University of Urbino Carlo Bo

Department of Biomolecular Sciences – DISB

Ph.D. Programme - Sciences of Life, Health and Biotechnologies

Curriculum - Biochemical and Pharmacological Sciences and Biotechnology

Cycle – XXXIV

Development of new biological drugs for the treatment of fungal infections

Thesis written thank to the financial contribution of Marche Region
as provider of the Innovative Ph.D. project.

Academic discipline: Biochemistry - BIO/10

Supervisor: Professor Mauro Magnani

Ph.D. Student: Dr. Tania Vanzolini

Co-supervisor: Tomas Di Mambro Ph.D.

Academic year

2020/2021

INDEX

INTRODUCTION

FUNGI

Among the living beings, fungi represent an autonomous kingdom since they preserve a unique combination of features proper alternatively of plants and animals. Fungi are immobile, heterotrophic, and eukaryotic organisms mainly obligate aerobes even if facultative aerobes exist. There is a great distinction that defines this group, it is the case of macromycetes and micromycetes; the former, mushrooms, form fruiting bodies visible to the naked eye [1] whereas the latter are subdivided in unicellular (yeasts), pluricellular (filamentous fungi or moulds) and dimorph (can switch the morphology from yeast to filamentous form and backwards according to the different environmental conditions) [2].

Yeasts usually are single round-oval cells with sizes generally bigger compared to bacteria and typically ranging around 3-6 μm [3]. They present a classic intracellular composition with a nucleus, organelles like mitochondria, vacuoles and membranous structures that remind the Golgi apparatus, all immersed in the cytoplasm and bordered by the cell membrane. Beyond the cell membrane, the fungal wall is a rigid architecture that gives shape and protection to the cell despite the nutritional exchanges and the ligand-receptor interactions. The chemical composition of the wall depends on the age, morphology and resistance mechanisms of the species and strains, but more than 80% consists of carbohydrates [4]. The main components are chitin that produces a thick net with its β-1,4-linked N-acetylglucosamine fibrils, mannan, a D-mannose polymer set up with α-1,6-linkages and α-1,2- and α-1,3- bonds for the branches, and glucan, a polymer composed by D-glucose. The most prevalent glucans have glucose molecules connected linearly with β-1,3- glycosidic linkages and branched with β-1,6 bonds but, to a lesser degree, the linear connections can be β-1,6 as well [5, 6] (Fig. 1).

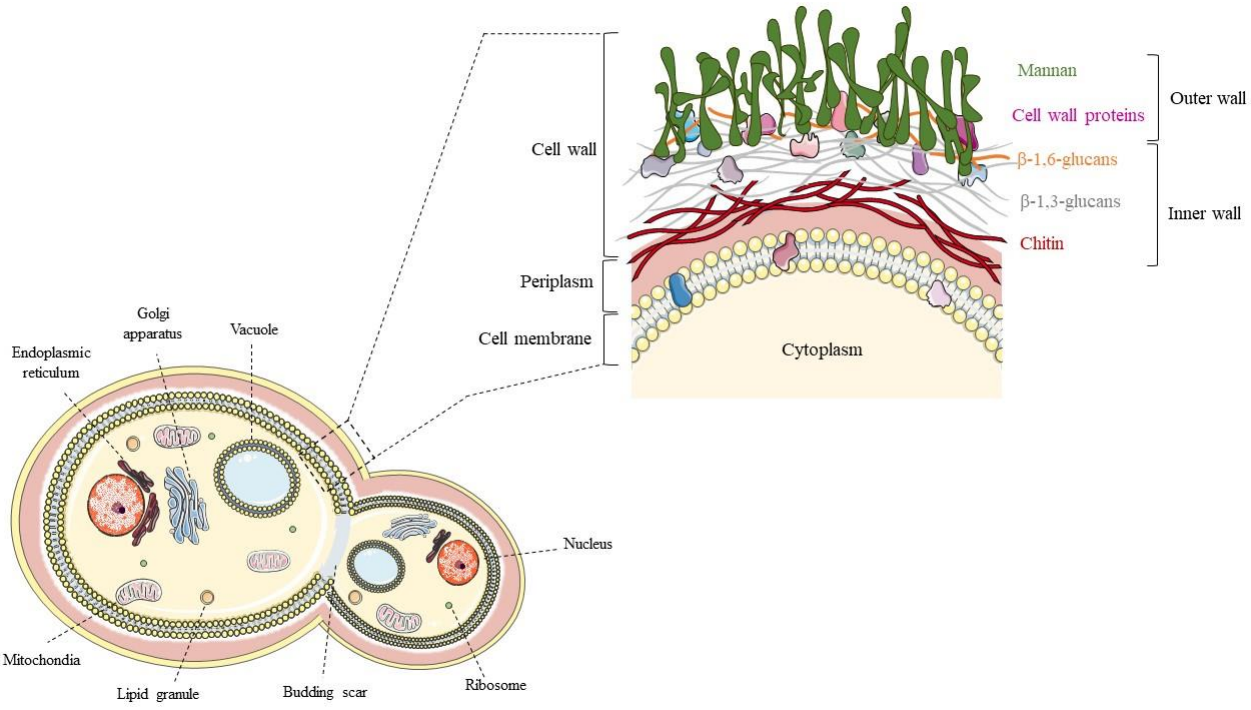

Figure 1. Representation of the intracellular composition and wall structure of a yeast cell. *C. albicans* was selected as model.

The moulds or filamentous fungi have a characteristic morphology composed of filaments deriving from cells that stretch and branch to form an intricate aggregate of hyphae called mycelium. The essential functions of moulds take place primarily in the vegetative mycelium but from that, some reproductive hyphae are arranged above to produce a reproductive mycelium from which the spores will be released. Hyphae are the structural units of the mycelia; they have a tubular and filamentous aspect that can reach a length of 50 μm with diameters of 4-6 μm [7]. Hyphae are classified in septate if they do have wall invagination called septa, and coenocytic if they don't. However, septa are always incomplete and never totally close a compartment, thus permitting a facilitated circulation through pores of nutrients and little organelles like mitochondria, ribosomes and sometimes nuclei. In septate hyphae there is always at least one nucleus in each compartment while in the coenocytic, nuclei are mobile elements dispersed in the cytoplasm. As for yeasts, the vacuole, the endoplasmic reticulum, and the Golgi apparatus are clearly recognizable as well, and outside the cell membrane, the wall is well organized with a great abundance of chitin (more than 70%) followed by glucans and a variable content of other carbohydrates, proteins, and lipids [8, 9, 10]. After differentiation, septa will maintain their dimension therefore the hyphal growth is granted by an apical elongation. In the top of the hyphae, a peculiar organelle born from the aggregation of vesicles, the spitzenkörper, undergoes the process of exocytosis contributing both to the cell membrane thank to its vesicle membranes, and to the cell wall through the components that it contained [11]. The hyphal growth and the increment direction are conditioned by environmental factors and septa are completely closed just in case of the urgent need to preserve the mycelium scarifying a part of a hypha that has been damaged or compromised by other microorganisms (Fig. 2).

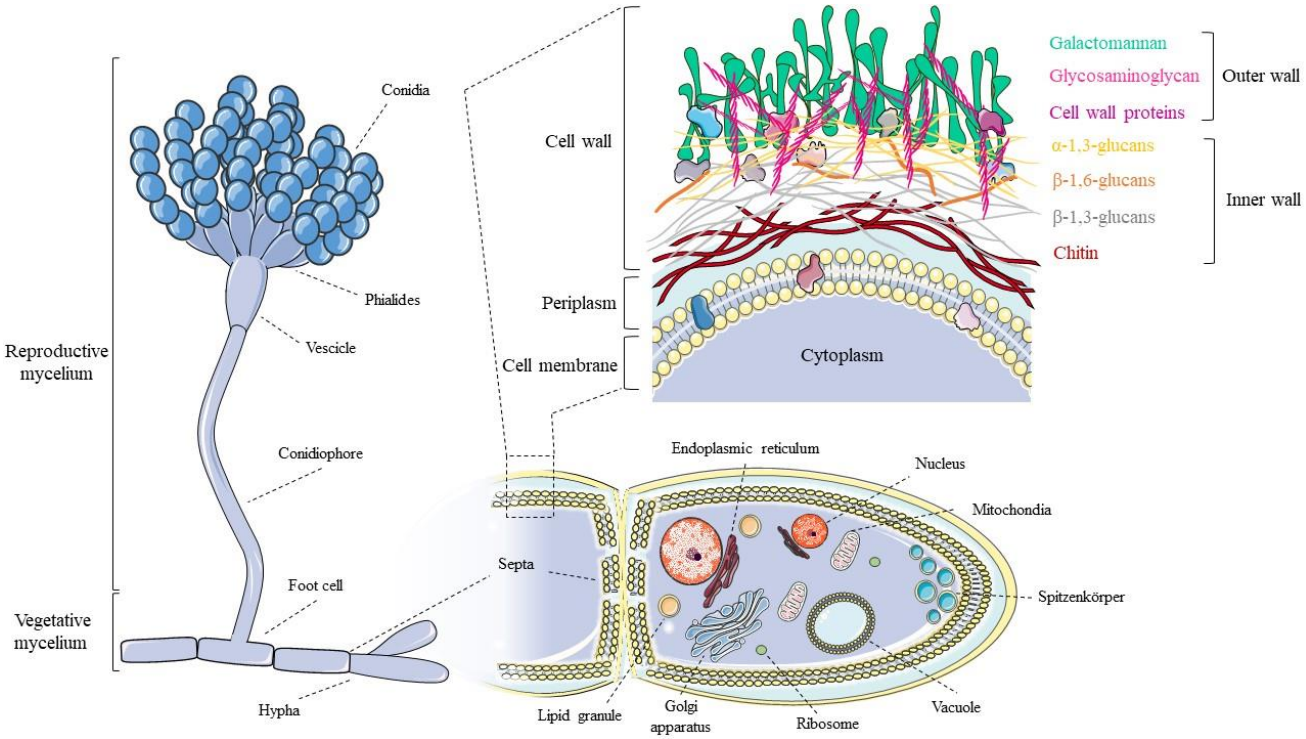

Figure 2. Representation of the intracellular composition and wall structure of a hypha of a mould. *Aspergillus fumigatus* was selected as model.

In nature another different behaviour has been found, the yeast-like fungi or dimorphic fungi can substantially change their morphotype assuming the yeast or the hyphal form in response to external conditions [12]. Even if some yeasts can produce septate hyphae, most of them protrude pseudo-hyphae which derive from a subsequent budding of a bud that keeps being attached to the originator cell. At this level they can also branch or produce bunches that form the vegetative pseudo-mycelium; the reproductive pseudo-mycelium doesn't exist. Because of this generating method, pseudo-hyphae have more pronounced shrinkages and for this reason, the cytoplasmic connections are limited or absent [13].

As a result of their intrinsic nutritive characteristics, fungi can be saprophytes borne by dead decomposing organic material or commensals, symbionts, or parasites of different superior organisms like plants, animals, and humans. According to the most recent estimates, there is a total of 5.1 million species of fungi [14], and more than 600 of them are related to humans as part of the microbiome or as pathogens [15].

Fungi have two major reproduction methods: the sexual and the asexual reproduction. In the life cycle of a fungus these two ways can be either present or being alternated or mutually exclusive. For what concerns yeasts, they often face a binary scission or a budding with the asymmetric detachment of a bud. Both are the result of the mitotic process [16]. Eventually they can also use sporulation preferring the asexual type compared to the sexual. Moulds can rather fragment the fruiting body or undergo asexual or sexual sporulation. Asexual spores may be produced in hyphal specialized structures like conidia in the conidiophores and sporangiospores in the sporangium or accumulated and released in response to a modification of the hyphal architecture such as arthrospores spread through the hyphal fragmentation, chlamydiospores, thick-walled spores collected in a swelling of the hyphal tract and blastospores born by budding. The sexual spores involve gametes of opposing mating types; typical examples are oospores and zygospores originated by conjugation, ascospores and basidiospores that take their name from the specific site of production and accumulation, respectively the asco in the fruiting body and the basidio in the hyphal apical part [17, 18, 19].

The kingdom of fungi recognizes different phyla and species. The classifications in the past were based mainly on the evolution, on the morphology and on the reproduction system of the fungus but new criteria raised and deeply modified the previous organization; among them, the genome sequencing studies broke new grounds but at the same time made the literature quite controversial [20, 21, 22, 23, 24]. The most updated taxonomic studies consider nine phyla of true fungi: Opisthosporidia, Chytridiomycota, Neocallimastigomycota, Blastocladiomycota, Zoopagomycota, Mucoromycota, Glomeromycota, Ascomycota and Basidiomycota [25, 26].

FUNGAL INFECTIONS

Fungi may be pathogens for plants (phytopathogens), animals and humans. Especially in the last two subjects, they can cause different disorders:

- Mycoses are infections that identify in fungi (or mycetes) their etiological agent. Fungi under consideration are true pathogens (or obligate pathogens) or opportunistic if they provoke infection only in particular and favourable conditions such as accidental penetration of the immunity barriers, a weakening of the immune system or the colonization of host-sites different from that in which they are confined as microbiome [27].
- Allergy or hypersensitivity due to the immune system cells' reaction to the antigens exhibited by ingested or inhaled spores [28, 29].
- Mycotoxicosis if the food or beverages ingested were contaminated by fungal toxic secondary metabolites [30].
- Mycetism in the case of ingestion of poisonous fungi [31].

Considering the aim of this project, this thesis will focus only on mycoses.

Human mycoses are classified into different groups given parameters like the level of penetration and diffusion of the infecting agent in the host tissues, and the specific characteristics of the microorganism.

- Superficial mycoses – are caused by fungi able to grow on the skin surface. In healthy individuals they don't lead to physiological damages but mainly aesthetic defects like the lack of melanin in correspondence of fungal colonies, whereas in immunocompromised patients a worsening can occur especially if the fungus reaches deeper tissues [32].
- Cutaneous mycoses – the fungal growth happens mainly in the epidermis with its keratin-rich layers but also in hair and nails. They are associated with macroscopic deformation, tissue damages and inflammation, and when the infection extends deeper, they can evoke pathologic changes [32].
- Subcutaneous mycoses – they are due to the penetration into the deep layers of the skin like the connective tissue, the subcutaneous layer until muscles and bones. They rise a great inflammatory state but rarely become systemic. These mycoses are particularly difficult to treat, and surgical interventions are indeed often required [32].
- Opportunistic mycoses – they belong to commensal fungi that settle immunocompromised patients, hosts with a debilitated immune system or immune deficiencies [33].

- Systemic mycoses – they are infections that primarily originate in the lungs and then reach the bloodstream and subsequently other organs and districts arising the most important, harmful, and strongest immunity response [34].

The onset and clinical development of a mycosis are closely related to predisposing factors; some of them are proper of the physio-pathological conditions of the host like age, pregnancy state, immunodeficiencies, HIV/AIDS, immunosuppressive treatments, diabetes mellitus, malignancies, alteration of the microbiome, etc., but some other are external to the host such as the behaviour, the environment, invasive devices, and the nature of the fungus [35, 36]. Obviously, the susceptibility of the host to the pathogen is individual and while in immunocompetent subjects the resistance is guaranteed by an efficient machinery able to defend and protect the organism, in immunodeficient or debilitate patients the fight is harder and mostly entrusted to the antifungal treatments available.

HOST IMMUNITY AGAINST FUNGAL INFECTIONS

In order to accomplish the infection, the pathogenic fungus should settle and start the reproduction and the colonization in a suitable host district but fortunately, the mechanisms adopted by a competent immune system manage to avoid both the invasion and the expansion, and in case of infection already in progress, to stop it reducing also the damages produced by the exacerbation of the inflammation. The immune system arranges in the aspecific or primary immunity, and in the specific or secondary immunity. The former is the intrinsic capacity to oppose microorganisms and their products, while the latter refers to the ability to distinguish and destroy every specific pathogen and its metabolites meeting, processing, exposing, and adapting to it [37, 38]. The first barriers that microorganisms encounter are the skin and the mucous which, besides resulting as physical shields, produce also secretions like sweat, tears, saliva, acid and mucus rich in enzymes as lysozyme and antimicrobial peptides as defensins [39, 40]. If the pathogen can penetrate in deeper layers, it will confront some effectors of the aspecific immunity: neutrophils, monocytes, macrophages, and dendritic cells [41]. In general immune cells can recognize pathogens through molecular profiles on their surfaces (the pattern recognition receptors-PRRs), that interact with molecular profiles proper just of the pathogen (pathogen-associated molecular patterns - PAMPs). The interaction between PRRs and PAMPs triggers transmembrane signals like MyD88 and Syk-CARD9 that promote the antifungal activity [41, 42, 43]. The receptors involved are mainly toll-like receptors (TLRs), in particular, TLR2 and TRL4 on the plasma membrane which bind mannans, N- and O-linked mannans, lipomannans, phospholipomannans and glucuronoxylomannans. TLR9 are instead in endosomes and recognize fungal DNA [41, 44, 45]. There are nucleotide-binding oligomerization domain-like receptors (NLRs), retinoic acid-inducible gene1-like receptors and C-type lectin receptors (CLRs) [45]. In the latter family there have been identified dectin-1 and dectin-2 (which heterodimerize with dectin-3 [46]), specific for β-glucans and α-mannans respectively, CD23 for both β-glucans and α-mannans [47], galectin for β-

galactosides [48], mannose receptor and dendritic cells specific intercellular adhesion molecule grabbing nonintegrin receptor (DS-SIGN) selective for mannose, fucose, mannosylated and fucosylated molecules and N-acetylglucosamine, glycans macrophage-inducible C-type lectin receptor (mincle) activated by glyceroglycolipid and mannitol-linked fatty acids, and finally complement receptor 3 (CR3) [44, 45, 47] and lactosylceramide receptor (LacCer) for β-glucans [49]. The recognition of the pathogen has different results: phagocytosis, the release of cytokines and reactive oxygen species (ROS), the antigen loading in the major histocompatibility complex and the activation of the T-cells responses. Fungi are killed through different mechanisms based on the specie and on the morphotype, as proof, the internalization by neutrophils of yeasts and conidia but the production of NADPH-oxidase-dependent neutrophil extracellular traps (NETs) for moulds and for fungi which develop hyphae and pseudo hyphae [50, 51]. Monocytes, macrophages, neutrophils, and dendritic cells engulf microorganisms and fuse the phagosome with the lysosome to process them through reactive oxygen and nitrogen intermediates moreover, macrophages undergo the polarization in M1 or M2 in case of classical activation and pro-inflammatory behaviour or in alternative activation with an anti-inflammatory trend when there is the persistence of the fungi inside them [52]. All these effectors also release a great number of antimicrobial peptides, ROS, chemokines, type I interferons as IFN-γ and cytokines both pro- and anti-inflammatory like IL-17, IL-12, IL-1β, IL-10, IL-2, IL-23, IL-6, TNF-α and, as result, also the redox-sensitive factor NF-κB. All these mediators are useful in promoting the recruitment of other immune cells and in boosting the antifungal activity, but they are also necessary for the differentiation of the T-helper lymphocytes. Macrophages and dendritic cells are indeed antigen-presenting cells (APCs) able to expose on their surfaces the antigens through the major histocompatibility complex (MHC) class II to naïve T cells. In this way, CD4+ T-helper lymphocytes can differentiate in different subpopulations: Th1, Th2, Th17 and Treg cells. They are involved in fungal infections and must balance the pro- and anti-inflammatory status avoiding exacerbations [45, 53]. B lymphocytes are APCs as well, but they usually present the antigens to already-activated T-cells which, in response, activate plasma cells producing both specific antibodies and memory cells [54]. Th1 and Th17 have a strong pro-inflammatory behaviour while Th2 and Treg contain the inflammation hindering the proliferation and the differentiation in Th1 and Th17 and promoting the M2 polarization; their objective is the reduction of the host tissue damage although allowing the fungal persistence. Microorganisms have developed different mechanisms of immune evasion for example, the coating or masking of PAMPs, the inhibition of the phagosome-lysosome fusion or of the opsonization, the degradation of the complement factors, the secretion of catalase, superoxide dismutase or toxins like candidalysin, the upregulation of efflux pumps to neutralize the AMPs, and the modulation of the immunity response promoting the Th2 differentiation and the M2 polarization to enhance the survival rate [44, 55]. In the case of immune evasion, there are several other strategies to fight with, for instance, if the microorganisms have escaped the phagocytosis and have poured out in the cytosol, they will be processed in the proteasome and then bond to MHC class I and presented to CD8+ T-cytotoxic lymphocytes [56]. Sometimes their activation may also come from a cross-presentation of extracellular antigens using MHC class I by dendritic cells [57]. CD8+ T-cytotoxic lymphocytes differentiate in subpopulations like Tc1, Tc2 and Tc3. While Tc1 cells are dedicated to the cell killing through degranulation

of perforin, grandzymes and granulysin, and Tc3 differentiates in Tc17 for the long-term antifungal immunity, Tc2 seems to suppress the immunity response [44, 58]. Natural killers, even if considered part of the primary immunity, are cytotoxic cells, hence degranulate and release perforin and granzymes and produce pro-inflammatory cytokines like IL-17 and IFN-γ and soluble factors as GM-CSF and RANTES [59]. There is significant evidence that some other immunity cells contribute consistently to the control of the fungal infection, among them mast cells [60], basophils, eosinophils [61], MDSCs, γδT, MAIT and iNKT [44]. Some antifungal drugs are fungistatic and not fungicidal therefore the participation of the immune system is fundamental for the resolution of a fungal infection, and this highlights the risk for people who don't benefit from a competent immunity both for pathological reasons and for immunosuppressive therapies.

ANTIFUNGAL DRUGS

Conversely to the antibacterial world which has always been in the eye of the storm and felt faster times of new targets and compounds development, only a poor arsenal of molecules and limited targets are available for antifungal drugs, thus probably for the similarities between fungal cells and host cells. Fungal infections have been a neglected issue that subtly grew for decades until they were brought to light only when it was figured out as one of the most serious health problems of our time and for the near future. Currently, there are four major classes of drugs used in clinic and veterinary; they are polyenes, azoles, echinocandins and pyrimidine analogues.

- **Polyenes**

Amphotericin B is the absolute representative of the polyene class. It is a fungicidal able to interfere in the ion homeostasis of the fungal cell establishing hydrophobic interactions with ergosterol of the membrane and creating pores. It induces an accumulation of reactive oxygen species as well and both mechanisms contribute to cell death. From its discovery in 1955, more than 200 polyenes were developed but amphotericin B keeps being the drug of choice especially for systemic mycoses [62, 63]. Although its high efficiency, the main limitations are represented by nephro- and hepatotoxicity, infusion reactions and electrolyte anomalies [64, 65] therefore, from the deoxycholate form, new formulations were elaborated in order to ameliorate both the safety and the effectiveness. Lipid-based formulations consist of the liposomal charging of the drug or of a complex formation. A colloidal dispersion of amphotericin B was developed but is not available on the market [66].

- **Azoles**

After their discovery, azoles became quickly the first-line drugs [66]. Apart from few exceptions, they are considered organism-dependent fungistatic/fungicidal [67] and can inhibit the cytochrome P450-dependent lanosterol-14α-demethylase, an essential enzyme in the synthesis of ergosterol [68, 69]. This class contains both imidazole- and triazole-active group molecules since several modifications in the structure followed one

another and gave rise to different generations. The first generation is occupied for instance by clotrimazole, ketoconazole, miconazole, butoconazole, econazole, bifonazole, terconazole, tioconazole etc. which present the imidazole ring. The scarce water-solubility was an obstacle as well as the limited oral bioavailability and side effects like gastrointestinal and endocrine alterations and hepatotoxicity. Even if their uses, especially for invasive infections, decreased over time, they are still adopted in topical preparations. After that, the second and the third generations saw their birth with the coming of the triazole ring in the formula and with structural changes that progressively made them more effective and hydrosoluble to say nothing of extended-spectra, better pharmacokinetics and pharmacodynamics, the possibility of new formulations and lower toxicities. In the second generation we find fluconazole and itraconazole while in the third, voriconazole, posaconazole, isavuconazole, ravuconazole and albaconazole [64]. The great usage that is done not only as treatment but also in prophylaxis and in pre-emptive circumstances permits them to be widely used also in medical and surgical fields [66, 70]. Despite they are well tolerated few restrictions have been highlighted like the QT prolongation, the teratogenicity, and the drug-drug interactions of triazoles [64, 71, 72].

- **Echinocandins**

Echinocandins represent the most recent class of antifungal drugs starting its development in the early 2000s [73]. They are semisynthetic lipopeptides which found in fermentation metabolites of different microorganisms their main structure [62]. Echinocandins inhibit in a non-competitive manner the UDP-glucose-β-1,3-D-glucan-β-3-D-glucosyltransferase also known as β-1,3-D-glucan synthase, an essential enzyme for the synthesis of β-1,3-glucans, fundamental components of the fungal cell wall. β-1,3-D-glucan synthase is a complex formed by two subunits, one regulatory, Rho1, and one catalytic, Fks; in particular, Fks is encoded by three genes, FKS1, FKS2 and FKS3. Echinocandins seem to target specifically FKS1 gene [74]. Based on the fungus but also on the specie and strain, echinocandins can be considered fungistatic or fungicidal. The echinocandins that had the most success and reached the market are caspofungin, micafungin and anidulafungin. Their features like the potent activity associated with the broad-spectrum, the good pharmacokinetic and pharmacodynamic and the high safety and few drug-drug interactions make them suitable as first line drugs especially in nosocomial candidemia [66].

- **Pyrimidine analogues**

5-Flucytosine is the only component of this class. From its approval in the 1960s it has been seen for a long time just as antimetabolite for cancer treatment, but its low antineoplastic activity made it shift towards the antimicrobial pipeline as an antifungal drug. 5-Flucytosine is a fluorinated analogue of cytosine and for this reason it can easily enter the fungal cells through the cytosine permease and be deaminated by cytosine deaminase to 5-fluorouracil. Then 5-fluorouracil is converted into 5-fluorouridine triphosphate able to be incorporated in fungal RNA hence, to alter the aminoacylation of tRNA and to inhibit the protein synthesis. At the same time 5-fluorouracil, when metabolized into 5-fluorodeoxyuridine monophosphate, inhibits the thymidylate synthase, an enzyme essential for DNA synthesis and nuclear division [62]. This double mechanism of action makes 5-flucytosine a potent drug especially in candidiasis and cryptococcosis, but it can be used

only in combination with other drugs like amphotericin B because of the rapid development of resistance [75]. It has high oral bioavailability but a brief half-life. The interactions with other drugs are few but the main limitations are referred to bone marrow suppression and hepatotoxicity [64].

Allylamines

Allylamines represent a small family of molecules that target the squalene epoxidase (or squalene monooxygenase) an enzyme needed for the ergosterol synthesis [76]. They aren't commonly used in clinics except for dermatophytes against which they are fungicidal [77]. Terbinafine, naftifine but also pentamidine and some derivatives like butenafine or amorolfine are examples of squalene epoxidase inhibitors.

NEW TARGETS AND NEW APPROACHES

Among the relatively new targets, it is important to mention the calcineurin pathway. Calcineurin is a Ca^{2+}/calmodulin activated protein phosphatase 2B essential for activating stress responses especially inside the host, but it also plays a role in fungal growth, morphotype change, virulence, and resistance development [78]. It is the target of immunosuppressors like tacrolimus and cyclosporine A, mainly used to avoid rejection after transplantations [76, 79]. Their action is fulfilled by the binding to immunophilins that impair the interaction of calcineurin to its substrates. The major limitation is represented by the serious consequences on the immune systems and for this reason, different efforts in bordering the side effects but maintaining the antifungal activity have been considered [80]. One significant example is APX879, the successor of tacrolimus that presented high efficacy in *in vivo* cryptococcosis infections but low immunosuppression [81]. Moreover, tacrolimus received large interest also in combination with caspofungin, making it fungicidal for C*andida* and *Aspergillus* species, echinocandins- and azoles-resistant as well [82, 83, 84, 85]. With azoles it showed a synergistic effect against the biofilm formation [86] with particular attention to fluconazole, with which it can reverse partially the azole resistance [87]. This pathway must be further explored especially because new molecules have been discovered as calcineurin inhibitors, few examples are vasostatin-I, a peptide derived from chromogranin A, and some of its shorter fragments like chromofungin and catestatin which are active both against yeasts and filamentous fungi [88] and tamoxifen, an anticancer that is supposed to interfere in the calcineurin pathway [89]. Calcineurin effectiveness is often associated with one of its upstream regulators, it is the case of the heat shock protein 90 (Hsp90), a chaperon involved in stress signalling pathways, virulence, and resistance [76]. It is a good target for inhibitors since it seems to be implicated in around 10% of the total protein pathways of a yeast [90]. In order to get its role more complicated, Hsp90 regulates the morphology of fungi differently, its inhibitors induce indeed filamentation in *Candida* spp. [91] and repress it in *Aspergillus* spp. with negative outcomes in germination and conidiation [92]. In combination with amphotericin B, fluconazole and echinocandins improved the antifungal activity, reduced the mortality rate, and impaired the evolution of resistance [93]. Mycograb (efungumab) is a monoclonal antibody specific for Hsp90 that demonstrated great efficiency in invasive candidiasis [94] but that

never reached the market because of quality and safety issues while geldanamycin and its derivatives, despite their antitumoral properties, have shown good antifungal effects but their use is restricted for drawbacks like hepatotoxicity [95]. Furthermore, part of their toxicity is related to the cross inhibition of Hsp90 of the host; about this, more selective inhibitors are currently under investigation and CMLD013075 is indeed an exquisite example [96]. Hsp90 also regulates the signalling of the protein kinase C cascade, essential for the calcineurin activation but also for the maintaining of the cell wall integrity as well as the growth, the morphotype, the resistance, and the stress responses [97]. The main enzyme of this cascade is Pkc1, hence its inhibition reduced the virulence *in vivo* and conferred hypersensitivity to several drugs making also the fungistatic drugs fungicidal. It seems that the PKC pathway permits the fungal survival to stress stimuli through the mitogen-activated protein kinase (MAPK) cascade and for this reason an upstream inhibition can implicate the lack of Mkc1 [93, 97]. Cercosporamide is a selective inhibitor of Pck1 [98]. Going up to the top of the Hsp90-calcineurin-PKC axis, the histone deacetylases (HDACs, also called lysine deacetylases, KDACs) control the expression and function of different proteins, Hsp90 included. Some of these proteins are fully involved in the fungal virulence hence inhibitors of these enzymes are strategic moves. Noteworthy is Hos2 since it regulates Hsp90 deacetylation and its activity therefore inhibitors of Hos2 like MGCD290 revealed to be extremely efficient especially in synergistic combination with azoles and echinocandins against *Candida* and *Aspergillus* spp. [99, 100] Trichostatin A is another HDAC inhibitor that displayed enhancement with azoles in *C. albicans* and with caspofungin in *Aspergillus* spp. [101] In addition to that, other interesting enzymes work at this level such as the deacetylase HST3 that, when inhibited, by nicotinamide demonstrated antifungal properties or the acetyltransferases whose genetic depletion conferred hypersensitivity to fluconazole [102]. Essentially inhibitors of calcineurin, Hsp90, Hos2 and Pkc1 represent actors that play at different but interconnected layers of the same piece. All four approaches are extremely promising in treating fungal infections.

Even if sphingolipids are components of the eukaryotic membranes, several studies have established that the biosynthesis pathways in fungi and in host cells are significantly different, therefore the enzymes involved or the genes encoding them could be optimal antifungal targets. Sphingolipids like inositol phosphoryl ceramide and glucosylceramide are responsible for virulence and for drug resistance [103, 104]. Acylhydrazones like BHBM, its derivative D13, D2 and D0 affect the glucosylceramide synthesis and are useful for infections of different pathogenic fungi [105] while aureobasidin A and its derivatives inhibit the inositol phosphoryl ceramide synthase [106]. Myriocin inhibits serine palmitoyltransferase, an essential enzyme in the synthesis of sphingolipids [107] while fumonisin and australifungin act on the ceramide synthase whose impairment makes *C. neoformans* avirulent [108]. Apart from them, a monoclonal antibody against glucosylceramides that reduces the host inflammation [109] and Cerezyme, a recombinant enzyme able to hydrolyse fungal glucosylceramides both tested in cryptococcosis [110], are interesting results coming from biotechnological studies. A similar discourse can be done for the Ras pathway: Ras are guanosine triphosphate proteins (GTPases) associated with the membrane and involved in some protein transduction, virulence, morphotype switch, and vital processes [111, 112]. Ras can reach the plasma membrane both in a palmitoylated and not-palmitoylated form. There, it undergoes some post-translational modifications essential for its biological activity, and finally, it is activated by the

interactions with guanosine nucleotide exchange factors (GEFs). The inhibition of palmitoylation, of post-translational modifications such as farnesylation or prenylation, of the interaction with GEFs, with its common substrates or with Ras-related proteins like RhbA could be brilliant approaches [113, 114, 115, 116]. Some successful molecules are manumycin A, a farnesyl transferase inhibitor, efficient against *C. neoformans*, *C. albicans* and *A. fumigatus* [117, 118] ethylenediamine inhibitor #2, tipifarnib, lonafarnib active in farnesylation inhibition in *cryptococcosis* [117, 119] and farnesyltransferase inhibitor III able to block the yeast-hyphal change in *C. albicans* through farnesyl transferase inhibition [120], actinoplanic acid A and its desmethyl analogue [121]. Standing in the post-translational modifications field, some proteins are supplemented with a glycosylphosphatidylinositol (GPI) group that allows the protein to travel from the endoplasmic reticulum to the plasma membrane and to the cell wall. An altered biosynthesis of the GPI-anchor resulted in defective morphology and attenuated virulence both in *C. albicans* and in *A. fumigatus* meaning that some GPI-anchored proteins have a role in the fungal pathogenesis [122, 123]. The GPI-anchor biosynthesis became thereby a source of targets like the acyltransferase Gwt1 inhibited by gepinacin, APX001A (E1210) and its prodrug fosmanogepix (APX001 or E1211) [124], BIQ, G365, G884, and the phosphoethanolamine transferase-I targeted by YW3548, M743 and M720 [125].

One of the most attractive and newest targets is represented by the trehalose biosynthesis. Its absence in mammalian cells reduces enormously the host toxicity. Trehalose is a storage carbohydrate useful as a carbon source for processes like glycolysis, fungal germination, and sporulation and is an important player in stress conditions [126]. Its pathway involves two main enzymes: the trehalose 6-phosphate synthase 1 (Tps1) and the trehalose 6-phosphate phosphatase (Tps2) [127]. It has been seen that the deletion of their genes affected *Cryptococcus* spp., *C. albicans* and *Aspergillus* spp. growth, survival and virulence and *Aspergillus* spp. germination moreover, a compromised Tps2 causes an accumulation of trehalose 6-phosphate leading to cell death [128, 129, 130, 131, 132, 133]. Even if the trehalose is such a delicious target just few studies have identified effective inhibitors; among them there is validamycin A [133]. As for the trehalose pathway, some components involved in the glyoxylate cycle are completely absent in mammalian cells. The glyoxylate cycle seems to be important for virulence and survival, especially after macrophagic engulfment. It is similar in some ways to the tricarboxylic acid cycle with which it has in common three enzymes, the citrate synthase, the aconitase, and the malate dehydrogenase. The glyoxylate cycle makes also use of two other unique enzymes, the isocitrate lyase (ICL) and the malate synthase (MS) [134]. Mohangamide A and mohangamide B are efficient inhibitors of ICL in *C. albicans* [135], argentilactone and its semi-synthetic analogues inhibited ICL in *Paracoccidioides* and some other compounds targeting MS are still under investigation [136].

With the term orotomides, the microbiological world has identified a completely new class of antifungal drugs. Their target is represented by the dihydroorotate dehydrogenase (DHODH) involved in the biosynthesis of pyrimidines. The depletion of pyrimidines leads to bocks in the DNA/RNA synthesis and in the lipid and carbohydrate precursors productions. Olorofilm F901318 is an excellent inhibitor that can be selective for fungal DHODH even if the enzyme was found also in mammals. The only negative point is the narrow spectrum that includes moulds and dimorphic fungi but not yeasts [137].

Among the promising targets, some can be found in the mitochondria. They are the organelles adhibited to the energy production through the oxidative phosphorylation and the tricarboxylic acid cycle and even if some intermediates and enzymes are shared by both fungi and host cells, there are some fungus specific proteins suitable for new antifungal compounds action [138]. The greatest results of this approach are represented by ATI-2307 and ilicicolin H. The first is an arylamidine able to inhibit both the complex III and IV of the respiratory chain interfering inevitably in the mitochondrial membrane potential [139] while the second acts on the mitochondrial cytochrome bc_1 reductase [140]. Both have been tested on *Candida*, *Cryptococcus* and *Aspergillus* spp. showing great potential, efficacy, and selectivity [140, 141]. Some other known molecules have been found to have antifungal effects altering the mitochondrial function, few examples are represented by artemisinin that inhibits the mitochondrial NADH dehydrogenase, quercitin that affects the oxidative stress operating on some electron membrane transport proteins, histatin 5 that disrupts the ATP synthesis machinery [142] and few antibiotics like linezolid, azithromycin, and minocycline [79].

Being comprehensive regulators of a multitude of pathways, the TOR protein kinases, when inhibited by the immunosuppressant rapamycin, showed antifungal activity against different fungi, blocking their growth and reversing azole resistance. Its main limitation is the immunosuppressive activity but some derivatives with reduced drawbacks but still effective are under investigation [143].

Some new strategies, looking at the current antifungal mechanisms, are directed toward the cell wall components or toward the enzymes that produce them. Nikkomycin Z, for instance, is a competitive inhibitor of the chitin synthase because of the structural similarities with the substrate uridine diphosphate (UDP)-N-acetyl glucosamine [144]. It has additive and synergic relationships with azoles and echinocandins in aspergillosis, candidiasis and coccidioidomycosis [145]. Polyoxins have the same mechanism as nikkomicins and together with plagiochin E and lectins and fungal secondary metabolites inhibit the chitin synthesis [144]. Another example is represented by the monoclonal antibody 2G8 and the humanized H5K1 whose antigens are selectively β-1,3-glucans of the fungal cell wall. The first has proved its efficacy in candidiasis, aspergillosis and cryptococcosis but with the limitation of its murine nature [146, 147] while the second has great potential against *Candida* spp., even if it is still under exploration on other pathogenic fungi and presented synergic combination with amphotericin B and echinocandins [148]. Some other molecules are in phase III clinical trials, it's the case of rezafungin (SP3025 or CD101) and ibrexafungerp (SCY-078) respectively a lipopeptide that can enter the class of echinocandins and a triterpene glycoside both acting on the β-1,3-glucan synthase [149, 150]. All these roads have the advantage to damage the wall, proper just of fungi without repercussions for the host.

A total new branch of antimicrobials addresses iron-related pathways. This gave the inspiration also for the development of new antifungal drugs. Iron is hijacked by fungal cells and is needed for many processes that confer the typical virulence factors. The main objective is the impairment or the exploiting of the iron assimilation and different strategies have been adopted: some antifungal peptides were conjugated to the siderophores in order to be incorporated inside the cells where they are released to carry out their task [151, 152]; the interference on the synthesis of siderophores through the inhibition of enzymes like the nonribosomal

peptide synthetases, the polyketide synthase, the phosphopantetheine transferase and the nonribosomal peptide synthetases-independent siderophore synthetases [153]. In this context, an expletive example is represented by celastol that, acting on the flavin-dependent monooxygenase siderophore A, inhibited *A. fumigatus* growth [154]. Other methods are the usage of iron chelators or the substitution of iron with gallium [155]. Lipocalins, especially ASP-2397, is a cyclic hexapeptide whose precise mechanism of action remains unknown, but it seems to chelate Al^{3+} and Fe^{3+} and to be translocated inside the fungal cell through the siderophore iron transporter 1 (Sit1) preventing the cations hijacking. It showed good selectivity because of the lack of the Sit1 in mammalian cells, and high potency against different fungi [156]. Ciclopirox has a similar mechanism of action sequestering Al^{3+} and Fe^{3+} [157, 158].

Other interesting approaches concern for instance the mitosis inhibitors like griseofulvin, a polyketide that affects the tubulin of the mitotic fuse [159], glutathione blockers like haloprogin [158, 160], or, with the same ratio, inhibitors of the superoxide dismutase, catalase and peroxidases that are tightly correlated to the remotion of ROS produced by the immune system cells making the fungal cell unable to protect itself [158]. Salinomycin is active against some yeasts and filamentous fungi especially in combination with polymyxin B [161]. AR-12 is a celecoxib analogue with little information about its mechanism of action. It is a protein kinase inhibitor that seems to operate both on acetyl fungal coenzyme A synthetase 1 (causing a downstream repercussion on the metabolism and especially on the histone acetylation) and on Hsp90 and Hsp27 chaperons' production, downregulating their genes and reducing, in this way, the host immune response [162]. Some cyclooxygenase inhibitors showed antibiofilm activity by inhibiting the prostaglandin E2 biosynthesis [62]. Some antimicrobial peptides, proteins, lectins, fungal and plant secondary metabolites are currently under investigation as both antifungal compounds and as enhancers if used in combination with commercially available drugs [142]. At the same time, several studies are ongoing on the repurposing of drugs that had the approval for other diseases [79]. There haven't been licensed any antifungal vaccine yet even if different groups are working on them and on adjuvants. Due to a multiplicity of obstacles, those research lines are still big challenges [163]. Furthermore, the metabolomic, proteomic and lipidomic sciences in combination with computational biology have granted great steps forward in the identification of new targets and compounds in faster times [164, 165, 166]. In this way, the reach of the clinical phases and the market can be facilitated and improve substantially the patients' treatment and survival.

DIAGNOSIS

The diagnosis is another important issue, especially for fungal infections. Despite the development of new diagnostic agents and techniques, the fungal identification, in order from the most used to the least used, still resorts to the examination at the microscope, to histopathology, to microbial cultures, to antigen detections, to serological tests and to molecular analyses [167]. The first three processes are not always accurate, and they often

delay the diagnosis because of the intrinsic properties of fungi like the slow growth in plates or liquid medium. Sometimes they are followed by susceptibility testing in order to find the MIC and the breakpoints for a correct use of antifungal drugs [168], but this delays even more the beginning of the antifungal treatment being dangerous for patients and negatively affecting their recovery or survival [169]. In addition to that, these procedures are less precise and certain, especially if compared to more recent techniques as molecular and immunological assays but, about them, the information available in the online platforms are little and the databases are poor and limited to few and more common mycoses [170]. The presence in the market of diagnostic kits for antigen detection is restricted as well and the sensitivity and the specificity are not always optimal [171, 172, 173]. Last but not least, there is patient variability: the symptoms are diversified from subject to subject even if the infection is caused by the same fungal pathogen [174]. In this regard, the degree of infection, the comorbidity and physio-pathological and pharmacological conditions like immunodeficiency or immunosuppressive treatments, are associated with the fastest progressions and with the worst outcomes. This sad view highlights the urgent need for not just new antifungal drugs but also for new diagnostics, data and techniques that can make the diagnoses clear, easy and quick to perform, robust, sensitive and specific.

RESISTANCE

Nowadays the failure of antifungal treatments is often related to fungal resistance. The resistance to a drug can be intrinsic or acquired. In the first case, the microorganism already has the genes enabling it to survive in the presence of certain concentrations of the antimicrobial compound, without any previous exposure. The second type of resistance occurs as an adaptive response to a direct contact with the antifungal drug that permits the fungus to stay alive when exposed again to the same drug or class, making it inefficient [168]. This phenomenon has spread worldwide encouraged also by people's bad behaviours. The extensive use of antifungal molecules in agriculture has created big reservoirs of resistant fungal populations [175] moreover, the poor compliance of the patents together with prolonged or repetitive treatments and prophylaxes, sub-therapeutic doses, frequent exposures to infective agents and low competence of the immune system, are all factors favouring the rise of resistances [168]. Looking in depth at the genetic features of fungi, the sexual and asexual reproductions, aneuploidy, the genome flexibility [176], and the capacity to take up mutations are considerable advantages especially if combined with densely populated communities like those in biofilms. As if that was not enough, the number of infections has increased also promoted by the environmental pressures such as the climate changes that have significantly influenced the birth of new species like *C. auris*, their geographical area of distribution by affecting their vectors and, as result, their susceptibility to the available antifungal drugs [177]. The European Committee on Antimicrobial Susceptibility Testing (EUCAST) and the Clinical and Laboratory Standards Institute (CLSI) monitor the resistance to antifungals through standardised methodologies giving clinical breakpoints and finding the minimum inhibitory concentration (MIC), useful tools for the choice of the antifungal drug and its dosage in patient treatment. However, the appearance of new species often with

intrinsic resistance and the scarce reliability of susceptibility tests towards some drugs and species make the resistance evaluation hard [178].

Despite the great use that has been done of amphotericin B, the resistance phenomena are luckily uncommon. The few cases identified reported mutations in the genes that encode for the enzymes involved in the ergosterol biosynthesis (alterations in ERG3, ERG5, ERG11, deletion in ERG11, mutations in ERG1, ERG2, ERG6, ERG11 [179]), the up-regulation of the stress responses like the thickening of the cell wall [180], the over-activation of Hsp70 and Hsp90 [181, 182], the increased activity of the catalase and the superoxide dismutase [183].

Azoles have been used for a long time and most of the mechanisms of resistance address this antifungal class. There have been found mutations in the heme-binding site in order to impair the binding of azoles to the Fe^{3+} portion preventing its obstruction, but also in the cytochrome P450-dependent lanosterol 14a-demethylase sequence, hence in ERG11 in yeasts and in *cyp51A* in moulds, producing their overexpression [184, 185]. As for amphotericin B, several alterations take place to modulate the stress responses and among them, those that involve the Hsp90, Sgt1, calcineurin, histone deacetylases, and PKC, are the most significant. Mutations in ERG3, even if associated with a lower degree of resistance, are important for the cross-resistance with polyenes [186, 187]. However, the most prevalent mechanism exploits the up regulation of efflux pumps. The membrane-associated efflux pumps are classified into two major groups, the ATP-binding cassette also called ABC and the major facilitators (MFs). Both undergo an increase in number and in activity through mutations in genes like CDR1, CDR2 and MDR1 in *Candida* spp. and in the respective homologs in other fungi [185, 188, 189]. The loss of heterozygosity as well as the modulation of the number of chromosomal copies [190, 191] are other effective strategies adopted by fungi to survive antifungals. In addition, the inactivation of the mitochondrial complex I [192], mutations in the mitochondrial superoxide dismutase or in mitochondrial membrane proteins suggest a complex and tangled correlation between mitochondrial function and resistance phenomena [193].

Echinocandins resistance is mainly associated with mutations in the genes encoding the subunits of the β-1,3-D-glucan synthase, therefore FKS1 and just recently FKS2. These alterations can both lower the affinity of the drug to the target and lead to an overexpression [187, 194]. Mutations in the mismatch repair gene MSH1 have been shown giving resistance both to azoles and to echinocandins [66, 195] but these alterations are quite infrequent and rarely transmitted [196]. Other mechanisms of resistance also engage the participants to the stress-response pathways like Hsp90, Hog, calcineurin and PKC [197]. The fungal cell wall is extremely affected by both the mutations in FKS genes and in the modulation of the stress-related processes: the glucans biosynthesis depends on the β-1,3-D-glucan synthase while the chitin production relies on chitin synthase which is directly regulated by calcineurin [198].

5-Flucytosine is never used alone because of the surprisingly high incidence of resistance development. It has been estimated that 1 yeast cell in a population of 10^{6-7} faces an alteration leading to lower susceptibility [199]. The most recurring mutations are associated with the genes encoding proteins involved in 5-flucytosine uptake and conversion hence, FcyB of the cytosine permease, Fcy1 and Fcy2 of the cytosine deaminase and Fur1 of

uracil phosphoribosyl transferase [200]. Other mechanisms have been seen but are less common and specie specific.

Some evidence has demonstrated that resistance can be overcome by higher doses or by treatments with other antifungal drugs or classes. There are also some examples of resistance reversion especially when compounds are used in combination, but this issue keeps expanding rapidly and mowing down an impressive number of lives. Even though several molecules are in late clinical trials and some other innovative approaches are currently under investigation, there are too few options markedly available and too often limited in their use by side effects. The risk to encounter new species with intrinsic resistance and the possibility to develop acquired resistance add a tragic and dangerous accent to this scenario already afflicted by this serious problem.

EPIDEMIOLOGY

The Global Action Fund for Fungal Infection estimated that more than 300 million people are affected by fungal infections every year [201] and more than 1.5 million of them have a fatal fate [202]. In certain regions, invasive infections of specific fungi have a mortality rate that overcomes the 50% [203] and from epidemiological data, it seems that the fungal burden has increased particularly in the 20th century [204] probably with the extensive use of immunosuppressive drugs like sterols, chemotherapy, antibiotics, surgical procedures, transplantations, haemodialysis, and invasive devices. In this context, the probability to contract a fungal infection has raised as well as the number of possible susceptible hosts. The age, the immune system status but also morbidities like diabetes, malignancies, HIV/AIDS, and chronic obstructive pulmonary disease, have a great impact both on the development of the infection and on the clinical progression [205]. Different clades are rapidly expanding all over the world also facilitated by environmental changes and by intercontinental travels moreover, the birth of novel multidrug-resistant fungi together with the increase of the resistances are dramatically threatening the global health [206, 207].

Although superficial mycoses are the most spread and frequent infections, in proportion, invasive mycoses have the highest rate of mortality and morbidity, therefore they represent a heavy healthy and economic burden [203]. *Candida albicans*, *Aspergillus fumigatus*, *Cryptococcus neoformans*, *Pneumonystis jirovecii*, dimorphic fungi and mucormycetes are responsible for most serious fungal diseases worldwide [208] and *Candida*, *Aspergillus*, *Cryptococcus* and *Pneumonystis* spp. alone are estimated to be accountable for 2 million infections and more than 90% of the reported deaths [203].

Candida spp. are the most common pathogens causing bloodstream infections. *C. albicans* is the prevalent specie with its presence in 80% of the total infections but in recent years there has been a surprising shift towards the non-*albicans Candida* (NAC) species [27]. Twenty-year studies demonstrated that NACs gained the upper hand moving to 10-40% of the systemic infection from 1970 to 1990 and to 35-65% from 1995 to 2015

[209] while *C. albicans* dealt with a decrease from 57.4 to 46.4% from 1997 to 2016 in systemic infections [210]. The most troublesome NACs are represented by *C. glabrata*, *C. tropicalis*, *C. parapsilosis*, and *C. krusei* especially for their intrinsic and acquired resistance to first-line antifungal drugs [211] even if multi-drug resistance is still common among them [212]. Another new specie is creating great concern: *C. auris*, from its discovery in 2009 in Japan [213], started its expansion in 47 countries [214]. Currently, 5 phylogenetic clades have been identified in different geographical areas and their whole-genome sequence analyses have established that they emerged almost simultaneously [215, 216]. They often have intrinsic resistances to azoles with 90% of the strains being resistant to fluconazole in the US, but polyenes and echinocandins suffer from low efficacies as well, being 30% of the strains resistant to amphotericin B and 5% to echinocandins [216, 217]. One of the most worrying aspects is represented by the presence of multidrug resistance strains: even if 70% of the strains are resistant to just one antifungal class, 25% are resistant to two and the 1% to three classes [207]. Furthermore, *C. auris* has the capacity to colonize and persist not just in districts of living hosts but also on abiotic surfaces of the environment. Noteworthy are the cases of *C. auris* presence in several nursing and hospital facilities despite the containment measures adopted [218, 219]. For these reasons and for the high mortality rate (39% within 30 days and 58% within 90 days) the Centers for Disease Control and Prevention (CDC) has declared this specie as an urgent threat [220, 221].

Aspergillus spp. are environmental moulds, but they are also responsible for more than 85% of the systemic infections caused by moulds [208, 222]. 4.4% of the population develops an invasive infection every year that corresponds to around 200 000 people worldwide with 1.1-1.8 subjects every 100 000 [223]. The most prevalent specie is *A. fumigatus* touching 92% of the total invasive infections followed by *A. flavus*, *A. niger* and *A. terreus* [224]. Generally, invasive infections are proper of immunocompromised patients, and in this population, the mortality rate overcome 60% with 33.1% for adults within 30 days and 37.5% for children in intensive care units [225, 226, 227]. The contact with *Aspergillus* spp. occurs through spores dispersed in the environment and especially in the air, and for this reason, the primary site of infection is often the respiratory tract. From there, the infection may become disseminated.

Cryptococcus spp. are environmental fungi as well, and the etiological factor of infections mostly fatal like cryptococcal meningitis. It is often associated with HIV/AIDS subjects becoming the third most prevalent disease in these patients [228] and it has been estimated that in the zones with a high level of HIV transmission like that Sub-Saharian, one million cases per year have been recorded and 650 000 are the deaths [229]. There are two most prevalent species, *C. neoformans* that tends to affect more the immunocompromised patients and *C. gattii* which turns to immunocompetent individuals [230]. There are other species, but they have been found just occasionally and only in immunocompromised people. The alarming awareness concerns the intrinsic resistance of almost all the species to echinocandins [231].

Pneumocystis spp., and more specifically, *Pneumocystis jirovecii* causes more than 400 000 pneumonia every year [203, 208]. The contact occurs by inhalation of cysts, and the infection progresses mainly asymptomatically in childhood whereas in immunocompromised patients and in subjects with chronic lung diseases the

colonization becomes more dangerous [232]. In a European study with both HIV- positive and negative subjects, the incidence of *Pneumocystis jirovecii* pneumonia was 1.5 per 100 000 with a mortality of 9.5% and interestingly higher for HIV-negative patients [211].

ANTIBODIES: FULL-LENGTH AND scFv FORMATS

Antibodies are glycosylated proteins produced and released from plasma cells after B lymphocytes activation and maturation. Antibodies are effectors of the adaptive immunity hence they recognize and bind their specific antigen that may be components of microorganisms or toxins. Their binding can modify the chemical and structural composition as for antitoxins, but usually, the opsonization of microorganisms prevents penetration in deeper tissues, activates the complement reaction, attracts phagocyting cells like macrophages and neutrophils and favours the antibody-dependent cell-mediated cytotoxicity (ADCC) carried out by natural killers [233]. Different antibody isotypes exist but despite their structural and functional variability, they have a common organization. Antibodies are always constituted by four polypeptide chains, two identical heavy chains and two identical light chains. Chains arrange in a Y-shape with the heavy chains coupled in pairs with the light chains through disulphide bonds and non-covalent interactions. This is considered the antibody monomer. Both the heavy and the light chains have constant regions (C) and variable regions (V). The former are portions of the sequence that don't undergo frequent variations while the latter contain regions that present a high level of variability. In particular, these regions are called complementary determining regions (CDRs). They are hypervariable loops distributed among framework regions and are directly involved in the binding with the antigen [234]. The variable regions of both the heavy and light chain with the first domain of the constant regions are called antigen-binding fragment (Fab) while the remaining domains of the constant regions are known as fragment crystallizable (Fc) region and are the portions that interact with the complement mediators, or with other effectors of the immune system. This is also the section of the antibody that is glycosylated: the extent and the exact portion depend on the isotype, but it is essential for the Fc receptor-mediated recognition and activity [235]. Antibodies are classified based on the primary structure of the heavy chains. Five antibody isotypes exist: IgM, IgD, IgG, IgA and IgE (with IgG being the most abundant). While IgD, IgG and IgE are monomers, IgA (in particular secretory IgA) work as dimer and IgM as pentamer. Their different amino acid sequence is responsible not just for the chemical and physical properties but also for their different biological activities [236, 237]. The advent of recombinant technologies let the opportunity to develop several antibody fragments; among them, the single-chain fragment variables (scFvs) are composed of only the variable regions of the heavy and light chains connected by a short linker peptide (usually 15-20 amino acids and rich in Glycine for flexibility and in hydrophilic residues for solubility [238, 239]). Compared to the full-length antibodies (150 kDa), scFvs have smaller sizes (~25 kDa) that enable them to reach not-easily accessible antigens, to better penetrate tissues, to be rapidly removed from the bloodstream and to reduce the immunogenicity risk because of the lack of the Fc portion (Fig.3). Production costs are lower, there is no need for animal immunization and

novel techniques like phage display have substantially contributed to the antibody fragments development [240]. On the other side, a rapid clearance can be considered also a disadvantage, especially for therapeutic applications, as well as the lower binding affinity and stability and the tendency to aggregate. Diverse formats promote the possibility to use their singular features for different therapeutic and diagnostic applications. Full-length antibodies are perfectly appropriate for systemic use while fragments, with their brief half-life, are suitable for topical treatments of as diagnostic [241, 242]. A great bottleneck associated not just to scFvs but in general to every antibody both full-length and fragment format, is their not-human nature. The majority have been produced by mammalian cells therefore the possibility to induce the production of human anti-mouse antibodies (HAMA) [243] is high. For this reason, operations of genetic engineering have tried to reduce this immunogenicity risk. Chimeric, humanized, and human antibodies are the results of these efforts. The insertion in human scaffolds of the murine variable regions of the heavy and light chains gave birth to chimeric antibodies, the retention of just the murine CDRs in a human antibody backbone represents the rationale of humanized antibodies while human antibodies are totally human [243, 244, 245] (Fig. 4). Thanks to the progress in antibody manipulation, several antibodies in different formats reached the market and some others are currently in late clinical trials slowly becoming the dominant products in the biopharmaceutical market [246].

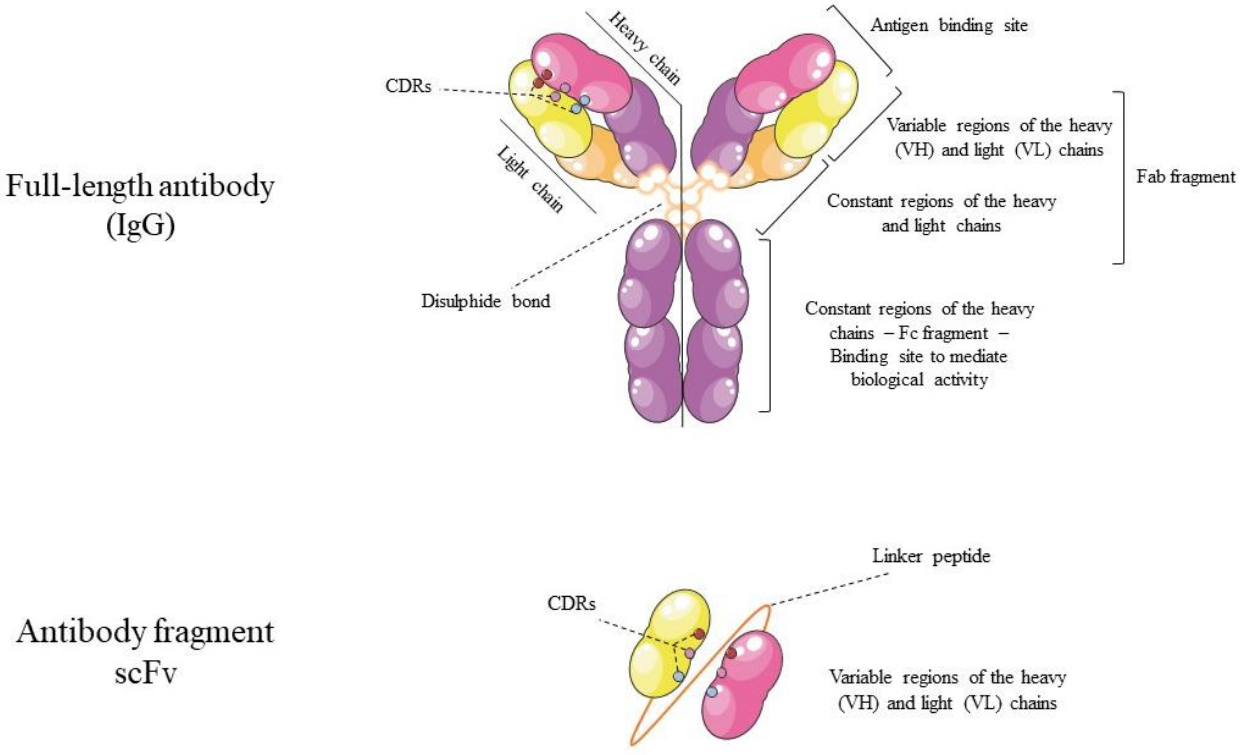

Figure 3. Simplified representation of the structure of a full-length antibody igG and of a scFv

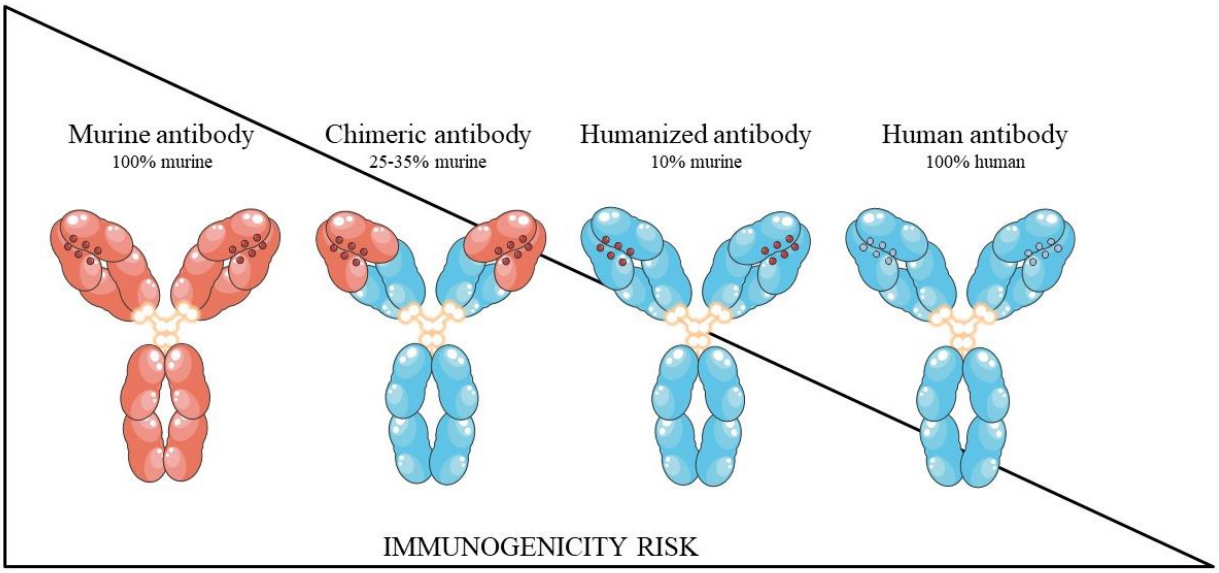

Figure 4. Schematic representation of the relation between the immunogenicity risk and the differently engineered antibodies.

THE MURINE MONOCLONAL ANTIBODY 2G8

Looking for a glycol-conjugate vaccine against pathogenic fungi, Professor Antonio Cassone's group found that laminarin conjugated with the protein carrier CRM197 had a protective action towards both systemic and vaginal infections by *C. albicans* [146]. This protection was due to the immunogenicity of the complex that led to the production of antibodies anti-β-glucans. These antibodies were purified, and the majority was represented by the IgG class. They demonstrated protection also in naïve mice, thus because they bond *C. albicans* hyphae and inhibit its growth. The same happened with *A. fumigatus* and *C. neoformans* both encapsulated and acapsular strains [147]. The monoclonal antibody born and tested in these studies was the monoclonal antibody 2G8, an IgG2b able to recognize laminarin, a β-1,3-glucan and, with lower reactivity, pustulan, a β-1,6-glucan. To gain more information about the protection capacity, two antibodies with the same complementarity-determining regions but different isotypes (the original mAb 2G8 IgG2b and the mAb 1E12, an IgM) were studied. The results obtained showed that 2G8 performed always better than 1E12, concluding that the structure may affect the epitope recognition, hence the efficacy [247]. On the other hand, the murine nature of 2G8 was a great obstacle for its use especially considering the future steps towards the clinical trials and, eventually, the entry into the market. From these results, a great investigation started with the aim to humanize the monoclonal antibody 2G8 both maintaining the full-length format and using smaller ones.

AIM OF THE STUDY

Considering the increasing interest in the discovery and advancement of novel antifungal agents, the great concern generated by both the resistance insurgence and spread, and the appearance of new species bringing intrinsic resistance to one or multiple drugs, I have started this project with the aim to develop a totally new humanized monoclonal antibody in both full-length and fragment formats based on the preliminary but high-promising results obtained with the murine monoclonal antibody 2G8. This thesis represents an exquisite example of the application of a biotechnological compound to the microbiological world and an almost unique approach for the treatment of drug-resistant fungal infections.

STRUCTURE OF THE THESIS

This thesis was written following the guidelines provided by the University of Urbino Carlo Bo.
Every chapter is organized reproducing a paper format.
If a chapter is composed by a published paper, it is presented according to the policy of the journal.

This thesis is divided into 5 chapters.
Chapter 1 reports a published paper in authors' accepted manuscripts format integrated with the supplementary information.
Chapters 2, 3, 4 and 5 describe results which have not been published yet.
The references of the Introduction and of chapters 2, 3, 4 and 5 can be found in the section "References" at the end of the thesis.

CHAPTER 1

Published paper

Di Mambro, T., Vanzolini, T., Bruscolini, P. et al.

A new humanized antibody is effective against pathogenic fungi in vitro.

Sci Rep 11, 19500 (2021).

Received	Accepted	Published
25 June 2021	09 September 2021	30 September 2021

DOI

https://doi.org/10.1038/s41598-021-98659-5

A new humanized antibody is effective against pathogenic fungi *in vitro*

Tomas Di Mambro[ag*], Tania Vanzolini[a], Pierpaolo Bruscolini[bc], Sergio Perez-Gaviro[dbc], Emanuele Marra[e], Giuseppe Roscilli[e], Marzia Bianchi[a], Alessandra Fraternale[a,] Giuditta Fiorella Schiavano[f], Barbara Canonico[a], and Mauro Magnani[ag]

[a]: Department of Biomolecular Sciences, University of Urbino "Carlo Bo", 61029 Urbino, Italy

[b]: Instituto de Biocomputación y Física de Sistemas Complejos (BIFI), Universidad de Zaragoza, 50018 Zaragoza, Spain

[c]: Departamento de Física Teórica, Universidad de Zaragoza, 50009 Zaragoza, Spain

[d]: Centro Universitario de la Defensa, 50090 Zaragoza, Spain

[e]: Takis s.r.l, Via di Castel Romano 100, 00128 Rome, Italy

[f]: Department of Humanities, University of Urbino "Carlo Bo", 61029 Urbino, Italy

[g]: Diatheva s.r.l., Via Sant'Anna 131/135, 61030 Cartoceto, Italy

[*]: Address correspondence to Tomas Di Mambro, **tomas.dimambro@uniurb.it**, **t.dimambro@diatheva.com**

Tomas Di Mambro and Tania Vanzolini contributed equally to this work as first authors.

Tomas Di Mambro: **tomas.dimambro@uniurb.it**, **t.dimambro@diatheva.com**, Tania Vanzolini: **t.vanzolini@campus.uniurb.it**, Pierpaolo Bruscolini: **pier@unizar.es**, Sergio Perez-Gaviro: **spgaviro@unizar.es**, Emanuele Marra: **marra@takisbiotech.it**, Giuseppe Roscilli: **roscilli@takisbiotech.it**, Bianchi Marzia: **marzia.bianchi@uniurb.it**, Alessandra Fraternale: **alessandra.fraternale@uniurb.it**, Giuditta Fiorella Schiavano: **giuditta.schiavano@uniurb.it**, Barbara Canonico: **barbara.canonico@uniurb.it**, Mauro Magnani: **mauro.magnani@uniurb.it**

ABSTRACT

Invasive fungal infections mainly affect patients undergoing transplantation, surgery, neoplastic disease, immunocompromised subjects and premature infants, and cause over 1.5 million deaths every year. The most common fungi isolated in invasive diseases are *Candida spp., Cryptococcus spp., and Aspergillus spp*. and even if four classes of antifungals are available (Azoles, Echinocandins, Polyenes and Pyrimidine analogues), the side effects of drugs and fungal acquired and innate resistance represent the major hurdles to be overcome.

Monoclonal antibodies are powerful tools currently used as diagnostic and therapeutic agents in different clinical contexts but not yet developed for the treatment of invasive fungal infections. In this paper we report the development of the first humanized monoclonal antibody specific for β-1,3 glucans, a vital component of several pathogenic fungi. H5K1 has been tested on *C. auris,* one of the most urgent threats and resulted efficient both alone and in combination with Caspofungin and Amphotericin B showing an enhancement effect. Our results support further preclinical and clinical developments for the use of H5K1 in the treatment of patients in need.

INTRODUCTION

More than 300 million people have serious fungal diseases and there are over 1.5 million deaths every year. Pathogenic fungi cause life-threatening infections such as fungaemia, pneumonia, chronic pulmonary aspergillosis, bronchopulmonary aspergillosis and cryptococcosis [1, 2]. These pathologies affect mainly patients undergoing transplantation, surgery and neoplastic disease, immunocompromised subjects and premature infants. Annually are reported about 3,000,000 cases of chronic pulmonary aspergillosis, 223,100 cases of cryptococcal meningitis complicating HIV/AIDs, 700,000 cases of invasive candidiasis, 500,000 cases of *Pneumocystis jirovecii* pneumonia, 250,000 cases of invasive aspergillosis, 100,000 cases of disseminated histoplasmosis, over 10,000,000 cases of fungal asthma [3]. Of the existing five million fungal species (spp.), only 300 are considered dangerous for humans, and ~ 10% of them are recurrent. The most common fungi isolated in invasive diseases are *Candida* spp., *Cryptococcus* spp., and *Aspergillus* spp.. The mortality rate for invasive candidiasis is about 40% [4], from 20 to 30% for cryptococcosis [5] and 20% for aspergillosis. These data are referred to wealthy countries with a fully functional healthcare, while where resources are limited the death rate surpasses 50% [6].

Candidiasis is the second most frequent fungal infection [7]. *C. albicans* is the most prevalent specie but the number of infections caused by non-*albicans Candida* species (NACs) is increasing. Moreover, the massive use of antifungal drugs has determined the selection of species with an innate resistance or higher tolerance. Together, *C. albicans*, *krusei*, *parapsilosis*, *glabrata* and *tropicalis* represents the 80% of the total cases of infections [8] and 49.5% of them are caused by NACs. The different geographical diffusion determines not just the prevalence of one specie over the others but also the influences that it therefore receives, the different virulence, susceptibility, resistance, and risk factors. In line with these considerations the mortality is still high because the detection methods are often not species-specific, and the diagnoses are delayed as well as adequate antifungal therapies [9, 10, 11, 7].

In addition to all these complications, the discovery of new frightening fungal species makes the race for drugs more urgent. This is the case of *C. auris* which appeared for the first time in 2009 [12] and has spread rapidly all over the world. It commonly presents multidrug resistance to every class of antifungal drugs. The Minimum Inhibitory Concentration (MIC) of different strains for fluconazole range from 32 to ≥ 64 mg/L while for voriconazole it is 16 mg/L. Around 30% of the strains have a low susceptibility to Amphotericin B (MIC ≥ 2 mg/L) and recent studies have confirmed an increasing resistance to echinocandins (MIC ≥ 8 mg/L) [13, 14]. *C. auris* is tolerant to high salt concentrations (where it tends to assume a rudimental pseudo-hyphal form) and to high temperatures (42 °C) [15]. *C. auris* can adhere to biotic and abiotic surfaces and colonize them for weeks and months becoming a very serious problem for the invasive devices used in the hospitals [13]. Part of its danger also comes from biofilm formation and from the production of phospholipases and proteinases [16]. This profile is probably not complete, but it does provide a reasonable explanation for 60% mortality [13].

Facing these alarming numbers, more and more efforts have been spent in finding new antifungal drugs or in improving those already on the market. Yet, nowadays there are still just four leading classes of antifungal drugs: polyenes, pyrimidine analogues, azoles and echinocandins [17, 18, 19, 20]. The lack of new therapeutic agents is mostly due to the large hurdles to overcome.

Toxicity represents the first issue of current and new antifungal agents. The action spectrum of antifungal agents should be balanced, not too limited but also not too broad: effective against several species but not subject to early resistance. They should be stable and have limited off-target interactions and a known pharmacokinetic. The way of administration may be chosen preferring the patient compliance and considering hypothetical comorbidities. The choice between a complete eradication or just a control of the infection is crucial, especially in consideration of the problem of resistance and tolerance [21, 20].

Despite a lot of antifungal entities and new targets under investigation [17, 20], none of them has joined the market yet.

Among the novel therapeutic strategies, to treat fungal diseases, the employment of monoclonal antibodies (mAbs) appears as a great step forward. Monoclonal antibodies are promising therapeutic and diagnostic tools in different clinical contexts such as cancer, infective and autoimmune diseases [19]. Thanks to their high specificity for the determinant antigen, several mAbs were developed to treat fungal infections and reduce their bottlenecks but unfortunately none of them reached the clinical trials because of their murine nature (with the exception of Mycograb, [22, 23]).

Monoclonal antibody 2G8 is a successful murine mAb that showed *in vitro* activity against *Candida* spp. and *Aspergillus* spp. It showed a strong efficacy *in vivo* in a systemic mouse model of *Candida* infection and in a rat model of vaginal candidiasis [24]. The activity was verified also on *Cryptococcus neoformans*, confirming the capability to bind and inhibit the growth and capsule formation of this fungal species both *in vitro* and *in vivo* [25]. However, the murine source of this antibody precludes the possibility to use it in humans.

In this paper we reported the development and the characterization of a new humanized monoclonal antibody derived from mAb 2G8 and able to recognize β-1,3 glucans of pathogenic fungi such as *Candida* spp. These polysaccharides are vital components but hard to be reached because of the β-1,6-glucans, mannans and their glyco- and proteo-conjugates masking able to avoid the recognition by the host immune system. This new antibody has been obtained by the implementation of several different humanization procedures initially resulting in the selection of inactive candidates. By the combination of multiple approaches and after several attempts, we were finally able to select hmAb H5K1. It is stable and effective, at least *in vitro*. This antibody has also been tested in combination with several common antifungal drugs obtaining very interesting results.

RESULTS

Humanization of the murine VH and VL from mAb 2G8

The study required different humanization approaches. The first protocol resorted to the CDR-grafting method [26] and produced four sequences, with different degrees of backward mutations.

The humanization process based on the MG-score [27] generated a trajectory that stopped at 42 mutations from the initial sequence in the second protocol (IMGT definition of the CDRs), and at 35 mutations in the third protocol (Kabat definition). Since the MG-score is inferred from a database of observed human variable-region sequences but does not include any explicit biophysical information on stability against aggregation, the most human-like sequence found is not guaranteed to be also the best hit for further development. For this reason, we used CamSol [28] to study the expected solubility of the resulting trajectories and refine the choice of potential candidates to test in the laboratory, as explained in Methods ("Fig. S1" and "Fig. S2" in Supplementary Information reports the CamSol score).

Indeed, sequences starting from step 7 on both IMGT and Kabat trajectories are above the human-murine threshold score (see Methods); on the other hand, the documentation of the CamSol Intrinsic tool states that scores larger than 1 denote highly soluble regions, while scores smaller than -1 indicate poorly soluble ones. As a trade-off between the above considerations, we chose the VH sequence corresponding to sequence 19 and the VL of sequence 36 along the IMGT trajectory, and the VH of sequence 15 and VL of sequence 24 in the "Kabat" trajectory. Also, we considered the scFv corresponding to the VH and VL of sequence 19 in the IMGT case, and of sequence 15 in the Kabat case. Notice that in the latter sequences, the VHs are the same as those individually chosen before, but the VLs are different, so that we end up with only one choice of VH sequence and two choices of VL sequences for each trajectory. Table 1 reports the sequences obtained from both the humanization approaches.

Table 1. identifiers of the heavy and light chains selected for further experimental inquiry, according to the protocol described in the text. The identifier names are related to our internal naming scheme.

Heavy-chain sequence identifier	Position in trajectory ("I":IMGT; "K":Kabat; "C": CDR-grafting)	Light-chain sequence identifier	Position in trajectory ("I":IMGT; "K":Kabat; "C": CDR-grafting)
H1	C, 1	K1	C, 1
H3	C, 3	K3	C, 3
H5	I, 19	K5	I, 36
		K7	I, 19
H6	K,15	K6	K, 24
		K8	K,15

To identify the best binders of the humanized 2G8 antibody, the four different heavy chains (H_1, H_3, H_5, H_6) were combined with the seven different light chains (K_1, K_3, K_5, K_6, K_7, K_8) in a high-throughput microscale production system. The corresponding supernatants containing different antibodies were tested in ELISA assays for their binding to Laminarin.

The four supernatants with the highest binding ability (H5 K1; H5 K3; H5 K5; H5 K7) (Fig.1) were purified to confirm the previous results and, among these four antibodies (tested at 8 scalar dilutions (1:2) starting from 5 μg/ml), the combination heavy:light H5K1 was chosen because it was the best performer in the ELISA assay.

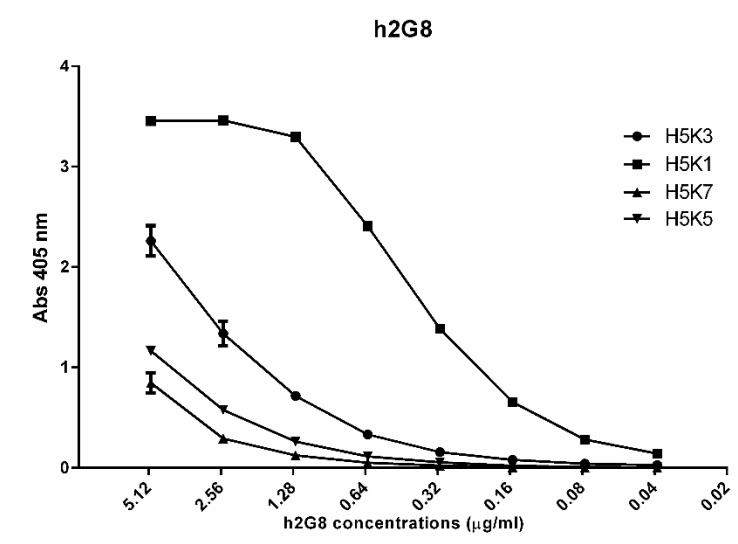

Figure 1. ELISA test performed to detect the activity of the four antibodies.

Characterization of the humanized mAb H5K1

For the antibody characterization a medium scale production was executed using the EXPICHO Expression and it was purified by affinity chromatography. The structural integrity and the absence of aggregates were confirmed by SDS-PAGE (Fig. 2) and HPLC-SEC analysis (Fig. 3).

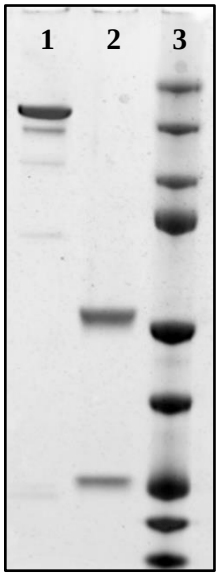

Figure 2. SDS-PAGE
1: H5K1 not reduced,
2: H5K1 reduced,
3: Marker.
Full-length blot is presented in Supplementary Figure 2.

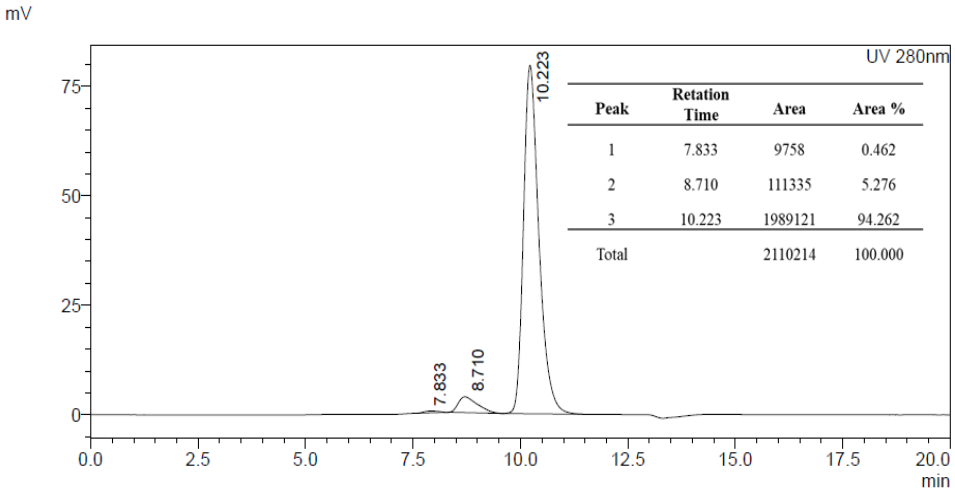

Figure 3. HPLC-SEC analysis of H5K1

The purified mAb H5K1 was tested in ELISA first using laminarin as a target. Fig. 4A shows the activity of the humanized H5K1 against laminarin compared to the murine 2G8. The IC_{50} values of the humanized and murine mAbs estimated from these data were respectively 0.06 and 0.120 µg/ml. This data, together with the predictive ability of the test performance of the interpolated ROC curves (Fig. 4B), their AUCs (0.85 for H5K1 and 0.77 for the murine 2G8) and the Kd evaluated with a competitive ELISA ($3\text{-}5x10^{-10}$ M mean 4 with n=4) support the superiority of the humanized antibody compared to the original murine one. In addition, in order to check the specificity, H5K1 was tested also with ELISA whose coating were respectively mannan, chitin and β-1,6-glucans extracted from *C. albicans* cells (Fig. 4C, D, E). It demonstrated to bind weakly chitin and β-1,6-glucans and only at higher concentrations while for what concerns mannan, H5K1 seems to bind but with an IC_{50} almost 3.5-fold higher than IC_{50} with laminarin (0.205 µg/ml). To further investigate the specific binding of H5K1 to β-1,3-glucans a competitive assay was performed through immunofluorescence. Fig. S3 in Supplementary Information reports a progressive decrease of H5K1 binding to *C. auris* cells with the increase of laminarin:H5K1 ratio.

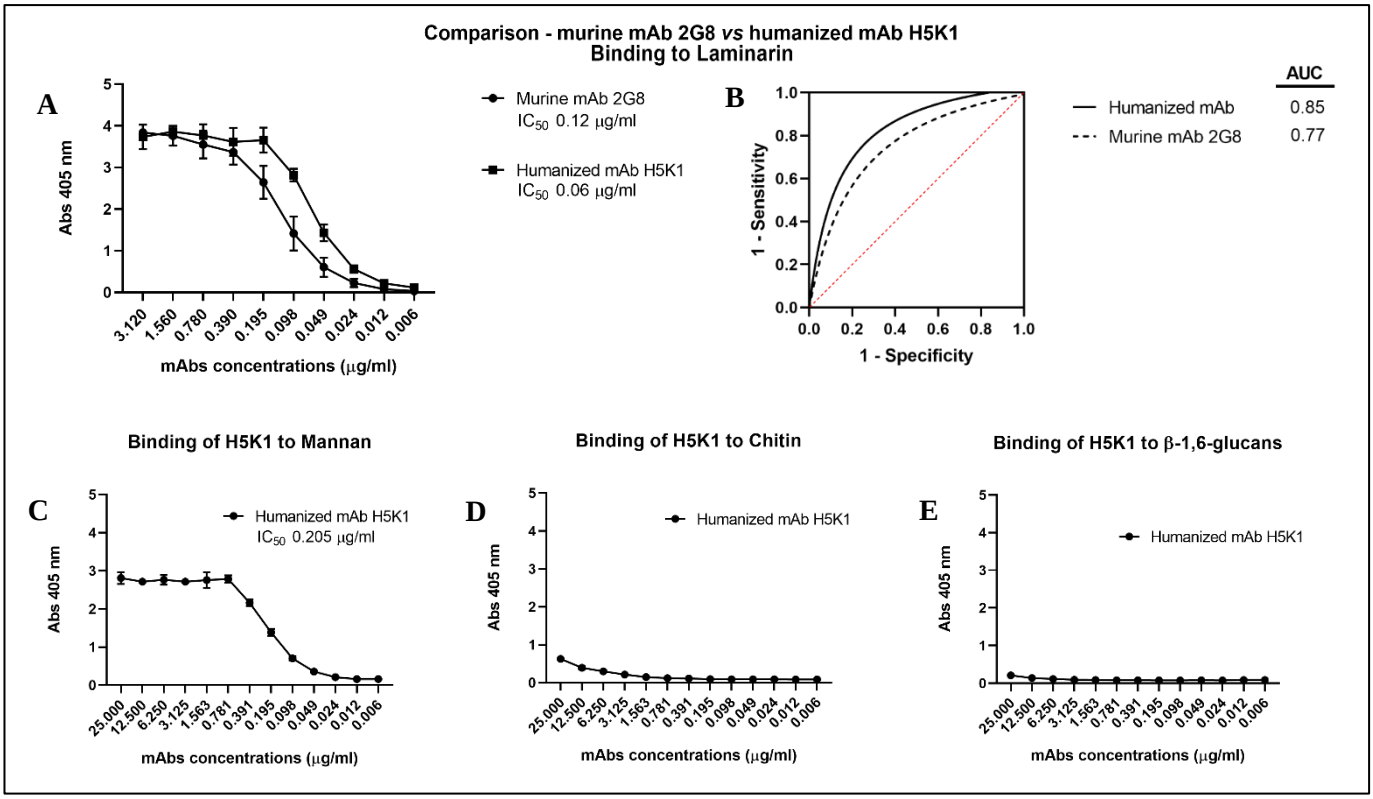

Figure 4. Binding to laminarin: comparison between the murine mAb 2G8 and the humanized H5K1 through ELISA assay (A) and the interpolated ROC curves of the ELISA assays' mean (B).
Binding to the other cell wall components: mannan (C), chitin (D) and β-1,6-glucans (E).

Flow cytometry and immunofluorescence

Figure 5 A, enables us to quantify the brilliance/efficiency of the mAb, placing a marker defining the area of positivity for the molecule investigated (histogram referred to hmAb treatment). As highlighted, almost 100% of events express the antigen, however the net expression was precisely defined by Mean Fluorescence Intensities (MFI) values, taking into account the MFI values of hmAb 2G8 (blu histogram – MFI: 35932) by the ratio with the related MFI from FITC-conjugated secondary Ab (red histogram – MFI: 219) the fold of increase is 164, if compared to controls (Fig. 5 B). Several studies in murine models of candidemia using *C. albicans* showed increased representation of β-glucan and chitin in the cell wall during infection and drug treatment [29]. Although similar detailed studies are not yet available for *Candida auris*, the cell wall remains dynamic and can alter its structure depending on the environment and carbon source the fungi encounter, as well as in response to cell wall stress [30]. Flow cytometric (Fig. 5) and immunofluorescence analyses show the ability of the H5K1 to recognize and bind β-1,3-glucans on the surface of *C. auris* and highlight that hmAb is able to trace *C. auris* at a single cell level (without aggregation of fungal cells by the antibody presence; see Fig. S4 in Supplementary Information), independently from the environment, following dynamic fluctuations of cell wall, as demonstrated by the histograms (that reveal different MFI values, but clearly define more than 97% of the sample). Moreover, apart from *C. auris*, H5K1 revealed to be able to bind also other *Candida* species such as *Candida albicans* both in hyphal and yeast form (see also S5 in Supplementary Information), and *Candida glabrata* (clinical isolate), but also *Aspergillus fumigatus* and *Fusarium solani* conidia (clinical isolates) (Fig. 6, Vid. 1 A-B).

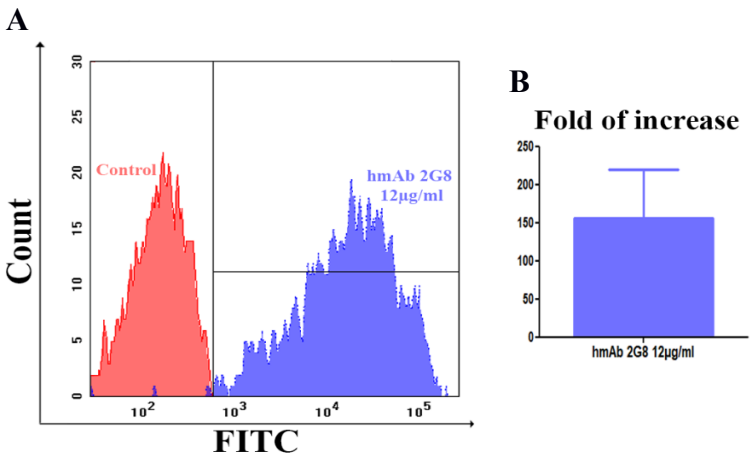

Figure 5. (A) Binding analysis by flow cytometry. Overlays of red histogram (from control sample) and blue histogram (from hmAb 2G8-labelled sample). (B) MFI fold of increase between the sample and the control.

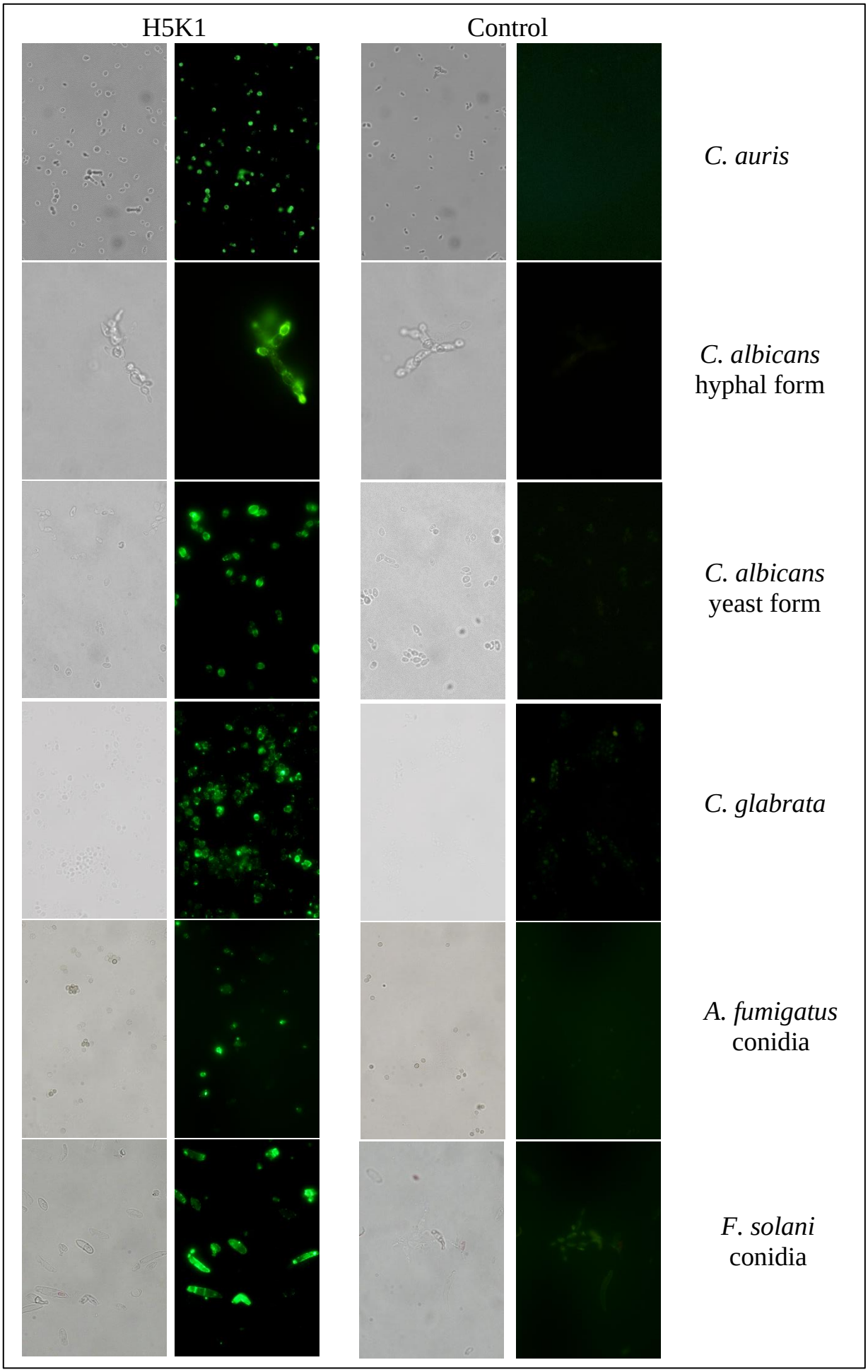

Figure 6. Binding analysis by means of immunofluorescence technique. Green fluorescence and bright-field images.

Growth inhibition assay and adhesion assay

From the CFU counts, it appears that H5K1 provides a statistically significant effect on the inhibition of the *C. auris* cell growth at all the doses tested (Fig. 7 A) ranging over 70% for 250 and 100 µg/ml and over 60% for 50 µg/ml and a statistically significant reduction in fungal adhesion to mammalian cells of 51.5% (Fig. 7 B).

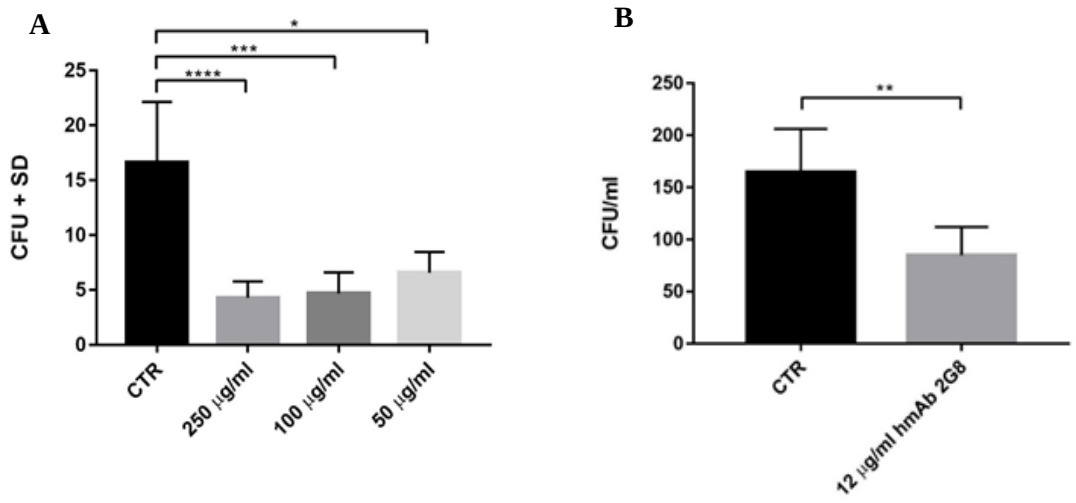

Figure 7. A) growth inhibition assay. B) adhesion assay. *p<0.05, **p<0.01, ***p<0.001, ****p<0.0001

Phagocytosis assay

Macrophages protect the body from damage and disease by targeting antibody-opsonized cells for phagocytosis. Contour plots FITC vs LTDR (Fig. 8 A), illustrates the applied phagocytosis assay. In particular, LTDR labels Lysosomes of human macrophages, whereas FITC is the fluorescence used to trace *Candida auris*. The test was carried out after 15, 30 and 180 minutes from *Candida*/macrophages interaction, in a 1:1 ratio. Upper contour plots show the experiment related to *C. auris* not pre-treated with the antibody, whereas the bottom contour plots depict the experiment on *Candida* labelled by the unconjugated antibody. Briefly, red events represent not engulfing macrophages, blu events represent *Candida*-engulfing macrophages, and green events the residual free *Candida* in the samples. Results are statistically reported in scattergrams (Fig. 8 B). As it is known, cooperative binding of antibody Fc domains to macrophage FcγR receptors triggers phagocytic cup formation in a process of adhesion and eventually internalization with phagosome closure. Scatter grams highlight a higher percentage of engulfing macrophages (Fig. 8 B) for all the time points investigated, after labelling *Candida auris* with the antibody. In fact, opsonization of *C. auris* may lead to additional FcγRI binding, increased adherence and internalization, and enhanced phagocytosis. This cascade of events in antibody labelled samples is confirmed also by residual *Candida auris* which undergoes a reduction at each time point, with the best result of more than half reduction after 180 minutes (Fig. 8 C). This highlights that the H5K1 immunomodulatory effects are not restricted to the percentage of actively phagocyting macrophages. Finally, as last consideration, in hmAb-pre-treated samples, macrophages seem more efficient, as demonstrated also by the functionality of their lysosomes (Fig. 8 D) in fact, it is known, that induced damages to macrophage lysosome crucially contribute to fungal virulence [50].

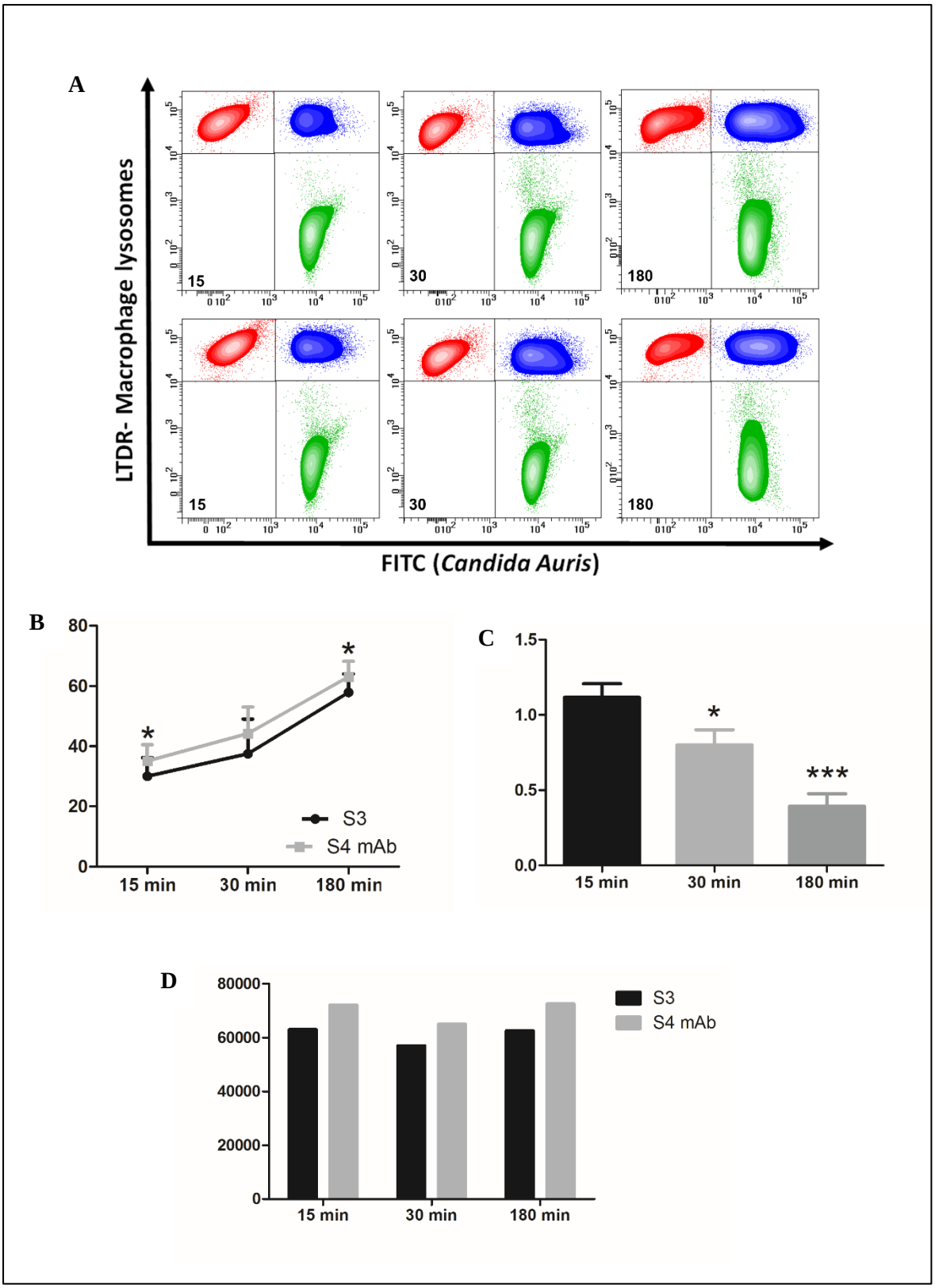

Figure 8. A) FITC vs LTDR at 15, 30 and 180 minutes; in the upper plots *C. auris* cells weren't pre-treated with the antibody while in the lower plots *C. auris* cells were pre-treated with H5K1. B) Percentage of phagocyting macrophages. C) Fold of decrease of residual *Candida auris* after treatment with the antibody. D) Lysosome function.

Minimal Inhibitory Concentration (MIC) assays

Figure 9 shows the results of MIC assays obtained by testing antifungals caspofungin (CAS) and amphotericin B (AMB) alone and in combination with hmAb H5K1 against *C. auris*. With the term MIC50 we refer to the lowest concentration that inhibits the 50% of the growth compared to drug-free control and with MIC90, the lowest concentration that inhibits the 90% of the growth compared to drug-free control. After 24 hours (Fig. 9 A) the MIC50 (red line) breakpoints of CAS alone and in combination with H5K1 are found at 0.0625 µg/ml with little dependence on H5K1 concentration. On the contrary at 48 hours (Fig. 9 B), the action of H5K1 is more pronounced, and MIC50 is established at 0.25 µg/ml for CAS alone, while at 0.125 µg/ml when in combination with the antibody. This corresponds to a reduction of 1 dilution of CAS concentration (from 0.25 to 0.125 µg/ml). CAS and the humanized mAb are assumed as synergic by definition [31, 32]. For AMB, at 24 hours (Fig. 9 C), the drug alone has a MIC50 (red line) and MIC90 (green line) at 0.5 µg/ml whereas, with 2.5 µg/ml of H5K1, MIC50 and MIC90 are respectively at 0.125 µg/ml and 0.25 µg/ml. Notably with 25 and 250 µg/ml of H5K1, MIC50 shifts at 0.0625 and MIC90 at 0.125 µg/ml. At 48 hours (Fig. 9 D), AMB alone has MIC50 and MIC90 at 1 µg/ml, while with 2.5 µg/ml of hmAb, MIC50 decreases to 0.5 µg/ml. The combination with 25 µg/ml of hmAb fixes MIC50 and MIC90 together at 0.25 µg/ml while with 250 µg/ml of the humanized mAb, MIC90 is at 0.25 µg/ml and MIC50 at 0.125 µg/ml. In Tables 2,3,4 and 5 are reported the percentage of inhibition at 24 and 48 h.

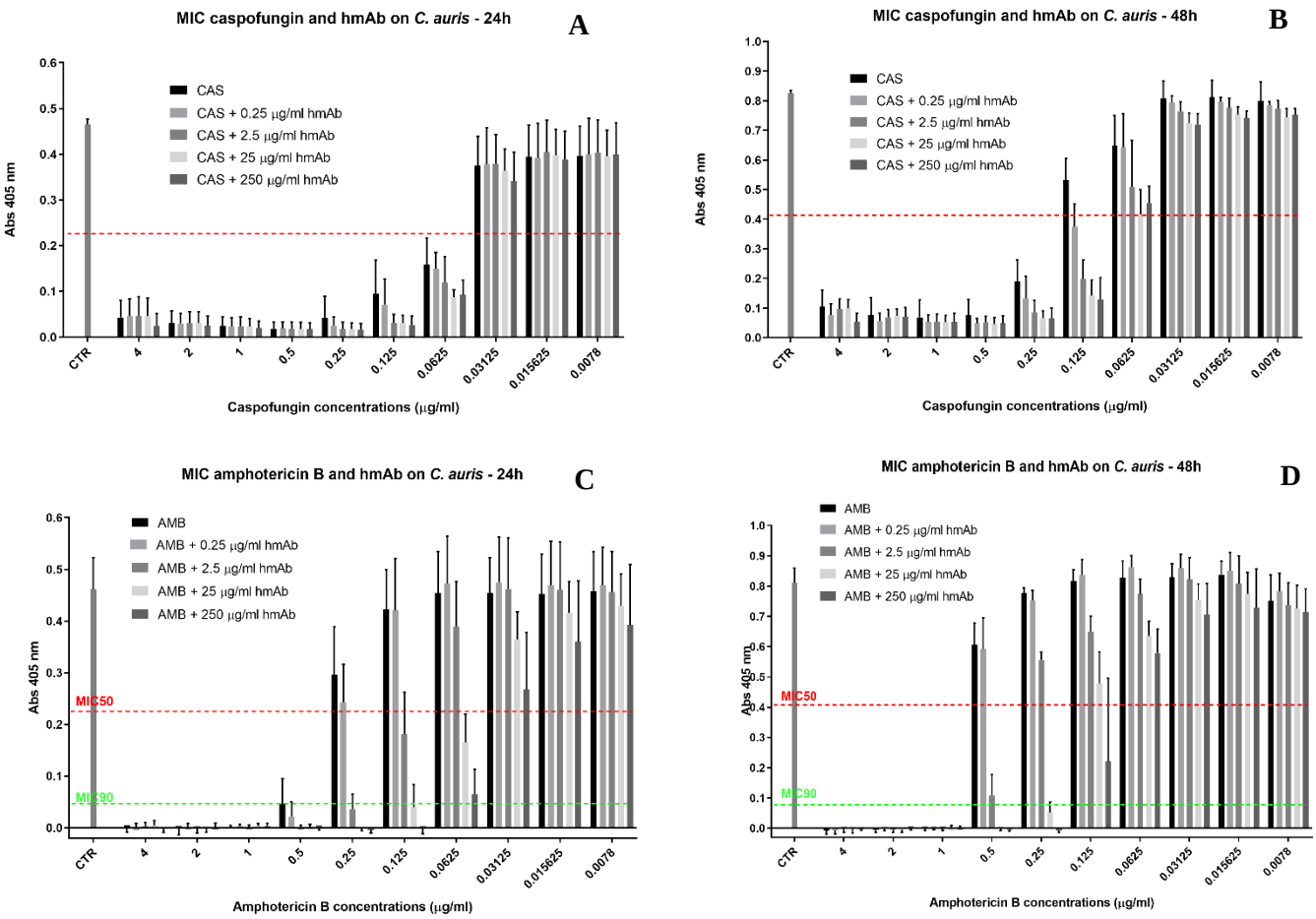

Figure 9. Figures 8A and 8B, MIC assays of caspofungin alone and in combination with different concentrations of humanized H5K1 at 24 and 48 hours. Figures 8C and 8D, MIC assays of amphotericin B in combination with different concentrations of humanized H5K1 at 24 and 48 hours.

Table 2. Percentage of growth inhibition at 24 h of CAS and CAS in combination with H5K1. The MIC50 breakpoints are marked with ∗.

Drug µg/ml	CAS	CAS in combination with:			
		0.25 µg/ml H5K1	2.5 µg/ml H5K1	25 µg/ml H5K1	250 µg/ml H5K1
4	90.3	89.7	89.6	89.6	94.5
2	93.1	93.3	93.1	93.0	94.2
1	94.5	94.7	94.6	94.8	95.7
0.5	95.8	95.7	95.9	95.8	96.1
0.25	90.4	94.4	96.0	95.8	96.2
0.125	79.0	94.0	93.1	93.1	94.0
0.0625	∗68.1	∗69.1	∗77.1	∗80.4	∗79.3
0.03125	16.5	15.6	15.4	18.9	23.8
0.0156	11.9	12.6	9.8	11.3	13.3
0.0078	11.5	11.0	9.9	11.7	10.8

Table 3. Percentage of growth inhibition at 48 h of CAS and CAS in combination with H5K1. The MIC50 breakpoints are marked with ∗

Drug µg/ml	CAS	CAS in combination with:			
		0.25 µg/ml H5K1	2.5 µg/ml H5K1	25 µg/ml H5K1	250 µg/ml H5K1
4	89.6	90.8	88.3	88	93.4
2	93	93.2	91.7	91.1	91.4
1	93.9	93.5	93.5	93.7	93.6
0.5	93	94.1	93.7	94.4	94.1
0.25	∗79.1	86.7	89.6	92	92
0.125	37.6	∗54.6	∗76	∗82.8	∗84.5
0.0625	23.7	22.1	38.3	49.6	45.1
0.03125	4.4	3.8	7.5	12.3	12.8
0.0156	3.8	3.6	5.8	8.9	10.3
0.0078	5.3	4.9	6.3	10	8.8

Table 4. Percentage of growth inhibition at 24 h of AMB and AMB in combination with H5K1. The MIC50 breakpoints are marked with ∗. The MIC90 breakpoints are marked with †.

Drug µg/ml	AMB	AMB in combination with:			
		0.25 µg/ml H5K1	2.5 µg/ml H5K1	25 µg/ml H5K1	250 µg/ml H5K1
4	98.8	99.8	98	97.8	98.7
2	99.8	99.4	99.8	99.8	99.1
1	100	99.8	100	100	99.8
0.5	∗†90.7	∗†95.2	100	100	100
0.25	35.1	46.6	†91.7	99.6	100
0.125	7.2	8.3	∗60.4	†91.3	†100
0.0625	0	0	13.5	∗62.6	∗84.8
0.03125	1.1	0	0	20.7	41.8
0.0156	1.8	0	0	9.6	21.6
0.0078	0.5	0	0	6.5	15

Table 5. Percentage of growth inhibition at 48 h of AMB and AMB in combination with H5K1. The MIC50 breakpoints are marked with ∗. The MIC90 breakpoints are marked with †.

Drug µg/ml	AMB	AMB in combination with:			
		0.25 µg/ml H5K1	2.5 µg/ml H5K1	25 µg/ml H5K1	250 µg/ml H5K1
4	100	100	100	100	100
2	100	100	100	100	100
1	∗†100	∗†100	†100	100	100
0.5	25.5	27.2	∗86.7	100	100
0.25	4.4	7.3	31.6	∗†93.5	†100
0.125	0	0	20	41.1	∗72.8
0.0625	0	0	4.9	21.7	28.7
0.03125	0	0	0	7.2	13
0.0156	0	0	0.6	4.7	10.4
0.0078	7.6	3.7	9.1	10.6	12

Time-kill curve assay

A time-kill curve based on the data from MIC assays was elaborated to evaluate how the H5K1 combined with CAS and AMB could improve their basal activity on *C. auris* (Fig. 10). At 24 h and 48 h, when at 0.25 and 0.125 µg/ml CAS efficiency starts decreasing (Fig. 10 A), the presence of hmAb ameliorated the drug efficiency. In particular, the combination of 0.25 µg/ml CAS + 250 µg/ml H5K1 maintained a constant fungistatic trend all over time, while the combination with 0.125 µg/ml CAS resulted in a recovery slower than with CAS alone (Fig. 10 B). The combination of CAS 0.25 µg/ml and H5K1 ensures more than 1log difference both at 24 and 48 hours and the combination with 0.125 µg/ml shows more than 1log difference at 24 hours and more than half log at 48 hours as reported in Table 6. Coming to AMB, we observe that even if it is a fungicidal, its efficiency alone starts decreasing at doses lower than 0.5 µg/ml and it is visible only after 24 h (Fig. 10 C). The presence of H5K1 prompts for an earlier efficacy already at 6 hours as reported in Table 7. Moreover, the combination shows a better effect with almost every concentration of AMB than the drug alone, in terms of cells revival with a reduction still ≥3 log at 24 h with AMB 0.25 µg/ml (Fig. 10 D). According to the standardized method [33], the synergic effect between two agents is revealed with a difference ≥2 log in their respective growth decreases after 24 hours. The strong synergy between AMB and H5K1 is evident from data shown in Table 8.

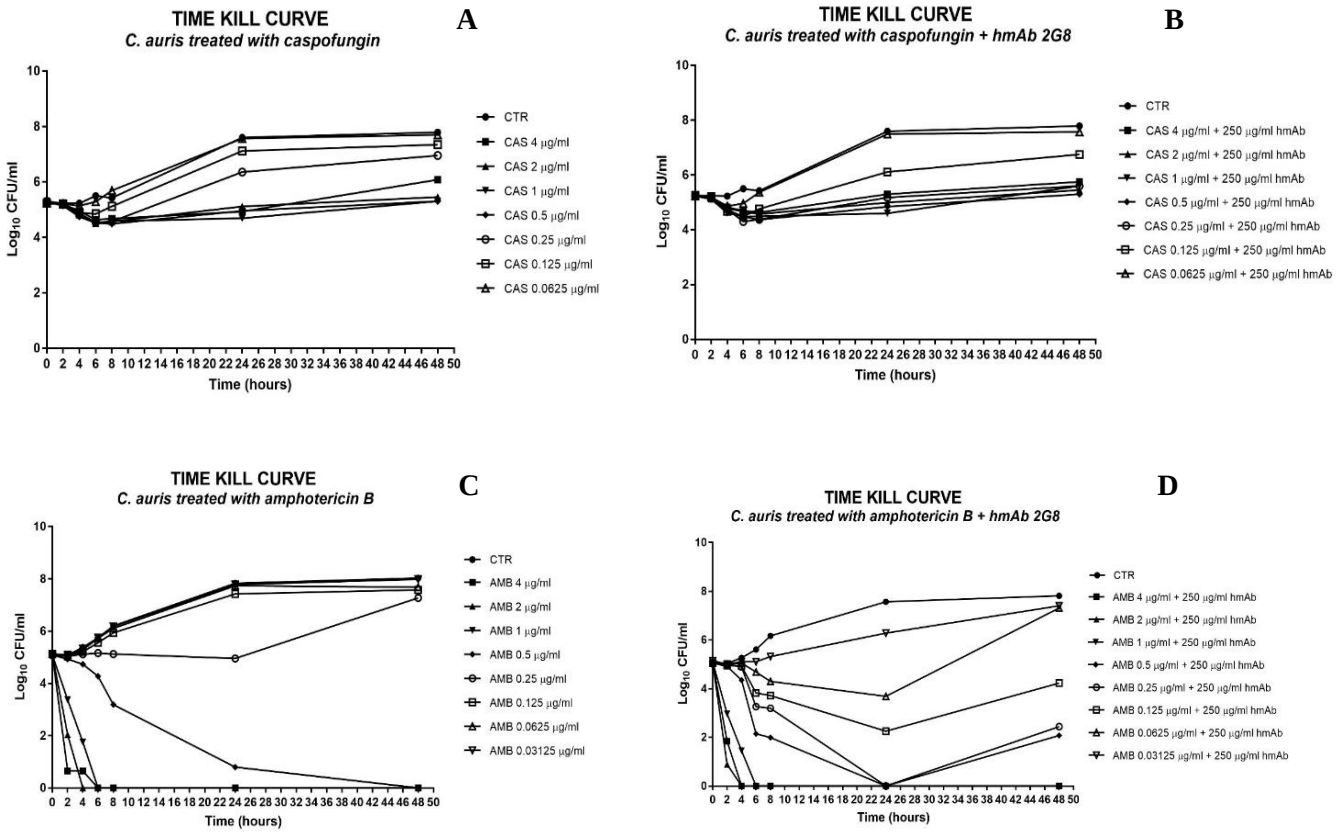

Figure 10. Time-kill curve of caspofungin (A and B) and amphotericin B (C and D) alone and in combination with H5K1

Table 6. Δlog of the respective samples with the starting inoculum as evaluation of hmAb contribution in combination treatment**.**

	24 h	48 h
CAS 0.25 µg/ml	-1.11	-1.71
CAS 0.25 µg/ml + 250 µg/ml H5K1	-0.02	-0.46
CAS 0.125 µg/ml	-1.88	-2.10
CAS 0.125 µg/ml + 250 µg/ml H5K1	-0.87	-1.51

Table 7. Δlog of the samples with the starting inoculum. The fungistatic effect is in white and the fungicidal in grey color.

	0 h	**2 h**	**4 h**	**6 h**	**8 h**	**24 h**	**48 h**
AMB 4 µg/ml	0.06	≥3Log	≥3Log	≥3Log	≥3Log	≥3Log	≥3Log
AMB 4 µg+250 µg/ml H5K1	0.08	≥3Log	≥3Log	≥3Log	≥3Log	≥3Log	≥3Log
AMB 2 µg/ml	0.05	≥3Log	≥3Log	≥3Log	≥3Log	≥3Log	≥3Log
AMB 2 µg+250 µg/ml H5K1	0.10	≥3Log	≥3Log	≥3Log	≥3Log	≥3Log	≥3Log
AMB 1 µg/ml	0.05	1.77	≥3Log	≥3Log	≥3Log	≥3Log	≥3Log
AMB 1 µg+250 µg/ml H5K1	0.05	2.16	≥3Log	≥3Log	≥3Log	≥3Log	≥3Log
AMB 0.5 µg/ml	0.05	0.21	0.41	0.86	1.95	≥3Log	≥3Log
AMB 0.5 µg+250 µg/ml H5K1	0.09	0.22	0.78	≥3Log	≥3Log	≥3Log	≥3Log
AMB 0.25 µg/ml	0.07	0.10	0.02	-0.02	0.02	0.19	-2.13
AMB 0.25 µg+250 µg/ml H5K1	0.11	0.13	0.25	1.88	1.95	≥3Log	2.66
AMB 0.125 µg/ml	0.01	0.11	-0.07	-0.42	-0.80	-2.28	-2.44
AMB 0.125 µg+250 µg/ml H5K1	0.09	0.20	0.21	1.31	1.42	2.88	0.91
AMB 0.0625 µg/ml	0	0.07	-0.14	-0.59	-0.97	-2.59	-2.57
AMB 0.0625 µg+250 µg/ml H5K1	0.09	0.15	0.09	0.46	0.84	1.45	-2.17
AMB 0.03125 µg/ml	0.01	0.05	-0.19	-0.62	-1.04	-2.65	-2.85
AMB 0.03125 µg+250 µg/ml H5K1	0.07	0.13	0.01	0.03	-0.18	-1.14	-2.26

Table 8. Δlog between amphotericin B effect and the corresponding combination with H5K1.

AMB concentrations	**Δlog: AMB – AMB + 250 µg/ml H5K1**	
	24 h	**48 h**
0.25 µg/ml	4.95	4.79
0.125 µg/ml	5.16	3.35
0.0625 µg/ml	4.04	0.4

DISCUSSION

Invasive fungal infections affect mainly patients undergoing transplantation, surgery, neoplastic disease, immunocompromised subjects and premature infants and cause over 1.5 million deaths every year. Their treatment is challenging, with drugs' toxicity and acquired and innate fungal resistance representing the major hurdles to overcome [20].

Monoclonal antibodies are powerful tools currently used as diagnostic and therapeutic agents in different clinical contexts. With over 60 monoclonal antibodies in late-stage clinical studies and an estimated global market of $125 billion, these biological drugs are the main candidates of the future medicine as the current circumstance of Covid-19 pandemic has taught us [34, 35, 36, 37, 38]. The humanized mAb H5K1 presented in this work and derived from the murine mAb 2G8 [24, 25], is able to recognize and bind selectively β-1,3-glucans in the fungal wall. Several key points emerging from our findings can be highlighted:

i) First of all, from the methodological point of view, this study represents the first experimental test of the humanization protocol proposed in [27]. Our findings suggest that the approach is not perfect and there is margin for further improvement: the overall best sequence scores poorly in CamSol solubility score (so we suspect that it is aggregation-prone, even though we have not tested it experimentally); moreover, the sequence H5K1, that we have finally chosen for further analysis, being the best performer in ELISA assay, is a combination of a heavy chain obtained by MG-optimization, and a light chain obtained by CDR-grafting. On the other hand, all the four best-performing sequencies in the ELISA assay have the heavy chain found by MG-optimization, and the third and fourth of them also have the light chain found by this protocol; therefore, the MG approach, especially when combined with Camsol for further refinement, appears as an interesting tool to identify candidate hits for humanization.

ii) Second, the humanization process has not changed the capability of the mAb to bind the antigen as shown in the ELISA assay. Furthermore, experimental outputs revealed that H5K1 performs better than the original murine 2G8. The binding activity is confirmed also in *in vitro* assays on *C. auris, C. albicans, C. glabrata* cells and on *Aspergillus fumigatus and Fusarium solani* conidia, as demonstrated by microscopy and flow cytometry analyses. Intrigued by those promising results, we assessed whether the binding of hmAb could affect cells growth and adhesion, as it is the case for the murine mAb [39]. As reported in the results section, in growth inhibition and adhesion assays mAb H5K1 displayed an activity which confirms the positive effects already obtained with the murine 2G8.

iii) Third, the opsonization activity of H5K1 to *C. auris* cells determines an improvement of the engulfment by macrophages which result more efficient as shown by their active lysosomes compared to the controls and from the residual *C. auris* that decreases significantly with the passing of time.

iv) Finally, we found that the co-administration of our antibody with some commercially available antifungal drugs could provide an important benefit. FLC, CAS and AMB were chosen as the best representatives of their

classes and tested with and without mAb H5K1 on *C. auris*. While with FLC we obtained just a little difference upon adding the antibody (data not shown), in combination with CAS and AMB, hmAb played an essential role in terms of concentration required to reach the desired effect and time of action. Well known are the side effects and the toxicity of AMB especially at high concentrations [40], hence the possibility to reduce the therapeutic doses is a hopeful perspective, especially for patients' compliance and treatment adherence. CAS is more tolerated and safer, but some studies highlighted negative drug-drug interactions and, even worse, CAS (as well as other antifungals) are blamed to act as selectors of resistant species when used at too low concentrations [41].

In the MIC assay the combination mAb H5K1-CAS, synergic by definition, brings to a 1:2 dilution concentration shift at 48 hours, which was also found in the time kill curve, where the hmAb makes the fungistatic effect still effective and preserved at very low concentrations all over time. When combined with amphotericin B, the hmAb had a more incisive impact both at 24 and 48 hours, but time kill curve was essential to define the presence of a synergism. The combination performs always better than the drug alone and the fungicidal effect is visible earlier and at concentrations at which amphotericin B alone has already lost it. We believe there is an important contribution of our hmAb even at earlier time points and at higher drug concentrations, although we cannot detect this effect, because of the heavy fungistatic and fungicidal effects of drugs alone against a non-resistant strain.

Notably, the combinations could have a fundamental role in the treatment of resistant species where the drugs alone have little or no effects even at high doses. Further studies are needed to test this hypothesis, as well as to check the action on other fungal strains and *in vivo*.

In view of the results obtained, we are optimistic that our new humanized mAb H5K1 could be a substantial player in the fight against fungal infections since it has all the qualities to reach clinical trials both alone and in combination with other drugs.

MATERIALS AND METHODS

Cell lines

In our studies we used *C. auris* (strain DMS 21092) as fungal model, *Candida albicans* (ATCC 10231), clinical isolates of *Candida glabrata*, *Aspergillus fumigatus* and *Fusarium solani*, cervical carcinoma HeLa cells (ATCC) and CHO cells (ExpiCHO-S Cells, Thermo Fisher Scientific).

Humanization process

An analysis of murine 2G8 VH and VL against IgBlastTool [42] murine databases (IMGT mouse V genes, IMGT mouse D genes, IMGT mouse J genes) brought to the substitution of the non-homologous amino acids to decrease the value of the *instability index* calculated with ExPasy [43]. The modified murine VH and VL underwent CDR-grafting following two methodologies: the first analysed the whole VH and VL sequences, the second just the Framework Regions (FRW). The latter method produced the VH and VL sequences with the lowest instability index and for this reason they were compared with the most similar ones in PDB, and the non-homologous amino acids were substituted. Some amino acids were back mutated to the murine ones.

The other two protocols use the MG-score and the humanization approach introduced in [27], resorting to statistical modelling of the variable regions of human antibody sequences: VH and VL regions were aligned according to the AHo scheme and juxtaposed, to yield a unique VH-VL sequence of length 298 amino acids (including gaps); then, the two protocols just differ in the choice of the CDR regions to be kept fixed: in one case, they coincided with residues chosen for the CDR-grafting protocol above, while in the second case, CDR residues were those corresponding to the Kabat numbering scheme. In Figure 11 we show a schematic representation of both the CDR-grafting and MGM humanization process. This approach, that includes residue-residue correlations both within and between heavy and light chains, strongly depends on which residues are kept fixed, as belonging to CDR regions: starting from the murine sequence, the method implies mutating one residue at a time, choosing the mutation (at any site and to any amino-acid) that yields the greatest increase in the MG-score. This method does not guarantee to reach the highest score (i.e. the most humanlike sequence with the given CDRs), but it finds the local maximum closest to the initial murine sequence, with the smallest number of mutations (i.e. the shortest path to it). The trajectories in sequence space thus produced contain several sequences that are above the human-murine threshold [27] and thus constitute potential hits. These sequences were further analysed with CamSol Intrinsic Server [28, 44], to check explicitly their tendency towards aggregation. Since CamSol uses local sequence information for prediction, the latter could be affected by the presence of the artificial contiguity between the C-term of the VH chain and the N-term of the VL chain in the alignment used in the design step above: for this reason, we analysed separately the VH and VL chains with CamSol, and also the scFv constructs, with a common linker between the two chains. This allows to pick, along the Kabat trajectory, separately the VH and VL sequences that have the least tendency towards aggregation, among those that score above the murine/human threshold, and also, the scFv that best copes with

the requirements of having a good MG-score and a good solubility; the same was done for the other protocol, with the IMGT trajectory.

Having observed [27] that the correlations between VH and VL are quite smaller than correlations within VH and VL regions, we consider, for further experimental testing, the VH-VL combinations corresponding to the scFv sequences, and also the constructs obtained by combining in all possible ways the 2 VH and VL sequences thus obtained, together with those obtained with the CDR-grafting protocol. In the end, excluding repetitions, a total of 28 combinations of VH and VL were used to develop new full-length antibodies.

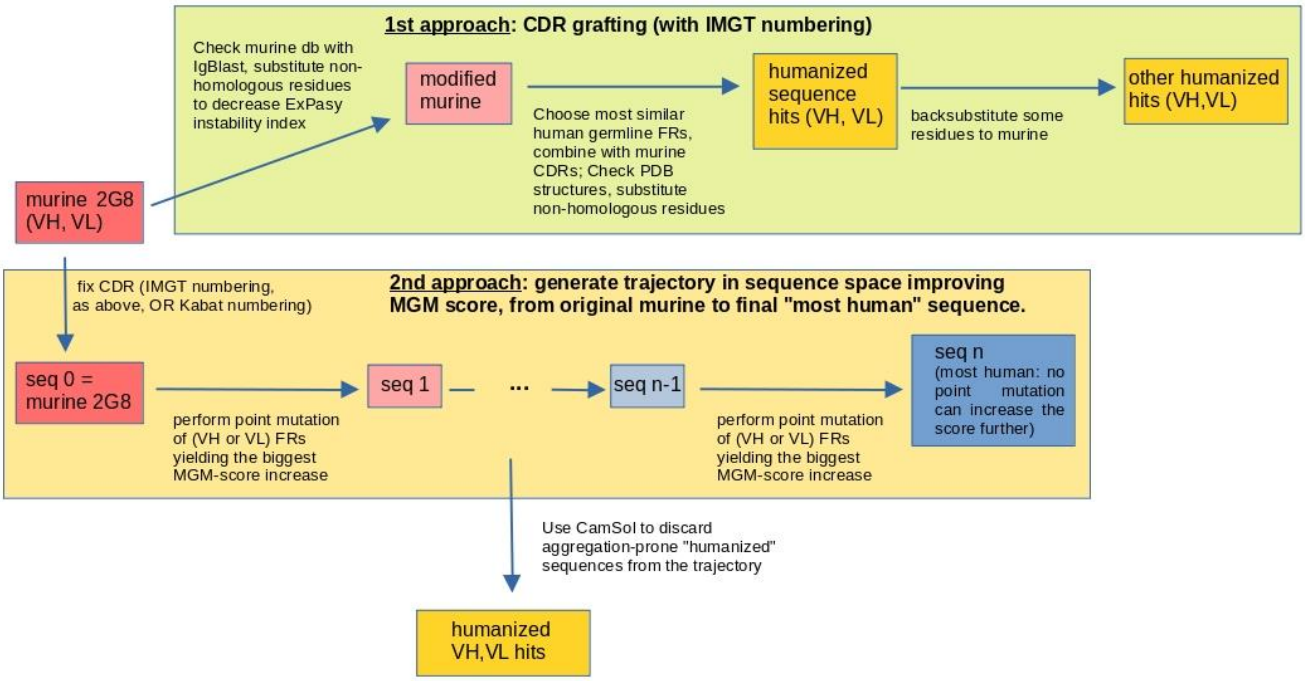

Figure 11. Flowchart of the humanization process: humanized sequences (in gold) are obtained according to either CDR grafting (above) or iterated MGM-score-based mutations (below); the latter approach yields a trajectory of increasingly human sequences from the original, murine one (red) to the final sequence, that cannot be further improved under point mutations (blue). CamSol Intrinsic server is used to select, among the sequence on this trajectory, the humanized hits as the ones that are sufficiently human and sufficiently soluble.

Antibody production

Recombinant antibodies were constructed in vitro using recombinant DNA technology. Antibody heavy and light variable fragments were synthesized based on sequences information obtained after humanization. They were then cloned into vectors for the expression in eukaryotic system and containing the human IgG1 heavy chain or the kappa light chain constant regions to create full length heavy and light chain constructs. Full length IgG1 heavy and kappa light chain genes were co-transfected in a high-throughput microscale system. 3 ml of CHO-S cells culture was transfected using the EXPICHO Expression system (Thermo Scientific™) according to the information supplied by the manufacturer. After one week, supernatants were collected for further analysis. The antibody production on a medium scale was carried out with the same expression system.

Antibody purification

Supernatants containing antibodies were centrifuged, filtered 0.22 μm to remove cells and debris and batch purified by affinity chromatography using TOYOPEARL AF-rProtein A HC-650F resin (Tosoh Bioscience LLC).

Antibodies were eluted with Buffer Citrate 0.1 M pH 3, neutralized with an alkaline solution and dialyzed in PBS1X with slide-A-Lyzer (Thermo Scientific™). Purity of the antibody was checked by SDS-PAGE analysis that was performed under reducing/non-reducing conditions according to the standard method. Endotoxin levels were evaluated by Pierce™ LAL Chromogenic Endotoxin Quantitation Kit (Thermo Scientific™) and the presence of aggregates analysed through HPLC-SEC analysis.

Mannan, chitin and β-1,6-glucans extraction

From an overnight inoculum of *C. albicans*, the cells were extracted with 3% NaOH for 1 hour at 80°C. The suspension was centrifuged; the alkali-extracted supernatant was used for the precipitation of mannan through Fehling's reaction while the pellet was digested overnight with Kitalase lytic enzyme (FUJIFILM Wako Pure Chemical Corporation) containing β-1,3-glucanase but not chitinase or β-1,6-glucanase. The digested product was centrifuged: the supernatant composed mainly by the remaining β-1,6-glucans was dialysed against 10 mM Tris-HCl (pH 7.5) to remove digested β-1,3-glucanas while the precipitate representing chitin was solubilized. Phenol-sulfuric acid method was used for the polysaccharides' quantification [49].

Competitive binding in immunofluorescence

12 μg/ml of H5K1 was added to different concentrations of laminarin in PBS 3% BSA in order to reach the following laminarin:H5K1 ratios: 40:1, 16:1, 4:1, 1:1 and 0:1. The solutions were left react at 37°C for one hour then were put in contact with $3.0x10^6$ *C. auris* cells coming from an overnight inoculum. After 1 hour the cells were centrifuged, washed, and marked for 1 hour with anti-human IgG FITC antibody (Abcam, ab97224) 1:150 in PBS + 3% BSA. The cells were washed before and after fixing with paraformaldehyde (Carlo Erba) 4% for 1 hour at 4 °C and finally they were resuspended in 100 μl of PBS. The samples were analysed through immunofluorescence microscope.

ELISA Assay

96-well plates were coated with 50 µg/ml laminarin (Sigma-Aldrich, L9634) or extracted mannan, chitin and β-1,6-glucans in 0.05 M carbonate buffer pH 9.6 overnight at 4 °C. Nonspecific interactions were blocked with 100 µL/well blocking solution, 3% (w/v) BSA in PBS-Tween 20 (8 g/L NaCl, 0.2 g/L KH_2PO_4, 2.9 g/L $Na_2HPO_4 \cdot 12\ H_2O$, 0.2 g/L KCl, 0.05% (v/v) Tween 20, pH 7.4) at 37 °C for 1h. The plates were then incubated with decreasing concentrations of humanized mAb 2G8 (from 3.12 µg/ml to 0.006 µg/ml, each concentration was tested in triplicate) in blocking solution for 2 h at 37 °C. At the same temperature and for the same time 100 µL Goat anti-human-HRP (Meridian Life Science, Inc., G5G16-0482) diluted 1:500 in blocking solution were poured in each well. After every single passage, the plates were washed 5 times with PBS-Tween 20. To reveal the binding, 100 µL of 5 mg-ABTS tablet (Roche Diagnostics) dissolved in 12 ml of sodium citrate 0.05 M, pH 3 and supplemented with 1:1000 dilution hydrogen peroxide (Carlo Erba) were added and after 15, 30, 45 and 60 min the absorbance at 405 nm was measured with a Microplate Reader (Bio-Rad). For the whole measuring time the plates were left in the dark. IC50 analysis of ELISA test was performed with Prism. The test was performed in triplicate.

Competitive binding in ELISA

Antigen-coated and blocked microplate was prepared as reported above in Materials and Methods ELISA assay. 0.06 µg/ml of H5K1 (concentration of IC_{50}) were left incubating for 1 h at 37 °C with serial dilutions of laminarin (from 400 to 0.000045 µg/ml) in blocking solution. Then, the serial dilution solution of laminarin and antibody were added to the plate and left for 1 hour at 37 °C. The plate was washed and 100 µL/well of Goat anti-human-HRP (Meridian Life Science, Inc., G5G16-0482) diluted 1:500 in blocking solution was added to the plate and incubated for 1 h at 37°C. After washing the binding was revealed with 100 µl/well of 5 mg-ABTS tablet (Roche Diagnostics) dissolved in 12 ml of sodium citrate 0.05 M, pH 3 and supplemented with 1:1000 dilution hydrogen peroxide (Carlo Erba). The absorbance was read at 405 nm after 15, 30, 45 and 60 min.

Flow cytometry and immunofluorescence

From an overnight inoculum, microorganism cells or conidia were washed with RPMI+MOPS (0.165 M, pH 7) and $3.0x10^6$ cells were pelleted, resuspended in Phosphate buffered saline (PBS) containing 3% (w/v) BSA (Bovine Serum Albumin Sigma Aldrich) and put in contact with 12 µg/ml of the H5K1 for 1 hour at room temperature. The cells and the conidia were washed with PBS and marked with anti-human IgG FITC antibody (Abcam, ab97224) 1:150 in PBS + 3% BSA for 1 hour. The cells and conidia were washed and fixed with paraformaldehyde (Carlo Erba) 4% in PBS 1 hour at 4 °C. After fixing and washing with PBS, the pellet was resuspended in 400 µl of PBS and splitted in two tubes. The samples of *Candida auris* were analysed respectively using flow cytometry and immunofluorescence while the others just in immunofluorescence [45]. A Flow cytometer (FACScanto II, BDBioscences, Erembodegem, Belgium), equipped with three lasers (488nm, 633nm, 405nm) was employed to collect and quantitate FITC fluorescence from different samples. Both

autofluorescence and fluorescence derived from aspecific binding of FITC-conjugated secondary Ab were quantitated by flow cytometry.

Growth Inhibition Assay

The growth inhibitory activity of H5K1 was tested as reported by Magliani [46], with some modifications. In brief, 150-250 cells of *C. auris* in 10 µl of PBS were incubated with 100 µl of hmAb at 250, 100 and 50 µg/ml (each concentration was tested in triplicate) and incubated for 18 h at 37 °C. The inhibition was evaluated by seeding the yeast on Potato Dextrose Agar (PDA) ((Sigma-Aldrich) plates. The plates were incubated at 37° C for 48 h and the inhibition was calculated by count of the CFU. The assay was performed in triplicate in three different days. [25, 39].

Adhesion assay

In order to investigate a potential protective effect of H5K1 in preventing fungal adhesion to human cells, *C. auris* cells were left adhering to a monolayer of HeLa cells together with the humanized mAb 2G8. $1.0x10^4$ cervical cancer cells HeLa were resuspended in RPMI + *10% FBS (pH 7) and plated in a 96-well plate for 2 hours at 37 °C + 5% CO_2. After incubation the cells not yet attached at the bottom of the wells were washed away with RPMI + MOPS (0.165 M, pH 7) and $1.0x10^4$ cells of *C. auris* resuspended in RPMI + MOPS (0.165 M, pH 7) were put on to reach a 1:1 ratio HeLa:yeast cells. Together with the yeast, 12 µg/ml of the humanized mAb 2G8 were added. PBS pH 7 was used in the control. The plate was left at 37 °C for 1 hour and after washing 5 times, HeLa cells were lysed with PBS 0.1% Triton X-100 pH 7 for 15 min. RT. The suspension was plated in PDA plate and incubated at 37 °C for 48 hours. This experiment has been repeated two times in triplicate [47, 39].

Monocytes preparation

Cultures of macrophages were prepared from leukocyte buffy coats obtained from healthy donors. Briefly, the peripheral blood mononuclear cells were isolated by Lymphoprep density gradient medium (Stemcell Technologies) and monocytes were separated from lymphocytes by adherence to plastic dishes. Monocytes were cultured in RPMI containing 10% foetal calf serum and 1% antibiotics at 37°C in a 5% CO_2 atmosphere for 10-12 days, at which time the monocytes had matured into macrophages and formed a monolayer.

Phagocytosis assay

From an overnight inoculum, *C. auris* cells were washed with RPMI+MOPS (0.165 M, pH 7) and labelled with 1 mg/ml Fluorescein-5-isothiocyanate (FITC, Sigma-Aldrich) in PBS for 10 minutes RT. After washing 250 µg/ml of H5K1 were left interacting for 1 hour at 37°C. Meanwhile macrophages were treated with 100 nM LysoTracker Red (Thermo Fisher Scientific, Waltham, MA, USA) for 45 minutes and washed with PBS. Yeasts and macrophages were counted in order to have a final ratio *C. auris* cells:macrophages 1:1. They were left 15, 30 and 180 minutes at 37°C and then washed and fixed with paraformaldehyde (Carlo Erba) 4% in

PBS 20 minutes at 4 °C. After washing again, the cells were scraped gently and acquired by flow cytometry. 15,000 cell events were acquired for each sample [52].

MIC assays

To evaluate the susceptibility of *C. auris* to CAS and AMB and their combination with H5K1, we followed the EUCAST antifungal MIC microdilution method [48]. Antifungal drugs were purchased from Sigma-Aldrich. CAS and AMB concentration ranges analysed were reported in EUCAST document. Those concentrations were tested alone and in combination with 0.25, 2.5, 25 and 250 µg/ml of humanized antibody. The wells with 100 µl of 2X final antifungal drugs concentration in RPMI 2% G medium were inoculated with 100 µl (1-5 x 10^5 CFU/ml) of yeast suspension of *C. auris*. The monoclonal antibody was added to the samples of yeast suspension to test the drug-antibody combination. The plates were incubated at 37 °C for 24 and 48 hours and read after incubation at 405 nm with a Microplate Reader (Bio-Rad). With the term MIC50 we consider the lowest concentration that inhibits the 50% of the growth compared to drug-free control and with MIC90, the lowest concentration that inhibits the 90% of the growth compared to drug-free control. The assays were performed three times in triplicate.

Time-kill curve assays

Based on MIC results a restricted range of drug concentration was used (4, 2, 1, 0.5, 0.25, 0.125 and 0.0625 µg/ml for caspofungin and 4, 2, 1, 0.5, 0.25, 0.125, 0.0625 and 0.03125 µg/ml for amphotericin B). In each well of a 96-well plate, 100 µl of 2X final antifungal drugs concentration in RPMI 2% G medium and 100 µl containing 1-5 x 10^5 CFU/ml of *C. auris* suspension were put together. 250 µg/ml of humanized antibody was added to see the effect of the combination. 5 mM phosphate buffer was used as control. The plates were incubated at 37 °C for 0, 2, 4, 6, 8, 24 and 48 h. The samples were spread (10-fold dilutions were used when necessary) in PDA plates and left at 37 °C for 48 hours before the CFU counting. Time-kills for strain-drug combination were performed a single time.

Statistical analysis

Data were plotted and analysed by GraphPad Prism 8 software. The statistical significance in adhesion and phagocytosis assays were assessed through a two-tailed Student's *t* test while in growth inhibition results, the statistical significance was assessed by One-way Anova test.

ACKNOWLEDGEMENTS

We gratefully thank Professor Antonio Cassone and Professor Francesco Barchiesi for their aid, support and useful suggestions. The work was partially supported by Diatheva s.r.l. P. Bruscolini acknowledges funding by MICINN (grant FIS2017-87519-P) and by DGA (E30_17R, E30_20R).

AUTHOR CONTRIBUTIONS

T.D.M. and T.V. were responsible for the experimental design, the execution of the experiments, data collection and interpretation. P.B, S.P.G. and T.D.M developed and identified the humanized monoclonal antibodies. E.M. and G.R. produced the humanized monoclonal antibodies. M.B., A.F., G.F.S and B.C. contributed to the experimental execution. All authors analyzed and discussed the results. T.D.M., T.V. and M.M wrote the article. All authors reviewed the manuscript.

COMPETING INTERESTS

T.D.M. is employees at Diatheva s.r.l., E.M. and G.R. are employees at Takis s.r.l., M.M. holds shares in Diatheva s.r.l. Both companies have interest in developing antifungal agents. All the other authors do not have any conflict of interest.

DATA AVAILABILITY

All data generated and analyzed during this study are included in this published article (and its Supplementary Information files) and available from the corresponding author on reasonable request.

REFERENCES

1. Perlin, D. S., Rautemaa-Richardson, R. & Alastruey-Izquierdo, A. The global problem of antifungal resistance: prevalence, mechanisms, and management. *Lancet Infect Dis* **17**, e383–e392 (2017).
2. Armstrong-James, D. *et al.* Immunotherapeutic approaches to treatment of fungal diseases. *Lancet Infect Dis* **17**, e393–e402 (2017).
3. Bongomin, F., Gago, S., Oladele, R. O. & Denning, D. W. Global and Multi-National Prevalence of Fungal Diseases-Estimate Precision. *J Fungi (Basel)* **3**, (2017).
4. Andes, D. R. *et al.* Impact of treatment strategy on outcomes in patients with candidemia and other forms of invasive candidiasis: a patient-level quantitative review of randomized trials. *Clin Infect Dis* **54**, 1110–1122 (2012).
5. Bratton, E. W. *et al.* Comparison and temporal trends of three groups with cryptococcosis: HIV-infected, solid organ transplant, and HIV-negative/non-transplant. *PLoS One* **7**, e43582 (2012).
6. Nyazika, T. K. *et al.* Cryptococcus neoformans population diversity and clinical outcomes of HIV-associated cryptococcal meningitis patients in Zimbabwe. *J Med Microbiol* **65**, 1281–1288 (2016).
7. Whibley, N. & Gaffen, S. L. Beyond Candida albicans: Mechanisms of immunity to non-albicans Candida species. *Cytokine* **76**, 42–52 (2015).
8. Salazar, S. B. *et al.* An Overview on Conventional and Non-Conventional Therapeutic Approaches for the Treatment of Candidiasis and Underlying Resistance Mechanisms in Clinical Strains. *J Fungi (Basel)* **6**, (2020).
9. Giacobbe, D. R. *et al.* Changes in the relative prevalence of candidaemia due to non-albicans Candida species in adult in-patients: A systematic review, meta-analysis and meta-regression. *Mycoses* **63**, 334–342 (2020).
10. Costa-de-Oliveira, S. & Rodrigues, A. G. Candida albicans Antifungal Resistance and Tolerance in Bloodstream Infections: The Triad Yeast-Host-Antifungal. *Microorganisms* **8**, (2020).
11. Dadar, M. *et al.* Candida albicans - Biology, molecular characterization, pathogenicity, and advances in diagnosis and control - An update. *Microb Pathog* **117**, 128–138 (2018).
12. Satoh, K. *et al.* Candida auris sp. nov., a novel ascomycetous yeast isolated from the external ear canal of an inpatient in a Japanese hospital. *Microbiol Immunol* **53**, 41–44 (2009).
13. Friedman, D. Z. P. & Schwartz, I. S. Emerging Fungal Infections: New Patients, New Patterns, and New Pathogens. *J Fungi (Basel)* **5**, (2019).

14. Cortegiani, A. *et al.* Epidemiology, clinical characteristics, resistance, and treatment of infections by Candida auris. *J Intensive Care* **6**, 69 (2018).

15. Rossato, L. & Colombo, A. L. Candida auris: What Have We Learned About Its Mechanisms of Pathogenicity? *Front Microbiol* **9**, 3081 (2018).

16. Short, B. *et al.* Candida auris exhibits resilient biofilm characteristics in vitro: implications for environmental persistence. *J Hosp Infect* **103**, 92–96 (2019).

17. Gintjee, T. J., Donnelley, M. A. & Thompson, G. R. Aspiring Antifungals: Review of Current Antifungal Pipeline Developments. *J Fungi (Basel)* **6**, (2020).

18. Faustino, C. & Pinheiro, L. Lipid Systems for the Delivery of Amphotericin B in Antifungal Therapy. *Pharmaceutics* **12**, (2020).

19. Di Mambro, T., Guerriero, I., Aurisicchio, L., Magnani, M. & Marra, E. The Yin and Yang of Current Antifungal Therapeutic Strategies: How Can We Harness Our Natural Defenses? *Front Pharmacol* **10**, 80 (2019).

20. Perfect, J. R. The antifungal pipeline: a reality check. *Nat Rev Drug Discov* **16**, 603–616 (2017).

21. Berman, J. & Krysan, D. J. Drug resistance and tolerance in fungi. *Nat Rev Microbiol* **18**, 319–331 (2020).

22. Matthews, R. C. *et al.* Preclinical assessment of the efficacy of mycograb, a human recombinant antibody against fungal HSP90. *Antimicrob Agents Chemother* **47**, 2208–2216 (2003).

23. Bugli, F. *et al.* Human monoclonal antibody-based therapy in the treatment of invasive candidiasis. *Clin Dev Immunol* **2013**, 403121 (2013).

24. Torosantucci, A. *et al.* A novel glyco-conjugate vaccine against fungal pathogens. *J Exp Med* **202**, 597–606 (2005).

25. Rachini, A. *et al.* An anti-beta-glucan monoclonal antibody inhibits growth and capsule formation of Cryptococcus neoformans in vitro and exerts therapeutic, anticryptococcal activity in vivo. *Infect Immun* **75**, 5085–5094 (2007).

26. Lefranc, M.-P. *et al.* IMGT unique numbering for immunoglobulin and T cell receptor variable domains and Ig superfamily V-like domains. *Dev Comp Immunol* **27**, 55–77 (2003).

27. Clavero-Álvarez, A., Di Mambro, T., Perez-Gaviro, S., Magnani, M. & Bruscolini, P. Humanization of Antibodies using a Statistical Inference Approach. *Scientific Reports* **8**, 14820 (2018).

28. Sormanni, P., Aprile, F. A. & Vendruscolo, M. The CamSol method of rational design of protein mutants with enhanced solubility. *J Mol Biol* **427**, 478–490 (2015).

29. Mf, N. *et al.* Quantitative Analysis of Candida Cell Wall Components by Flow Cytometry with Triple-Fluorescence Staining. *Journal of Microbiology and Modern Techniques* **2**, (2017).

30. Lee, K. K. *et al.* Yeast species-specific, differential inhibition of β-1,3-glucan synthesis by poacic acid and caspofungin. *The Cell Surface* **3**, 12–25 (2018).

31. Chen, D., Zhang, H., Lu, P., Liu, X. & Cao, H. Synergy evaluation by a pathway-pathway interaction network: a new way to predict drug combination. *Mol Biosyst* **12**, 614–623 (2016).

32. Dent, P., Curiel, D. T., Fisher, P. B. & Grant, S. Synergistic combinations of signaling pathway inhibitors: Mechanisms for improved cancer therapy. *Drug Resist Updat* **12**, 65–73 (2009).

33. Pfaller, M. A., Sheehan, D. J. & Rex, J. H. Determination of fungicidal activities against yeasts and molds: lessons learned from bactericidal testing and the need for standardization. *Clin Microbiol Rev* **17**, 268–280 (2004).

34. Gaughan, C. L. The present state of the art in expression, production and characterization of monoclonal antibodies. *Mol Divers* **20**, 255–270 (2016).

35. Reichert, J. M. Antibodies to watch in 2017. *MAbs* **9**, 167–181 (2017).

36. Carter, P. J. & Lazar, G. A. Next generation antibody drugs: pursuit of the 'high-hanging fruit'. *Nat Rev Drug Discov* **17**, 197–223 (2018).

37. Kaplon, H. & Reichert, J. M. Antibodies to watch in 2018. *MAbs* **10**, 183–203 (2018).

38. Wang, C. *et al.* A human monoclonal antibody blocking SARS-CoV-2 infection. *Nature Communications* **11**, 2251 (2020).

39. Torosantucci, A. *et al.* Protection by anti-beta-glucan antibodies is associated with restricted beta-1,3 glucan binding specificity and inhibition of fungal growth and adherence. *PLoS One* **4**, e5392 (2009).

40. Laniado-Laborín, R. & Cabrales-Vargas, M. N. Amphotericin B: side effects and toxicity. *Rev Iberoam Micol* **26**, 223–227 (2009).

41. Ullmann, D. A. J. Review of the safety, tolerability, and drug interactions of the new antifungal agents caspofungin and voriconazole. *Current Medical Research and Opinion* **19**, 263–271 (2003).

42. IgBlast tool. https://www.ncbi.nlm.nih.gov/igblast/.

43. SIB Swiss Institute of Bioinformatics | Expasy. https://www.expasy.org/.

44. Home :: Chemistry of Health - software. http://www-cohsoftware.ch.cam.ac.uk//index.php.

45. Singh, S. *et al.* The NDV-3A vaccine protects mice from multidrug resistant Candida auris infection. *PLoS Pathog* **15**, e1007460 (2019).

46. Magliani, W. *et al.* Therapeutic potential of antiidiotypic single chain antibodies with yeast killer toxin activity. *Nat Biotechnol* **15**, 155–158 (1997).

47. Bhattacharya, S., Holowka, T., Orner, E. P. & Fries, B. C. Gene Duplication Associated with Increased Fluconazole Tolerance in Candida auris cells of Advanced Generational Age. *Sci Rep* **9**, 5052 (2019).

48. Arendrup, M. C. *et al.* EUCAST DEFINITIVE DOCUMENT E.DEF 7.3.2. 21 (2020).

49. Kitamura, A., Someya, K., Hata, M., Nakajima, R. & Takemura, M. Discovery of a Small-Molecule Inhibitor of β-1,6-Glucan Synthesis. Antimicrob Agents Chemother 53, 670–677 (2009).

50. Davis, M. J. et al. Cryptococcus neoformans– Induced Macrophage Lysosome Damage Crucially Contributes to Fungal Virulence. J.I. 194, 2219–2231 (2015).

51. Canonico, B. et al. Honey flavonoids inhibit Candida albicans morphogenesis by affecting DNA behavior and mitochondrial function. Future Microbiology 9, 445–456 (2014).

52. Rudkin, F. M. et al. Single human B cell-derived monoclonal anti-Candida antibodies enhance phagocytosis and protect against disseminated candidiasis. Nat Commun 9, 5288 (2018).

SUPPLEMENTARY INFORMATION

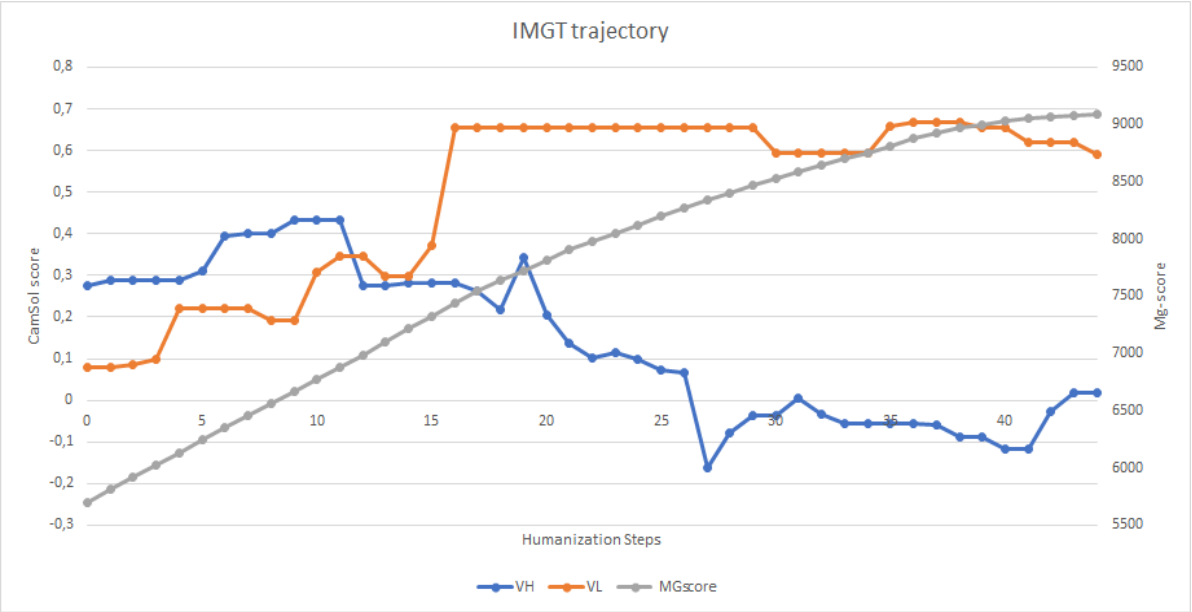

Figure S1 (supplementary information). CamSol Intrinsic solubility scores (mayor y-axes) and humanization MG-score (minor y-axes) for the humanization trajectories in sequence space starting from the murine sequence (step 0): the results for the second protocol described in Methods, upon fixing the CDR residues corresponding to the IMGT numbering. High CamSol score corresponds to high solubility; MG-scores above 6383 are classified as human.

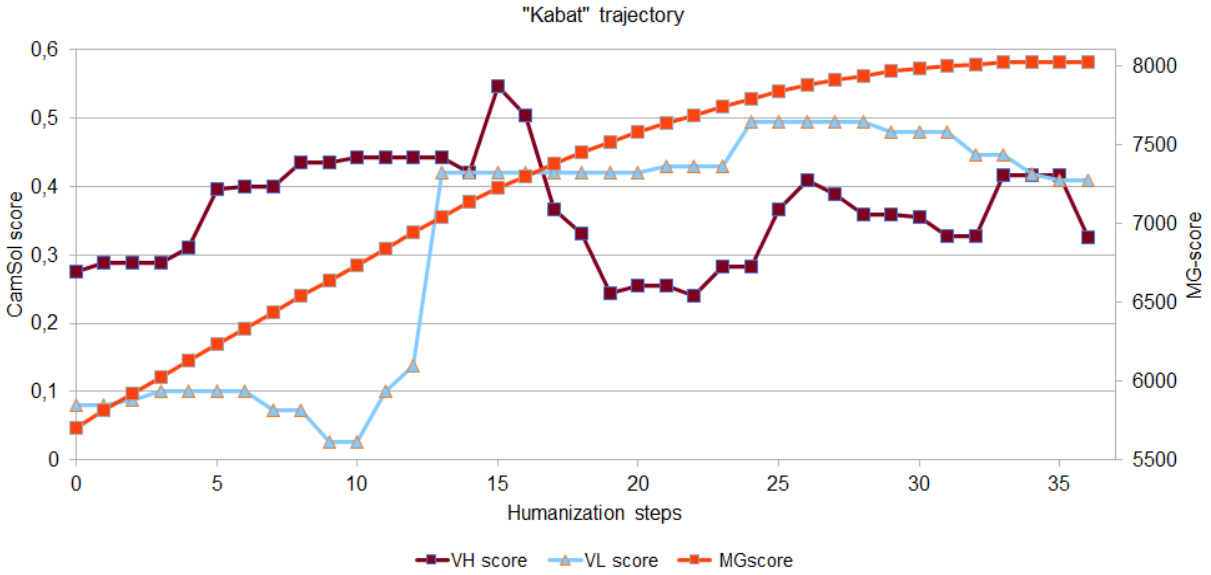

Figures S2 (supplementary information). CamSol Intrinsic solubility scores (mayor y-axes) and humanization MG-score (minor y-axes) for the humanization trajectories in sequence space starting from the murine sequence (step 0): the results for the third protocol, upon fixing the CDR residues corresponding to the Kabat numbering. High CamSol score corresponds to high solubility; MG-scores above 6383 are classified as human.

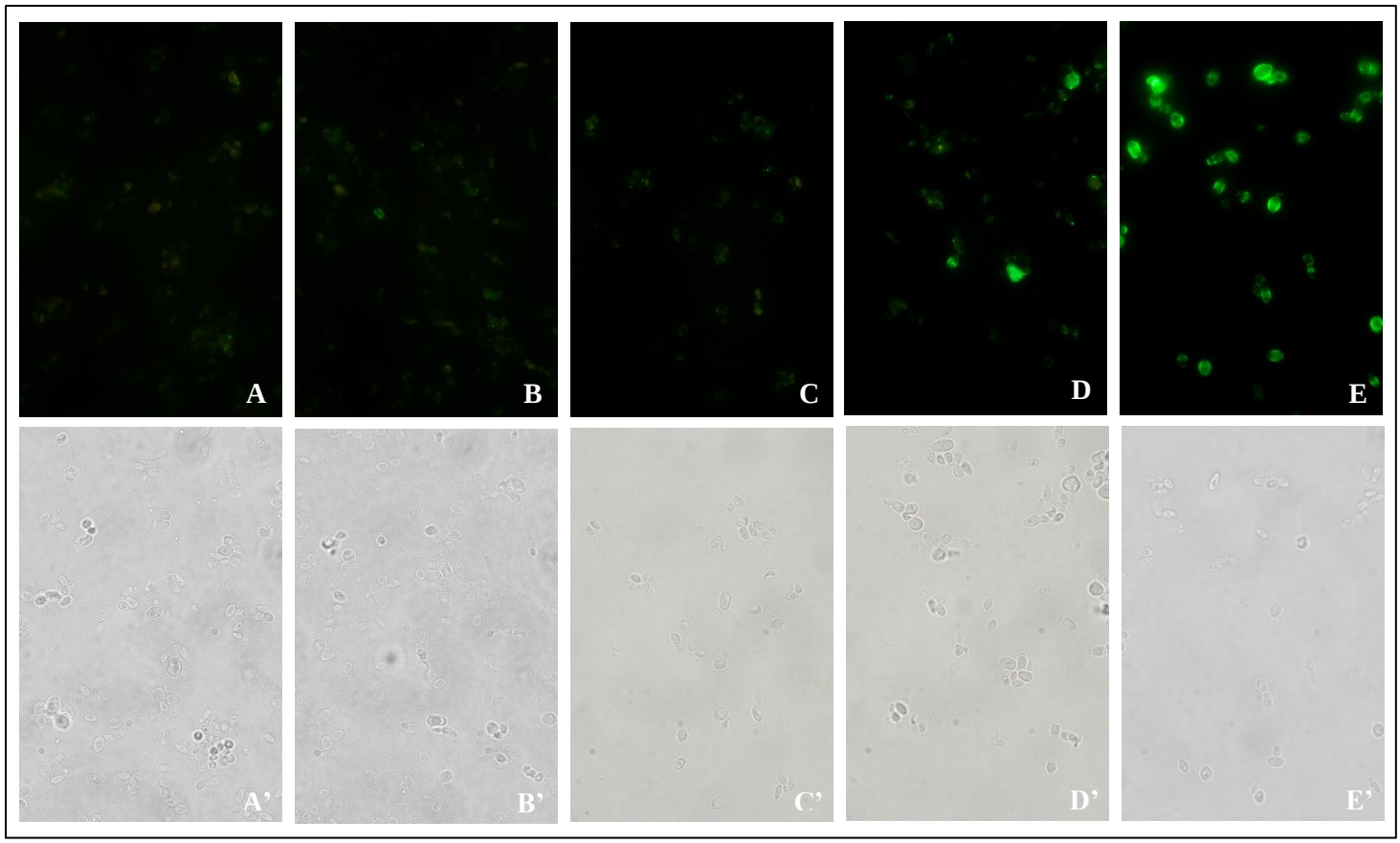

Figure S3 (supplementary information). Competitive binding of H5K1 to *C. auris* cells after treatment with different concentrations of laminarin. PBS pre-treatment was used as control. Considering that the humanized antibody is bivalent, and that more than one antibody can bind a single laminarin polysaccharide, the ratios laminarin:H5K1 in μg/ml were respectively: A-A' 40:1, B-B' 16:1, C-C' 4:1, D-D' 1:1, E-E' 0:1.

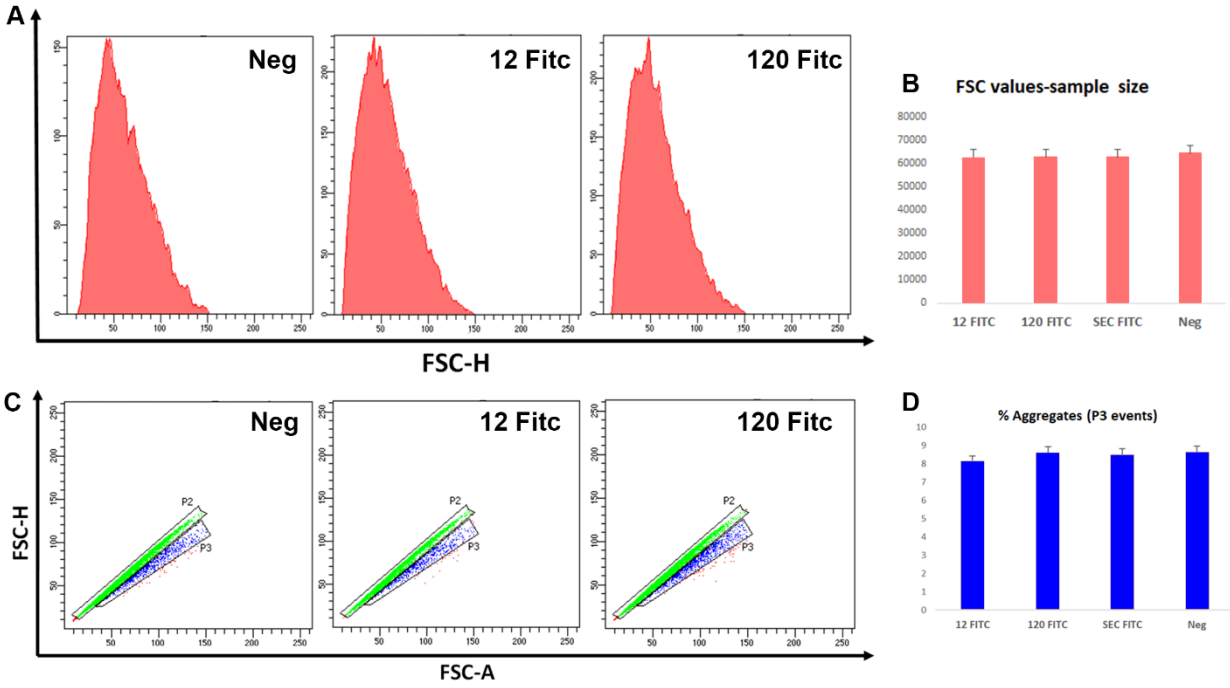

Figure S4 (supplementary information). Flow cytometry is also suited for measurements of cell size, interaction, aggregation or shape using non-labelled cells by means of analysing their light scattering characteristics. Yeast aggregation is not induced by antibody labelling, as demonstrated by flow cytometric detection of both total event size (FSC histogram (A-B)) and dimensional aggregates (dot plot FSC-A vs FSC-H (C-D)) Data were collected as FSC values and percentages of aggregates.

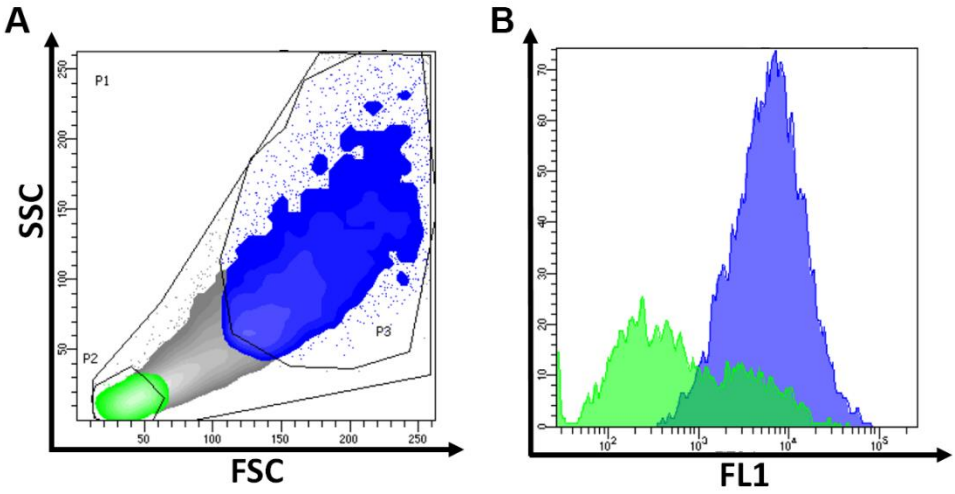

Figure S5 (supplementary information). Fluorescence Intensity highlights a differential labelling of the antibody on different subpopulations of *Candida albicans* during hyphal transition. Green events represent small cells, putative scarce residual yeasts, partially germinating [51], whereas blue events represent hyphal morphogenetic state (hyphal aggregates, scarcely represented rare excluded from the analysis) (A). Hystogram (B) overlays puts in light a higher Mean Fluorescence Intensity (MFI) on blue events in respect to the green ones, in agreement with the higher presence of 1,3 Beta-glucan in hyphal state, as reported [24].

Vid. 1 A. Binding analysis by means of immunofluorescence technique – Control FITC

Vid. 1 B. binding analysis by means of immunofluorescence technique – hmAb H5K1 FITC

(Available at **https://doi.org/10.1038/s41598-021-98659-5**)

CHAPTER 2

AFM analysis of *C. auris* cells treated with fluconazole, caspofungin, amphotericin B, hmAb H5K1 and its combinations with the antifungal drugs

I wish to express my gratitude to

Professor Michele Menotta

ABSTRACT

Mycoses are increasingly impacting the health of the population and particularly on specific subject categories with a compromised immune system. The resistance phenomenon and the rise of new species are creating concern and, consequently, an interest in developing new therapeutic agents against pathogenic fungi. H5K1 is a humanized monoclonal antibody that binds selectively β-1,3-glucans, vital components of the fungal cell wall, hence attractive targets to reach an antifungal effect. Since *Candida auris* is considered an urgent threat by the CDC and one of the three leading causes of morbidity and mortality worldwide, it has been used as fungal model to investigate the effect of H5K1 on the cell surface both alone and in combination with commercially available antifungal drugs (fluconazole, caspofungin and amphotericin B). By an extensive exploration through the atomic force microscope, H5K1 was revealed to have a role in the perturbation of the fungal cell wall that reflects in the loss of the whole cell integrity. Moreover, it contributes substantially to the alterations caused especially by caspofungin and amphotericin B.

INTRODUCTION

Mycoses are opportunistic infections caused by fungi. They can colonize biotic and abiotic surfaces and become progressively more dangerous when diffuse in deeper tissues or into the bloodstream. Subjects with a debilitated immune system and immunocompromised patients have the highest probability to contract severe fungal infections [1]. In particular, candidemia is one of the most common systemic infections worldwide with an incidence of 7.0/100,000 people per year in the US [2] and 3.88/100,000 in Europe [3]. Invasive candidiasis is associated with a high mortality rate [4] and for this reason, *Candida* spp. are considered serious threats. The spread of acquired resistance and the rise of species with intrinsic and sometimes multidrug resistance worsen even more the scenario [5]. Among the new pathogens, *C. auris* has gained sad interest in the last decades to the point that it is considered by the Centers for Disease Control and Prevention an urgent global health threat [6]. More than 90% of the isolates have an innate resistance to one antifungal class, more than 30% to two classes and 1% to all three major classes [6]. These numbers match with its rapid spread from 2009 in Japan [7] to over 47 countries worldwide [8] and with its high mortality rate which ranges from 32 to 66% [9, 10].

Here the choice to use *Candida auris* as specie-to-be tested favored also by its prevalent yeast-like morphotype [11, 12].

Fungi are eukaryotic organisms hence they have a complex and dynamic intracellular organization confined by a phospholipidic bilayer. Over the membrane, several polysaccharide/-proteo-conjugate layers are arranged to form the fungal wall. The inner and the outer layers are the most conserved and the main differences are

related to the content variability among species or to the switch yeast-to-hyphal morphotype typical of some species like *Candida* spp. [13].

The inner layer of *Candida* spp. is composed of microfibrils of antiparallel chitin chains stabilized by H-bonds, and of a flexible network of branched β-1,3-glucans organized in single or in polymer chains [14]. Chitin and β-1,3-glucans represent the real backbone of the fungal wall and the strength, and the shape of the cells derive from their chemical and physical properties. Even if less abundant (20% vs 40%) β-1,6-glucans are fundamental to link chitin and β-1,3-glucans to the glycosylphosphatidylinositol remnants of the outer layer-cell wall proteins (CWPs) [15] while α-glucans are absent in *Candida* spp. [16].

β-1,3-glucans are promptly recognized by Dectin-1, a C-type lectin type II transmembrane receptor expressed mainly on myeloid cells [17], but the O- and N-linked mannoproteins of the outer layer are aligned perpendicularly in order to form a fibril coat able to reduce their exposition. Moreover, the high hydrophobicity of mannans confers resistance, low permeability and low porosity to the cell wall making it difficult also for the antifungal drugs to penetrate [18, 19]. In the outer layer there are also several CWPs like adhesins and invasins, functional for the host infection.

Fungal species can have substantial differences in the number of proteins, lipids and carbohydrates. Notably, *C. auris* presents fewer CWPs and enzymes involved in the cell wall remodeling if compared to *C. albicans* but more structural lipids [20]. They have similar levels of mannan and glucans, but chitin is more abundant in *C. auris* thus explaining probably part of its higher natural resistance against some antifungal classes [21].

H5K1 is a humanized monoclonal antibody able to recognize and bind selectively β-1,3-glucans which are fundamental and vital for several pathogenic fungi [22]. The aim of this study is to investigate through the atomic force microscope the effect on the cell surface of H5K1 and of its combinations with a representative from the three major antifungal classes (fluconazole for azoles, caspofungin for echinocandins and amphotericin B for polyenes). The focus will be done on the differences in the topographic and sub-topographic domains and in the chemical distribution on the surfaces. Data were acquired in both in non-contact and tapping modes.

EXPERIMENTAL DETAILS

Materials

C. auris DSM 21092 was purchased from Leibniz Institute DSMZ-German Collection of Microorganisms and Cell Cultures GmbH, Germany; the humanized monoclonal antibody H5K1 was produced by Takis s.r.l., Italy; caspofungin, fluconazole, amphotericin B, RPMI (powder) and MOPS were bought from Sigma-Aldrich, Germany, while paraformaldehyde 37% w/v was acquired from Carlo Erba reagents s.r.l., Italy.

Sample preparation

From an overnight inoculum in RPMI + MOPS (0.165 M, pH 7), a *C. auris* suspension was washed and resuspended in phosphate buffered saline (PBS). $3x10^6$ *C. auris* cells were treated respectively with the humanized mAb H5K1, with fluconazole, caspofungin and amphotericin B at sub-MIC concentrations and with the combination of hmAb H5K1 with the mentioned antifungal drugs for 1 hour at 37°C. *C. auris* cells in PBS were used as control. The samples were washed three times with PBS before fixing them with paraformaldehyde 4% for 1 hour at 4 °C. Finally, the samples were washed again and resuspended in 18MΩ water. The samples were layered on fresh muscovite mica and dried by nitrogen flow.

AFM analyses

AFM analysis was carried out with an XE-100 Atomic Force microscope (PARK Systems Inc., Suwon, South Korea). The microscope was equipped with a 50 µm scanner controlled by the XEP 1.8.6 software. The XY stages and the Z scan were set in closed-loop manner and in high voltage mode.

The speed scan was set between 0.2 Hz and 1.5 Hz. The cantilevers used in this study were Non-Contact High Resonant (NCHR) tips (spring constant between 35 and 44 N/m) with a typical resonant frequency between 200 and 300 kHz. The instrument was set in true non-contact mode and topography, amplitude, error, and phase signals were acquired during the imaging.

Amplitude signal images were used for topographic subdomains contrast enhancement while the phase images were adopted for surface chemical characterization.

The Force Modulation Microscopy (FMM) was achieved by using a NSC14 tip (5N/m) and the local nanomechanical properties were tested by amplitude and phase signals.

For the force/distance spectroscopy analysis (F/D) a calibrated NCHR tip (39.7 N/m) was employed. Briefly, at least 4 points were randomly chosen in the middle of each cell and F/D assay was performed. The tip moved forward the samples for 1 mm at 10 nm/s, while the retrace velocity was set at 50 nm/s with a force limit of 3 mN. The stiffness of the sample was determined from the slope of the force-separation curve in the contact region and reported as nanoNewton.

Statistical analyses

Data inferred by Park XEI software (PARK Systems Inc., Suwon, South Korea) were analyzed by GraphPad Prism. The statistical Kruskal-Wallis analysis of variance (ANOVA) on uncorrected Dunn's test for multiple comparisons was adopted.

RESULTS AND DISCUSSION

Candida auris cells were treated with sub-MIC concentrations of the antifungal drugs fluconazole (FLC), caspofungin (CAS) and amphotericin B (AMB), with the humanized monoclonal antibody H5K1 (hmAb), and with their combinations. Cells treated with PBS were used as control.

Image-surface profile parameters chosen for topographic and sub-topographic analyses are the main descriptors used to delineate the cell morphology and the surface [23, 24]. Together with roughness parameters they are sensitive indicators of cell's health state [25]. They are suitable for monitoring the damages caused by specific agents on biological samples [26] and in our case the effects of antifungal compounds on *C. auris* cells. To have a complete sight of the results, force modulation microscopy was adopted to probe the nanomechanical properties in relation to the topographic images [27] and finally the cellular stiffness was considered to evaluate the cytoskeletal structure and to have an indication of the integrity and of the mechanics of the cells [28].

From a preliminary analysis of the 1μmx1μm topographic images, there is evidence of the cell wall perturbation due to the presence of topographic alterations leading to a more inhomogeneous surface compared to the control cells (Fig.1).

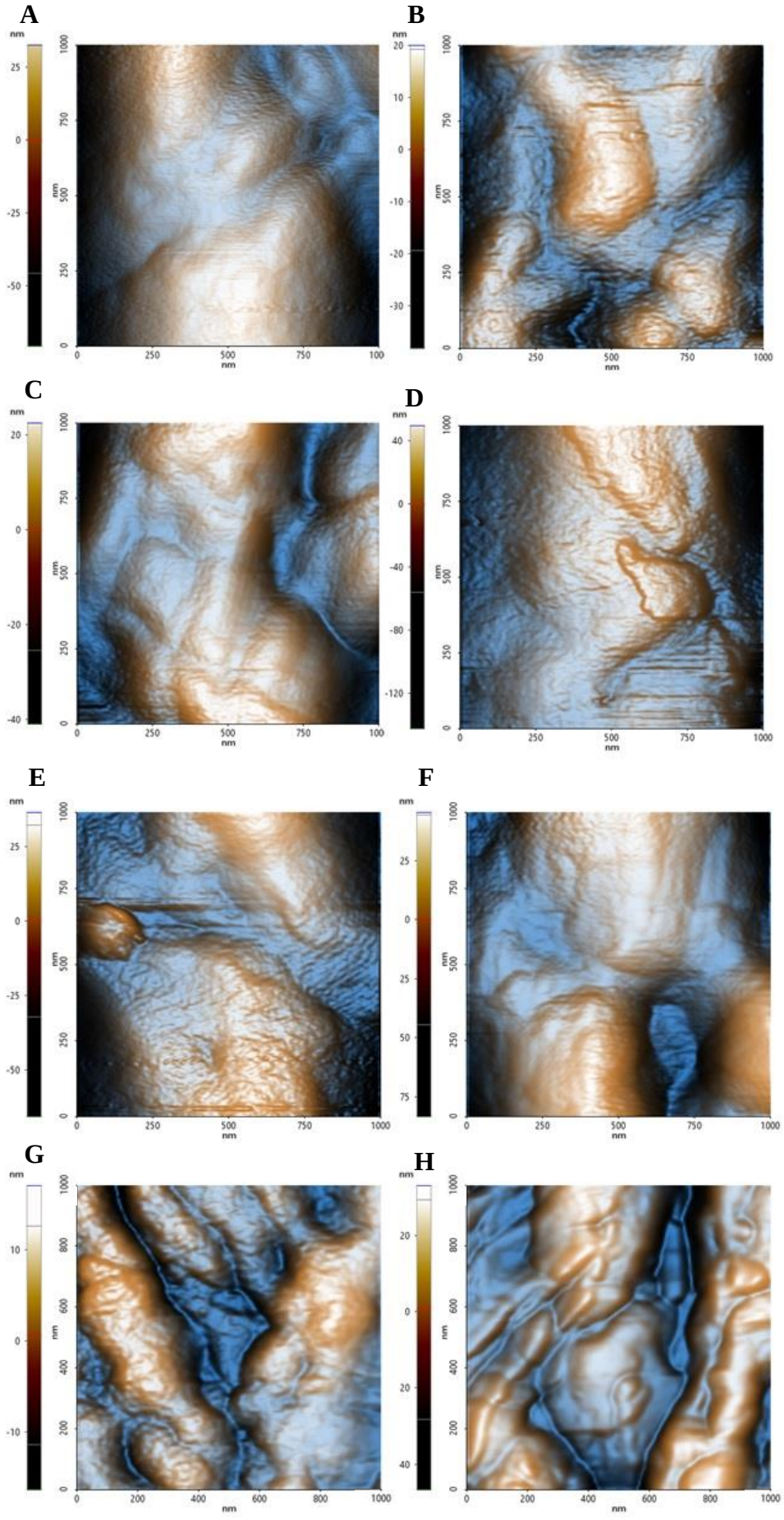

Figure 1. Topographic images of *C. auris* cell surface. **A** Control, **B** treatment with hmAb H5K1, **C** treatment with fluconazole, **D** treatment with the combination of hmAb H5K1 and fluconazole, **E** treatment with amphotericin B, **F** treatment with the combination hmAb H5K1 and amphotericin B, **G** treatment with caspofungin, **H** treatment with the combination of hmAb H5K1 and caspofungin.

In order to numerically describe these alterations, the mean spacing of profile irregularities (Sm) and the average wavelength of the profile (λa) were evaluated as spatial parameters, while the average absolute slope (Δa) was estimated as hybrid factor (Fig. 2). For what concerns the Sm (Fig. 2 A), while for the control an average spacing of ~113 nm was calculated, for hmAb H5K1 and CAS + hmAb treated cells the Sm values were lower and statistically significant, thus meaning a higher frequency of topographical changes. This outcome was also confirmed by using λa parameter (Fig. 2 B). In fact, hmAb H5K1 treated sample and hmAb H5K1 in combination with fluconazole and caspofungin samples showed a statistically significant decrement of λa compared to the control sample (Table 1). The average absolute slope (Δa) (Fig. 2 C) was considered to characterize the magnitude of the topographical variations. By this parameter statistical differences were noted in amphotericin B, caspofungin and caspofungin + hmAb H5K1 treated samples. Taken together these data suggests that changes in surface roughness were induced by hmAB H5K1 alone or in combination with other drugs.

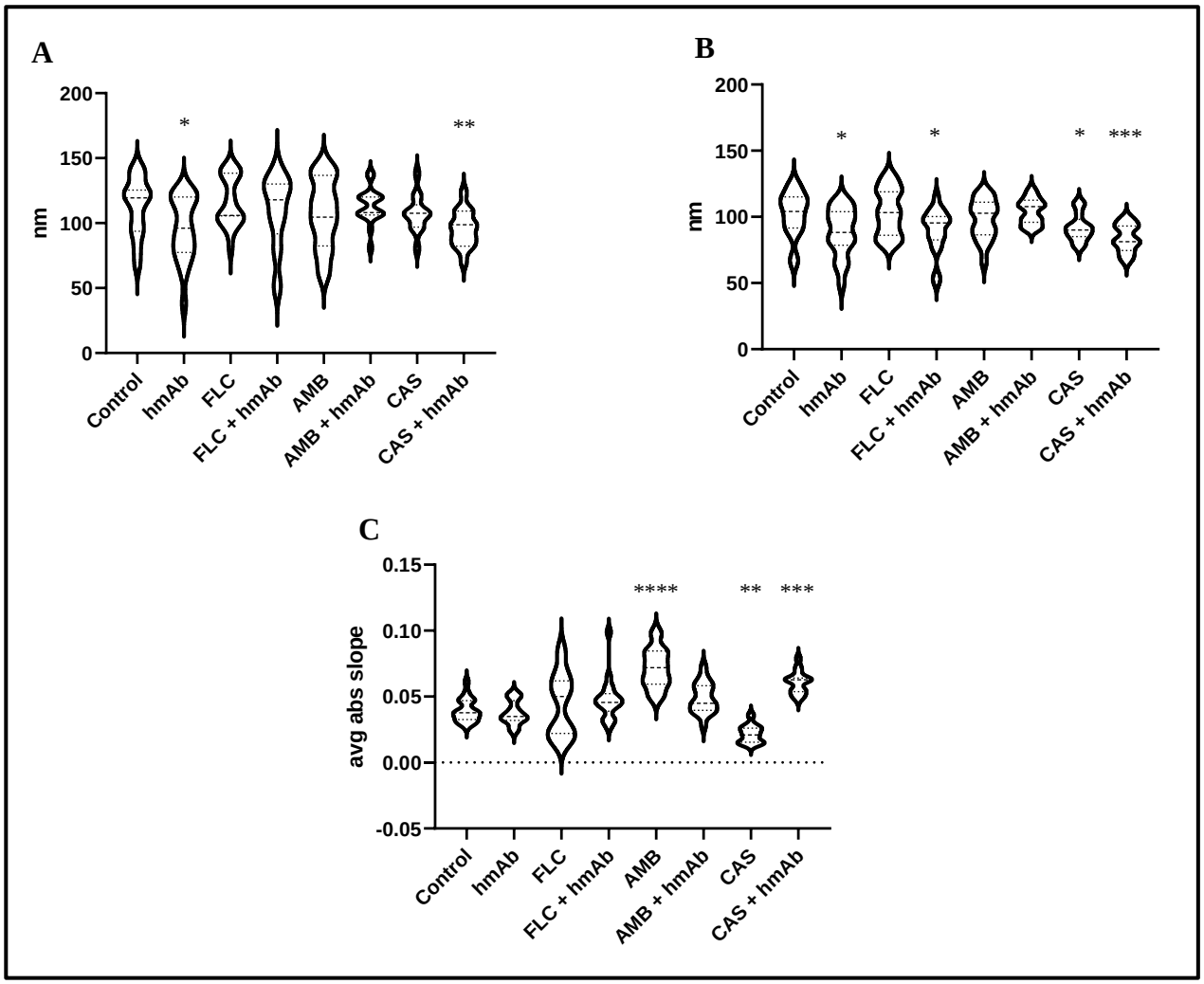

Figure 2. A: spacing mean of the irregularities of the profile (Sm); B: average wavelength (λa); C: average absolute slope (Δa) of the wave function from topographic analyses. The statistical significances are referred to the comparison with the control.

In the amphotericin B treated sample the Δa distribution showed higher values probably indicating the presence of sharper vertical variations possibly caused by the capacity of AMB aggregates to produce digging after their embedding in surface rich in ergosterol [22]. This digging appears to be just the prelude to the typical pores produced by amphotericin B [22]. The combination of hmAb with caspofungin produces a similar trend hence we are likely to suppose that the enhancement of hmAb H5K1 on caspofungin can lead to an effect comparable to that of amphotericin B on the surface. Of note the statistically significant decrease of Δa in presence of caspofungin alone. We speculate that it could be due by the unmasking activity of caspofungin [29].

To further confirm changes in surface topography the images obtained by tip amplitude signal were used to improve the topographic image contrast, allowing to emphasize sub-nanometric structures (Fig. 3). In the control, segmentations are denser while in samples treated with all the antifungal drugs domains undergo alterations that become even more slacken in the presence of hmAb. Again, by measuring the average wavelength of the profile belonging to the amplitude signal, all samples differ from the control (Fig 4). This evidence suggests that there are differences in molecules distribution (glucans) on the surface of the cells. Since the λa increased in all treated samples (Table 1), it is possible to suppose that the cell wall components were displaced away by the treatments.

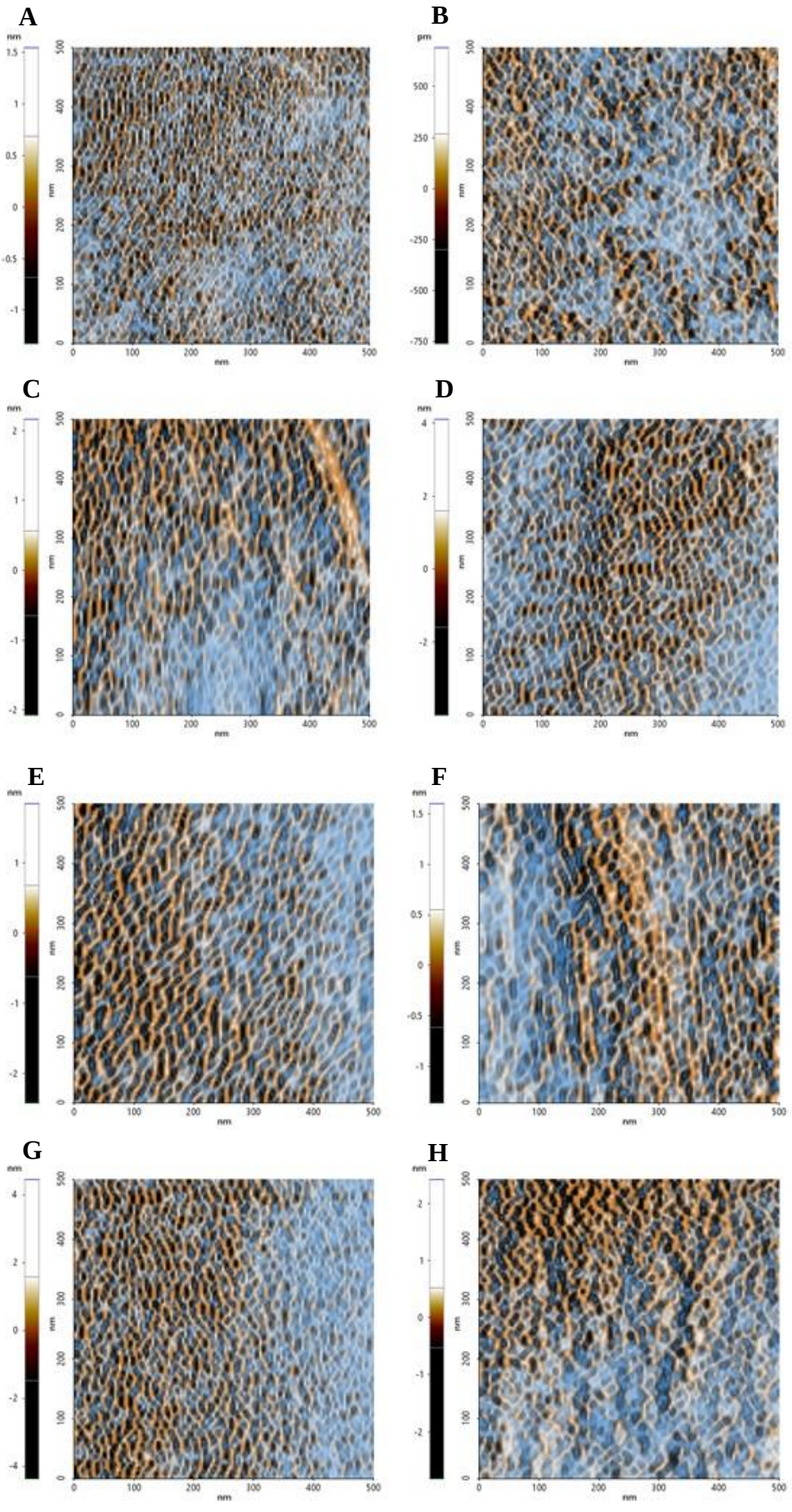

Figure 3. *C. auris* cell surface. Images obtained from amplitude signal analysis. **A** Control, **B** treatment with hmAb H5K1, **C** treatment with fluconazole, **D** treatment with the combination of hmAb H5K1 and fluconazole, **E** treatment with amphotericin B, **F** treatment with the combination hmAb H5K1 and amphotericin B, **G** treatment with caspofungin, **H** treatment with the combination of hmAb H5K1 and caspofungin.

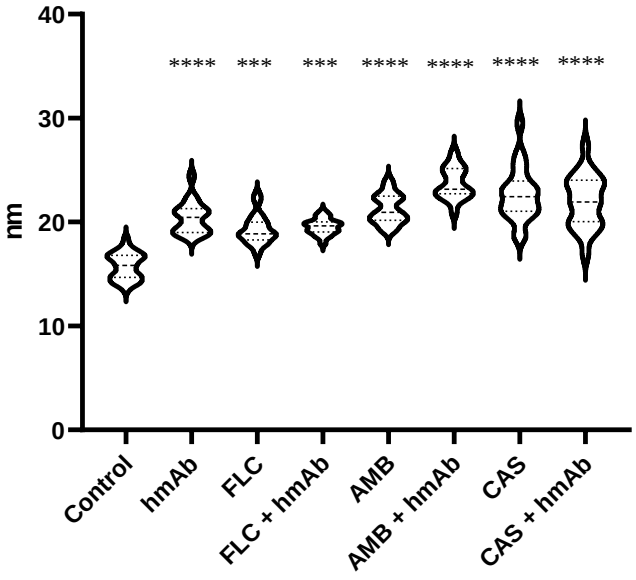

Figure 4. Average wavelength of the NCM amplitude signal profile. The statistical significances are referred to the comparison with the control.

The surface composition alteration was also assayed by non-contact mode phase imaging (Fig 5). Control samples showed a homogeneous distribution of the phase signal whereas all treated cells exhibited a variegate phase signal distribution, quantitatively measured as peak-to-valley mean-height roughness (RPV roughness) (Fig 6 and Table 1). hmAb H5K1 provided the major contribution to the roughness, and this is highlighted by the statistically significant difference in RPV of hmAb H5K1 monotreatment and of its combinations compared to the control. Fluconazole and amphotericin B used alone weren't statistically significant while caspofungin was and this is consistent with the results obtained by Hasim et Al. that reported an increase of roughness in *C. albicans* treated with caspofungin probably due to the β-1,3-glucans unmasking [29, 30]. Interesting is the different distribution of the RPV values: those of control and of the antifungals' monotreatments are more homogeneous while in the presence of hmAb H5K1 alone and in combination with fluconazole or caspofungin the phase signal roughness is increased, consequently to a wider distribution of the molecules on the surface.

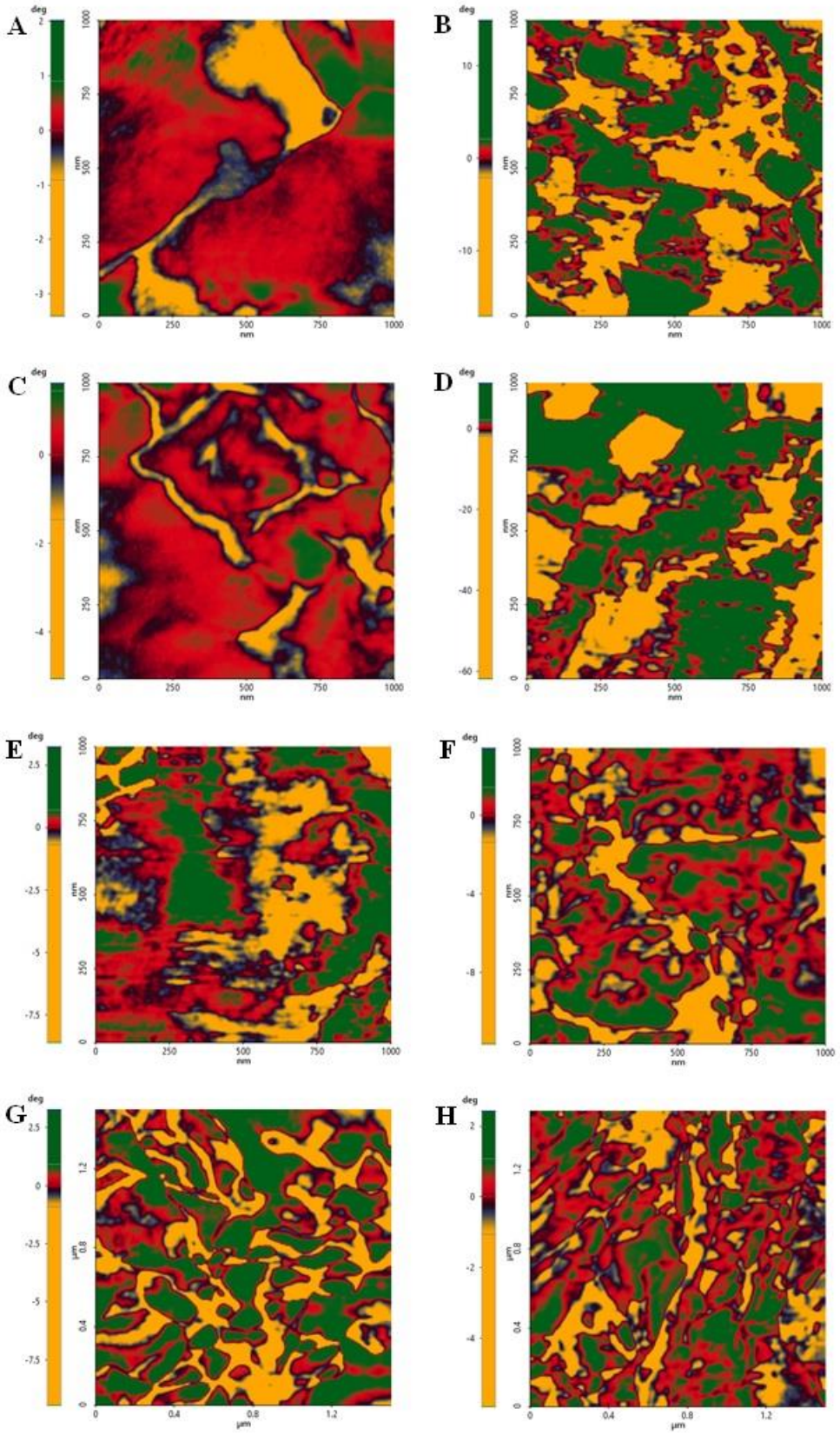

Figure 5. Non-contact mode analysis of chemical variations on *C. auris* surface. **A** Control, **B** treatment with hmAb H5K1, **C** treatment with fluconazole, **D** treatment with the combination of hmAb H5K1 and fluconazole, **E** treatment with Amphotericin B, **F** treatment with the combination hmAb H5K1 and amphotericin B, **G** treatment with caspofungin, **H** treatment with the combination of hmAb H5K1 and caspofungin.

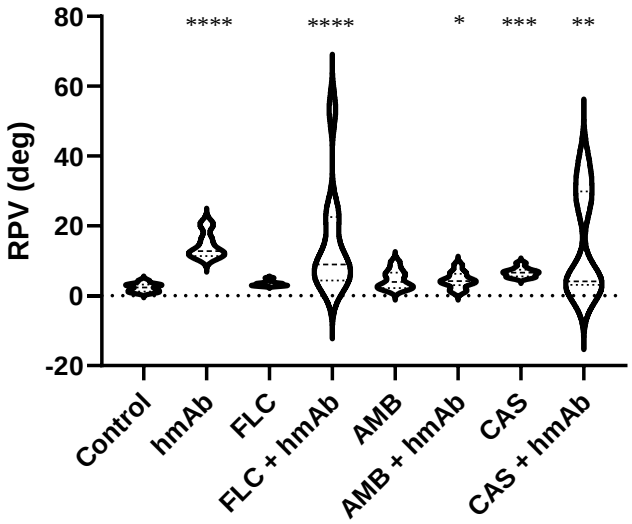

Figure 6. Phase signal distribution measured as RPV roughness. The statistical significances are referred to the comparison with the control.

The surface alterations induced by the treatments were also assayed by nanomechanical approaches. The force modulation mode was used to investigate the amplitude and the phase signals to obtain information about the local stiffness and elasticity (Fig. 7). The middle amplitude values are dependent on analyzed regions and are little informative. Anyway, the median of the amplitude signal was higher in the presence of hmAb H5K1 alone and in combination with amphotericin B and caspofungin (Fig. 8 A). indicating stiffer surfaces compared to the control. The FMM amplitude roughness revealed that nanomechanical proprieties dependent on molecules arrangement were altered in samples treated with amphotericin B, caspofungin and caspofungin + hmAb (Fig. 8 B). Concerning elasticity proprieties, FMM phase roughness revealed that samples treated with amphotericin B, amphotericin B + hmAb and caspofungin + hmAb (Fig. 8C) were altered compared to the control sample. Again, the less informative FMM phase signal medians showed differences between control samples treated with hmAb, with the combination FLC + hmAb and with the combination CAS + hmAb (Fig. 8 D). We can suppose that the bispecific binding of hmAb H5K1 to its antigen can locally stiffen the superficial structures and this could also explain the wider distribution of both FMM amplitude and phase signals. This phenomenon is perceivable also when hmAb is used in combination (Table 1).

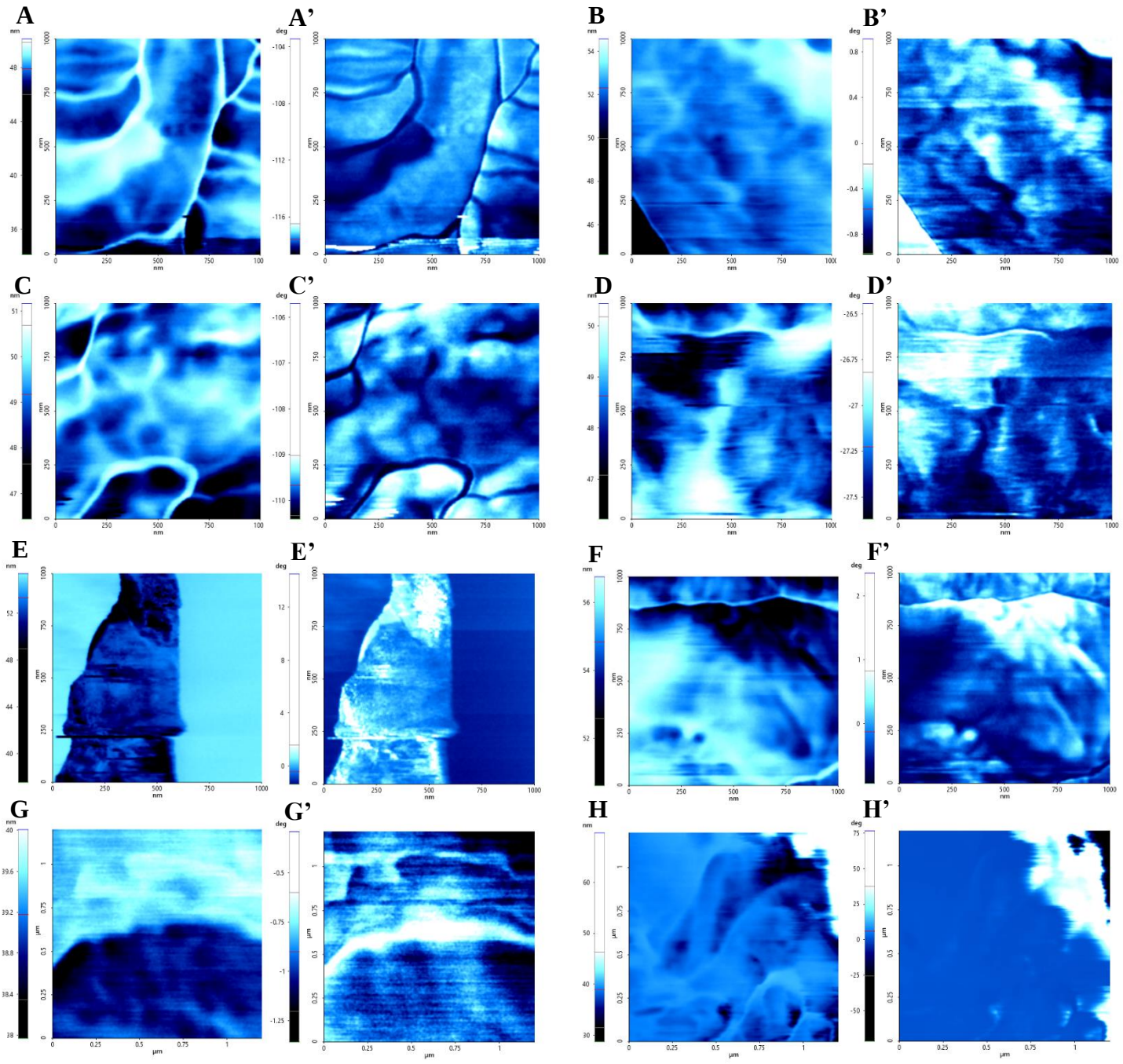

Figure 7. Analysis of the amplitude (letters) and of the phase signal (marked letters) in force modulation mode. **A/A'** Control, **B/B'** treatment with hmAb H5K1, **C/C'** treatment with fluconazole, **D/D'** treatment with the combination of hmAb H5K1 and fluconazole, **E/E'** treatment with amphotericin B, **F/F'** treatment with the combination hmAb H5K1 and amphotericin B, **G/G'** treatment with caspofungin, **H/H'** treatment with the combination of hmAb H5K1 and caspofungin.

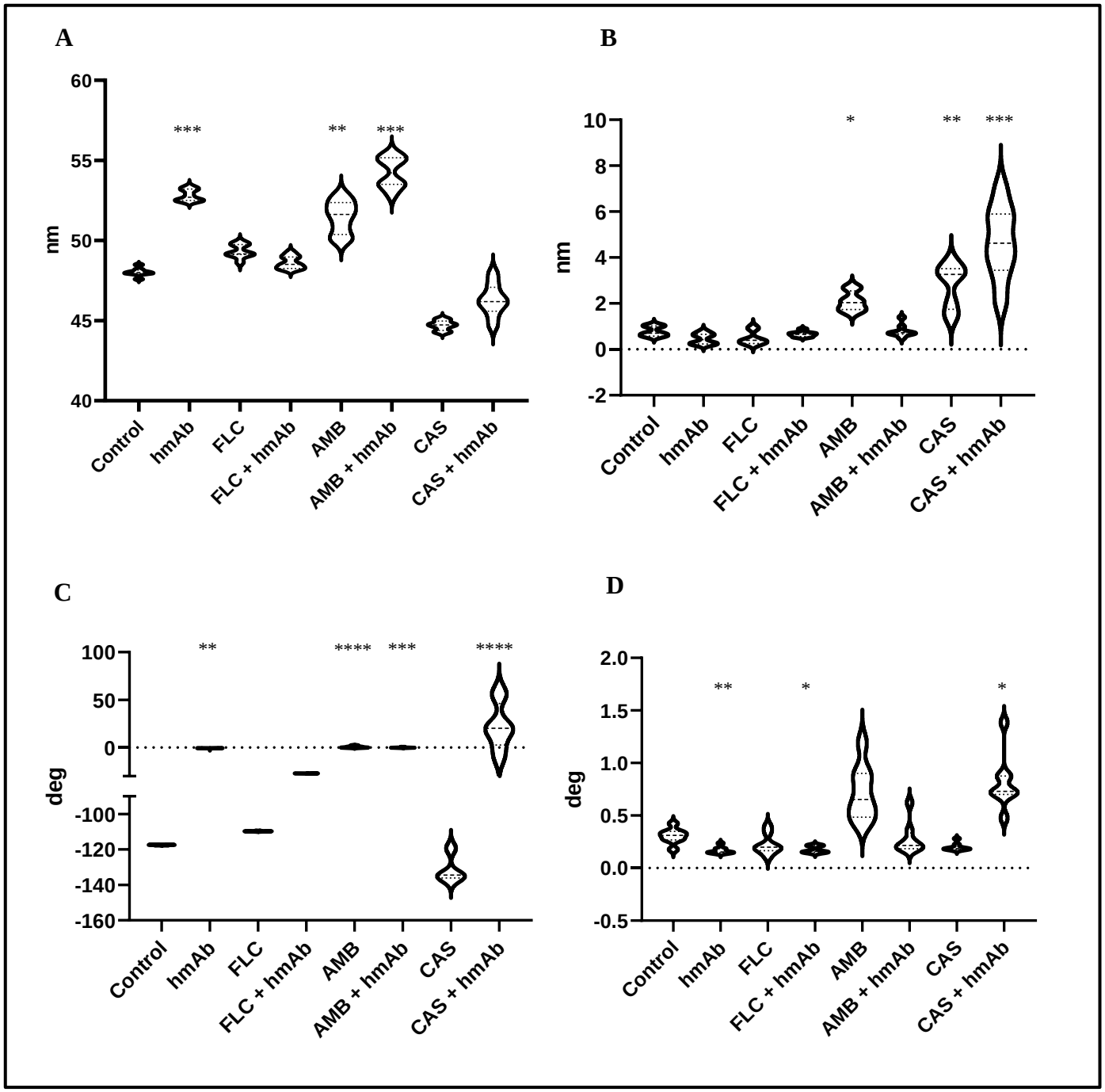

Figure 8. Superficial FMM analysis: A – median of the amplitude signal, B – roughness of amplitude signal, C – median of the phase signal, D – roughness of phase signal.

In order to assess the effects of the treatments not just locally but also globally, points of the cell surface were randomly selected and undergone to physical deformation to calculate a deeper cellular stiffness. Fluconazole, amphotericin B, their combination with hmAb and the combination of caspofungin + hmAb presented lower stiffness values than the control sample (Table 1) meaning that the deep structure integrity was altered as well. Easy-deformable zones reflect the weakening of the whole cell (Fig. 9).

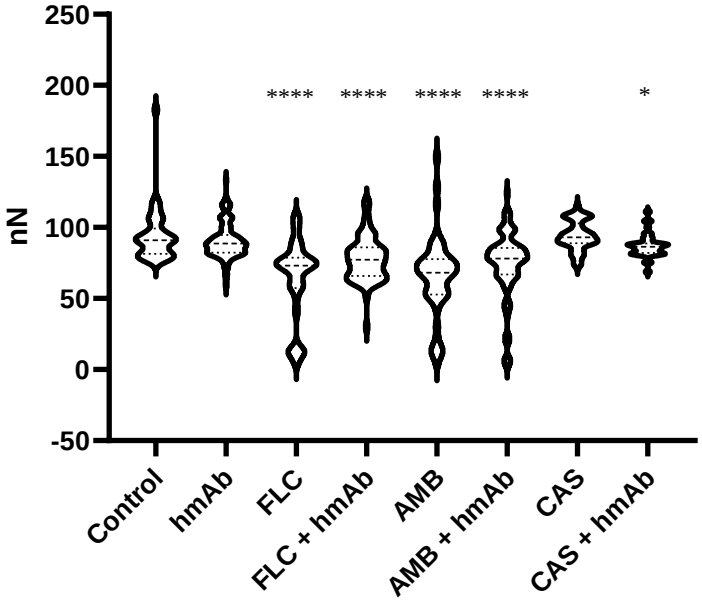

Figure 9. Stiffness analysis on a macrozone.

Table 1. Mean ± SEM of the parameters considered during the analyses.

		Control	hmAb	FLC	FLC + hmAb	AMB	AMB + hmAb	CAS	CAS + hmAb
Sm	Mean	113	95.35	116.6	109.1	107.4	113.1	107.4	95.57
	SEM	4.231	5.703	4.42	6.562	6.017	3.011	3.893	3.561
λa	Mean	102.4	88.28	103.8	89.8	98.21	104.3	91.87	83.9
	SEM	3.86	4.187	4.013	3.955	3.442	2.214	2.863	2.669
Δa	Mean	0.03957	0.03766	0.04411	0.04804	0.07142	0.0491	0.02152	0.06089
	SEM	0.002013	0.002065	0.005429	0.003777	0.003403	0.002667	0.001888	0.002214
Amp. λa	Mean	15.76	20.41	19.28	19.55	21.24	23.72	22.68	22
	SEM	0.226	0.3403	0.3008	0.1623	0.2981	0.3503	0.5463	0.5393
Phase (deg)	Mean	2,351	14,47	3,398	14,96	4,678	4,518	6,706	14,66
	SEM	0,3692	1,141	0,2260	4,825	0,8359	0,7139	0,4113	4,757
Striffness (nN)	Mean	93,91	90,40	64,27	77,73	65,45	74,38	94,21	87,09
	SEM	1,905	1,015	2,445	1,204	2,666	1,664	1,011	0,7766
FMM amp. (nm) median	Mean	48,02	52,83	49,33	48,62	51,47	54,25	44,70	46,29
	SEM	0,09034	0,1310	0,1500	0,1401	0,3634	0,3379	0,1075	0,3530
FMM phase (deg) median	Mean	-117,5	-0,7914	-109,8	-27,14	0,5188	-0,1118	-131,3	22,06
	SEM	0,06237	0,3164	0,05930	0,02724	0,3150	0,1230	2,678	8,552
RPV amp. (nm) FMM	Mean	0,7805	0,4575	0,4768	0,6619	2,087	0,8000	2,793	4,668
	SEM	0,07615	0,08226	0,1023	0,04104	0,1489	0,09742	0,3344	0,5578
RPV phase (deg) FMM	Mean	0,3060	0,1678	0,2251	0,1769	0,7158	0,2786	0,1989	0,8104
	SEM	0,02552	0,01144	0,03402	0,01159	0,09190	0,05332	0,01286	0,09302

CONCLUSIONS

The drug resistance phenomenon and the lack of new therapeutic agents highlight the urgency in finding novel effective strategies for the treatment of fungal infections. The humanized monoclonal antibody H5K1 is an exquisite example of a step forward towards the application of biotechnological entities to a world almost completely ruled by synthetic compounds.

Even without the presence of the immune system apparatus, H5K1 not only was revealed to bind β-1,3-glucans of the fungal cell wall as seen in previous studies, but also to affect the cell integrity resulting as an enhancer for drugs like caspofungin and amphotericin B.

Summarizing our results, we demonstrated that: i) H5K1 disturbs *C. auris* topography producing irregularities and bumpy aspects especially when combined with caspofungin. ii) The perturbation extends also to the subdomains which appear more slacken and where molecular modifications occur. iii) hmAb alone but also caspofungin, amphotericin B and their combination with the antibody cause changes in the chemical distribution of the surface. iv) H5K1 increase the roughness when used alone and in combination. v) The presence of hmAb tends to stiffen the zones in which the binding to β-1,3-glucans occurs. vi) With almost every treatment *C. auris* cells are more deformable than the control; however, hmAb emphasizes the structural fragility especially if compared to the respective antifungal drug used alone. In conclusion, this study wants to show the perturbating effects produced on *C. auris* by hmAb H5K1 alone and in combination with commercially available antifungal drugs but also to demonstrate that AFM is a valuable tool for the investigation of microorganisms and of their morphological, structural, and biochemical changes induced by drug treatments.

CHAPTER 3

hmAb H5K1 activity

against clinical isolates of *C. glabrata*

Work currently in progress

I wish to express my gratitude to

Simona Fioriti Ph.D.

Gianluca Morroni Ph.D.

Professor Francesco Barchiesi

Professor Barbara Canonico

Caterina Ciacci Ph.D.

Professor Michele Menotta

INTRODUCTION

The global spread of antifungal resistance [1] together with the appearance of new strains sometimes intrinsically multidrug-resistant are seriously threatening public health [2, 3]. Moreover, the environmental changes [4], the massive use of antifungal agents in agriculture [5], the use of invasive surgeries and medical devices and the increase of subjects at risk are slowly worsening the situation [6]. Even if *C. albicans* is the most diffuse specie and keeps being the leading cause of invasive candidiasis, the rise of non-*albicans Candida* species (NACs) have significantly changed the fungal panorama [7]. In particular, the diagnoses have identified in *C. glabrata* and *C. parapsilosis* the most frequent fungal pathogens after *C. albicans*, sometimes also exceeding it in some settings [8, 9]. In particular, *C. glabrata* cases have been having increasing trends in different parts of the world becoming a concerning emergence. USA, Canada, and the North and the Centre of Europe seem to be the most struck areas [10] and the zones in which *C. glabrata* is responsible for more than 15% of the total *Candida*-related systemic infections [10, 11] and is the third most common cause of nosocomial infections [12]. Furthermore, *C. glabrata* often presents lower susceptibility to fluconazole [13] and other antifungal agents with well-known mechanisms as the mutation in FKS genes to grant resistance to echinocandins [14] and in ERG genes to reduce susceptibility to polyenes [15, 16]. Although *C. glabrata* is not able to form hyphae, it manages to adhere and colonize both biotic and abiotic surfaces and to form a biofilm. In particular, the biofilm is a virulent feature that guarantees protection from the host immune system and from some antifungal drugs [17]. *C. glabrata* showed generally the lowest metabolic activity and the smallest biomass compared to the other NACs but, to the other side, a high number of proteins and carbohydrates in the matrix [18, 19]. In this study, we used four strains of *C. glabrata* isolated from bloodstream infections. Two of them (85.40 and 1324Y) have mutations in FKS genes that make them less susceptible to echinocandins and one strain (406486) hyper producer of biofilm. These strains were exploited to test the antifungal activity of hmAb H5K1, a novel humanized monoclonal antibody able to bind selectively β-1,3-glucans, vital components of the fungal cell wall. H5K1 efficacy was previously evaluated on *C. auris* both alone and in combination with markedly available antifungal drugs [20]. The aim of this study is to confirm the activity of hmAb H5K1 on other *Candida* species, also echinocandin-resistant and biofilm hyper producer and to deeply investigate its eventual role in biofilm production.

MATERIAL AND METHODS

Microorganisms

Four *C. glabrata* strains (406486, 391216, 85.40 and 1324Y) were isolated from patients affected by bloodstream fungal infections. Two strains, 85.40 and 1324Y have a mutation in FKS genes making them less susceptible to echinocandins while 406486 is a hyper producer of biofilm. *C. parapsilosis* ATCC 90018 was purchased. *C. parapsilosis* and *C. glabrata* were let grow in Sabouraud solid agar for the maintaining and in RPMI liquid medium + MOPS 0.165 M, pH 7 for the experiments.

Material

Antibody H5K1 was produced and purified by Takis S.R.L. RPMI, MOPS, amphotericin B (AMB), caspofungin, micafungin, anidulafungin (ANIDU) and fluconazole, Bovine Serum Albumin (BSA), XTT sodium salt and menadione were purchased from Sigma-Aldrich while Sabouraud CAF agar was bought from Liofilchem, the anti-human IgG FITC antibody (ab97224) from Abcam and the paraformaldehyde from Carlo Erba.

Flow cytometry and confocal microscopy

From an overnight inoculum, *Candida* stains cells were washed in RPMI+MOPS and ~10^6 CFU/ml were resuspended in PBS 3% (w/v) BSA and 12 μg/ml of hmAb H5K1 was added and left incubating for 1 hour at 37 °C (PBS was used for the positive controls). The cells were then washed with PBS and marked with anti-human IgG FITC antibody (Abcam, ab97224) diluted 1:150 in PBS 3% BSA for 1 hour. After washing again, the samples were fixed with paraformaldehyde 4% in PBS for 1 hour at 4 °C. Finally, after removing paraformaldehyde through washing the samples were resuspended in PBS and each of them was divided in two aliquots. An aliquot was used for the analysis at the flow cytometer (FACScanto II, BDBioscences, Erembodegem, Belgium), equipped with three lasers (488 nm, 633 nm, 405 nm) to evaluate the FITC fluorescence due to the conjugation to the hmAb compared to the cells' autofluorescence. The other was used in confocal microscopy.

Minimum inhibitory concentration

The minimum inhibitory concentration (MIC) was assessed following the microdilution method of EUCAST guidelines using *C. parapsilosis* ATCC as a reference strain. The antifungal drugs tested were amphotericin B, caspofungin, micafungin, anidulafungin and fluconazole. In brief, ~10^5 colony-forming units (CFU)/ml were treated with increasing concentrations of antifungal drugs for 24 hours at 37 °C. The determination of the MIC is based on the absorbance readings at 405 nm. For amphotericin B, MIC is considered as the lowest concentration giving the 90% growth inhibition compared to the control while for caspofungin, micafungin, anidulafungin and fluconazole is the lowest concentration giving the 50% of growth inhibition compared to the control.

Checkerboard assay

To see an eventual enhancement effect of the antibody H5K1 in combination with the antifungal drugs, ~10^5 CFU/ml of each strain were treated with serial 1:2 decreasing concentrations of antibody and compound both alone and in combination in a 96-well plate. The starting concentration of the antifungals was chosen as 1-fold higher compared to the MIC results while H5K1 starting concentration was based on previous studies. The plates were left in incubation at 37 °C for 24 hours and then the absorbance at 405 nm was read. FICI values were classified as follows: FICI ≤ 0.5 synergic, 0.5 <FICI ≤1 additive, FICI>1 indifferent. Every experiment was performed in duplicate.

Minimal fungicidal concentration

From the plates of the checkerboards an aliquot of the wells in which the absorbance was under the MIC value was serially diluted and spread on Sabouraud agar plates. After 24 hours of incubation at 37 °C, the CFU were counted. The minimal fungicidal concentration (MFI) considers a growth inhibition of 90%.

Time-kill curves

Based on the checkerboards and MCFs data, several concentrations of H5K1in correspondence of the MIC of anidulafungin and amphotericin B were selected and tested both alone and in combination. The sample with only *Candida* spp. was used as positive control while the treatments with the anidulafungin and amphotericin B alone were used to assess the additive and synergistic effects respectively. Briefly, ~10^5 CFU/ml of every strain were treated with PBS, hmAb, the antifungal drug and hmAb + antifungal drug for a total of 24 hours at 37° C. At 0, 4, 8 and 24 hours an amount of each sample was diluted, spread on Sabouraud agar plates and left incubating at 37° C. The count of the colonies was done after 24 hours. Synergy is defined as a ≥2 log decrease in CFU/ml between the combination and its most active constituent after 24 hours.

Atomic Force Microscopy

The bottom of the wells of a 12-well plate was covered with a round 35 mm-diameter dish and then ~10^6 CFU/ml in RMPI+MOPS were seeded. The cells of the four strains were incubated 24 hours at 37 °C with the aim to let them develop the biofilm. After washing with PBS, the cells were treated with 50 μg/ml of hmAb H5K1 and left incubating again for 24 hours at 37 °C. The cells were washed again before fixing with paraformaldehyde 4% in PBS for 1 hour at 4 °C. To better remove the paraformaldehyde, the samples were washed and finally, the glass sheets were gently removed and analyzed at the atomic force microscope. The instrument was set in true non-contact mode and topography, amplitude, error, and phase signals were acquired during the imaging.

Polysaccharide content

To evaluate the polysaccharide content the method of da Silveira et al. [21] was followed with a few modifications. ~10^6 CFU/ml in RMPI+MOPS were seeded in a 24-well plate and washed after 90 minutes

(adhesion phase). Then RPMI+MOPS was poured again in the wells with the addition of 50 μg/ml of hmAb H5K1 for the treated samples and PBS for the controls. The plate was incubated 24 hours at 37 °C and after washing with PBS the wells were scarpered in 1 ml of PBS. The cells were centrifuged at 10 000 g for 10 minutes at 4 °C and the pellet was resuspended in PBS and sonicated at 35 Watt in ice (5 cycles of 30 seconds and a pause of 1 minute). The samples were centrifuged again (10 000 g for 10 minutes at 4 °C) and the supernatants were collected. To see the polysaccharides' content the phenol/H_2SO_4 method was adopted. In brief, 200 μl of phenol (5% w/v) were added to 200 μl of supernatant and, after mixing, 1 ml of H_2SO_4 conc. was gently poured in. The samples were left 10 minutes RT and then left incubating 30 minutes at 30 °C. Finally, the absorbance was read at 485 nm and the glucan content was evaluated using a standard curve of glucose (0, 5, 10, 20, 40 and 80 μg/ml).

Biofilm assays

Using the same concentrations of the time-kill curves, hmAb H5K1, anidulafungin, amphotericin B and the combinations of the hmAb with each antifungal drug were tested in a biofilm inhibition and in a biofilm destruction assays. Both the metabolic activity and the biomass were evaluated. For the experiments ~10^6 CFU/ml in RMPI+MOPS were seeded in a 96-well plate. To see the eventual inhibition, the seeded cells were immediately treated with the agents alone and in combination (PBS was used as positive control and wells without seeding were the negative controls). The plate was incubated at 37 °C for 24 hours and after three washes, to assess the metabolic activity 20 μl of MTS (Promega) /PMS (Sigma-Aldrich) solution were added to 100 μl of PBS in the wells and after 3 hours the absorbance at 492 nm was read [22] while for the biomass 100 μl of crystal violet (0.1% in PBS) were added and left dying for 15 minutes at room temperature. After washing, ethanol 96% was added and left incubating for 15 minutes at room temperature. Absorbance was read at 570 nm [23]. For the biofilm disruption assay, the seeded cells were incubated 24 hours at 37° C before adding the treatments, then the methodology used is the same as before.

Statistical analyses

Data were analyzed by GraphPad Prism software. The statistical Kruskal-Wallis analysis of variance (ANOVA) on Dunn's test for multiple comparisons was adopted for the biofilm inhibition and disruption, two-way ANOVA with Sidak's multiple comparisons test was used for AFM data and the Wilcoxon signed-rank test for the polysaccharide content.

RESULTS

Flow cytometry and confocal microscopy

The fungal pathogen *Candida glabrata* is a common cause of candidiasis especially in immunocompromised patients. Especially in systemic infections *C. glabrata* may be present in both yeast and hyphal form [24] since the reversible transition from spherical budding yeast to pseudohyphal or hyphal filaments is influenced by body temperature, serum, pH and CO_2 concentration [25]. The two forms aren't just recognized by immune cells in a different way [26] but are also believed to have different roles: hyphae and pseudo hyphae facilitate tissue invasion, damage, and escape from host cells while yeasts tend to colonize mucosa, disseminate in the bloodstream, adhere to endothelial cells, and form biofilm [27]. Similar to other yeasts, *Candida glabrata* ages when it undergoes asymmetric, finite cell divisions which determine its replicative lifespan [28]. This study shows that in the analyzed phase, most of the *Candida glabrata* strains show a population consisting of over 30% unbudded cells (the subpopulation in green in figure 3) and of approximately 60% budded cells (the subpopulation in blue in figure 3). However, 406486 strain highlights an inversion of the frequencies of unbudded and budded cells (Fig.1). On the identified subpopulations, the MFI of our FITC-conjugated hmAb H5K1 was calculated, showing an increase of fluorescence intensities (corresponding to an increase of the hmAb H5K1 labelling) on the budded yeasts, as reported in literature [20]. Of note, 406486 shows a reduced MFI, in comparison to other strains, contemporary to a decreased percentage of budded cells (Fig. 2). It has been seen that the replicative fungal aging significantly affects the fungal resistance to phagocytic clearance and to drug treatments and that the old cells (budded cells) persist while the youngers (unbudded cells) are killed by neutrophils [29]. In our case, the ability to better recognize budding cells is an advantageous aspect hmAb H5K1. However, the net expression of MFI considering both the subpopulations is almost 100% for all the strains (97.9% 406486, 98.4% 391216, 98.2% 85.40 and 98.3% 1324Y) as shown in figure 3.

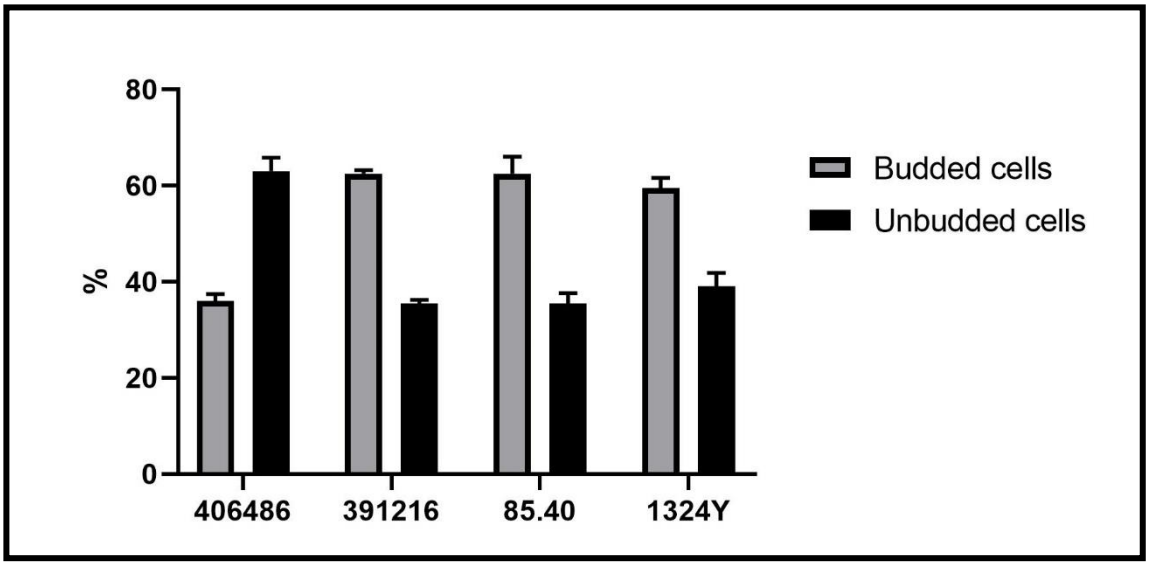

Figure 1. Flow cytometric analysis - percentage of unbudded and budded cells

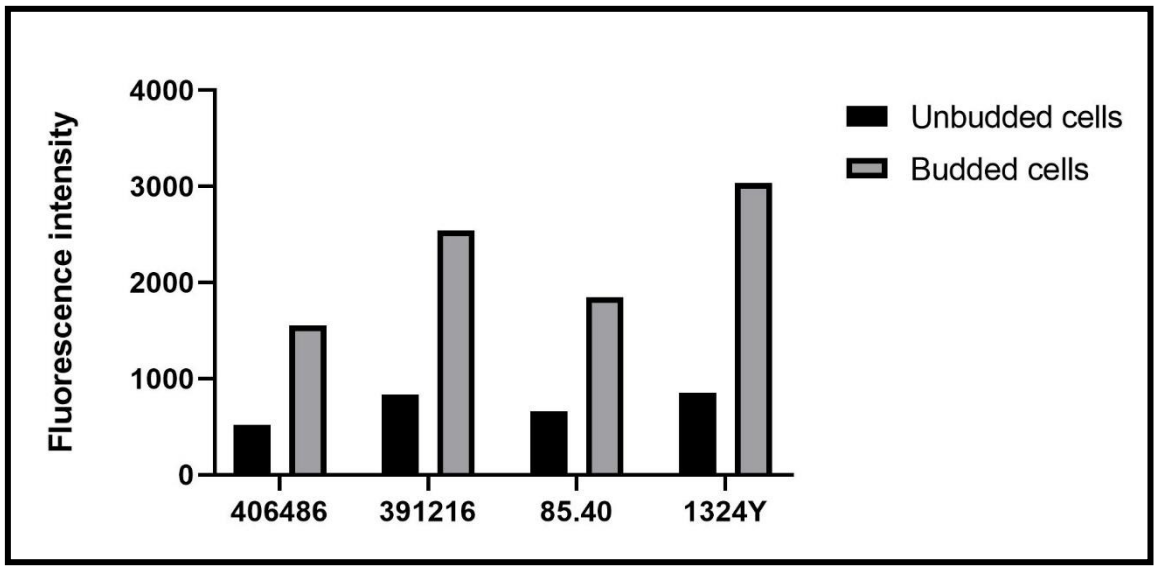

Figure 2. Flow cytometry analysis - MFI of unbudded and budded cells treated with hmAb H5K1

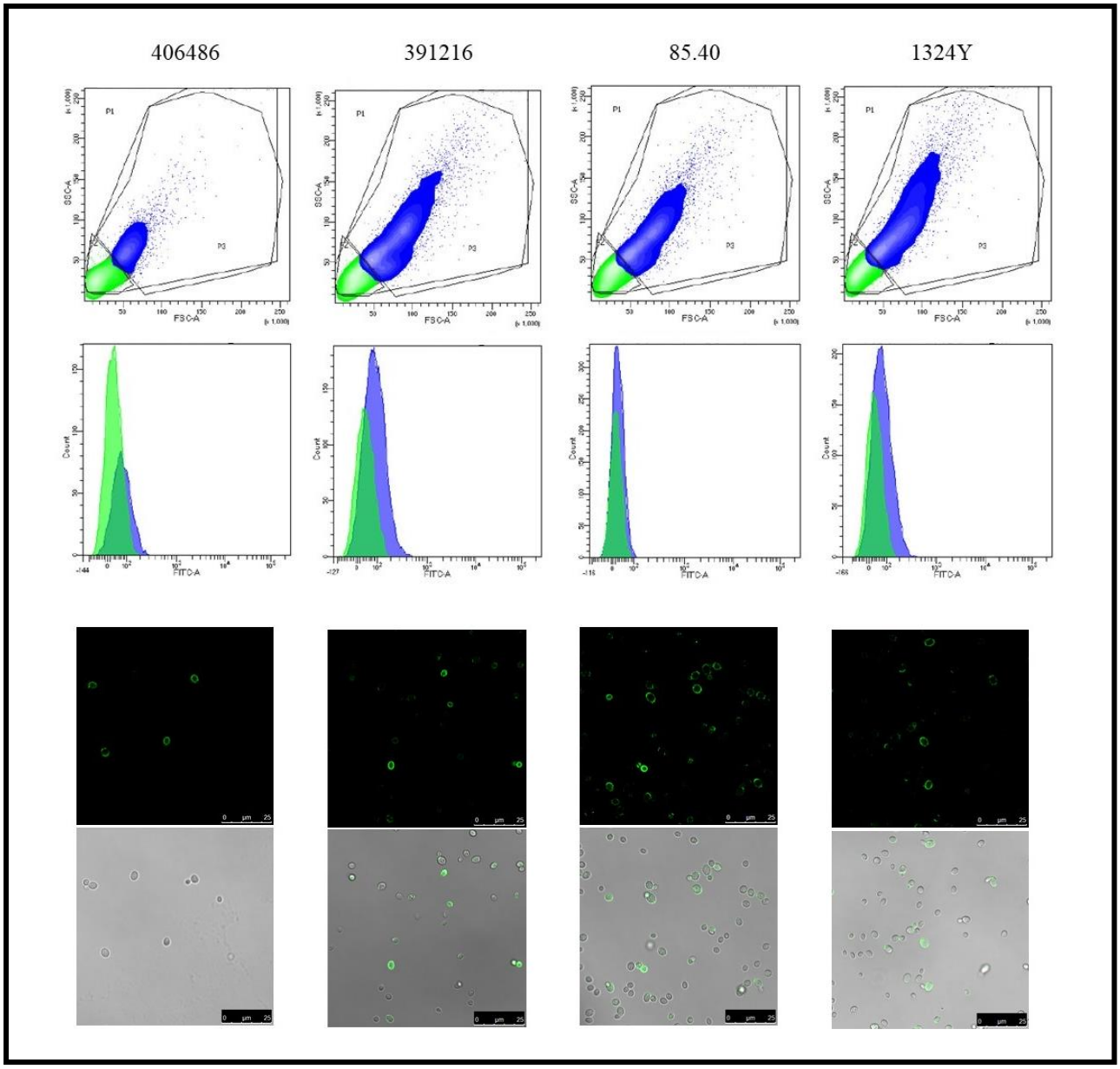

Figure 3. Binding analysis by flow cytometry (mean fluorescence intensity of the two subpopulations; in green the unbudded cells and in blue the budded cells) and confocal microscopy (green fluorescence and bright-field images).

Minimum inhibitory concentration

The four *C. glabrata* strains were treated with five antifungal agents with the aim to find the minimum inhibitory concentration for each of them (Table 1). While for amphotericin B the MIC values are the same, for the other drugs they vary more with similarities in pairs. The two strains without mutation in FKS genes (406486 and 391216), fairly and obviously present lower MICs for all the echinocandins except 406486 and the MICs for caspofungin are generally higher than those for micafungin and anidulafungin. This is quite normal and can be explained by the fact that caspofungin entered the clinic some years before the others and has been being a first-line drug, especially for candidiasis. Fluconazole has the highest concentrations of MIC, and this is consistent with its large use in the clinic.

	Antifungal drugs – MIC (μg/ml)				
C. glabrata strains	Amphotericin B	Caspofungin	Micafungin	Anidulafungin	Fluconazole
406486	0.5	0.5	<0.004	0.015	>16
391216	0.5	0.12	<0.004	0.015	>16
85.40	0.5	2	0.03	0.25	128
1324Y	0.5	0.25	0.016	0.06	>128

Table 1. MIC values expressed in μg/ml of the four *C. glabrata* strains for each antifungal drug.

Checkerboard assay and MFC

One representative of each antifungal class was selected to investigate the eventual enhancement effect born from the combination of the humanized antibody H5K1 with each of them on *C. glabrata* strains. Amphotericin B for the polyene class, anidulafungin for echinocandins and fluconazole for the azoles were tested in the checkerboard test. All the strains demonstrated a synergistic effect when treated with amphotericin B and the antibody as shown in figure 4 and demonstrated with FICI values lower than 0.5 as reported in Table 2. When H5K1 was combined with anidulafungin (Fig. 5) it revealed an enhancement resulting additive with FICI higher than 0.5 and finally, the combination with fluconazole appeared to have an indifferent effect (Fig. 6). In the MFC evaluation, the fungicidal activity was detected only at concentrations of amphotericin B 1-fold higher than the synergic combinations.

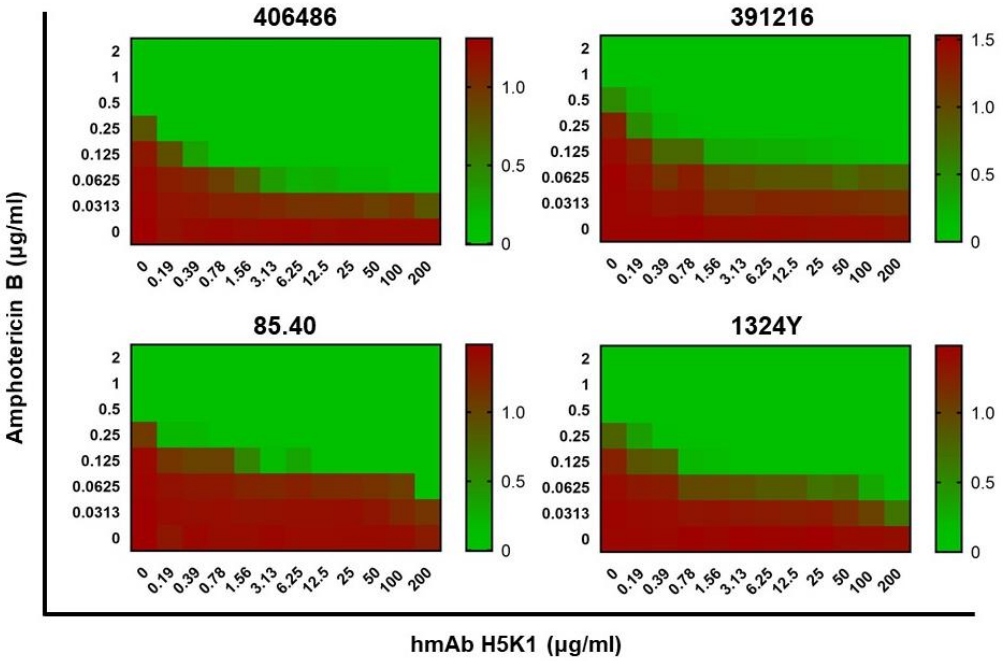

Figure 4. Checkerboards of the four *C. glabrata* strains treated with decreasing concentrations of amphotericin B, of H5K1 and of their combinations.

Table 2. Concentrations of hmAb H5K1 and amphotericin B that in combination gave the best FICI values. All the FICI values confirm a synergistic effect (synergy when FICI ≤ 0.5).

C. glabrata *strains*	Concentrations (µg/ml) hmAb / AMB	FICI
406486	0.78 / 0.125	0.252
391216	1.56 / 0.25	0.254
85.40	12.5 / 0.125	0.281
1324Y	3.13 / 0.125	0.258

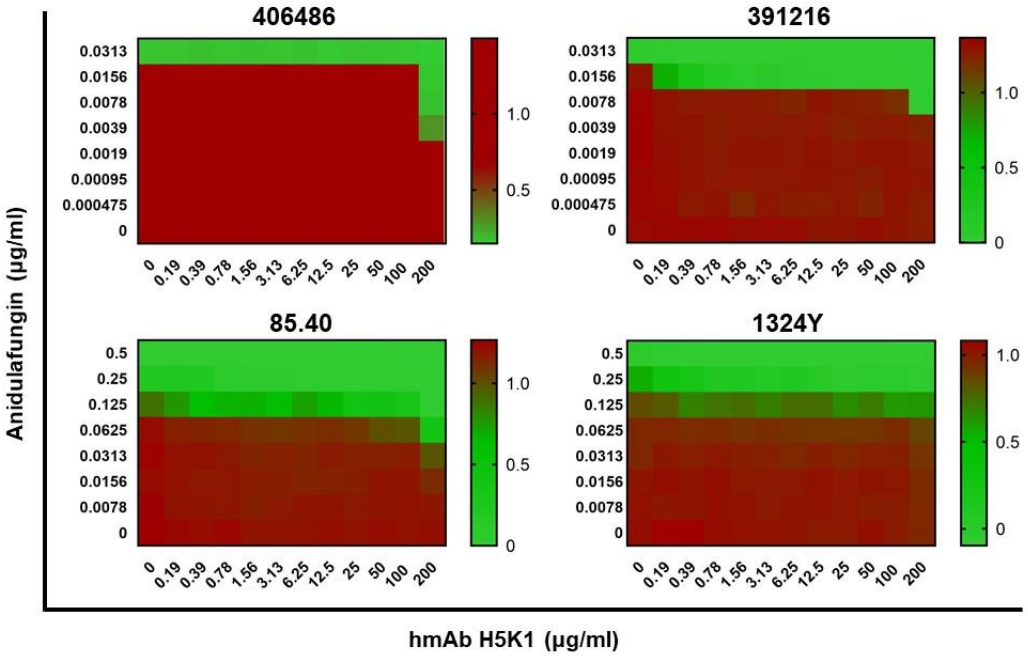

Figure 5. Checkerboards of the four *C. glabrata* strains treated with decreasing concentrations of anidulafungin, of H5K1 and of their combinations.

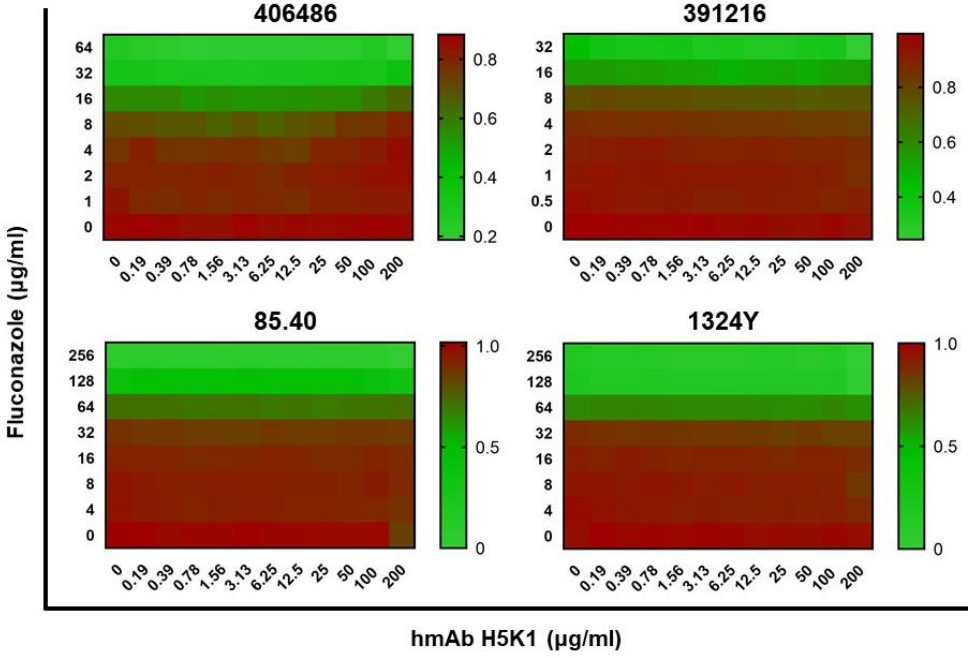

Figure 6. Checkerboards of the four *C. glabrata* strains treated with decreasing concentrations of fluconazole, of H5K1 and of their combinations.

Time-kill curves

Several concentrations of hmAb H5K1, amphotericin B and anidulafungin were tested in combination with the intent to confirm the synergy and the additivity respectively. The aim was to find not just the most active combination but to reach an effective combination with the lowest concentration of both hmAb H5K1 and antifungal drugs. When combined with sub-MIC concentrations of amphotericin B, H5K1 seemed to suggest a synergistic effect ($\Delta\log \geq 2$ between the most active agent and the combination) (Fig. 7). For 406486, 391216 and 85.40 the maximal log-difference occurs at 24 hours of treatment while for 1324Y already at 8 hours. On the other hand, the combinations with sub-MIC concentrations of anidulafungin never reached a 2-log difference but demonstrated an enhancement effect compared to the drug alone. This improvement of the activity of anidulafungin is totally due to hmAb H5K1 presence, thus confirming the previous results of additivity from checkerboards (Fig. 8). The most important contribution of H5K1 is recorded at shorter timepoints (4 and 8 hours) for all the strains with a decrease of the combinatorial effect at 24 hours for three out of four strains. These data are just preliminary, more replicates must be done.

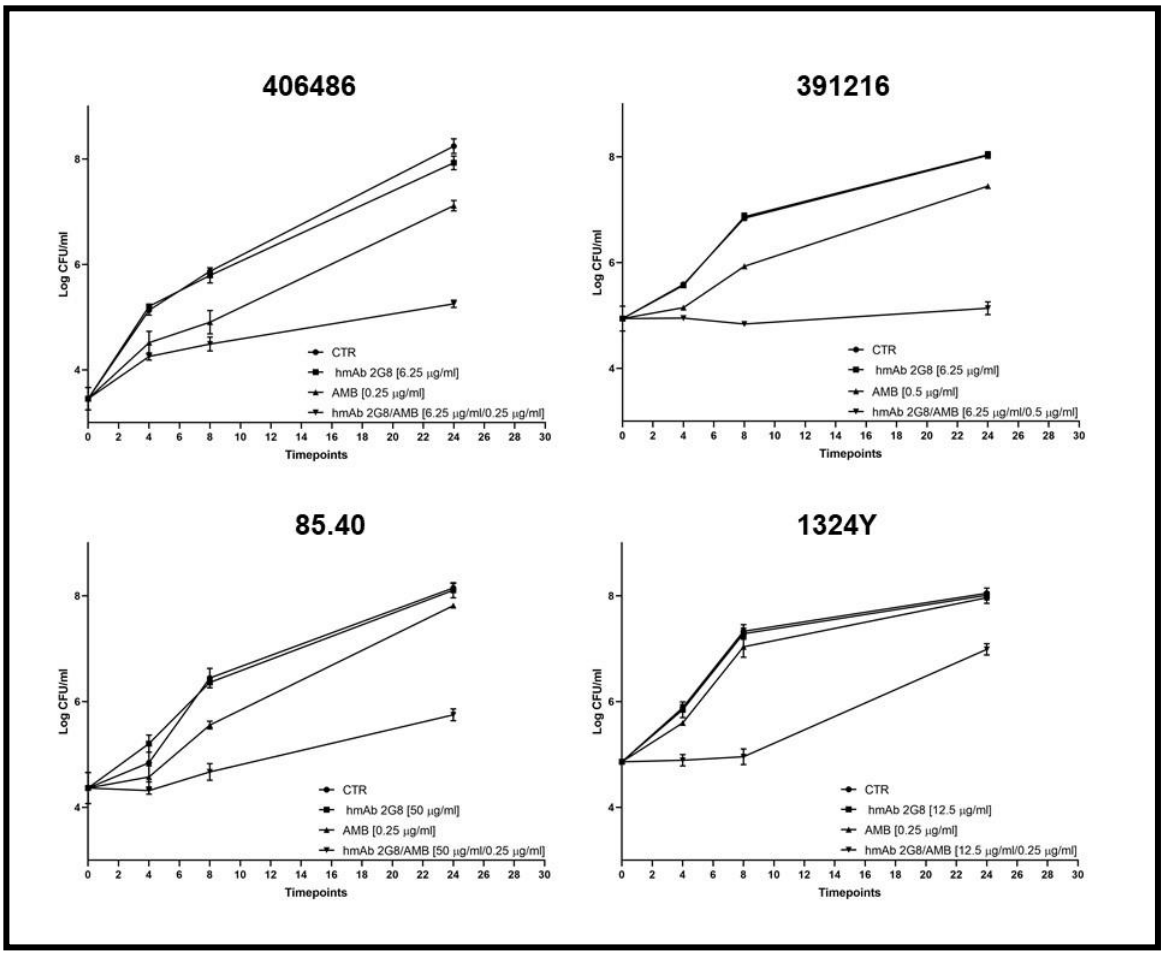

Figure 7. Time kill curves of the four *C. glabrata* strains treated with H5K1, amphotericin B, and their combination.

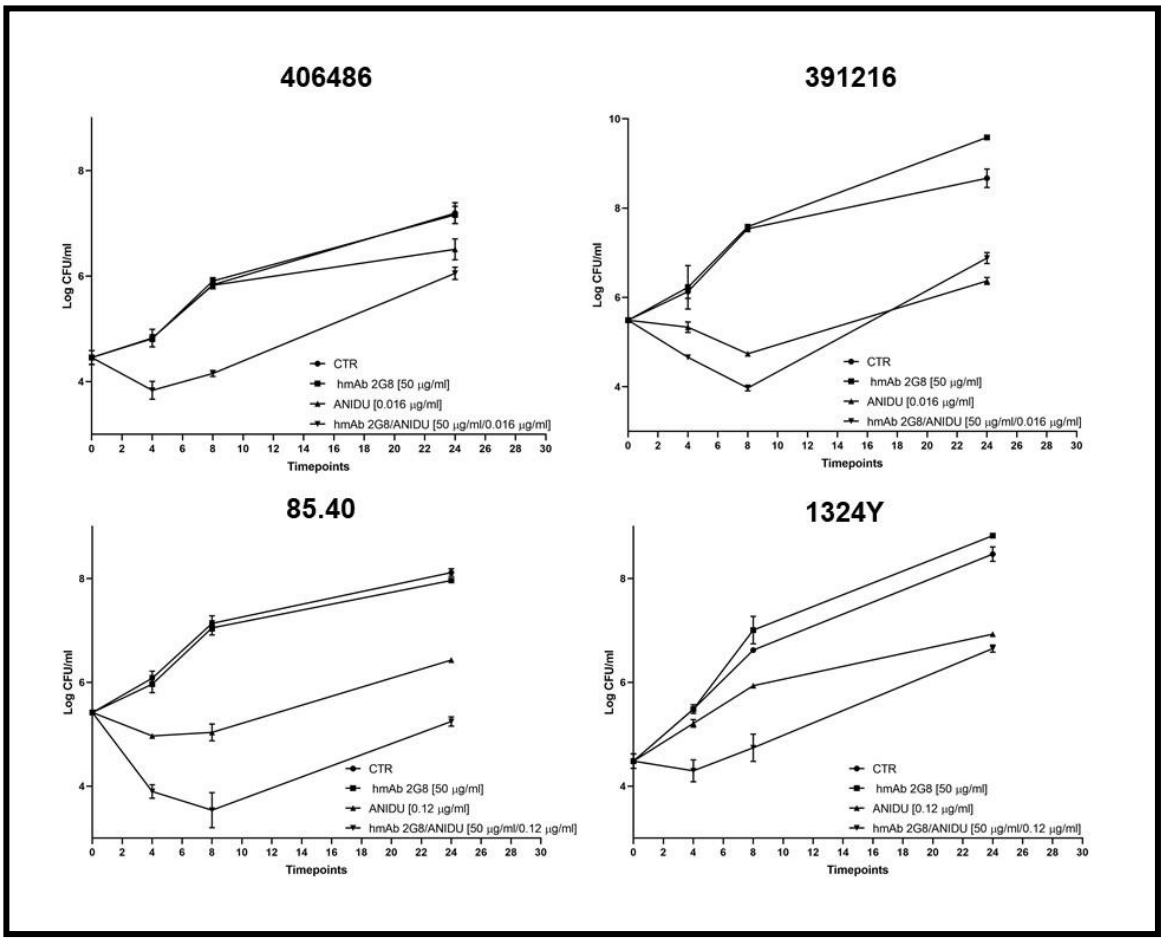

Figure 8. Time kill curves of the four *C. glabrata* strains treated with H5K1, anidulafungin, and their combination.

AFM analyses, **polysaccharides content** and b**iofilm assays**

In order to investigate the effect of hmAb H5K1 on biofilm formation, AFM analyses were performed on every strain. Both the length and the height of the biofilm were considered taking as baseline the dish surface and as end-measure spot the point of flex between *Candida* cells on a monolayer and the biofilm matrix (Fig. 9 A). The treatment with hmAb H5K1 caused a statistically significant reduction in the biofilm extension on 406486 strain (Fig. 9 B) and in the biofilm thickness on 391216, 85.40 and 1324Y strains (Fig. 9 C). Moreover, in the random sampling of the topographic images, from a visive analysis, there was a higher number of cells completely lacking in biofilm in the treated samples compared to the controls (Fig. 10). We can conclude that hmAb H5K1 has a perturbating effect on *C. glabrata* biofilm. After 24 hours from the beginning of hmAb H5K1 treatment, the polysaccharide content was measured as well. The matrix of fungal biofilm is mostly composed of polysaccharides, and in particular by glucans and mannans [30]. In light of the results obtained with AFM, the polysaccharide content was evaluated as well. The polysaccharide content underwent a statistically significant decrease with hmAb H5K1 treatment compared to the control in three strains out of four. The only strain that didn't face a decrease compared to the control was the hyper producer of biofilm 406486 (Fig. 11). Cellular metabolic activity during biofilm-forming and in a mature biofilm was considered and analyzed together with the biofilm biomass. The metabolic activity of the four strains was reduced in a statistically significant manner as well as the biomass in presence of the combination of hmAb H5K1 and amphotericin B during biofilm formation, meaning a strong inhibitory activity even compared to amphotericin B alone. In a mature biofilm the combination causes a reduction of the metabolic activity in every strain but not always it is statistically significant, and the biomasses reflect this trend (Fig.12). Neither anidulafungin nor its combination with hmAb H5K1 has strong inhibitory or disrupting activity on biofilm apart from a few exceptions. The general trend seems to lead to higher metabolic activity and increased biomass in the presence of the antibody and of sub-MIC concentrations of anidulafungin (Fig. 13).

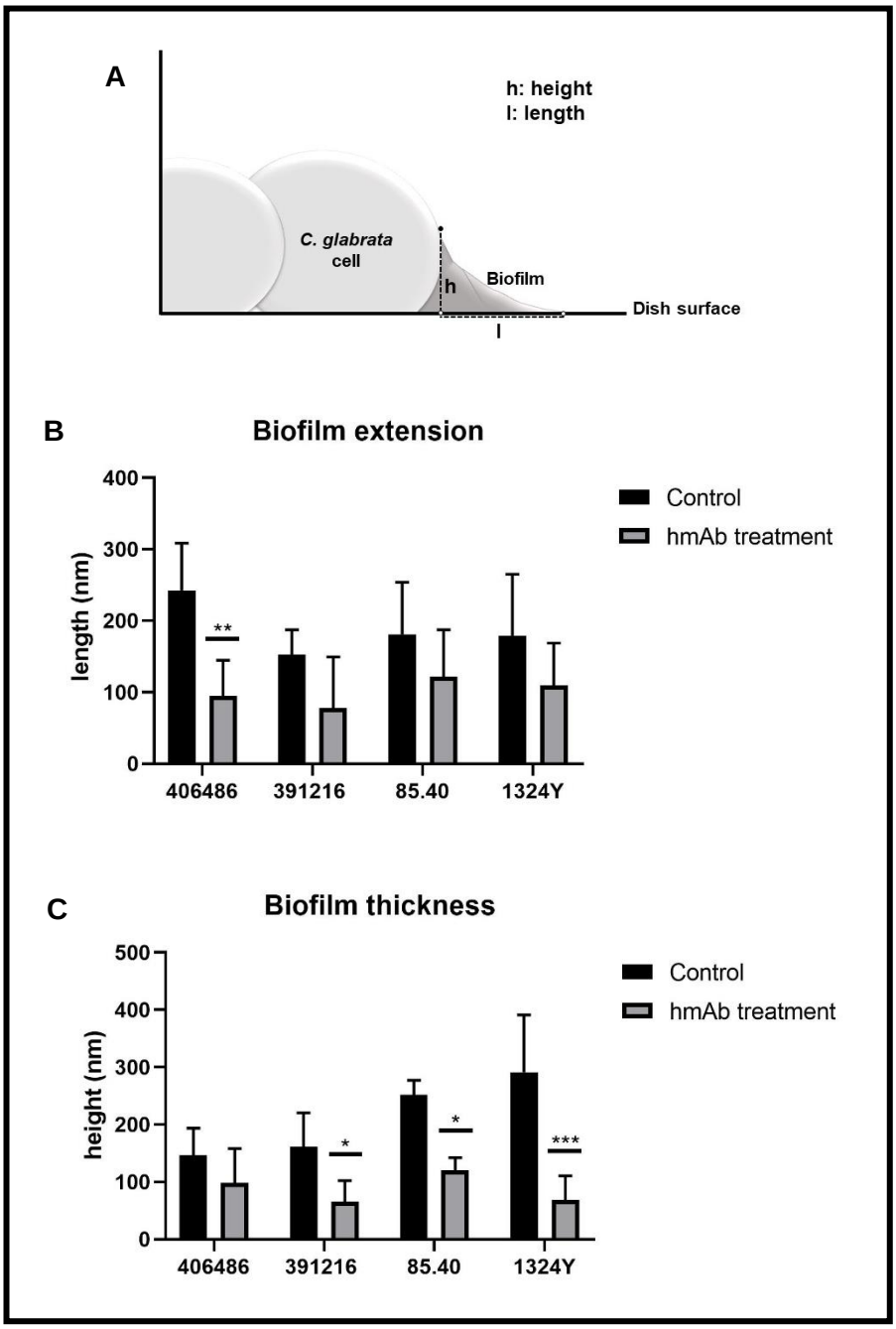

Figure 9. AFM analyses explanation of the measures considered (A). Evaluation of the extension (B) and of the thickness (C) of the biofilm with and without H5K1 treatment in all *C. glabrata* strains.

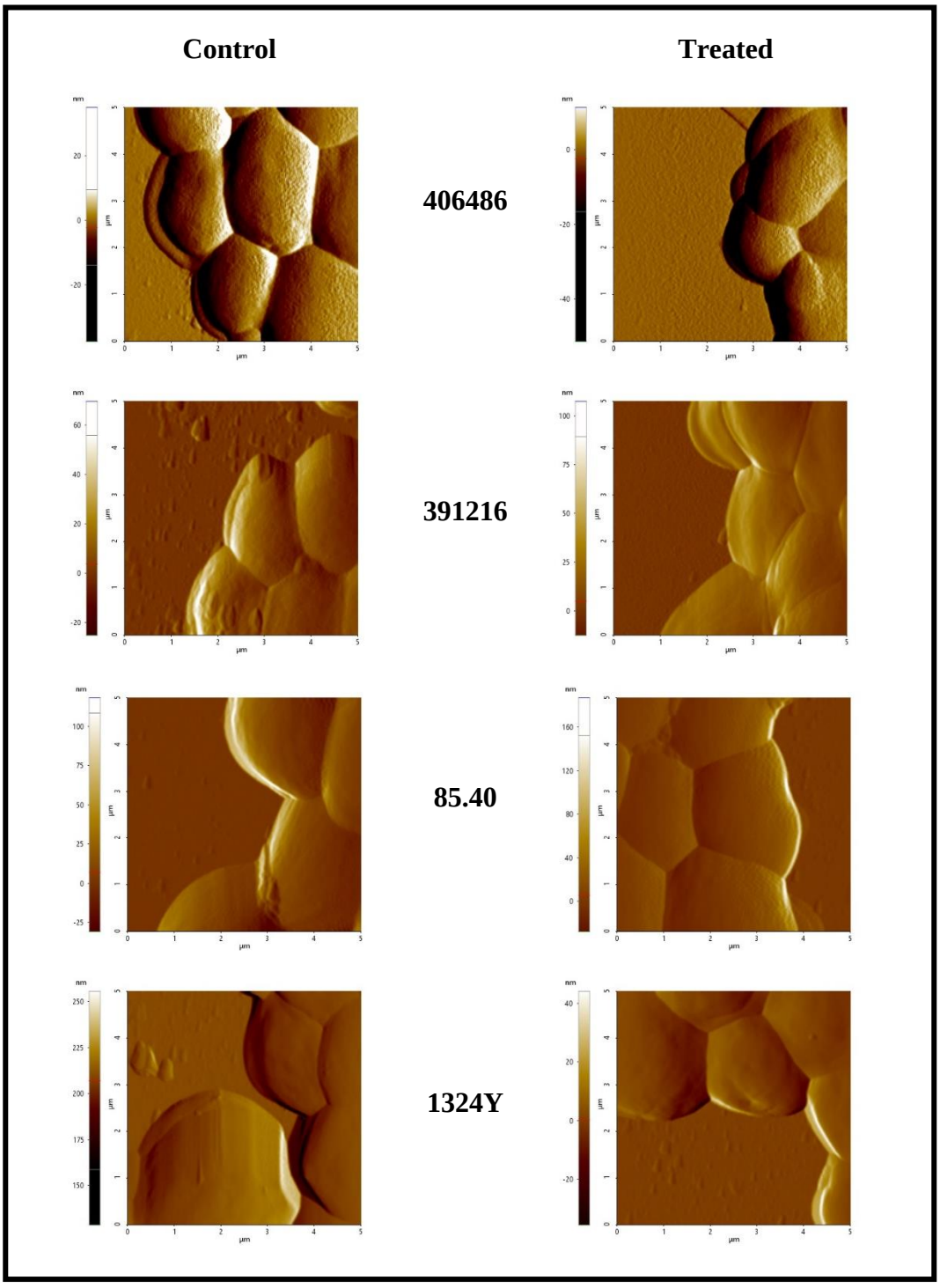

Figure 10. AFM images of the biofilm of the four *C. glabrata* strains with and without H5K1 treatment after 24 hours.

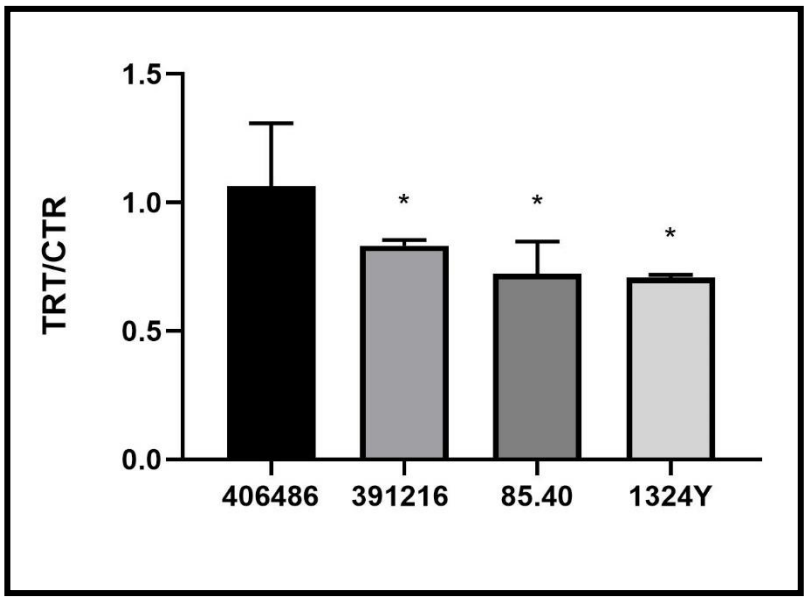

Figure 11. Polysaccharide content in the biofilm matrix – fold of decrease between the treated samples and the controls.

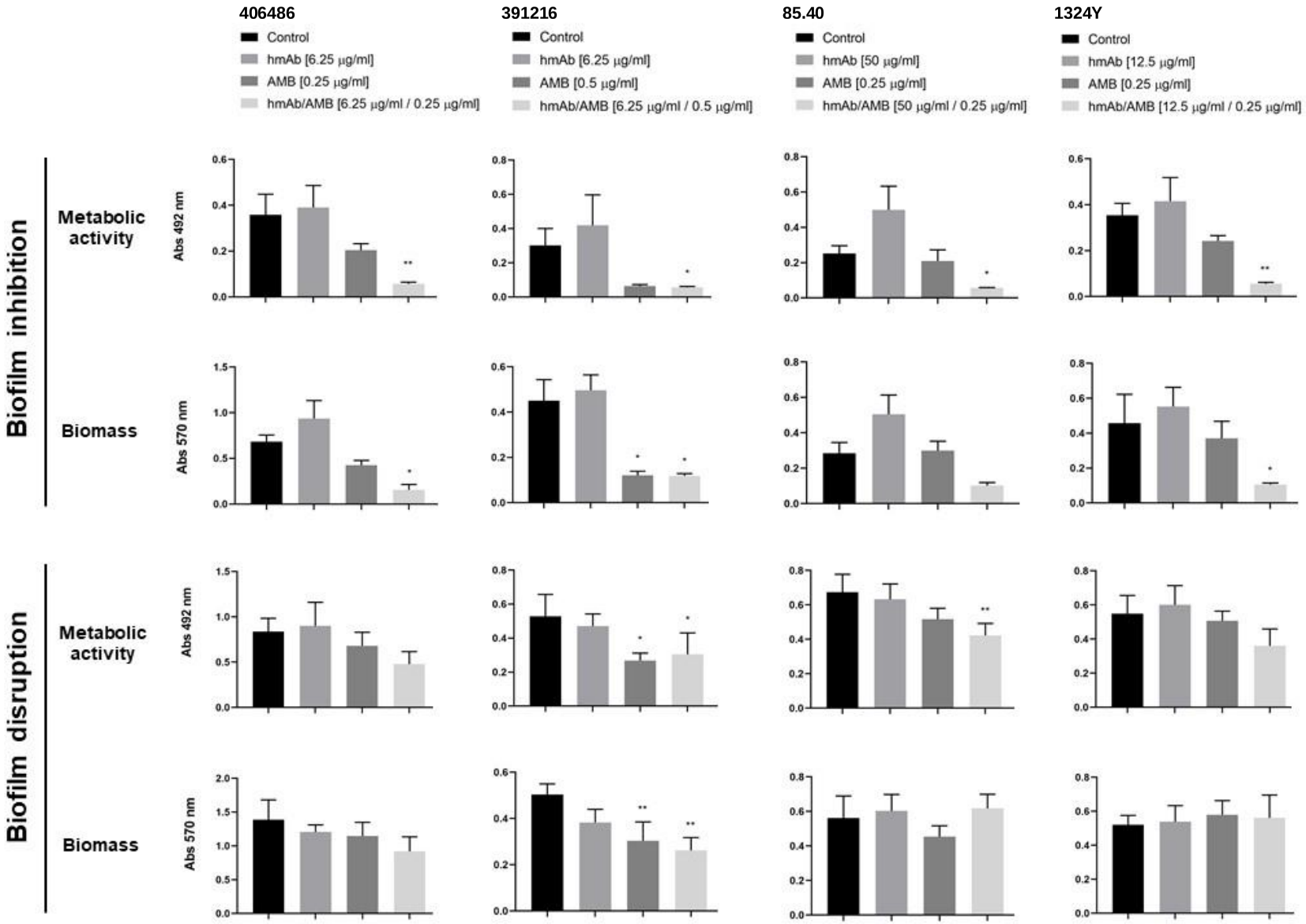

Figure 12. Biofilm inhibition and disruption experiments – Metabolic activity and biomass evaluation when *C. glabrata* cells are treated with hmAb H5K1, amphotericin B and their combination. The statistic significances are referred to the comparison with the control.

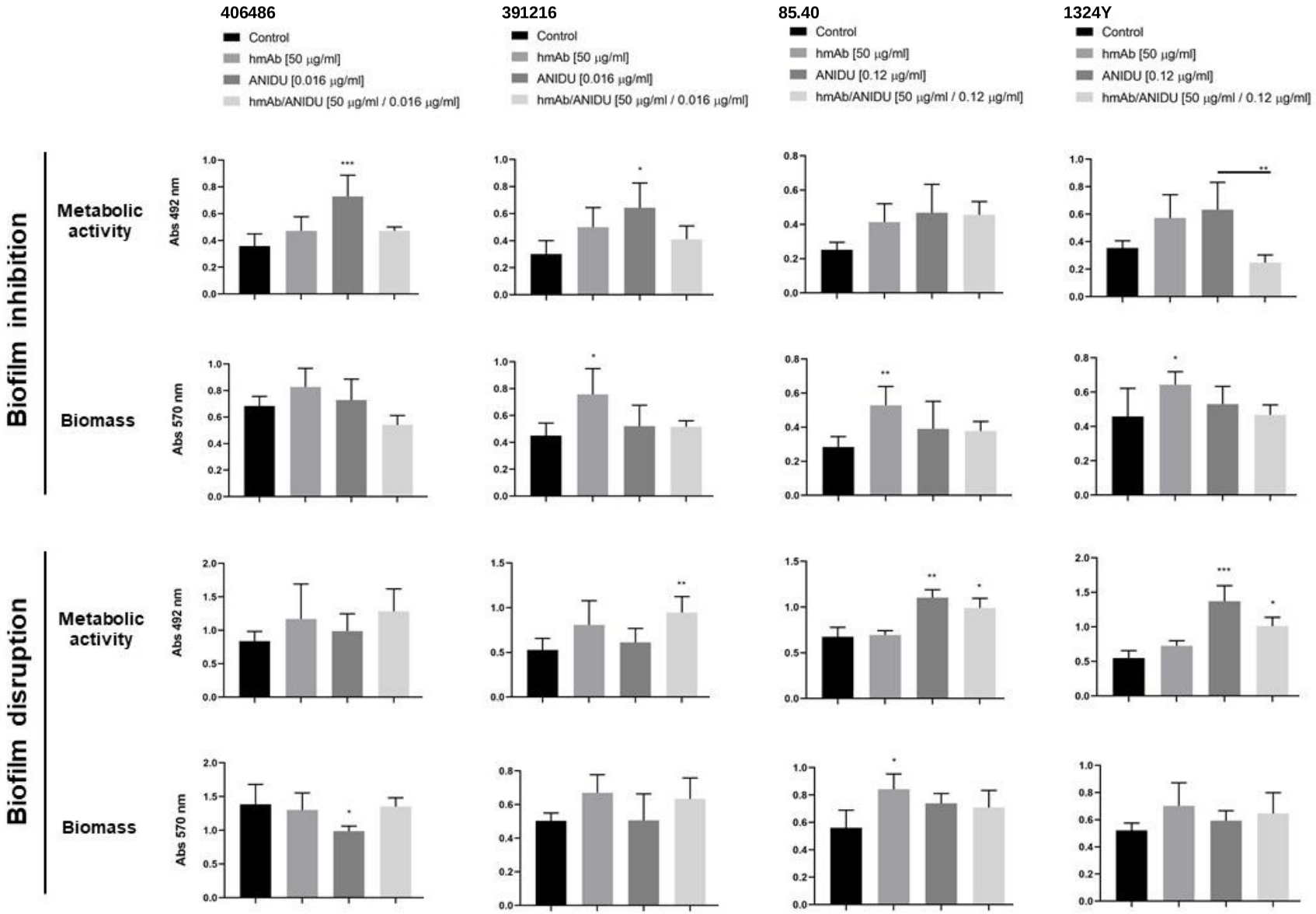

Figure 13. Biofilm inhibition and disruption experiments – Metabolic activity and biomass evaluation when *C. glabrata* cells are treated with hmAb H5K1, anidulafungin (ANIDU) and their combination. The statistic significances are referred to the comparison with the control.

DISCUSSION

C. glabrata is a non-*albicans Candida* specie that is causing great concern both for its large spread all over the world and for its intrinsic and acquired resistance to the mostly used first-line antifungal drugs. The aim of this study was to test the humanized monoclonal antibody H5K1 on *C. glabrata*. H5K1 was previously investigated on *C. auris* manifesting its greatest potential in combination with antifungals as amphotericin B and caspofungin. In this case, the aim is to find the lowest concentrations that in combination could maintain the synergy and the additivity in another *Candida* specie, precisely *C. glabrata* strains, biofilm-hyper producer and echinocandin resistant as well. In addition to that, we wanted to explore the hypothetical effect of hmAb both alone and in combination with antifungal drugs on the biofilm. For these reasons the research began from the binding capacity: H5K1 can bind every *C. glabrata* strain tested with almost 100% of FITC-positive cells moreover, an advantage is the ability to distinguish budded and unbudded cells hence the replicative aging which affects fungal resistance [29]. From these results, the checkerboards were essential to assess the possible enhancement effect of H5K1 in combination with three antifungal drugs chosen from different antifungal classes. Amphotericin B was the representative for the polyene class, anidulafungin for the echinocandins and fluconazole for azoles. The combination with amphotericin B was synergic for all four strains with the best FICI values abundantly under the threshold of 0.5. With anidulafungin, H5K1 had an additive effect while combined with fluconazole it demonstrated an indifferent effect. These results are consistent with those on *C. auris* but the added value consists in the concentrations of both the antifungal agents (the highest for both AMB and ANIDU was 0.25 μg/ml) and especially of the hmAb which are much lower compared to the previously used 250 μg/ml [20]. The fungicidal activity determined by the MFI was proper only of the combination with amphotericin B and at concentrations 1-fold higher compared to the FICI values. Considering these data and the previous ones we suppose that the booster effect of H5K1 is convenient only for echinocandins, and amphotericin B and can be applied to different *Candida* species. In order to confirm the synergy with amphotericin B and the additivity with anidulafungin, different combinations of concentrations of hmAb-AMB and hmAb-ANIDU were tested obtaining as a preliminary result, synergistic effects at sub-MIC concentrations of amphotericin B and additive effects at sub-MIC concentrations of anidulafungin, with hmAb H5K1 never overcoming 50 μg/ml. Furthermore, hmAb H5K1 seems to perturbate the biofilm integrity and the polysaccharide content (the latter in the "normal"-biofilm producers' strains). From the topographic analyses of the four strains treated or not with hmAb H5K1, it is evident that the antibody affects both the extension and the thickness of the biofilm matrix. Considering that the greater the extent of the biofilm, the thinner it is and vice versa, in the case of the biofilm-hyper producer strain there is a statistically significant difference in the matrix extension while for the other strains the reduction of thickness becomes statistically significant. We still don't understand the exact mechanism, but we suppose that its ability in binding β-1,3-glucans may be implicated in these outcomes. H5K1 is able to potentiate the effect of amphotericin B during biofilm formation meaning a strong inhibition with a statistically significant reduction of metabolic activity and decrease of biomass. The disruption of the biofilm is not as efficient, but the

combination performs always slightly better than amphotericin B alone. It is not surprising to see, sometimes a high biomass and a low metabolic activity: this happens when cells deep in the biofilm don't receive sufficient nutrients and die or because of the contact-dependent growth inhibition phenomenon [31,32]. The effect of the combination with anidulafungin is accentuated neither for the inhibition nor for the disruption of the biofilm. On the contrary, the metabolic activity and the biomass increased in presence of hmAb H5K1 and sub-MIC concentrations of anidulafungin. We speculate about the fact that since hmAb H5K1 causes a perturbation in the biofilm affecting its integrity, it can interfere in the contact-dependent growth inhibition re-activating yeast cells and stimulating an uncontrolled proliferation [30]. This could explain the high values of metabolic activity and biomass. If H5K1 is supported by a fungicidal compound as amphotericin B, the result is a potentiated activity as long as AMB can better reach *Candida* cells because of the antibody perturbation. This doesn't happen when the antibody is used alone or in combination with anidulafungin. Anidulafungin is fungistatic, it was used at sub-MIC concentrations and, as seen in time-kill curves, it starts losing its effect at 24 hours. We suppose that sub-MIC concentrations of anidulafungin alone have an effect like that of H5K1 hence, for the same reason, at the moment of absorbance evaluation we manage to see cells already metabolically active and abundant biomasses. In conclusion, the humanized H5K1 is effective also on *C. glabrata* specie, including strains echinocandins resistant and biofilm-hyper producer. It confirmed its enhancement effect in combinatorial treatments especially with amphotericin B and echinocandins even at lower concentrations and suggest having an effect also on the biofilm. We consider these results not just highly promising but extraordinary considering that H5K1 is a full-length antibody therefore its real potential can be revealed only in the presence of the immune system. Nevertheless, hmAb H5K1 demonstrated to be a powerful tool in managing fungal growth even in absence of immunity effectors. Further studies must be done, and other fungal species should be used (especially among filamentous fungi), but these data support the idea of hmAb H5K1 as a new drug candidate for the treatment of fungal infections and in particular of candidemia.

CHAPTER 4

Development of a humanised scFv derived from mAb 2G8 against pathogenic fungi

I wish to express my gratitude to

Professor Marzia Bianchi

Professor Rita Crinelli

INTRODUCTION

With the discovery of the double helix of the DNA by Watson and Crick, the age of gene technology started as well as the development of biological and biotechnological compounds that could be used in clinics [1, 2]. Novel techniques as the possibility to introduce foreign genes into an organism like bacteria together with the prospect to scale up the expression and the purification to have final clean products opened the route to a different approach to medicine [3, 4]. With the financial support of different companies [4, 5, 6], several biotechnological entities reached the market with a subsequent boom of the biotech sector [7]. In 1986 FDA approved the first ever monoclonal antibody, muromonab-CD3, a murine antibody anti-CD3 used for the prevention of transplant rejection [8]. Its mouse nature turned out to be a great obstacle since it stimulated the immune system giving severe immunogenicity reactions [9]. From that moment the humanization processes began, and the first result was revealed a few years later with natalizumab, a humanized monoclonal antibody anti-α4β1 integrin for the treatment of multiple sclerosis [10]. Almost simultaneously the antibody fragments raised interest, an example is the first chimeric antigen-binding fragment (Fab) anti-GPIIb/IIIa abciximab approved by FDA in 1994 for the inhibition of platelet aggregation in cardiovascular diseases [11]. The higher penetration given by the smaller sizes, the lack of glycosylation, hence the prospect of production in prokaryotic organisms and the low costs are the major advantages. However, the short half-life, the low stability and the risk of aggregation have limited a lot the entry into the market of several Fabs and single-chain fragment variables (scFvs) [12]. The monoclonal antibody 2G8 is a murine antibody IgG2b able to bind selectively β-1,3-glucans, fundamental components of the fungal cell wall, being effective against several pathogenic fungi both *in vitro* and *in vivo* [13, 14, 15]. The aim of this project is the development of a humanized scFv starting from the murine mAb 2G8 and the fine-tuning of a purification process able to make a clean product with an acceptable yield.

MATERIALS AND METHODS

Humanization of VH and VL regions of the murine monoclonal antibody 2G8

The amino acids sequence of the murine scFv has been analysed by ExPasy[16] to evaluate the *instability index*. The murine variable regions (VH and VL) were compared with the murine databases IMGT mouse V genes, IMGT mouse D genes and IMGT mouse J genes in *IgBlastToll* [17] software and were compared and mutated following the germlines found. The VH and VL were humanized by *IgBlastTool* launching their nucleotide sequences against the human germline databases IMGT human V genes, IMGT human D genes and IMGT human J genes [18,19]. According to CDR-grafting technique, two strategies have been explored: the first one was based on the analysis of the whole sequences of the murine VH and VL and the second strategy considered just the single frameworks. In both cases, the germlines with the highest identity with the initial sequences were selected and the non-homologous amino acids were changed only in framework regions (FRW). The two humanized scFvs (hscFv) were assembled and their *instability indexes* were analyzed again by ExPasy. The variable regions chosen were checked separately in PDB databases [20] and the output sequences with the closest homology and with an X-ray crystallographic resolution ≤ 2 Å were selected. In order to avoid the reduction of the target binding affinity and specificity, the amino acids in the Vernier Zone [21] positions were back-mutated to the original murine ones.

Humanized scFvs (hscFv) in VH-linker-VL and VL-linker-VH orientations: construction and cloning in pET22b (+)

The hscFv oriented in VH-linker-VL was synthesized *de novo* by GenScript and optimized with the codon usage for the expression in *E. coli* BL21(DE3) strain. The variable domains, joined with a linker of 15 amino acids $(G_4S)_3$, were cloned in pET22b (+) expression vector downstream pel B sequence, between Nco I and Hind III restriction sites, to have a periplasmic secretion, and a 6-Histidine tag at the C-terminus of the protein. The hscFv was obtained also in VL-linker-VH orientation. To build the reverse sequence, the variable regions were amplified separately by PCR endpoint with specific primers (Table 1) using the high-fidelity thermophilic DNA polymerase Vent DNA Polymerase (BioLabs). After purification with MiniElute PCR purification Kit (Qiagen), 50 ng of each purified variable region were used to create the new hscFv by SOE-PCR. The thermal profile of the reaction was: denaturation at 95 °C for 3 min, 5 cycles of denaturation at 95 °C for 1 min, annealing at 63 °C for 1 min and extension at 72 °C for 1 min, 5 cycles of denaturation at 95 °C for 1 min, annealing at 56 °C for 30 sec and extension at 72 °C for 1 min, 25 cycles of denaturation at 95 °C for 30 sec and extension at 72 °C for 1 min.

The resulting fragment was purified with the MiniElute Gel-extraction purification Kit (Qiagen) and was digested with Nco I and Hind III restriction enzymes, as for the expression vector pET22b (+). The ligase reaction was performed with Anza Ligase (ThermoFischer) enzyme and competent *E. coli* BL21(DE3) cells were transformed. The positive clones were checked by colony PCR and underwent a miniprep with QuiaPrep

Spin Miniprep Kit (Qiagen) to be sequenced. T7 promoter and T7 terminator primers were used for both colony PCR and sequencing.

Table 1. Primers used to amplify VL-linker-VH sequence. F: forward, R: reverse.

Sequence (5'>3')	F/R
5'-TTCCTGCCATGGACATTGTGATGACCCAGAC-3'	F
5'-ACCAGAGCCGCCGCCGCCGCTACCACCACCACCACGTTTGATTTCCACTTTGG-3'	R
5'-AGCGGCGGCGGCGGCTCTGGTGGTGGTGGTTCCCAGGTTCAACTGGTCCAAAG-3'	F
5'-GGAAGTTAAGCTTTTAGGAACTAACGGTCACCAGG-3'	R

Cloning of a monomer, dimer, and trimer of the human ubiquitin in pET45b (+)

The histidine-tagged ubiquitin-based expression vectors were constructed starting from the pET45b (+) (Novagen) plasmid backbone. The pET45b (+) was digested with Pml I and Bam HI in order to insert the coding sequence for one or more ubiquitin (Ub) monomers, in frame with the N-terminal His-tag, provided by the vector itself. The wild-type Ub coding sequence was PCR amplified from HeLa cDNA, obtained from total RNA purified with the RNeasy Plus Mini kit (Qiagen), reverse-transcribed using PrimeScript™ RT Master Mix (Perfect Real Time; Takara Bio Europe SAS, Saint-Germain-en-Laye, France), according to manufacturer´s instructions. Amplification of Ub coding sequence was performed with the Platinum Pfx DNA polymerase (Invitrogen, Carlsbad, CA, USA), according to the protocol, and the degenerate primers reported in table 2.

Table 2. Primers used to amplify a monomer, dimer, and trimer of ubiquitin. F: forward, R: reverse.

Sequence (5'>3')	F/R
5'-CGTCACGTCACGTGATGCAGATCTTCGTGAAGACC-3'	F
5'- ACGTGACGGGATCCACCGCGGAGACGGAGCACCAGGTGC-3'	R

The forward primer was engineered to be cut with Pml I restriction enzyme, while the reverse primer, carrying a Bam HI cutting site, was designed to allow the deletion of the translation stop codon at the end of the insert. Moreover, the presence of a Sac II cutting site in the reverse primer which matches with the last Ub codons

can be exploited to clone downstream any coding sequence hence, to obtain a fusion product with Ub at the N-terminus without any intervening amino acid residue and with an available internal Sac II cleavage site. The PCR conditions were: 2 min at 94 °C; 35 cycles of denaturation at 94 °C for 15 s, annealing at 62 °C for 15 s, and extension at 68 °C for 1 min. At the end of PCR cycles, the amplified products were analyzed through agarose gel electrophoresis. Ub is encoded in mammals by different genes which are transcribed in different mRNAs containing one (UBA52 and RPS27A) or more Ub CDS in tandem (3 for UBB and 9 for UBC, respectively) sharing a high homology. This explains the PCR output with the two degenerate primers reported above, which displayed different bands corresponding to one or multiples of Ub coding sequence (Fig. 1). The PCR products of Ub monomer, dimer and trimer were gel-purified by the Gel Extraction Kit (Qiagen), double-digested with Pml I and Bam HI and then inserted into the pET45b (+) vector cut with the same restriction enzymes. Screening and purification of positive clones were performed as above. All pET45b (+)/Ub constructs were validated and confirmed through DNA sequencing using a PE310 Perkin Elmer capillary sequencer.

Cloning of ubiquitin monomer-, dimer- and trimer-hscFv in pET45b (+) and ubiquitin dimer- and trimer-hscFv in pET22b (+)

The hscFv VL-Linker-VH was amplified from vector pET22b (+) with specific primers and was purified with the MinElute PCR Purification Kit (Qiagen). Based on the cloning vector, it was digested with different restriction enzymes: Pml I (Anza) and Bam HI (Anza) to clone inside the pET45b (+) downstream the 6-His tag and Ksp I (Roche, isoschizomer of Sac II) and Hind III (Anza) to introduce it in pET45b (+) downstream Ub-trimer/dimer/monomer (Fig.2). After the purification with MinElute PCR Purification Kit (Qiagen), the digested hscFv was ligated with each of the mentioned plasmids already digested and hydrolyzed with Calf-intestinal alkaline phosphatase (Anza). Competent *E. coli* BL21(DE3) cells were transformed then the colonies were checked by Colony PCR and used for a MiniPrep (QIAprep Spin Miniprep Kit Qiagen). The positive clones were sequenced. To obtain the Ub dimer and trimer hscFv with His Tag at C-terminus, the constructs Ub dimer-hscFv and Ub trimer-hscFv were amplified from the cloning vector pET45b (+) with specific primers containing Nde I and Hind III restriction sites. The amplified DNA fragments were purified with the Qiagen PCR purification kit and treated with Nde I and Hind III. The same enzymes were used to digest pET22b (+) to remove the pel B sequence (Fig.3). After the purification by Qiagen gel extraction kit, the digested constructs were ligated into the expression vector and used to transform competent *E. coli* BL21(DE3) cells. Bacteria were spread on agarose plates containing 100 µl/ml of ampicillin (Sigma-Aldrich) and the vectors with the right inserts were selected and expressed.

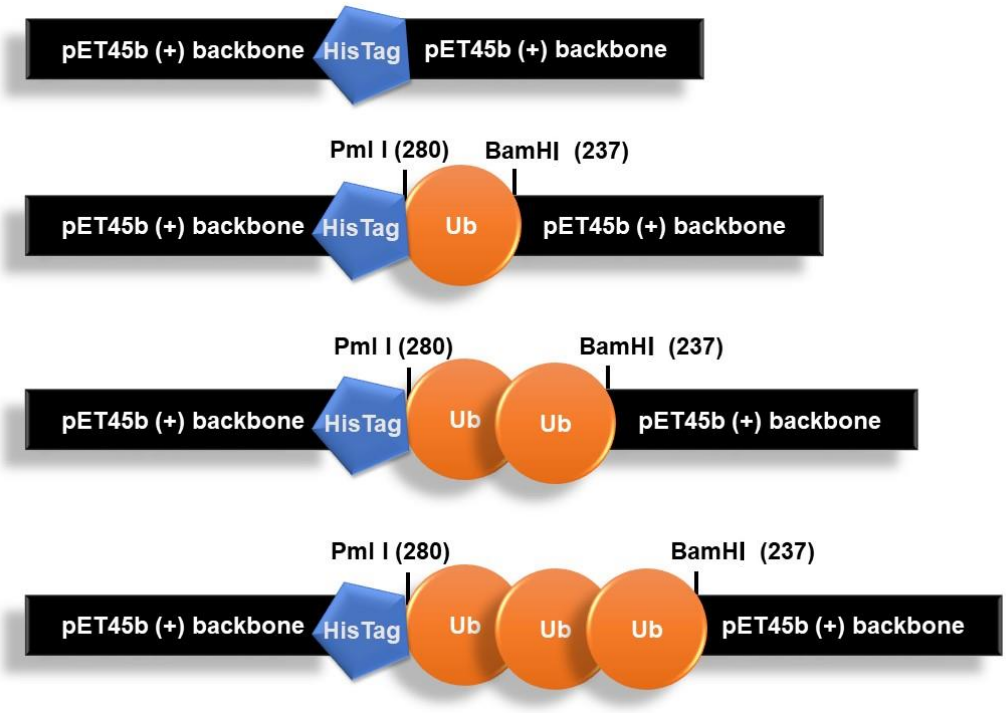

Figure 1. Cloning of Ub monomer, dimer ant trimer in pET45 b (+)

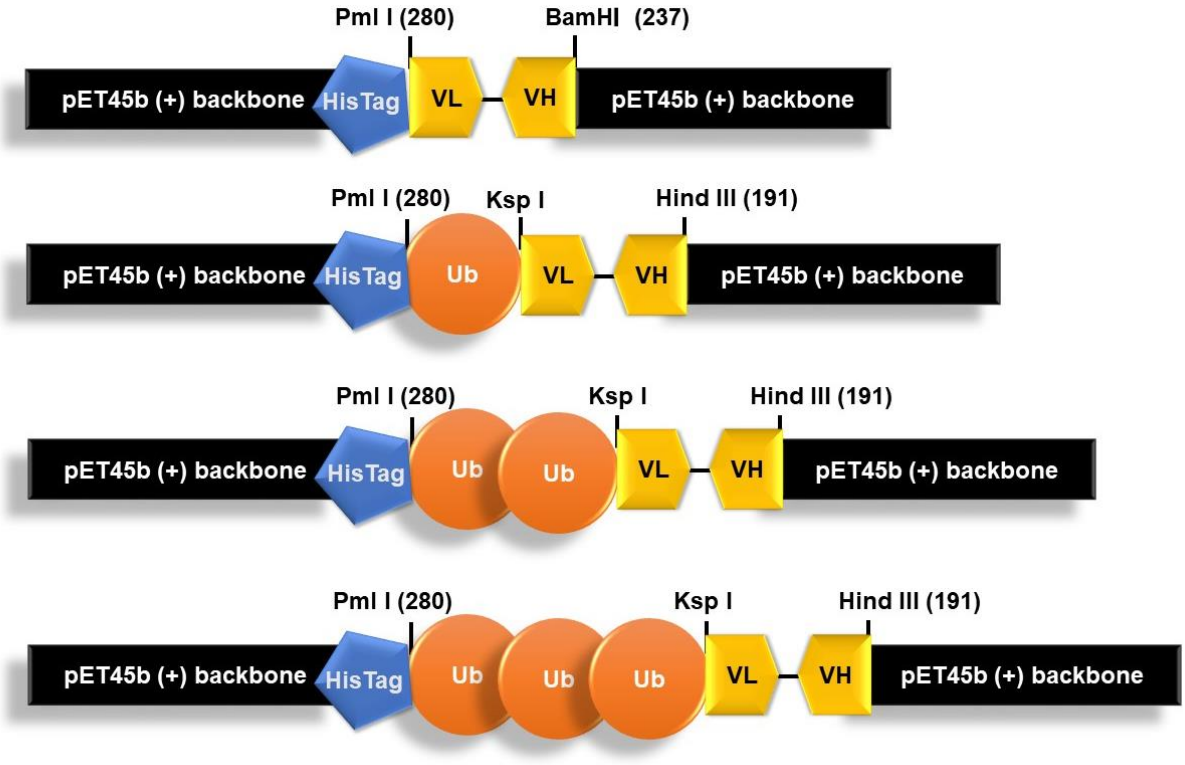

Figure 2. Cloning of scFv in pET45b (+) downstream Ub monomer, dimer, and trimer

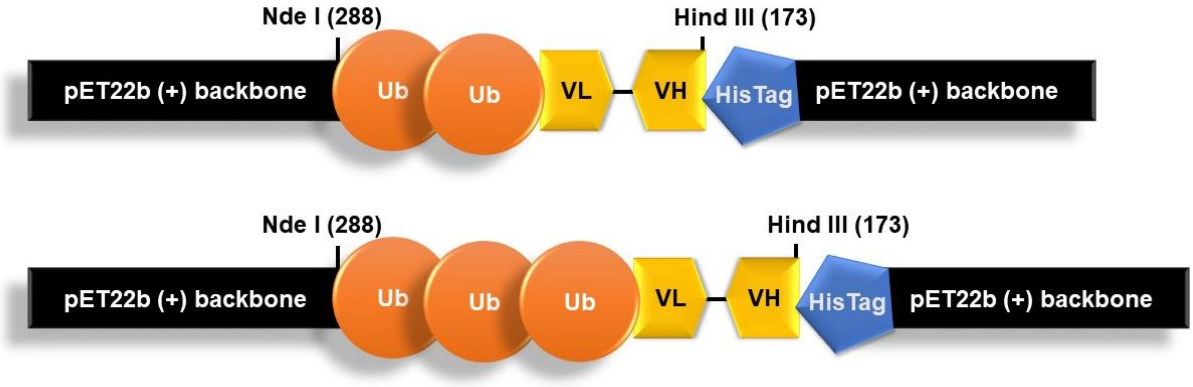

Figure 3. Cloning of Ub dimer scFv and Ub trimer scFv in pET22b (+)

Expression of hscFvs

A single colony of *E. coli* transformed with the respective plasmids, was inoculated into 20 ml of Louria-Bertani (LB) medium (10 g/L Trypton, 5 g/L Yeast Extract, 10 g/L NaCl pH 7.5) with ampicillin 100 µl/ml (A_{100}) and it was left shaking (190 rpm) overnight at 30 °C. After measuring the optical density at 600 nm, a part of the overnight culture was diluted in new LB medium+A_{100} to have a final optical density of 0.1. The suspension was put in agitation (190 rpm) at 25 °C until the OD_{600nm} reached an absorbance ranging from 0.6 to 0.8. An aliquot was removed and used as Not-Induced (NI) control. To induce the expression, isopropylthio-β-D-galactophyranoside (IPTG) (Sigma-Aldrich) was added in a final concentration of 0.5 mM and cells were cultured at 25 °C under constant shaking (200 rpm). The OD_{600nm} was measured every hour for 3 hours and every single time an aliquot of 10 ml was withdrawn. The aliquots were pelleted by centrifugation at 4 °C for 20 minutes at 3000 rpm, suspended in 0.5 ml of lysis buffer (phosphate buffer 20 mM, glycerol 10% (v/v), NaCl 0.3 M, β-mercaptoethanol (BME) 3 mM, PMSF 1 mM pH 7.4) and sonicated 3 times (Ultrasonic Cell Crusher 60 W, 30 sec in ice). The samples were centrifuged at 4 °C for 20 minutes at 12000 rpm and the supernatants, representing the soluble fractions, were separated by the pellets. The latter were resuspended in 0.5 ml of denaturing buffer (Urea 8 M, phosphate buffer 20 mM, glycerol 10% (v/v), NaCl 0.3 M, BME 10 mM, pH 8). After one cycle of sonication, the suspensions were left in agitation for one hour and then centrifuged for 20 minutes RT at 12000 rpm. The supernatants obtained represented the insoluble fraction. The protein concentrations of both the soluble and insoluble fractions were measured through the Bradford assay (Bio-Rad).

SDS-PAGE and western blot analysis

To evaluate the recombinant protein expression levels and the purification fractions, the samples diluted 1:2 in sample buffer 2X (Tris-HCl 0.5 M pH 6.8, SDS 2% (w/v), Glycerol 20% (v/v), Bromophenol blue) + 4% (v/v) β-Mercaptoethanol (BME), vortexed and heated in boiling water for 3 minutes were resolved in SDS-PAGE at the proper polyacrylamide concentrations. The proteins were visualized dying the gels with Brilliant Blue Coomassie R-250. To immunodetect the recombinant proteins the gels were electroblotted onto a nitrocellulose membrane (0.2 mm pore size) (Bio-Rad) 1 h at 100 V. The membranes were blocked with 3% BSA (Bovine Serum Albumin, Sigma-Aldrich) in TBS (Tris Buffer Saline) + Tween 20 (Sigma-Aldrich) 0.1% for 1 hour at room temperature and incubated overnight with Anti-6X His tag polyclonal antibody (OriGene) (1:3500 in blocking solution). After washing 3 times (10 min. each), the bands were detected by anti-rabbit horseradish peroxidase (HRP)-conjugated secondary antibody (Bio-Rad) (1:1000 in 3% milk in TBS + tween 20). The chemiluminescence detection method (WesternBright ECL, Advasta) allowed seeing the peroxidase activity.

Purification of Ub dimer- and trimer-hscFv VL-linker-VH His tag N-terminus and Ub dimer- and trimer-hscFv VL-linker-VH His tag C-terminus from the soluble fraction

500 ml *E.coli* pellet were suspended in 25 ml of lysis buffer (phosphate buffer 20 mM, glycerol 10% (v/v), NaCl 0.3 M, BME 3 mM, PMSF 1 mM, pH 7.4), disrupted by physical method with French Press (Avastin, Emulsiflex B15) between 10000 and 13000 Psi and centrifuged at 12000 rpm for 30 min at 4 °C to obtain soluble and insoluble fractions (Inclusion Bodies, Ibs). In order to purify the hscFvs with AKTA purifier chromatography system (GE Healthcare) by IMAC chromatography, the soluble fraction was charged in a 5 ml-HisTrap HP column (GE Healthcare, Bucks, UK) equilibrated with 5 CV (column volume) of loading buffer (phosphate buffer 20 mM, glycerol 10% (v/v), NaCl 0.3 M, BME 3 mM, pH 7.4). The column was washed with 20 CV of loading buffer and then with 5 CV for respectively 50, 250 and 500 mM of imidazole (Sigma-Aldrich) in loading buffer. Elution fractions were analyzed by SDS-PAGE 10% (v/v) and stained with Brilliant Blue Coomassie R-250.

Purification of Ub trimer-hscFv VL-linker-VH His tag N-terminus from inclusion bodies

The bacterial pellet coming from 500 ml of *E. coli* culture was treated as reported above. The insoluble fraction (inclusion bodies) was suspended in denaturing buffer (Urea 8 M, phosphate buffer 20 mM, glycerol 10% (v/v), NaCl 0.3 M, BME 10 mM and 30 mM of imidazole, pH 8) and incubated in agitation at room temperature for 60 minutes. The sample was centrifuged at 12000 rpm for 30 min. and the urea supernatant was collected. The hscFv purification was performed through AKTA purifier chromatography system by IMAC chromatography with 5 ml-HisTrap HP-column equilibrated with 5 CV loading buffer (Urea 8 M, phosphate buffer 20 mM, NaCl 0.3 M, glycerol 10% (v/v), BME 10 mM, imidazole 30 mM, pH 8). After the sample charging, the column was washed with 20 CV of loading buffer and the protein was refolded on column by a linear gradient of 30 CV to obtain a solution with 0.5 M of urea and 3 mM of BME. After this step, the column

was washed with 5 CV for 50, 250 and 500 mM of imidazole in 0.5 M Urea, 20 mM of phosphate buffer, 0.3 M NaCl, glycerol 10% (v/v), BME 3 mM, pH 8. Elution fractions were analyzed by SDS-PAGE 10% (v/v) and stained with Brilliant Blue Coomassie R-250.

Purification optimizations of Ub dimer hscFv VL-linker-VH His tag C-terminus from the soluble fraction

The first step of optimization concerned the change of the pH, and consequently of the buffers, opting for basic solutions of Tris-HCl. 500 ml of *E. coli* pellet were suspended in 25 ml of lysis buffer (Tris-HCl 20 mM, NaCl 0.3 M, glycerol 10 % (v/v), BME 3 mM, PMSF 1 mM, pH 8.5), disrupted by French Press and to separate the soluble and insoluble fractions. The soluble fraction was charged in a column with 30 ml Ni^{+2} Sepharose HP (GE Healthcare, Bucks, UK) and equilibrated with loading buffer (Tris-HCl 20 mM, NaCl 0.3 M, glycerol 10 % (v/v), BME 3 mM, pH 8.5). The column was washed with 20 CV of loading buffer and then with 5 CV for each imidazole concentrations (50, 250 and 500 mM in Tris-HCl 20 mM, NaCl 0.3 M, glycerol 10% (v/v), BME 3 mM, pH 8.5). The second step of optimization was developed with the aim to reach a higher level of cleaning of the fractions containing the hscFv by maintaining the same buffers therefore, after the sample charging in 30 ml Ni^{+2} Sepharose HP and the equilibration with loading buffer, a first step of 5 CV with imidazole 100 mM was applied to remove most of the proteins and then a gradient of 5 CV until 250 mM of imidazole. Elution fractions were analyzed by SDS-PAGE 10%. The fractions corresponding to the elution peak were collected, concentrated, and dialyzed against Tris-HCl 20 mM, NaCl 0.3 M, glycerol 10% (v/v), BME 3 mM, pH 8.5 to remove imidazole.

ELISA assay

A 96-well plate was coated with 50 µg/ml Laminarin (Sigma-Aldrich, L9634) in 0.05 M carbonate buffer pH 9.6 overnight at 4 °C. Nonspecific interactions were prevented with 100 µL/well of BSA 3% (w/v) in PBS-Tween 20 blocking solution (NaCl8g/L, KH_2PO_4 0.2g/L, $Na_2HPO_4 \cdot 12\ H_2O$ 2.9g/L, KCl 0.2g/L, Tween 20 0.05% (v/v), pH 7.4) at 37 °C for 1hour. The plate was then incubated with decreasing concentrations of hscFv (from 50 µg/ml to 0.10 µg/ml) in the blocking solution for 2 hours at 37 °C. 100 µL/well of freshly prepared Anti-6X His tag polyclonal antibody (OriGene) in blocking solution (1:500) were added and the plates were incubated at 37 °C for 1h. At the same temperature and for the same time 100 µL Goat anti-rabbit-HRP (Bio-rad) diluted 1:1000 in blocking solution was poured in each well. After every single passage, the plates were washed 5 times with PBS-Tween 20. To reveal the binding of the secondary antibody, 100 µL of 5 mg-ABTS tablet (Roche Diagnostics) dissolved in 12 ml of sodium citrate (0.05M, pH 3) and supplemented with 1:1000 dilution hydrogen peroxide (Carlo Erba Reagents) were added and after 15, 30, 45 and 60 minutes the absorbance at 405 nm was measured at the microplate reader (Bio-Rad). From the addiction of the ABTS solution, the plates were left in the dark.

RESULTS

Humanization of VH and VL regions of the murine monoclonal antibody 2G8

The murine amino acids sequence of the scFv 2G8 (VH-Linker-VL) was analyzed with ExPasy and the value of the instability index was 41.64. To decrease this value, the VH and VL regions were investigated separately through *"IgBlastTool"*. The murine germlines found to have the highest homology were IGHV1-9*01 for the VH (96,2%) and IGKV1-133*01 for the VL (97,7%). The substitution of the non-homologs amino acids (in VH: FRW1 I20→L, FRW2 L1→I, FRW3 S30→T, V35→I; in VL: FRW1 I2→V, S7→T, FRW3 F33→V) (Fig. 1 A), lowered the instability index until 37.05. These mutated variable regions were used for the humanization process. The first strategy recognized IGHV1-46*02 (74.7%) and IGKV2-30*01 (84.0%) as human germlines with the highest homology (data not shown). Regarding the second strategy the human germlines found for the VH murine frameworks were: IGHV1-3*02 for FWR1 (87.5 %), IGHV1-38-4*01 for FRW2 (77.1 %), IGHV169*06 for FRW3 (76.3 %) while for the VL murine frameworks: IGKV2-29*02 for FRW1 (84.6 %), IGKV2-28*01 for FRW2 (90.7 %), IGKV2-30*01 for FRW3 (86.3 %) (Fig. 1 B). Once the frameworks have been humanized, the two single chains were assembled and launched again in ExPasy. The best instability index, even if still too high, was obtained by the second strategy with a value of 41.10. The VH and VL of the selected hscFv were compared with the murine ones and back-mutations (VH FRW2 S40→R and FRW3 A61→N) were done to decrease the instability index to 37.01 (Fig. 1 C hVH1 and 1 D hVL1). Through their analysis in PDB the sequences obtained were: 3HC4 (Identities:80%, X-RAY diffraction: 1.62 Å [22]), 4KQ3 (Identities 80%, X-RAY diffraction: 1.92 Å [23]), 4JDV (Identities 72%, X-RAY diffraction: 1.65 Å [24]) for VH and 4DTG (Identities:84%, X-RAY diffraction: 1.80 Å [25]), 4LKX (Identities82%, X-RAY diffraction: 1.92 Å [26], 4LRI (Identities78%, X-RAY diffraction: 1.65 Å [27]) for VL. After the analysis of amino acid sequences, non-homolog amino acids in frameworks were changed (Fig. 1 C hVH2 and 1 D hVL2). According to several studies [21, 28] about the critical role of Vernier Zones in protein shaping, some amino acids were back-mutated in correspondence with these residues. The variable regions obtained were used to build the hscFv (Fig. 1 E).

Figure 1. A – first strategy: substitution of non-homologs amino acids in VH and VL sequences; B – second strategy: substitution of non-homologs amino acids in VH and VL frameworks; C – back mutations and mutations in the frameworks of the VH of the hscFv obtained from the second strategy; D – back mutations and mutations in the frameworks of the VL of the hscFv obtained from the second strategy; E – back-mutations in the Vernier Zones.

Protein expression of the humanized scFv (hscFv) in VH-linker-VL and in VL-linker-VH orientations cloned in pET22b (+)

The recombinant hscFv cloned in pET22b (+) downstream the pelB sequence and the His-tag at the C-terminus, was successfully expressed in *E. coli* BL21(DE3) mainly in inclusion bodies fraction. The cells were collected and analyzed at 1, 2 and 3 hours after induction with IPTG. The hscFvs' bands were found at the molecular weight of about 27 kDa. Despite the majority of scFvs are built as VH-linker-VL, some studies [29, 30, 31, 32] showed that the VL-linker-VH orientation ameliorates both the stability and the expression. These data revealed to be useful for our hscFv whose amount in the soluble fractions improved for the VL-linker-VH construct. Western immunoblotting confirmed the presence of the recombinant proteins (Fig. 2A and 2B). Although the hscFv VL-linker-VH amount in the soluble fraction was improved by the orientation, it was not enough to be purified and for this reason a preliminary purification from inclusion bodies was performed. After the solubilization of inclusion bodies in Urea 8 M buffer, the sample was loaded in a 5 ml HisTrap column under denaturing conditions. The hscFv was eluted with 250 mM of imidazole in Urea 0.5 M buffer. The purified fractions were mixed but after concentration, they produced protein precipitation therefore to improve the solubility and to avoid the precipitation tween 80 (Sigma-Aldrich) was added in all buffers following the same purification process. This strategy prevented the precipitation, but when the hscFv was tested for biological activity by ELISA it was impossible to determine the exact β-1,3-glucan-binding efficiency (data not shown).

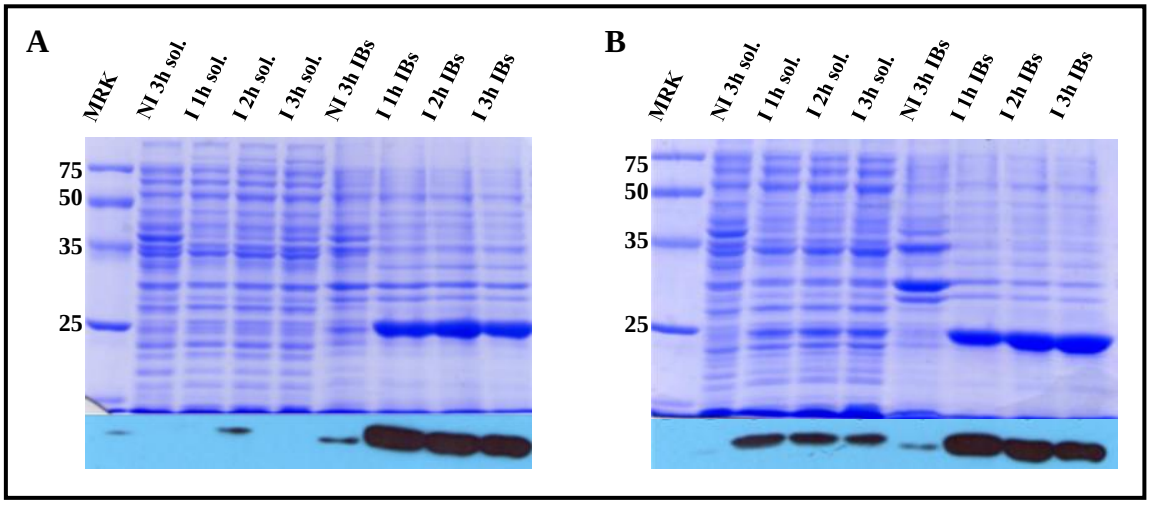

Figure 2. SDS-PAGE and western immunoblotting of hscFvs' expressions. A: VH-linker-VL, B: VL-linker-VH.

NI: not induced
I: induced
sol.: soluble fraction
IBs: inclusion bodies fraction

Expression of ubiquitin monomer-, dimer- and trimer-hscFv in pET45b (+) and ubiquitin dimer- and trimer-hscFv in pET22b (+)

The SDS-PAGE analysis (Fig. 3) shows hscFv cloned in pET45b (+), hence with the His-tag at the N-terminus, alone and with Ub monomer, dimer and trimer. An increase of hscFv in the soluble fraction is directly correlated with the number of ubiquitin subunits (Fig. 3 A, B, C and D). hscFv without Ub and Ub monomer-hscFv showed electrophoresis mobility in accordance with their molecular weight (MW) (without Ub ~27 kDa and with one subunit ~35 kDa) (Fig. 3 A and B), whereas Ub dimer- and trimer-hscFv bands were lower than expected (with two Ub subunits ~44 kDa and with three subunits ~52 kDa) and for this reason, the rightness of the sequences has been checked with nucleotide sequencing.

To produce the Ub trimer- and dimer-hscFv with His-tag at C-terminus, the constructs were amplified from pET45b (+) and cloned in pET22b (+) without pel B sequence (as for pET45b (+) vector) adopting the same expression conditions reported above. The expression analysis not only follows the pattern seen before but also shows an increase of the recombinant protein in soluble fractions (Fig. 3 C compared to E and D compared to F). The western immunoblotting analysis revealed the presence of the Ub dimer-hscFv His-tag C-term (Fig. 3 E).

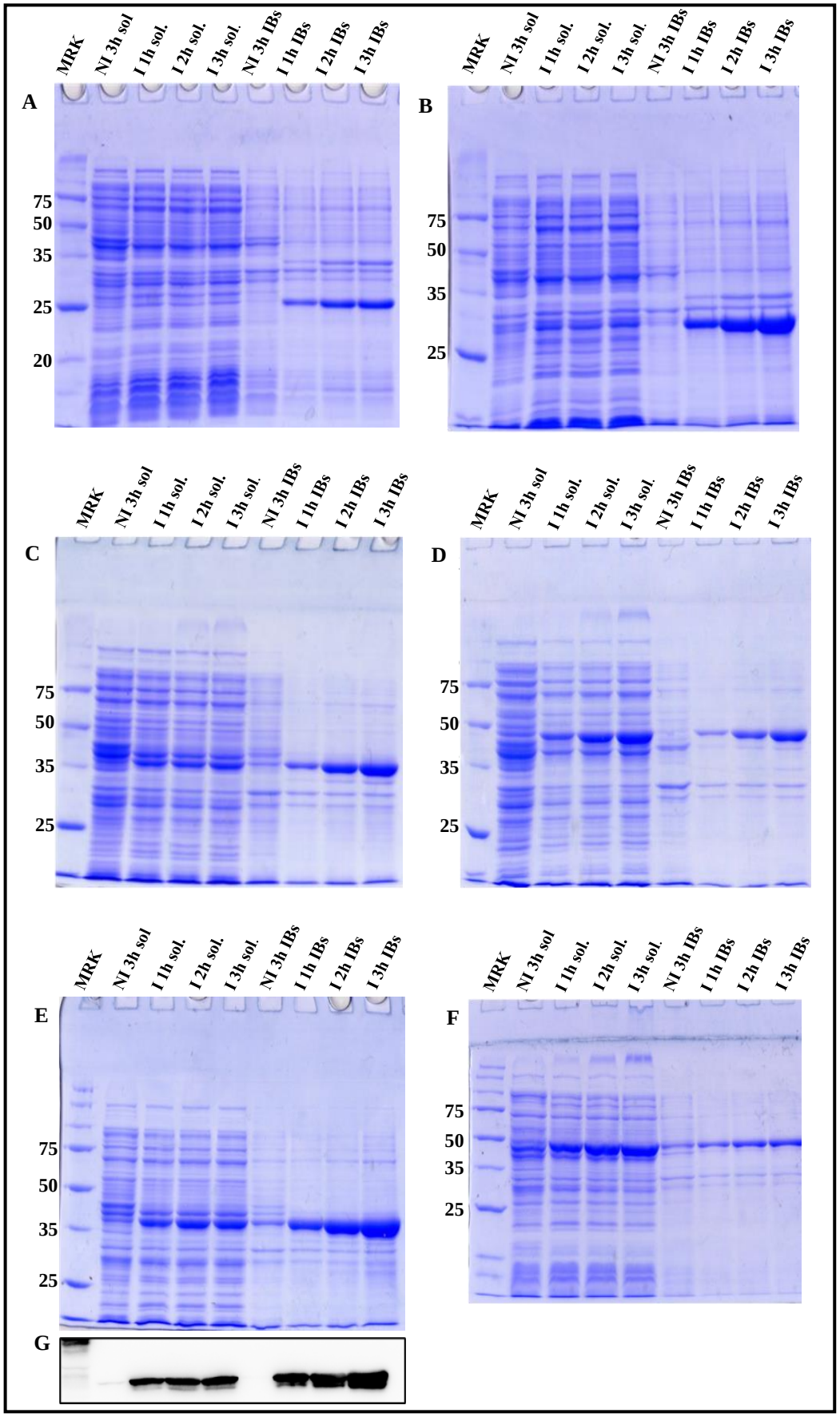

Figure 3. Images from A to D SDS-PAGE expression analysis of hscFv in pET45b (+); A: hscFv without Ub; B: Ub monomer-hscFv; C: Ub dimer-hscFV; D: Ub trimer-hscFv. Images E and F: SDS-PAGE expression analysis of hscFv in pET22b (+); E: Ub dimer-hscFv; F: Ub trimer-hscFv 3. G: western immunoblotting of Ub dimer-hscFv in pET22b(+).

Purification of ubiquitin dimer- and trimer-hscFv His-tag N-terminus from soluble fraction and of ubiquitin trimer-hscFv His-tag N-terminus from inclusion bodies

The soluble fraction coming from the lysate bacterial pellet was used to purify the recombinants Ub dimer- and trimer-hscFv His-tag N-terminus by IMAC nickel column. SDS-PAGE analysis of purification processes showed that the Ub dimer- and trimer-hscFv were found in flow-through fractions failing the binding in column (Fig.4 A and B). To evaluate if the His-tag could be insufficiently exposed when the protein is in native conditions, the same purification process was performed also under denaturing conditions using inclusion bodies of Ub trimer-hscFv His-tag N-terminus, the recombinant produced in higher quantity. In this case, part of the recombinant antibody bound the Ni^{+2} Sepharose resin and the elution fractions obtained with 250 mM of imidazole were analyzed by SDS-PAGE (Fig. 5). In light of these results, we supposed that the His-tag might be potentially masked and for this reason, we decided to change the His-tag position from N-terminus to C-terminus.

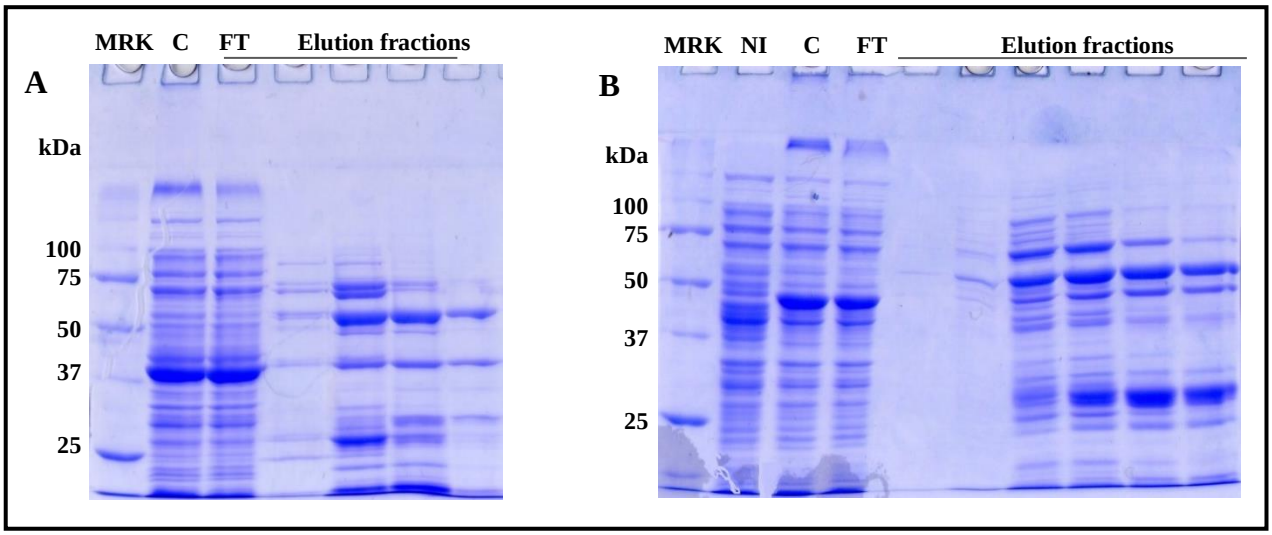

Figure 4. Purification of Ub dimer-hscFv His-tag N-terminus (A) and Ub trimer-hscFv His-tag N-terminus (B) from soluble fractions.

MRK: Marker
NI: not induced
C: sample charged in column
FT: flow-through

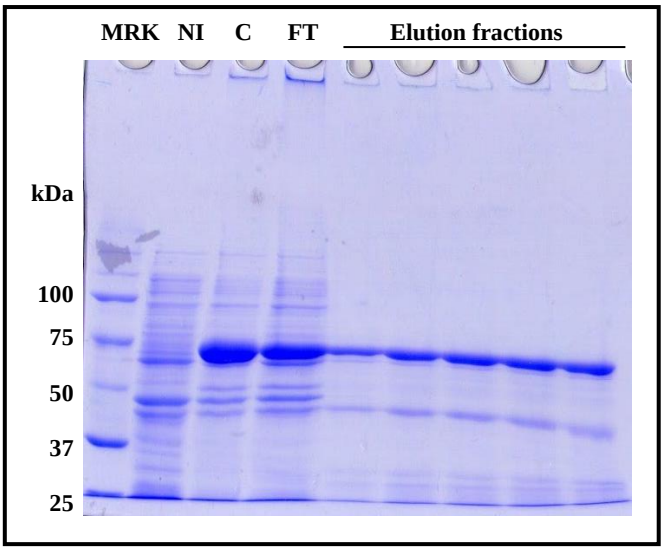

Figure 5. Purification of Ub trimer-hscFv His-tag N-terminus from inclusion bodies

MRK: Marker
NI: inclusion bodies' fraction not induced
C: sample charged in column
FT: flow-through

Purification of ubiquitin dimer- and trimer-hscFv His-tag C-terminus from the soluble fraction

The purifications of the soluble fractions of both Ub dimer- and trimer-hscFv with the His-tag at the C-terminus revealed that the new position is able to improve the protein binding to the column even though a portion keeps going to the flow-through (Fig. 6 A and B). The fractions obtained from purification were pooled, concentrated, and dialyzed to remove the imidazole. The products were tested in ELISA showing that Ub dimer-hscFv performed better than Ub trimer-hscFv. From here the choice to optimize the purification process just for the Ub dimer-hscFv (Fig.7).

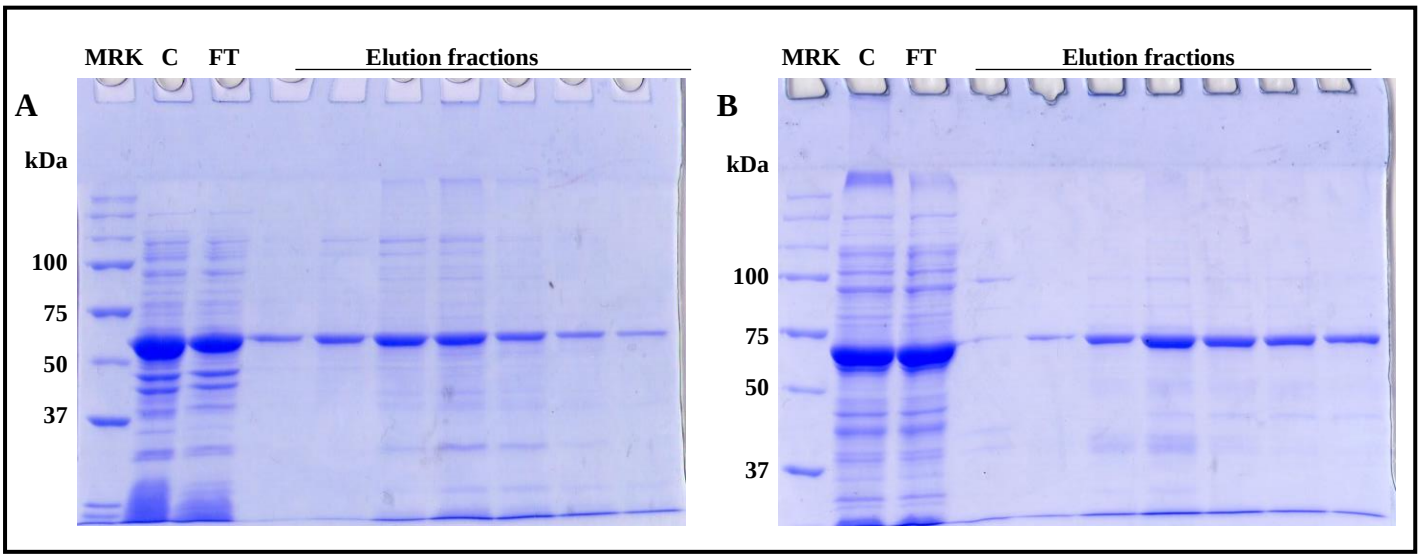

Figure 6. Purification of Ub dimer-hscFv His-tag C-terminus (A) and Ub trimer-hscFv His-tag C-terminus (B) from soluble fractions.

MRK: Marker
C: sample charged in column
FT: flow-through

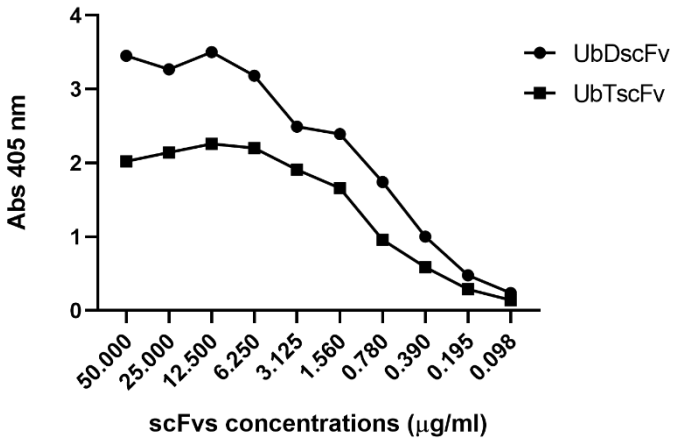

Figure 7. ELISA assay to compare the binding activity of Ub dimer-hscFv and Ub trimer-hscFv to laminarin antigen.

Optimized purifications of Ub dimer-hscFv His-tag C-terminus from the soluble fraction

Two peaks were obtained, the first at 100 mM of imidazole and the second during the gradient towards 250 mM. The fractions corresponding to the peaks were analyzed in SDS-PAGE. As shown in Fig. 8 no recombinant protein was found in the 100 mM- peak. HscFv was eluted at around 165 mM of imidazole as a single band denoting a good level of purity and at the expected MW. From 1L of bacterial culture, the yield was 40 mg.

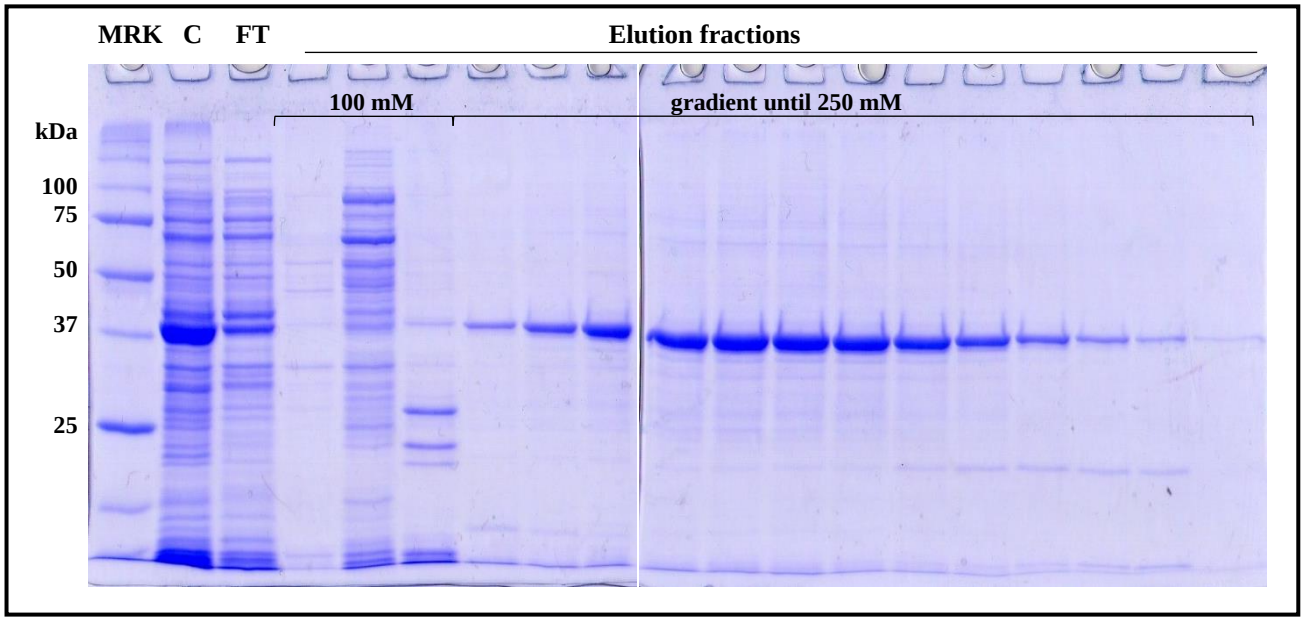

Figure 8. Purification of Ub dimer-hscFv at pH 8.5 – step at 100 and gradient until 250 mM of imidazole.

MRK: Marker
C: sample charged in column
FT: flow-through

DISCUSSION

Looking at the increasing interest of the pharmaceutical companies and research laboratories towards antibody-based treatments, the development of a humanized scFv becomes an interesting and tempting challenge. The IgG2b antibody 2G8 was an optimal candidate for this kind of study since it doesn't just bind β-1,3-glucans, fundamental components of the fungal cell wall, but also demonstrated its efficacy in inhibition of growth, adhesion and infection progression, both *in vitro* and *in vivo* against several pathogenic fungi.

Ub dimer-hscFv His-tag C-terminus is the result of a humanization process followed by a deep study aimed to express and purify a considerable amount of clean product. The humanization process was based on the CDR-grafting technique. The VL-VH orientation seemed to be a little more soluble than the VH-VL but the real contribution in terms of solubility was given by ubiquitin. The solubility increased with the number of ubiquitin monomers added in the sequence, but at the same time, the steric hindrance made the purification through His-tag difficult for both the Ub dimer- and the trimer-hscFv. The order changing, with the presence of the His-tag at the C-terminus improved the purification profile but the hscFvs were largely found in the flow-through. We suppose that the protein folding could still mask the tag of Histidine not allowing the binding to the column. Only the pH modification moving from the canonical 7.4 to 8.5 let a total protein binding thus suggesting a temporary and reversible conformational modification in basic conditions that probably implicate the His-tag exhibition. The Ub dimer-hscFv His-tag C-terminus was then collected resulting in a 40 mg clean product coming from 1L of bacterial culture. The binding capacity was maintained in ELISA meaning that the hscFv obtained was still efficient. Further studies on its activity and stability are ongoing.

CHAPTER 5

Characterization of the humanised scFv derived from mAb 2G8

Work currently in progress

I wish to express my gratitude to

Filippo Tasini Ph.D.

Federica Biancucci Ph.D. student

Professor Michele Menotta

Professor Barbara Canonico

INTRODUCTION

The use of monoclonal antibodies as therapeutics has met a rapid evolution mainly due to their computational identification and/or design combined with efficient and rapid screening methods [1]. Advances in recombinant antibody technologies promoted the manipulation of antibody fragments as well, allowing research, diagnoses, and therapies to benefit from several engineered products [2, 3, 4, 5, 6, 7]. In particular, single-chain fragment variables (scFvs), are recombinant antibody formats composed only by the variable regions of the heavy and of the light chains. Their smaller size and the consequently higher degree of penetration and facilitated access to the antigen, together with the better pharmacokinetic profile, the lower immunogenicity risk due to the lack of the Fc domain and the high production at low costs have drawn huge interest and several investments [6, 8, 9, 10]. Despite the advantages of scFvs compared to the respective full-length antibodies, several bottlenecks have been identified: scFvs often don't share with their parentals a good binding affinity, they suffer from a rapid clearance, they are less stable and tend to aggregate becoming immunogenic in any case [2, 10, 11]. These features limit a lot their therapeutic potential, nevertheless, some genetic and chemical modifications and suitable formulations are being explored [12, 13, 14, 15, 16]. In this study we continue the investigation of Ub-dimer-hscFv His-tag at the C-terminus (hscFv) which was previously humanized and optimized in order to make it soluble and purifiable. Our attempts are those of the improvement in the purity of the hscFv and of the evaluation of the binding to the specific antigen and of the stability, always monitoring the aggregation formation. Finally, the hscFv activity was tested on *Candida* spp. looking at the binding and at the growth inhibition both alone and in combination with antifungal drugs markedly available.

MATERIAL AND METHOD

Expression of hscFvs

E. coli transformed with pET45b (+) – Ub-dimer-hscFv His-tag at the C-terminus was used for the protein expression. In brief, a single colony was spread into Louria-Bertani (LB) medium (10 g/L Trypton, 5 g/L Yeast Extract, 10 g/L NaCl pH 7.5) with ampicillin 100 µl/ml and left growing overnight at 30 °C in agitation. Then the inoculum was diluted in 500 ml of LB to have an OD_{600} of 0.1 and incubated in agitation at 25 °C until an OD_{600} of 0.6-0.8. An aliquot was removed while the remaining culture was induced by isopropylthio-β-D-galactophyranoside (IPTG) (Sigma-Aldrich). The expression was carried on for three hours with withdrawals at every hour whereas the remaining volume was used for the purification. The aliquots were centrifuged, and the pellet lysed and sonicated three times (Ultrasonic Cell Crusher 60 W, 30 sec in ice). After centrifugation, the supernatants were collected (soluble fractions) while the pellets were resuspended in denaturing buffer (Urea 8 M, phosphate buffer 20 mM, glycerol 10% (v/v), NaCl 0.3 M, BME 10 mM, pH 8), sonicated once and left in agitation for 1 hour RT. Finally, the samples were centrifugated again and the supernatants were collected (insoluble fractions). The protein concentration was measured through Bradford assay (Bio-Rad) and the analysis of the aliquots was performed by SDS-PAGE and western-blot.

Purification with a negative passage in Q Sepharose and a positive passage in Ni^{+2} Sepharose

The remaining volume of the expression was centrifuged. *E. coli* pellet was lysed with lysis buffer (Tris-HCl 20 mM, glycerol 10% (v/v), NaCl 30 mM, BME 3 mM, PMSF 1 mM, pH 7.4), then the suspension underwent three passages in French Press and was centrifuged again. The supernatant was charged in Q Sepharose FF column (GE Healthcare, Bucks, UK) previously equilibrated with 5 CV of loading buffer (Tris-HCl 20 mM, glycerol 10% (v/v), NaCl 30 mM, BME 3 mM, pH 7.4). The column was washed with 20 CV of loading buffer and then with 5 CV for respectively 0.25, 0.5, 0.75, 1 and 2 M of NaCl in loading buffer. The flow-through and the elution fractions were analyzed by SDS-PAGE 10% (v/v) and stained with Brilliant Blue Coomassie R-250. Then the flow-through fractions were reunited, adjusted in pH until 8.5 and in NaCl concentration until 0.3M, concentrated, dialyzed, and charged in Ni^{+2} Sepharose HP (GE Healthcare, Bucks, UK). The Ni^{+2} Sepharose HP column was previously equilibrated with loading buffer (Tris-HCl 20 mM, NaCl 0.3 M, glycerol 10 % (v/v), BME 3 mM, pH 8.5). The first step of elution occurred with 100 mM of imidazole (5 column volume (CV)) while the hscFv was eluted during the gradient until 250mM of imidazole (5CV). The elution fractions were analyzed by SDS.PAGE then the fractions containing the hscFv were reunited, concentrated, dialyzed to remove imidazole, and used to perform different analyses.

SDS-PAGE and western blot analysis

Samples were diluted 1:2 in sample buffer 2X (Tris-HCl 0.5 M pH 6.8, SDS 2% (w/v), Glycerol 20% (v/v), Bromophenol blue) + 4% (v/v) of β-Mercaptoethanol (BME), vortexed and boiled for 3 minutes. Then they were charged and let running in polyacrylamide gel (10%) The proteins were dyed with Brilliant Blue

Coomassie R-250 whereas for immunodetection the gels were electroblotted onto a nitrocellulose membrane (0.2 mm pore size) (Bio-Rad) for 1 hour at 100 V. The membranes were blocked with 3% BSA (Bovine Serum Albumin, Sigma-Aldrich) in tris buffer saline (TBS) + Tween 20 (Sigma-Aldrich) 0.1% for 1 hour at room temperature and then incubated overnight with Anti-6X His tag polyclonal antibody (OriGene) (1:3500 in blocking solution). After washing 3 times (10 min. each), the membranes were incubated with anti-rabbit horseradish peroxidase (HRP)-conjugated secondary antibody (Bio-Rad) (1:1000 in 3% milk in TBS + tween 20). Bands were visualized with the enhanced chemiluminescence detection kit WesternBright ECL (Advansta) in a ChemiDoc MP Imaging System (Bio-Rad).

Mass spectrometry

Following the method of Zhang et al. [16], 10 pmol/µl of hscFv diluted in a solution of H_2O/acetonitrile 50:50 supplemented with formic acid 0.1% was injected for direct infusion into the Orbitrap Exploris 240 Mass Spectrometer (Thermo Fisher Scientific) equipped with electrospray ionization source. The analysis was performed at room temperature with an elution flow rate of 10 µl/min., in intact protein mode and the surface-induced dissociation (SID) was set at 60 V to help desolvation without fragmenting the hscFv and the resolution at 15 000. The resulting spectrum was the average of all the scans acquired in the mass range from 600 to 1400 mass-to-charge ratio (m/z) and deconvoluted with FreeStyle software (Thermo Fisher Scientific). The analysis was performed by the internal facility of the University of Urbino Carlo Bo – section of biochemistry and biotechnology.

Investigation of the aggregation behaviour

The aggregation behaviour of hscFv was evaluated in SDS-PAGE. First it was diluted 1:2 in sample buffer 2X (Tris-HCl 0.5 M pH 6.8, SDS 2% (w/v), Glycerol 20% (v/v), Bromophenol blue). The sample buffer was supplemented with 4% (v/v) of β-Mercaptoethanol (BME), 5 M of urea and 10 mM of EDTA, assaying all the possible combinations [17]. At the same time, BME was also substituted with different concentrations of DTT (1, 10, 50 and 100 mM) and the samples were and weren't boiled.

At the end of these analyses, the purified hscFv was dialyzed in order to change BME into 1,4-Dithiothreitol (DTT). DTT is a stronger reducing agent moreover, it is more stable, hence it is preferred for storage.

ELISA assay

A 96-well plate was coated with 50 µg/ml Laminarin (Sigma-Aldrich, L9634) in 0.05 M carbonate buffer pH 9.6 overnight at 4 °C. For 1 hour at 37 °C the plate was incubated with blocking solution (BSA 3% (w/v) in PBS-0.05% (v/v) tween 20, pH 7.4) then, decreasing concentrations hscFv were added and left to bind for 2 hours at 37 °C. Anti-6X His tag polyclonal antibody (OriGene) in blocking solution (1:500) were added and the plates and left incubating at 37 °C for 1hour. Then the Goat anti-rabbit-HRP (Bio-rad) diluted 1:1000 in blocking solution was left bind for 1 hour at 37 °C. After every single passage, the plates were washed 5 times with PBS-Tween 20. Finally, 100 µL of 5 mg-ABTS tablet (Roche Diagnostics) dissolved in 12 ml of sodium

citrate (0.05M, pH 3) and supplemented with 1:1000 dilution hydrogen peroxide (Carlo Erba Reagents) were left react in the dark for 15, 30, 45 and 60 minutes and the absorbance was read at 405 nm at the microplate reader (Bio-Rad).

Stability test

Aliquots containing hscFv were left at different temperatures for different time points (Table 1). The evaluation of the structural stability of the hscFv was performed through SDS-PAGE and western blot, while to assess its activity, the IC50 resulting from ELISA tests were compared.

Table 1. Schematic representation of the temperatures and time points for the stability test

Temperatures	37 °C	4 °C	-20 °C	-80 °C
Time points	3 days 1 week 2 weeks 3 weeks	3 days 1 week 2 weeks 3 weeks 1 month 2 months 3 months	1 month 2 months 3 months	3 months

Immunofluorescence and flow cytometry

Candida albicans and *Candida auris* were inoculated overnight in RPMI+MOPS (0.165M pH 7). In order to investigate *C. albicans* in both hyphal and yeast form, two inocula for this specie were prepared, one of RPMI+MOPS (0.165M pH 7) and the other RPMI+MOPS (0.165M pH 7) supplemented with 10% serum [18]. Inocula were washed and ~10^6 CFU/ml were resuspended in PBS 3% (w/v) BSA + 50 μg/ml of hscFv and left 1 hour at 37 °C. Cells were washed and incubated with Anti-6X His tag polyclonal antibody (OriGene) in blocking solution for 1 hour at 37 °C and then, with goat anti-mouse IgG1 Alexa Fluor 488 (Molecular Probes). After washing again, the samples were fixed with paraformaldehyde 4% in PBS for 1 hour at 4 °C. After washing again, each sample was resuspended in PBS and divided into two aliquots. An aliquot was used for the immunofluorescence microscopy while the other for the analysis at the flow cytometer (FACScanto II, BDBioscences, Erembodegem, Belgium), equipped with three lasers (488 nm, 633 nm, 405 nm) to evaluate the fluorescence intensity due to the conjugation to the hmAb compared to the cells' autofluorescence. The dialysis buffer was used at the place of the hscFv, while PBS replaced the other antibodies in the controls.

Minimum inhibitory concentration (MIC)

Confident about the results obtained with the humanized full-length antibody H5K1, hscFv was tested as well in combination with caspofungin (CAS) (Sigma-Aldrich) and amphotericin B (AMB) (Sigma-Aldrich) on *C. auris*. EUCAST guidelines for the microdilution method were followed. In brief, from an overnight inoculum of *C. auris* in RPMI+MOPS (0.165M pH 7), 1–5x10^5 CFU/ml were plated in a 96-well plate. The antifungal drugs concentrations were 10-fold serially diluted starting from 4 μg/ml, while the concentrations of hscFv tested were 0.25, 2.5 and 25 μg/ml. The plates were incubated at 37 °C for 24 and 48 hours. The absorbance was read at 405 nm with a Microplate Reader (Bio-Rad). For caspofungin we considered the concentrations that inhibit 50% of the growth compared to drug-free control (MIC50) while for amphotericin, the concentration that inhibits the 90% (MIC90) and the 50% (MIC50) of the growth compared to drug-free control. The dialysis buffer was used at the place of the hscFv. The assays were performed three times in triplicate.

RESULTS

Purification process

In view of a scaling up and with the aim to clean as much as possible Ub dimer-hscFv VL-linker-VH His tag C-terminus (hscFv) from other proteins and especially from endotoxins, a negative passage in Q Sepharose FF was introduced in the purification process before the step in Ni^{+2} Sepharose HP. As reported in Figure 1, the first passage was essential to remove some contaminants with the majority of the hscFv passing in the flow-through fractions. The fractions containing the hscFv were collected, reunited, adjusted in NaCl concentration and pH and charged in Ni^{+2} Sepharose HP column. This passage was previously validated and the elution of the hscFv occurred, as expected at around 165 mM of imidazole. The fractions seem cleaner compared to the purifications performed before with a single passage in Ni^{+2} Sepharose HP. The contribution of every single purification step is summarized in figure 3. The first band corresponds to the sample charged in Q Sepharose FF, the second band to result of the Q Sepharose FF purification and at the same time the sample charged in Ni^{+2} Sepharose HP and the third band the result of the Ni^{+2} Sepharose HP purification. The third band is cleaner from contaminants even if it presents some products of degradation and traces of aggregates. The yield obtained from around 500 ml of bacterial culture was ~18.8 mg meaning that there hasn't been a significant loss of material.

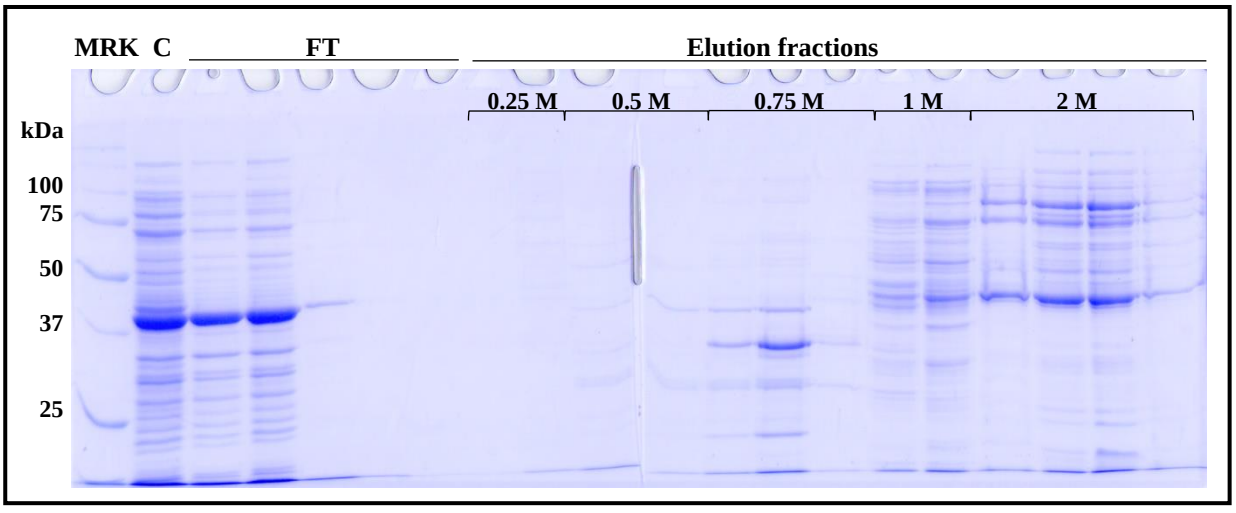

Figure 1. Purification of Ub dimer-hscFv: step in Q Sepharose FF, negative passage. Elution with 0.25, 0.5, 0.75, 1 and 2 M of NaCl.

MRK: Marker
C: sample charged in column
FT: flow-through

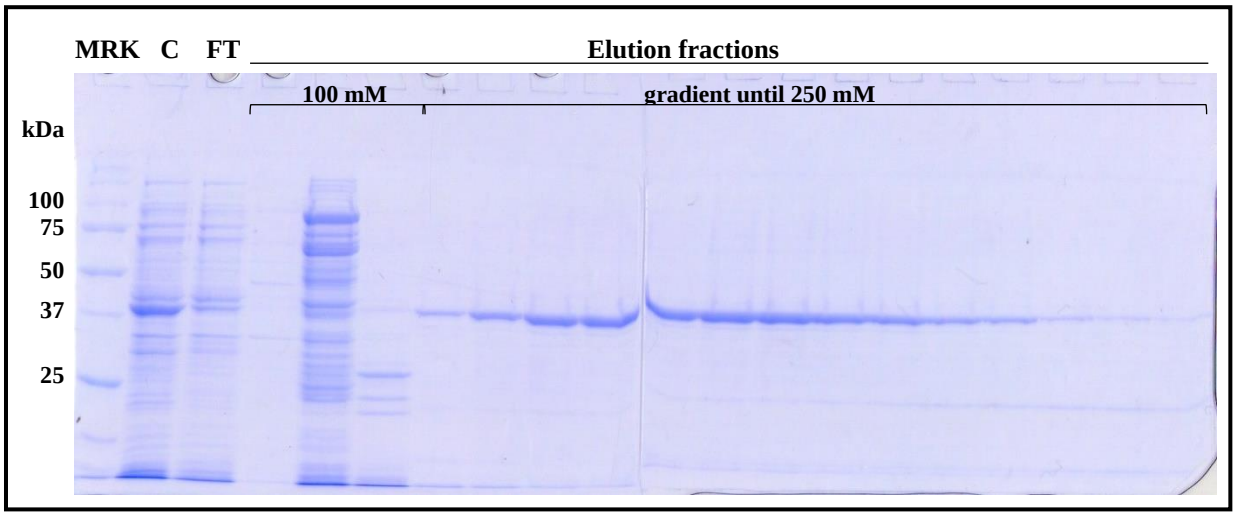

Figure 2. Purification of Ub dimer-hscFv: step in Ni^{+2} Sepharose HP, positive passage. First elution with 100 mM of imidazole followed by a gradient until 250 mM of imidazole.

MRK: Marker
C: sample charged in column
FT: flow-through

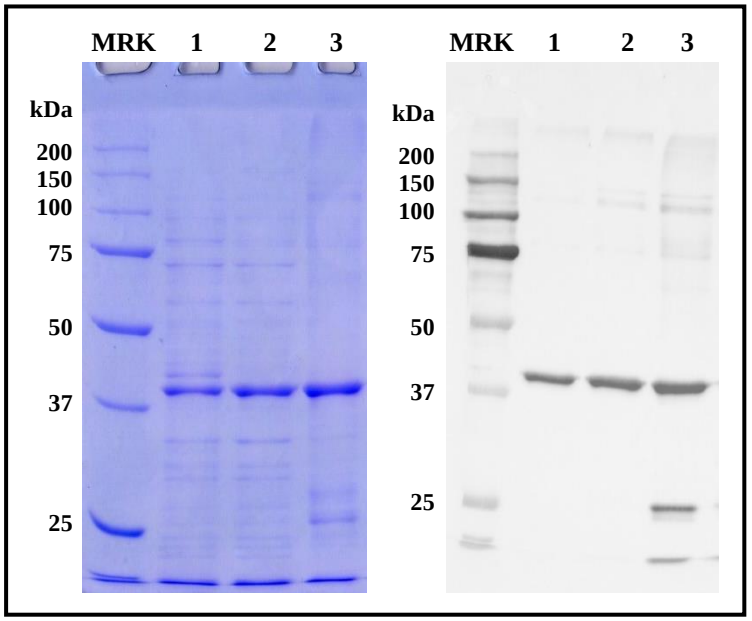

Figure 3. Sequence of the steps of the purification process and progressive higher level of purity of the hscFv.

MRK: Marker
1: soluble fraction of the bacterial culture charged in Q Sepharose FF
2: product of the negative passage in Q Sepharose/sample charged in Ni^{+2} Sepharose HP
3: product of the positive passage in Ni^{+2} Sepharose HP

Mass spectrometry

Figure 4 represents the average ESI mass spectrum with mass-to-charge (m/z) ranging between 600 and 1400. The hscFv was analyzed in its intact form and each peak of the resulting Gaussian distribution represents a different protonated level of the proteins present in the sample. The distribution proceeds from the most protonated to le least protonated species in a charged state ranging from 36+ to 63+. The corresponding deconvoluted mass spectrum (Fig. 5) shows that the most abundant peak belongs to the hscFv and represents almost 100% of the total proteins in the sample. The molecular mass is 44 519.89 Da; the other two most abundant species are cationized adducts of the hscFv with respectively 1 (44 497.35 Da) and 4 (44611.05 Da) Na^+ cations at the place of protons. The remaining peaks are probably degradation products of the hscFv and contaminants of the purification.

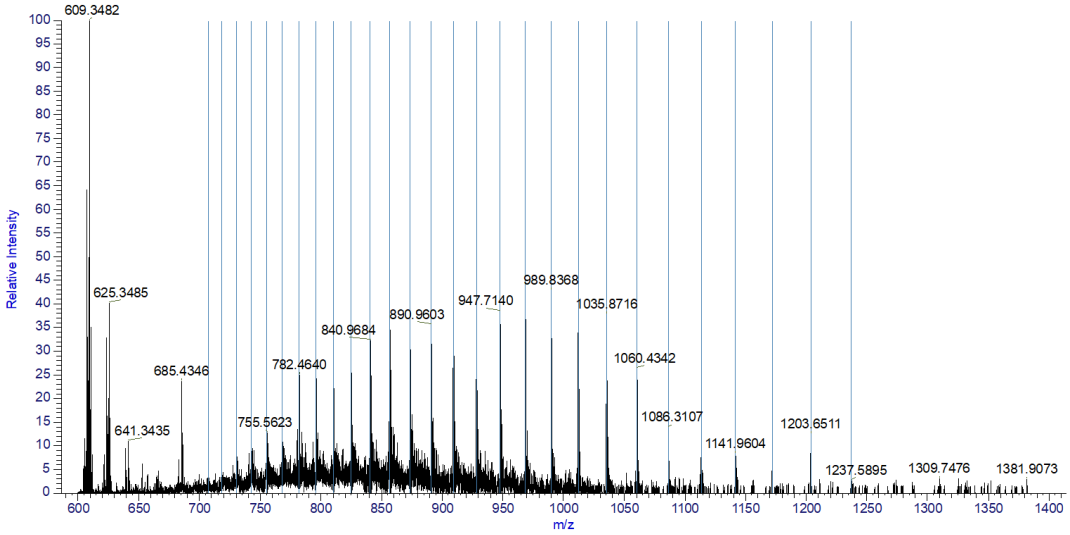

Figure 4. Positive ESI Orbitrap mass spectrum of the intact hscFv. m/z ranging from 600 to 1400 and charge ranging from 36+ to 63+.

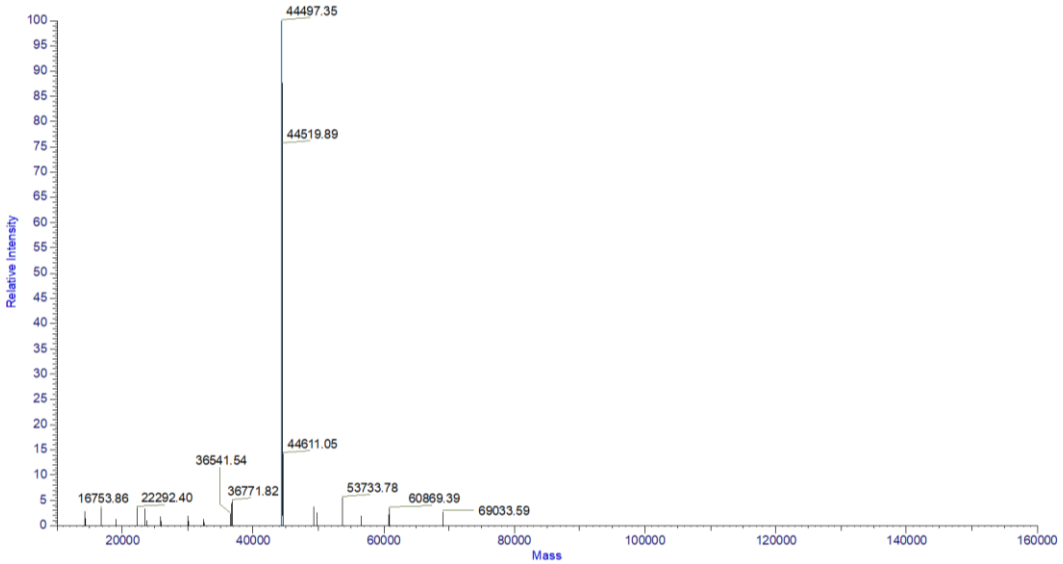

Figure 5. Deconvoluted mass spectrum showing the prevalence of the hscFv and of its cationized adducts.

Investigation of the aggregation behaviour

One of the major limits of the antibody fragments is their pro-aggregation behaviour and for this reason, electrophoretic analyses were performed to assess the presence and absence of aggregates. hscFv was dissolved in a common buffer (sample buffer) supplemented with BME, urea, EDTA and their combinations and boiled (Fig. 6) and with different concentrations of DTT not/boiling the samples (Fig. 7). In figure 6 it is evident that the 30 mM of BME used during the purification process are not sufficient for preventing the aggregation of the hscFv. Only by adding 4% of BME (~0.57 M) to the sample buffer it is possible to let the bands enter the gel and be resolved. The aggregates are clearly resistant to the denaturing action of urea and to the chelating activity of EDTA suggesting that the interactions responsible for the aggregates are neither aspecific nor metal-linked. The aggregates are sensitive to reducing conditions demonstrating that the 4 Cysteines in the sequence play a putative role probably creating both intra- and intermolecular disulphide bonds. Figure 7 confirms that the redox state gives a pivotal contribution to the aggregates' formation. In not boiling condition and in absence of DTT, the majority of hscFv can't penetrate the gel. With the same treatment, the addition of increasing concentrations of DTT promotes the progressive disaggregation starting from 1 mM of DTT and with a complete electrophoresis resolution already with 10 mM. Aspecific interactions have a minor influence, and it is evident comparing the samples with 1 mM of DTT boiled and not boiled. Interestingly in both figures is the presence of aggregates at around the double (~90 kDa) and the triple (~133 kDa) of hscFv molecular weight, meaning the presence of hscFv dimers and trimers.

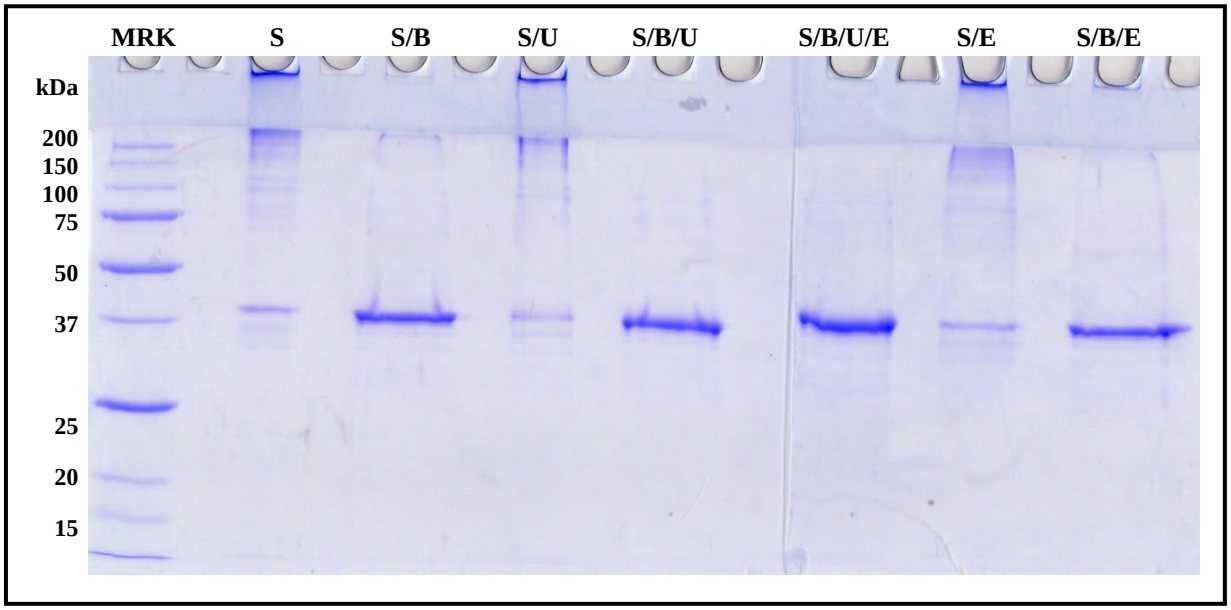

Figure 6. SDS-PAGE analysis of the hscFv to test the aggregation formation in presence of BME, urea and EDTA and their combinations added to the sample buffer solution. The samples were boiled.

S: sample buffer
B: 4% β-Mercaptoethanol (BME)
U: 5 M urea
E: 10 mM EDTA

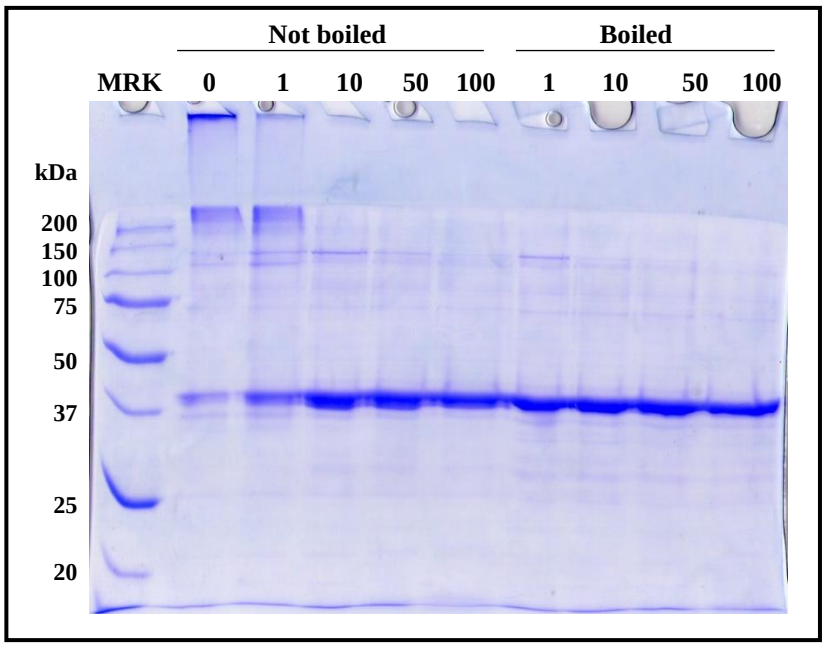

Figure 7. Electrophoretic analysis of the effect of the boiling and of increasing concentrations of DTT on hscFv aggregates. 0, 1 ,10, 50 and 100 mM are the concentrations of DTT. The first five samples weren't boiled while the last four were boiled.

ELISA assay

The hscFv coming from the purification, after concentration and dialysis, was tested in ELISA assay to assess its binding capacity to the β-1,3-glucan laminarin. The resulting IC_{50} is 0.403 ± 0.029 μg/ml (Fig. 8 A) and the AUC of the relative interpolated curve is 0.59 (Fig. 8 B).

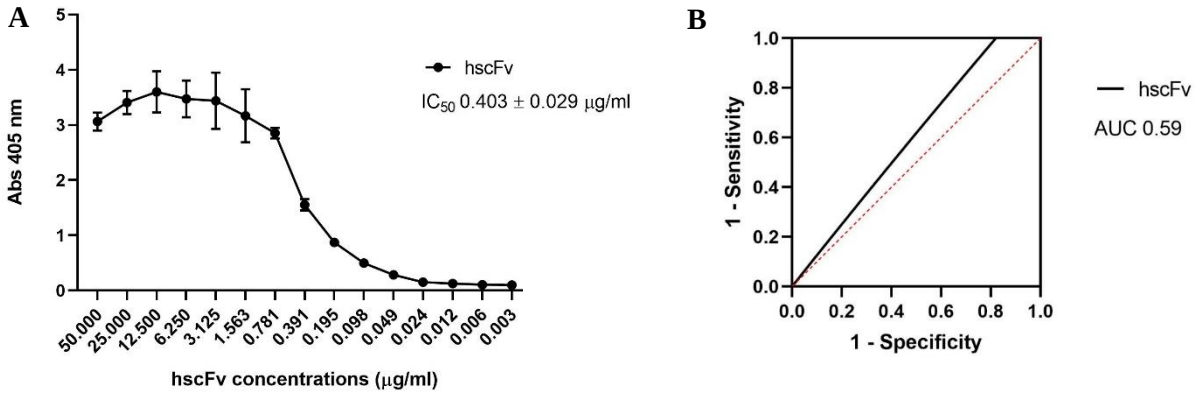

Figure 8. Binding of the hscFv to laminarin and evaluation through ELISA assay (A) and the interpolated ROC curve (B).

Stability test

Aliquots of the same stock solution containing the purified, concentrated, and dialyzed hscFv (Fig. 10 A) were separated and stored at different temperatures and for different time points. Already after 3 days at 37 °C, the hscFv started losing its binding ability (Fig. 9 A). Temperature played a dual role, the first was a direct effect on the hscFv while the second implies the DTT faster degradation hence, a huge aggregation of the hscFv in a shorter time. Both these concomitant events probably influenced the activity and the stability of the hscFv whose bands gradually disappeared for the aliquots at 37 °C leaving space only to aggregates (Fig. 10 B, C, D and E). At 4 °C the hscFv preserved the binding capacity with IC_{50}s ranging near the value of the beginning (Fig. 9 B). Only after one month the IC_{50} progressively increased, whereas the aliquots at -20° and -80° C, not just performed as at the starting point in terms of binding (Fig. 9 C and D) but they even didn't present more aggregates compared to the time 0 (Fig. 10 F, G and H)

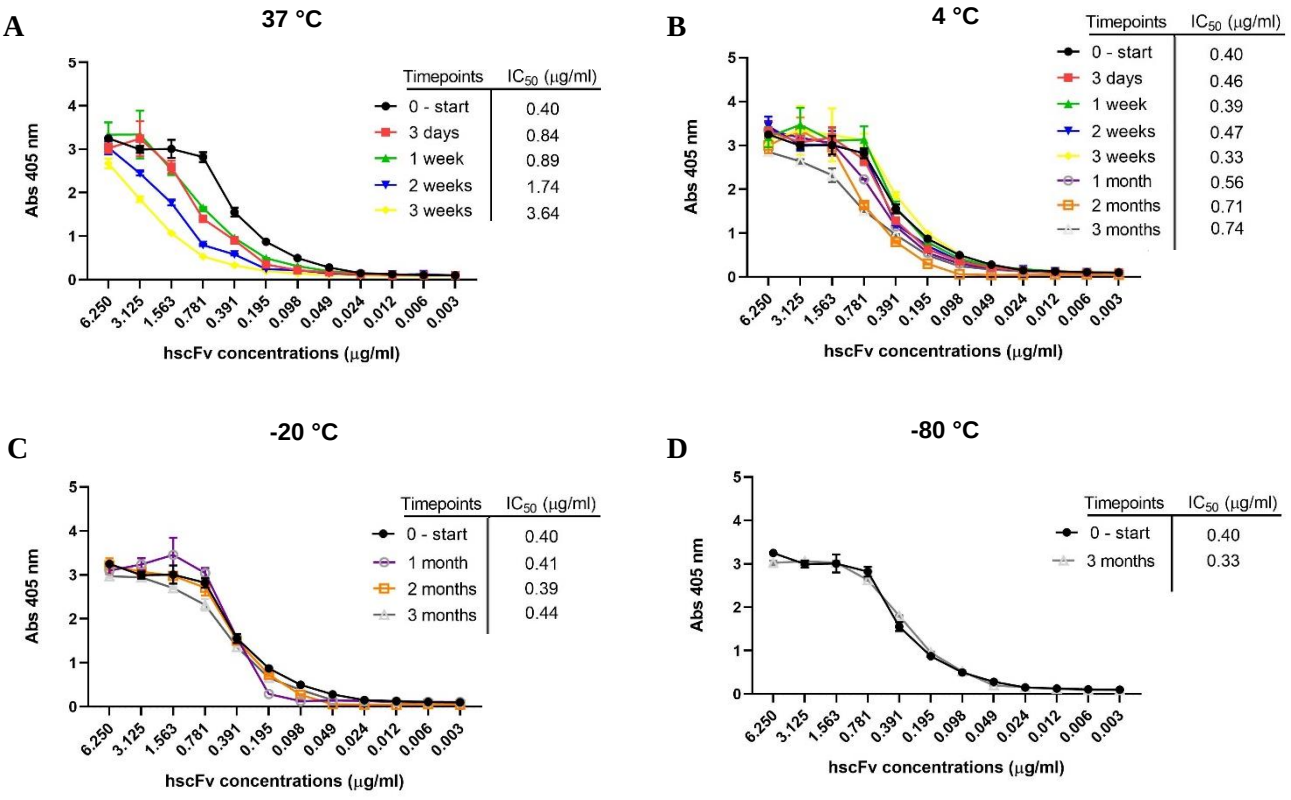

Figure 9. Stability test. Evaluation of the binding activity of hscFv when stored at 37° (A), 4° (B), -20° (C) and -80° C (D) for different time points.

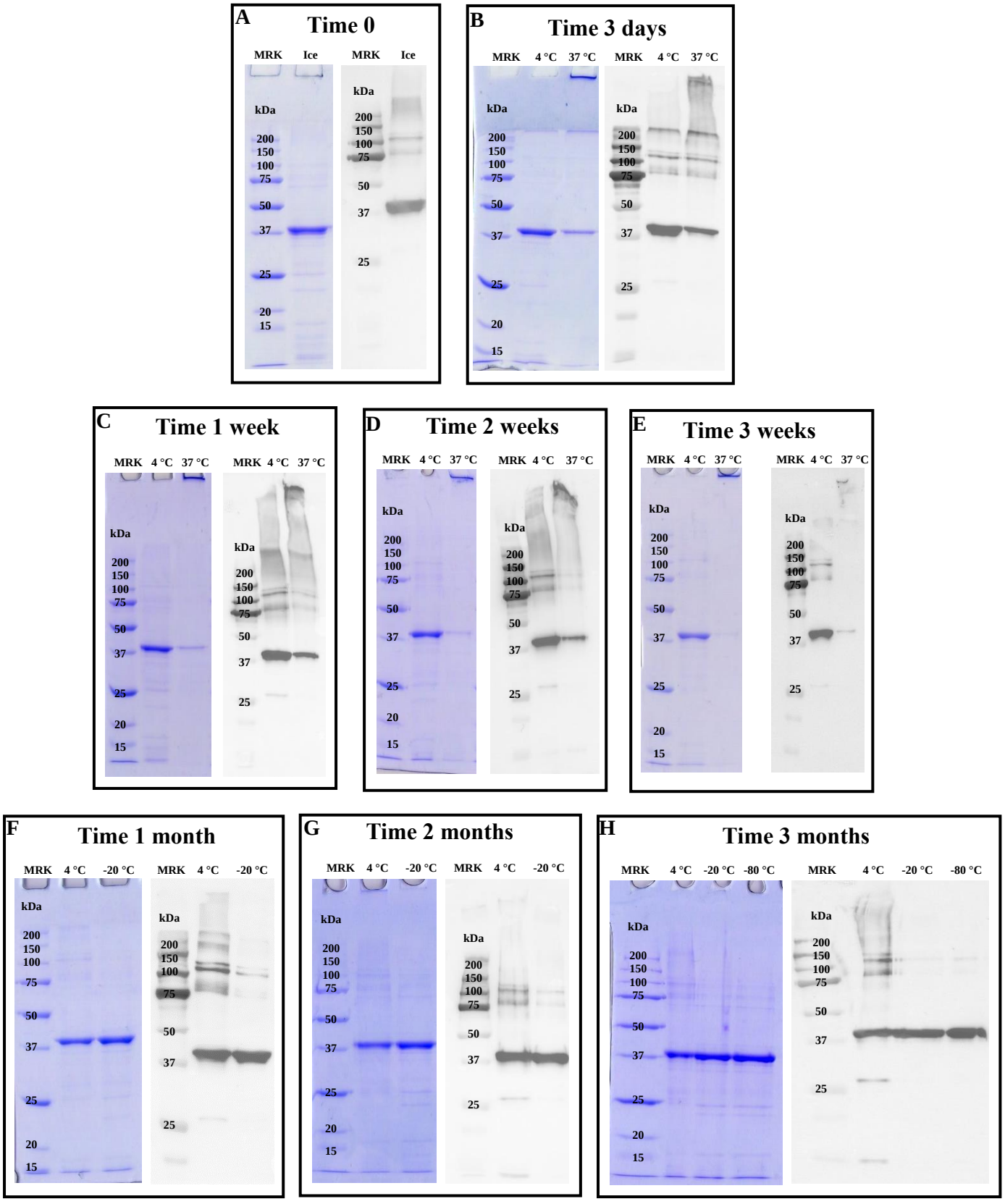

Figure 10. Stability test. Evaluation of the aggregation formation immediately after hscFv production (A) and when it is stored at different temperatures for 3 days (B), 1 week (C), 2 weeks (D), 3 weeks (E), 1 month (F), 2 months (G) and 3 months (H).

Immunofluorescence and flow cytometry

Until now the binding of hscFv to β-1,3-glucans was evaluated only in ELISA assays and using laminarin as antigen. Here we demonstrated its ability in recognizing and binding β-1,3-glucans on the cell wall of *C. auris* and *C. albicans* both in hyphal and yeast form (Fig. 11). Through flow cytometry analyses the fold of increase between the fluorescence of treated samples and the basal cell autofluorescence was calculated. For *C. auris* the fold of increase is about 50 while for *C. albicans* around 30.5. These values increase considerably considering the events at higher forward scatter (FSC) and side scatter (SSC): for *C. auris* becomes 120 and for *C. albicans* 54. The subpopulations considered are the budded cells for *C. auris* and the hyphae for *C. albicans* and represent respectively the 13% and the 66% of the entire samples (Fig. 12).

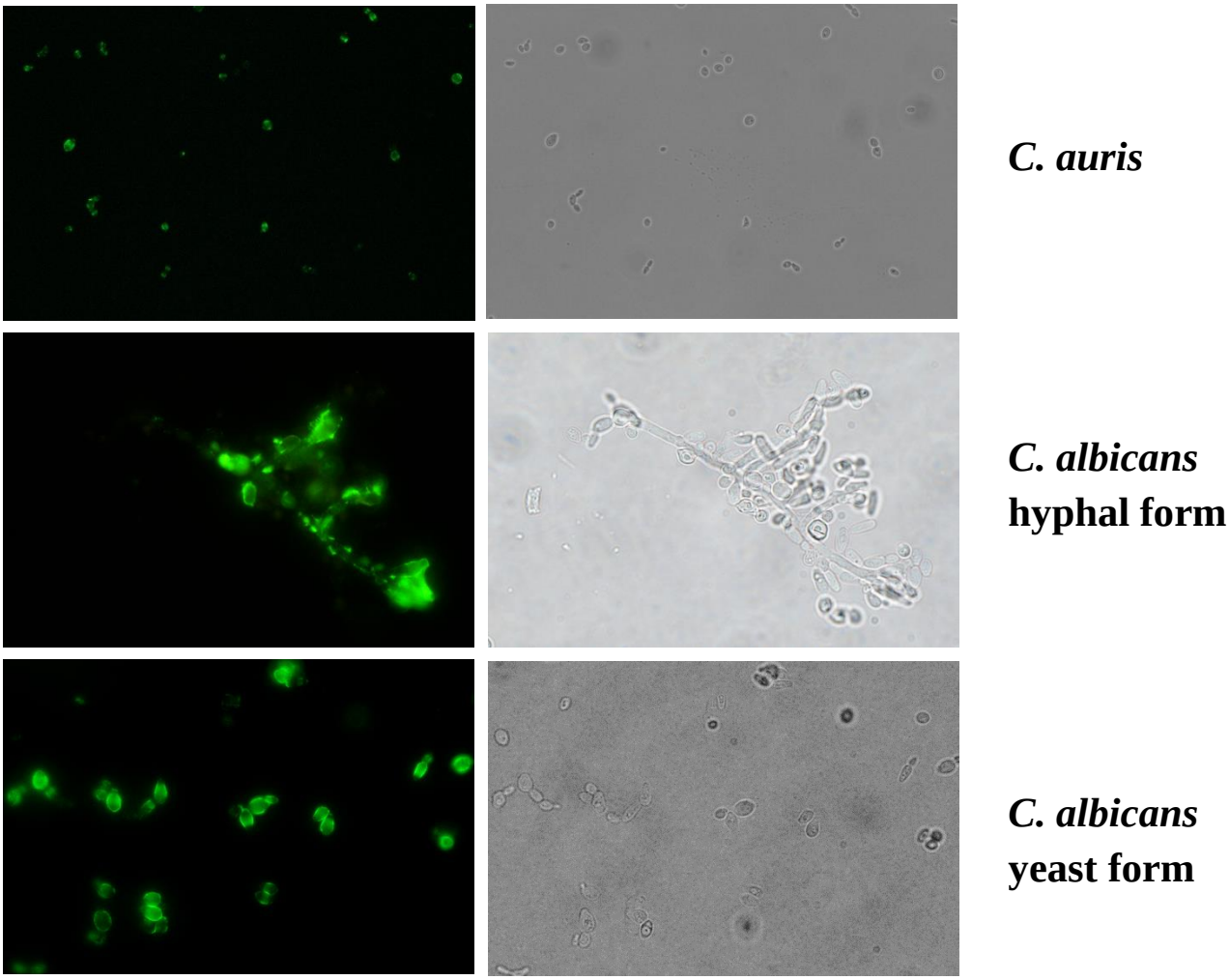

Figure 11. Immunofluorescence analysis to evaluate hscFv binding to β-1,3-glucans of *C. auris* and *C. albicans* cells. Green fluorescence and bright-field images.

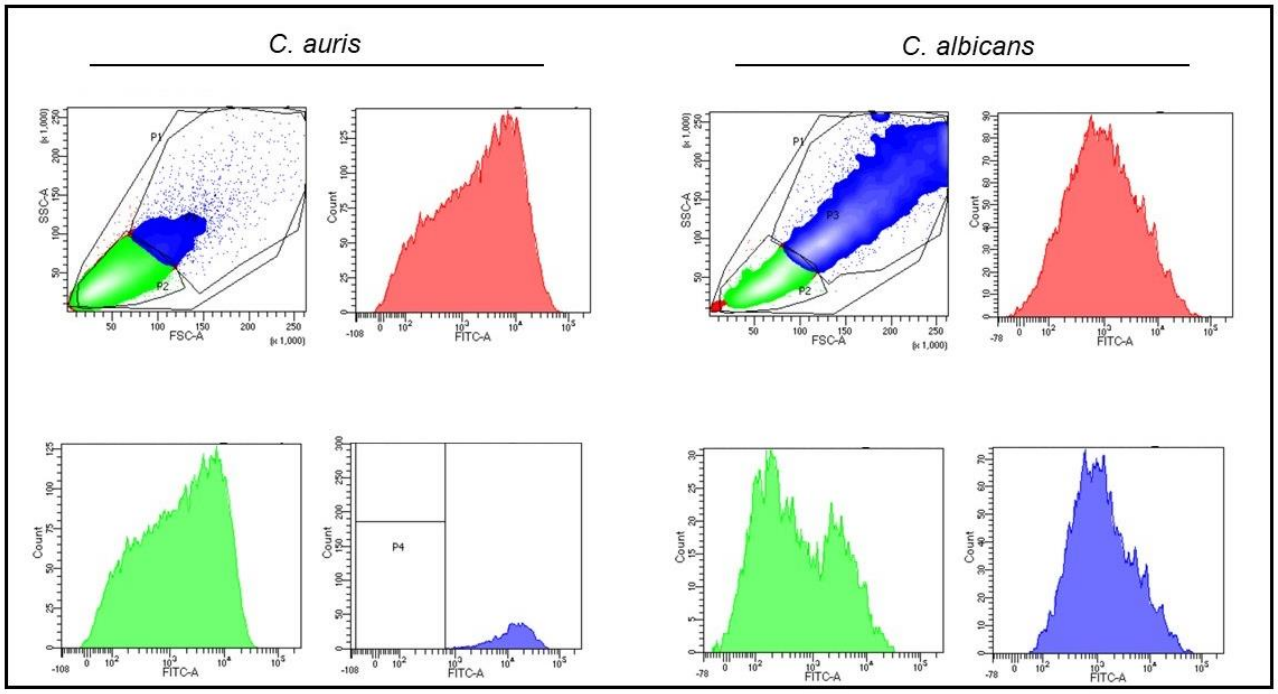

Figure 12. Flow cytometric analysis of MFI of *C. auris* and *C. albicans* cells treated with hscFv. On the left *C. auris* cells: in red the entire sample population; in green the subpopulation of the unbudded cells; in blue the subpopulation of the budded cells. On the right *C. albicans* cells: in red the entire sample population; in green the subpopulation of the cells in yeast form; in blue the subpopulation of the cells in hyphal form.

Minimum inhibitory concentration (MIC)

Looking at the promising results in flow cytometry and immunofluorescence, the hscFv was also investigated for its possible activity in combination with caspofungin (CAS) and amphotericin B (AMB). We considered MIC50 as the lowest concentration that inhibits 50% of the growth compared to drug-free control and MIC90 as the lowest concentration that inhibits 90% of the growth compared to drug-free control. For what concern caspofungin, positive results are visible already at 24 hours with the gradual loss of efficacy of CAS from 0.125 μg/ml and the retention of activity when combined with hscFv (Fig. 13 A). In particular, the combination with 25 μg/ml of hscFv permitted the MIC50 to shift of 2-fold dilutions from 0.125 μg/ml of caspofungin to 0.03125 μg/ml (Table 2). At 48 hours the effect doesn't disappear (Fig. 13 B), in fact the shift of MIC50 is maintained of 2-fold for the combination with 25 μg/ml of hscFv (from 0.25 to 0.0625 μg/ml of caspofungin) but appears, of 1-fold (from 0.25 to 0.125 μg/ml), also with 2.5 μg/ml (Table 3). Nevertheless, the best results were obtained with amphotericin B for which we considered both MIC90 and MIC50 (Fig. 14 A and B). At 24 hours both the combination with 2.5 μg/ml and with 25 μg/ml of hscFv caused a shift of 1-fold for the former and of 2-fold for the latter, for both MIC90 and MIC50 (MIC90 decreased from 0.25 μg/ml to 0.125

µg/ml with 2.5 µg/ml of hscFv and to 0.0625 µg/ml with 25 µg/ml of hscFv, whereas MIC50 decreased from 0.125 µg/ml to 0.0625 µg/ml when CAS is combined with 2.5 µg/ml of hscFv and to 0.03125 µg/ml when combined with 25 µg/ml of hscFv) (Table 4). The shift of MIC50 is extended also to the combination with 0.25 µg/ml of hscFv at 48 hours. While the fold-shifts for the combinations with 2.5 and 25 µg/ml of hscFv were maintained constant for MIC90, they increased of 1-fold for MIC50 (MIC90 decreased from 0.5 µg/ml to 0.25 with the addition of 2.5 µg/ml of hscFv and to 0.125 µg/ml with 25 µg/ml of hscFv while MIC50 decreased from 0.5 µg/ml to 0.25 µg/ml with 0.25 µg/ml of hscFv, to 0.125 µg/ml with 2.5 µg/ml of hscFv and to 0.0625 µg/ml with 25 µg/ml of hscFv) (Table 5).

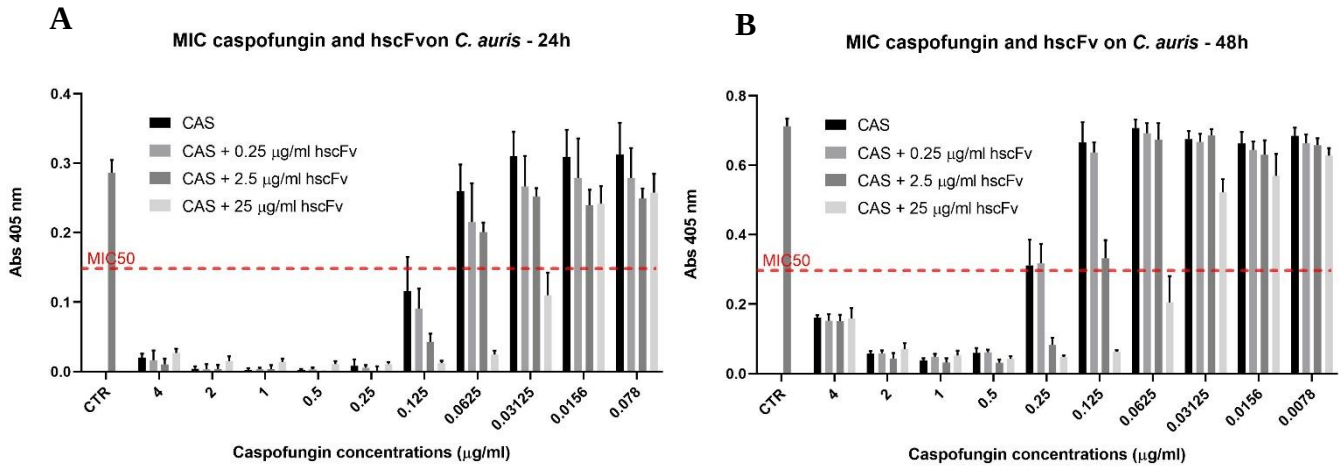

Figure 13. MIC assay of caspofungin (CAS) alone and in combination with different concentrations of hscFv at 24 (A) and 48 (B) hours.

Table 2. Percentage of growth inhibition of caspofungin (CAS) alone and in combination with hscFv at 24 hours. MIC50 breakpoints are marked with ∗.

Drug µg/ml	% growth inhibition - 24h			
	CAS	Combination CAS-hscFv (µg/ml)		
		0.25	**2.5**	**25**
4	93.0	94.3	96.3	90.6
2	98.6	98.9	98.6	94.7
1	99.1	98.8	98.7	95.1
0.5	99.0	98.8	100	96.2
0.25	97.0	98.0	100	96.3
0.125	59.2*	68.2*	85.0*	95.8
0.0625	9.1	24.7	29.8	91.4
0.03125	0	6.7	11.9	61.5*
0.156	0	2.4	16.2	15.1
0.0078	0	2.4	12.8	9.8

Table 3. Percentage of growth inhibition of caspofungin (CAS) alone and in combination with hscFv at 48 hours. MIC50 breakpoints are marked with ∗.

Drug µg/ml	% growth inhibition - 48h			
	CAS	Combination CAS-hscFv (µg/ml)		
		0.25	**2.5**	**25**
4	77.2	78.5	78.8	77.6
2	91.9	91.7	93.9	90.2
1	94.7	93.2	95.6	92.7
0.5	91.6	91.4	95.6	94.1
0.25	56.3*	55.4*	88.4	93.3
0.125	6.5	10.7	53.4*	91.1
0.0625	0.7	2.8	5.4	71.2*
0.03125	5.2	6.3	3.4	26.6
0.156	6.9	9.5	11.6	20.1
0.0078	3.9	6.9	7.7	12.0

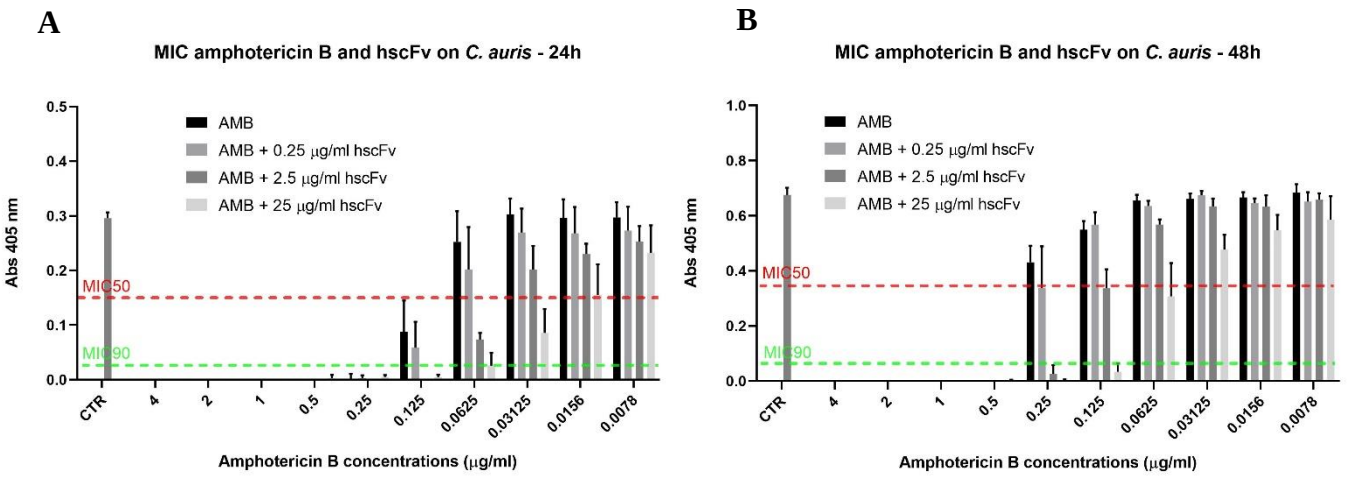

Figure 14. MIC assay of amphotericin B (AMB) alone and in combination with different concentrations of hscFv at 24 (A) and 48 (B) hours.

Table 4. Percentage of growth inhibition of amphotericin B (AMB) alone and in combination with hscFv at 24 hours. MIC50 breakpoints are marked with ∗ while MIC90 breakpoints are marked with †.

Drug µg/ml	% growth inhibition - 24h			
	AMB	Combination AMB-hscFv (µg/ml)		
		0.25	**2.5**	**25**
4	100	100	100	100
2	100	100	100	100
1	100	100	100	100
0.5	100	100	100	98.9
0.25	95.6†	99.0†	100	98.2
0.125	70.2*	80.1*	100†	98.4
0.0625	14.7	31.8	75.1*	91.3†
0.03125	0	8.9	31.8	71.0*
0.156	0	9.3	22.2	47.3
0.0078	0	7.6	14.4	21.5

Table 5. Percentage of growth inhibition of amphotericin B (AMB) alone and in combination with hscFv at 48 hours. MIC50 breakpoints are marked with ∗ while MIC90 breakpoints are marked with †.

Drug µg/ml	% growth inhibition - 48h			
	AMB	Combination AMB-hscFv (µg/ml)		
		0.25	**2.5**	**25**
4	100	100	100	100
2	100	100	100	100
1	100	100	100	100
0.5	100*†	100†	100	100
0.25	36.1	50.0*	96.0†	100
0.125	18.6	15.9	50.1*	94.9†
0.0625	3.1	5.9	15.9	50.4*
0.03125	2.3	0	6.1	29.4
0.156	1.3	4.2	6.2	18.8
0.0078	3.5	3.5	2.6	13.3

DISCUSSION

In this study we tried to characterize the hscFv previously humanized and optimized. The purification process was firstly improved in order to obtain a product pure as much as possible still maintaining a good yield. Here we are proud to present the result of a double-step purification process based on a negative passage in Q Sepharose FF and on a positive passage in Ni^{+2} Sepharose HP. The hscFv has a level of purity that touches almost 100%. The presence, even if little, of degradation products and of aggregates persuaded us to start immediately analyses about the nature of the aggregates and about the best buffer composition. The interactions behind the aggregate behaviour are sensitive to the presence of reducing agents as β-mercaptoethanol (BME) and 1,4-dithiothreitol (DTT), while were slightly susceptible the boiling/not boiling process and completely indifferent to the presence of urea and EDTA meaning that aspecific interactions play a minor role compared to the formation of intra-and intermolecular disulphide bonds. From these results the initial formulation was modified only in its reducing agent, therefore BME was substituted with DTT since it has stronger activity and is stabler. hscFv demonstrated to be able to recognize and bind β-1,3-glucans with an IC_{50} of 0.403 ± 0.029 μg/ml. To test the stability of the new formulation, tests were performed at different temperatures and for different time points. The formation of many aggregates and the total loss of the binding activity occurs within 3 weeks at 37° C probably because of a direct effect of the temperature on the hscFv and of an indirect effect given by the faster degradation of DTT. At 4° C, the hscFv demonstrated to maintain the binding capacity longer with a slight and slow decrease only after one month. Aggregate increased as well, especially if compared to the samples stored at -20° and -80° C that preserved completely both the binding activity and the monomeric form without traces of aggregates formation compared to the starting point. Not satisfied, we evaluated the binding of the hscFv also on *C. auris* and *C. albicans* cells, the latter both in hyphal and yeast form obtaining good results. The fold of increase of the mean fluorescence intensity in *C. auris* and *C. albicans* are respectively 50 and 30.5 but they considerably increase to 120 and 54 considering the subpopulations composed by budded cells for *C. auris* and cells in hyphal form for *C. albicans*. These subpopulations represent respectively 13% and 66% of the entire samples and are also the cells with the highest positivity for the hscFv. This is consistent with the information reported in the literature about a higher β-1,3-glucan exposition in bud scars and in hyphae [19, 20]. Finally, the hscFv activity on the pathogenic yeast *C. auris* was assessed through MIC assays and both alone and in combination with caspofungin and amphotericin B. hscFv alone doesn't affect the fungal growth but it contributes substantially to the activity of both caspofungin and amphotericin B especially when they are alone and lose their activity. Actually, MIC50 of caspofungin shifts of 2-fold concentration with 25 μg/ml of hscFv at 24 and 48 hours and of 1-fold with 2.5 μg/ml at 48 hours. With amphotericin B hscFv reaches its greatest potential with a decrease of MIC50 and MIC90 of 1-fold concentration with 2.5 μg/ml of hscFv and of 2 folds with 25 μg/ml at 24 hours while, if MIC90 fold decrease remains constant, the MIC50 shifts of 1-fold concentration with 0.25 μg/ml of hscFv, of 2 folds with 2.5 μg/ml and of 3 folds with 25 μg/ml. Further experiments must be done, especially to check the presence of additivity or synergy and to see whether the activity in combination is effective also on other fungal species

and genera. Since the small size of the hscFv it may be interesting to see its level of penetration, binding and activity in biofilm. Nonetheless, these highly promising preliminary results make us hopeful and intrigued.

FINAL CONCLUSION

The microbiological world and especially the fungal panorama is currently facing hard times with the rapid development and spread of resistance and the birth of new species intrinsically and sometimes multidrug-resistant. Noted the poor drug arsenal and the lack of effectiveness, an innovative approach had to be found. The application of biological drugs in this field has always been scarce and limited to a few attempts that almost always ended up with failures. In this study, we started from a candidate rich in activity potential but poor in safety and clinical future, the murine monoclonal antibody 2G8. 2G8 demonstrated to be able to bind selectively β-1,3-glucans, vital components of the cell wall of pathogenic fungi, and to be efficient in controlling fungal infections. Nevertheless, the murine nature was its major bottleneck, therefore I started my Ph.D. project with the aim to develop, produce and characterize a humanized antibody starting from 2G8. Two different antibody formats were evaluated: the single-chain fragment variable (scFv) and the full-length. These choices reflected two different ways of administration, hence diverse infection severity and urgency level. The full-length format was designed for systemic applications while the scFv, with its briefer half-life, for topical use.

The canonical CDR-grafting permitted the birth of a humanized single-chain fragment variable (hscFv). The orientation as VL-linker-VH and the presence of two ubiquitin monomers at the N-terminus and the His-tag at the C-terminus granted higher quantity, stability, and solubility. With many efforts, we managed to have a clean product (~40 mg from 1L of bacterial culture) with two steps of purification, a negative passage in Q Sepharose and a positive passage in Ni^{2+} Sepharose. hscFv is still able to bind β-1,3-glucans both as coated antigens and on *C. auris* and *C. albicans* cells and to affect the growth of *C. auris* when combined with caspofungin and amphotericin B. A black mark is represented by its tendency to aggregate forming disulphide bonds and, in a minor way, aspecific interactions. Studies on the best formulation led to the substitution of the reducing agent and to relatively long stability and retention of activity when stored at 4°, -20° and -80° C.

In the meanwhile, with a novel humanisation approach combining different humanization methods, the humanised full-length monoclonal antibody H5K1 was generated. It was soon compared to the murine 2G8 from which it took immediate distance in terms of performances showing better IC_{50}, AUC and K_d. Among pathogenic fungi, *Candida* spp. are the causes of many nosocomial infections and even though *C. albicans* is still the prevalent specie, over the past few years a mycological shift toward the non-*albicans Candida* (NAC) species has been recorded. Apropos *Candida auris* is one of the three leading causes of morbidity and mortality worldwide and is often associated with intrinsic multidrug-resistance and *Candida glabrata* is associated with higher mortality compared to other NACs. Both these species were considered as a fungal model to evaluate hmAb H5K1 effectiveness. H5K1 can bind selectively β-1,3-glucans on *C. auris*, *C. albicans* and *C. glabrata* cells and on *Aspergillus fumigatus* and *Fusarium solani* conidia. In particular, *C. auris*, *C. albicans* and *C. glabrata* had almost 100% of positive cells with a major binding propensity for budded cells and hyphae. Surprisingly H5K1 demonstrated activity alone in *C. auris* growth and adhesion inhibition and cell wall perturbation and in *C. glabrata* biofilm matrix alteration. However, the best activity was revealed in combination with amphotericin B and echinocandins on both *C. auris* and *C. glabrata* (of the latter two strains had low susceptibility for echinocandins and one was a biofilm hyper producer). H5K1 establishes additivity

with echinocandins and synergy with amphotericin B potentiating its fungicidal activity as well. This happens also at low concentrations of both hmAb H5K1 and of the antifungal drugs being an advantage considering the side effects of the available antifungal drugs used for prolonged periods and at high doses. In addition to its intrinsic and combinatorial efficacy, hmAb H5K1 keeps being a full-length antibody then able to be recognized by macrophages. As a matter of fact, after *C. auris* opsonization, macrophage efficiency increased, and the phagocytosis was enhanced.

In conclusion, hscFv and hmAb H5K1, both born from the murine hmAb 2G8, demonstrated comparable and sometimes better performances than their parental. They are effective *in vitro* especially in combination with amphotericin B and echinocandins showing to be able to modulate not just the fungal growth and adhesion but also the biofilm formation. The two different antibody formats are destined for different applications but in view of this fact, the full-length H5K1, suitable for systemic use, can also enhance the activity of phagocytic cells of the immune system.

The data showed in this thesis suggest that hscFv and hmAb H5K1 could be new drug candidates for the treatment of fungal infections and especially, candidiasis. Although the encouraging results, hscFv must be further explored while, noted the promising preclinical outcomes of hmAb H5K1, we are optimistic and hopeful about its rapid moving to clinical phases with the name of Dia-T51.

The considerable data resulting from these three years of Ph.D. were more than adequate for the patent submission of Dia-T51 (PCT/EP2021/080372).

REFERENCES

REFERENCES FOR INTRODUCTION

1. Falandysz, J., Treu, R. & Zhang, J. Call for papers: Special issue "Environment–Macromycetes (Fungi)–Edible Fungi". (2019).
2. Gorthi, L. V. Morphological Classification of Fungal Infections (Yeasts, Mold, Dimorphic). in Fungal Infections of the Central Nervous System: Pathogens, Diagnosis, and Management (eds. Turgut, M., Challa, S. & Akhaddar, A.) 23–30 (Springer International Publishing, 2019). doi:10.1007/978-3-030-06088-6_3.
3. Chay, C. et al. Isolation and identification of molds and yeasts in medombae, a rice wine starter culture from Kompong Cham Province, Cambodia. Food Res. 1, 213–220 (2017).
4. Rosenthal, A. L. & Nordin, J. H. Enzymes that hydrolyze fungal cell wall polysaccharides. The carbonhydrate constitution of mycodextranse, an endo-alpha (1 yields 4)-D-glucanase from Pencillium melinii. Journal of Biological Chemistry 250, 5295–5303 (1975).
5. Garcia-Rubio, R., de Oliveira, H. C., Rivera, J. & Trevijano-Contador, N. The Fungal Cell Wall: Candida, Cryptococcus, and Aspergillus Species. Frontiers in Microbiology 10, 2993 (2020).
6. Kang, X. et al. Molecular architecture of fungal cell walls revealed by solid-state NMR. Nat Commun 9, 2747 (2018).
7. Fungi: Experimental Methods In Biology, Second Edition. Routledge & CRC Press https://www.routledge.com/Fungi-Experimental-Methods-In-Biology-Second-Edition/Maheshwari/p/book/9781138199255.
8. Aronson, J. M. & Machlis, L. The Chemical Composition of the Hyphal Walls of the Fungus Allomyces. American Journal of Botany 46, 292–300 (1959).
9. Barbosa, I. P. & Kemmelmeier, C. Chemical Composition of the Hyphal Wall from Fusarium graminearum. Experimental Mycology 17, 274–283 (1993).
10. Fesel, P. H. & Zuccaro, A. β-glucan: Crucial component of the fungal cell wall and elusive MAMP in plants. Fungal Genetics and Biology 90, 53–60 (2016).
11. Riquelme, M. & Sánchez-León, E. The Spitzenkörper: a choreographer of fungal growth and morphogenesis. Current Opinion in Microbiology 20, 27–33 (2014).
12. Fernández, N. V., Cecilia Mestre, M., Marchelli, P. & Fontenla, S. B. Yeast and yeast-like fungi associated with dry indehiscent fruits of Nothofagus nervosa in Patagonia, Argentina. FEMS Microbiol Ecol 80, 179–192 (2012).

13. Sudbery, P., Gow, N. & Berman, J. The distinct morphogenic states of Candida albicans. Trends Microbiol 12, 317–324 (2004).

14. Blackwell, M. The Fungi: 1, 2, 3 … 5.1 million species? American Journal of Botany 98, 426–438 (2011).

15. One Health: Fungal Pathogens of Humans, Animals, and Plants. (American Society for Microbiology, 2019). doi:10.1128/AAMCol.18Oct.2017.

16. Characteristics of Fungi | Boundless Biology. https://courses.lumenlearning.com/boundless-biology/chapter/characteristics-of-fungi/.

17. Castrillo, L. A., Roberts, D. W. & Vandenberg, J. D. The fungal past, present, and future: Germination, ramification, and reproduction. Journal of Invertebrate Pathology 89, 46–56 (2005).

18. Ingold, C. T Fungal spores. Their libération and dispersal. T Fungal spores. Their liberation and dispersal. 4, (1971).

19. Heitman, J., Sun, S. & James, T. Y. Evolution of fungal sexual reproduction. Mycologia 105, 1–27 (2013).

20. Xu, J. Fungal species concepts in the genomics era. Genome 63, 459–468 (2020).

21. Tedersoo, L. et al. High-level classification of the Fungi and a tool for evolutionary ecological analyses. Fungal Diversity 90, 135–159 (2018).

22. Schüßler, A., Schwarzott, D. & Walker, C. A new fungal phylum, the Glomeromycota: phylogeny and evolution. Mycological Research 105, 1413–1421 (2001).

23. Spatafora, J. W. et al. A phylum-level phylogenetic classification of zygomycete fungi based on genome-scale data. Mycologia 108, 1028–1046 (2016).

24. O'Brien, H. E., Parrent, J. L., Jackson, J. A., Moncalvo, J.-M. & Vilgalys, R. Fungal Community Analysis by Large-Scale Sequencing of Environmental Samples. Applied and Environmental Microbiology 71, 5544–5550 (2005).

25. Xu, J. Fungal species concepts in the genomics era. Genome 63, 459–468 (2020).

26. Galindo, L. J., López-García, P., Torruella, G., Karpov, S. & Moreira, D. Phylogenomics of a new fungal phylum reveals multiple waves of reductive evolution across Holomycota. Nat Commun 12, 4973 (2021).

27. Gnat, S., Łagowski, D., Nowakiewicz, A. & Dyląg, M. A global view on fungal infections in humans and animals: opportunistic infections and microsporidioses. Journal of Applied Microbiology n/a.

28. Crameri, R. & Blaser, K. Allergy and immunity to fungal infections and colonization. European Respiratory Journal 19, 151–157 (2002).

29. Marinkovich, V. Fungal Hypersensitivity: Pathophysiology, Diagnosis, Therapy. Advances in applied microbiology 55, 289–307 (2004).

30. Peraica, M., RadicÂ, B., LucicÂ, A. & PavlovicÂ, M. Toxic effects of mycotoxins in humans. Bulletin of the World Health Organization 13 (1999).

31. Graeme, K. A. Mycetism: A Review of the Recent Literature. J Med Toxicol 10, 173–189 (2014).

32. Lombardi, G. et al. Superficial and subcutaneous mycoses. Microbiologia Medica 35, (2020).

33. Walsh, T. J. & Pizzo, P. A. Nosocomial fungal infections: a classification for hospital-acquired fungal infections and mycoses arising from endogenous flora or reactivation. Annu Rev Microbiol 42, 517–545 (1988).

34. Salzer, H. J. F. et al. Diagnosis and Management of Systemic Endemic Mycoses Causing Pulmonary Disease. Respiration 96, 283–301 (2018).

35. Arevalo, J. F., Fernández, C. F. & Mendoza, A. J. Chapter 41 - Fungal Infections. in Retinal Imaging (eds. Huang, D., Kaiser, P. K., Lowder, C. Y. & Traboulsi, E. I.) 366–374 (Mosby, 2006). doi:10.1016/B978-0-323-02346-7.50046-6.

36. Wohl, Y. & Tur, E. Environmental risk factors for mycosis fungoides. Curr Probl Dermatol 35, 52–64 (2007).

37. Jiang, S. Immunity against Fungal Infections. Immunol Immunogenet Insights 8, III.S38707 (2016).

38. Romani, L. Immunity to fungal infections. Nat Rev Immunol 4, 11–24 (2004).

39. Dropulic, L. K. & Lederman, H. M. Overview of Infections in the Immunocompromised Host. Microbiol Spectr 4, (2016).

40. Goodarzi, H., Trowbridge, J. & Gallo, R. L. Innate immunity: a cutaneous perspective. Clin Rev Allergy Immunol 33, 15–26 (2007).

41. Drummond, R. A., Gaffen, S. L., Hise, A. G. & Brown, G. D. Innate Defense against Fungal Pathogens. Cold Spring Harb Perspect Med 5, a019620 (2015).

42. Hatinguais, R., Willment, J. A. & Brown, G. D. PAMPs of the Fungal Cell Wall and Mammalian PRRs. in The Fungal Cell Wall : An Armour and a Weapon for Human Fungal Pathogens (ed. Latgé, J.-P.) 187–223 (Springer International Publishing, 2020). doi:10.1007/82_2020_201.

43. Plato, A., Hardison, S. E. & Brown, G. D. Pattern recognition receptors in antifungal immunity. Semin Immunopathol 37, 97–106 (2015).

44. Pathakumari, B., Liang, G. & Liu, W. Immune defence to invasive fungal infections: A comprehensive review. Biomedicine & Pharmacotherapy 130, 110550 (2020).

45. Romani, L. Immunity to fungal infections. Nat Rev Immunol 11, 275–288 (2011).

46. Zhu, L.-L. et al. C-Type Lectin Receptors Dectin-3 and Dectin-2 Form a Heterodimeric Pattern-Recognition Receptor for Host Defense against Fungal Infection. Immunity 39, 324–334 (2013).

47. Salazar, F. & Brown, G. D. Antifungal Innate Immunity: A Perspective from the Last 10 Years. JIN 10, 373–397 (2018).

48. Rezende, C. P. et al. Altered expression of genes related to innate antifungal immunity in the absence of galectin-3. Virulence 12, 981–988 (2021).

49. Hitoshi, N., Chihiro, I., Kenji, T., Hideoki, O. & Kazuhisa, I. Lactosylceramide is a Pattern Recognition Receptor that Forms Lyn-Coupled Membrane Microdomains on Neutrophils. Immunology, Endocrine & Metabolic Agents in Medicinal Chemistry (Under Re-organization) 8, 327–335 (2008).

50. Gazendam, R. P. et al. Human Neutrophils Use Different Mechanisms To Kill Aspergillus fumigatus Conidia and Hyphae: Evidence from Phagocyte Defects. J Immunol 196, 1272–1283 (2016).

51. Wu, S.-Y. et al. Candida albicans triggers NADPH oxidase-independent neutrophil extracellular traps through dectin-2. PLOS Pathogens 15, e1008096 (2019).

52. Gordon, S. & Martinez, F. O. Alternative Activation of Macrophages: Mechanism and Functions. Immunity 32, 593–604 (2010).

53. Speakman, E. A., Dambuza, I. M., Salazar, F. & Brown, G. D. T Cell Antifungal Immunity and the Role of C-Type Lectin Receptors. Trends in Immunology 41, 61–76 (2020).

54. Montagnoli, C. et al. A role for antibodies in the generation of memory antifungal immunity. Eur J Immunol 33, 1193–1204 (2003).

55. König, A., Müller, R., Mogavero, S. & Hube, B. Fungal factors involved in host immune evasion, modulation and exploitation during infection. Cell Microbiol 23, e13272 (2021).

56. Kumaresan, P. R., da Silva, T. A. & Kontoyiannis, D. P. Methods of Controlling Invasive Fungal Infections Using CD8+ T Cells. Frontiers in Immunology 8, 1939 (2018).

57. Gutiérrez-Martínez, E. et al. Cross-Presentation of Cell-Associated Antigens by MHC Class I in Dendritic Cell Subsets. Frontiers in Immunology 6, 363 (2015).

58. Nanjappa, S., Heninger, E., Wüthrich, M., Gasper, D. & Klein, B. Tc17 Cells Mediate Vaccine Immunity against Lethal Fungal Pneumonia in Immune Deficient Hosts Lacking CD4 T Cells. PLoS pathogens 8, e1002771 (2012).

59. Campbell, K. S. & Hasegawa, J. Natural killer cell biology: An update and future directions. Journal of Allergy and Clinical Immunology 132, 536–544 (2013).

60. Sakurai, A., Yamaguchi, N. & Sonoyama, K. Cell Wall Polysaccharides of Candida albicans Induce Mast Cell Degranulation in the Gut. Biosci Microbiota Food Health 31, 67–70 (2012).

61. 1.Ward, R. A. & Vyas, J. M. The first line of defense: effector pathways of anti-fungal innate immunity. Current Opinion in Microbiology 58, 160–165 (2020).

62. Houšť, J., Spížek, J. & Havlíček, V. Antifungal Drugs. Metabolites 10, 106 (2020).

63. Sergey, B. Z. Polyene Macrolide Antibiotics and their Applications in Human Therapy. Current Medicinal Chemistry 10, 211–223 (2003).

64. Nett, J. E. & Andes, D. R. Antifungal Agents: Spectrum of Activity, Pharmacology, and Clinical Indications. Infectious Disease Clinics of North America 30, 51–83 (2016).

65. Laniado-Laborín, R. & Cabrales-Vargas, M. N. Amphotericin B: side effects and toxicity. Rev Iberoam Micol 26, 223–227 (2009).

66. Perfect, J. R. The antifungal pipeline: a reality check. Nat Rev Drug Discov 16, 603–616 (2017).

67. Manavathu, E. K., Cutright, J. L. & Chandrasekar, P. H. Organism-Dependent Fungicidal Activities of Azoles. Antimicrob Agents Chemother 42, 3018–3021 (1998).

68. Mast, N., Zheng, W., Stout, C. D. & Pikuleva, I. A. Antifungal Azoles: Structural Insights into Undesired Tight Binding to Cholesterol-Metabolizing CYP46A1. Mol Pharmacol 84, 86–94 (2013).

69. Bodey, G. P. Azole Antifungal Agents. Clinical Infectious Diseases 14, S161–S169 (1992).

70. Allen, D., Wilson, D., Drew, R. & Perfect, J. Azole antifungals: 35 years of invasive fungal infection management. Expert Rev Anti Infect Ther 13, 787–798 (2015).

71. Pursley, T. J., Blomquist, I. K., Abraham, J., Andersen, H. F. & Bartley, J. A. Fluconazole-induced congenital anomalies in three infants. Clin Infect Dis 22, 336–340 (1996).

72. Cook, K. et al. QTc Prolongation in Patients Receiving Triazoles and Amiodarone. Open Forum Infectious Diseases 4, S84 (2017).

73. Sucher, A. J., Chahine, E. B. & Balcer, H. E. Echinocandins: the newest class of antifungals. Ann Pharmacother 43, 1647–1657 (2009).

74. Loh, B. S. & Ang, W. H. “Illuminating” Echinocandins’ Mechanism of Action. ACS Cent Sci 6, 1651–1653 (2020).

75. Flucytosine: Site of Action, Mechanism of Resistance and Use in Combination Therapy | SpringerLink. https://link.springer.com/chapter/10.1007/978-1-59745-180-2_27.

76. Mota Fernandes, C. et al. The Future of Antifungal Drug Therapy: Novel Compounds and Targets. Antimicrob Agents Chemother 65, e01719-20 (2021).

77. Bondaryk, M., Kurzątkowski, W. & Staniszewska, M. Antifungal agents commonly used in the superficial and mucosal candidiasis treatment: mode of action and resistance development. Adv Dermatol Allergol 30, 293–301 (2013).

78. Zheng, Y.-H., Ma, Y.-Y., Ding, Y., Chen, X.-Q. & Gao, G.-X. An insight into new strategies to combat antifungal drug resistance. Drug Des Devel Ther 12, 3807–3816 (2018).

79. Zhang, Q., Liu, F., Zeng, M., Mao, Y. & Song, Z. Drug repurposing strategies in the development of potential antifungal agents. Appl Microbiol Biotechnol 1–21 (2021) doi:10.1007/s00253-021-11407-7.

80. Nambu, M. et al. A calcineurin antifungal strategy with analogs of FK506. Bioorganic & Medicinal Chemistry Letters 27, 2465–2471 (2017).

81. Juvvadi, P. R. et al. Harnessing calcineurin-FK506-FKBP12 crystal structures from invasive fungal pathogens to develop antifungal agents. Nat Commun 10, 4275 (2019).

82. Vahedi-Shahandashti, R. & Lass-Flörl, C. Novel Antifungal Agents and Their Activity against Aspergillus Species. Journal of Fungi 6, 213 (2020).

83. Kontoyiannis, D. P., Lewis, R. E., Osherov, N., Albert, N. D. & May, G. S. Combination of caspofungin with inhibitors of the calcineurin pathway attenuates growth in vitro in Aspergillus species. Journal of Antimicrobial Chemotherapy 51, 313–316 (2003).

84. Onyewu, C., Blankenship, J. R., Del Poeta, M. & Heitman, J. Ergosterol Biosynthesis Inhibitors Become Fungicidal when Combined with Calcineurin Inhibitors against Candida albicans, Candida glabrata, and Candida krusei. Antimicrobial Agents and Chemotherapy 47, 956–964 (2003).

85. Lamoth, F., Juvvadi, P. R., Gehrke, C. & Steinbach, W. J. In Vitro Activity of Calcineurin and Heat Shock Protein 90 Inhibitors against Aspergillus fumigatus Azole- and Echinocandin-Resistant Strains. Antimicrobial Agents and Chemotherapy 57, 1035–1039 (2013).

86. Uppuluri, P., Nett, J., Heitman, J. & Andes, D. Synergistic Effect of Calcineurin Inhibitors and Fluconazole against Candida albicans Biofilms. Antimicrobial Agents and Chemotherapy 52, 1127–1132 (2008).

87. Maesaki, S. et al. Synergic effects of tactolimus and azole antifungal agents against azole-resistant Candida albican strains. J Antimicrob Chemother 42, 747–753 (1998).

88. Aslam, R. et al. Chromogranin A-derived peptides are involved in innate immunity. Curr Med Chem 19, 4115–4123 (2012).

89. Hai, T. P. et al. The combination of tamoxifen with amphotericin B, but not with fluconazole, has synergistic activity against the majority of clinical isolates of Cryptococcus neoformans. Mycoses 62, 818–825 (2019).

90. Zhao, R. et al. Navigating the Chaperone Network: An Integrative Map of Physical and Genetic Interactions Mediated by the Hsp90 Chaperone. Cell 120, 715–727 (2005).

91. Shapiro, R. S. et al. Pho85, Pcl1, and Hms1 Signaling Governs Candida albicans Morphogenesis Induced by High Temperature or Hsp90 Compromise. Current Biology 22, 461–470 (2012).

92. Lamoth, F., Juvvadi, P. R., Fortwendel, J. R. & Steinbach, W. J. Heat Shock Protein 90 Is Required for Conidiation and Cell Wall Integrity in Aspergillus fumigatus. Eukaryotic Cell 11, 1324–1332 (2012).

93. Singh, S. D. et al. Hsp90 Governs Echinocandin Resistance in the Pathogenic Yeast Candida albicans via Calcineurin. PLOS Pathogens 5, e1000532 (2009).

94. Karwa, R. & Wargo, K. A. Efungumab: a novel agent in the treatment of invasive candidiasis. Ann Pharmacother 43, 1818–1823 (2009).

95. Gorska, M. Geldanamycin and its derivatives as Hsp90 inhibitors. Front Biosci 17, 2269 (2012).

96. Whitesell, L. et al. Structural basis for species-selective targeting of Hsp90 in a pathogenic fungus. Nat Commun 10, 402 (2019).

97. LaFayette, S. L. et al. PKC Signaling Regulates Drug Resistance of the Fungal Pathogen Candida albicans via Circuitry Comprised of Mkc1, Calcineurin, and Hsp90. PLOS Pathogens 6, e1001069 (2010).

98. Sussman, A. et al. Discovery of Cercosporamide, a Known Antifungal Natural Product, as a Selective Pkc1 Kinase Inhibitor through High-Throughput Screening. Eukaryotic Cell 3, 932–943 (2004).

99. Pfaller, M. A., Rhomberg, P. R., Messer, S. A. & Castanheira, M. In vitro activity of a Hos2 deacetylase inhibitor, MGCD290, in combination with echinocandins against echinocandin-resistant Candida species. Diagn Microbiol Infect Dis 81, 259–263 (2015).

100. Pfaller, M. A. et al. Activity of MGCD290, a Hos2 histone deacetylase inhibitor, in combination with azole antifungals against opportunistic fungal pathogens. J Clin Microbiol 47, 3797–3804 (2009).

101. Bauer, I. et al. A Class 1 Histone Deacetylase with Potential as an Antifungal Target. mBio 7, e00831-16 (2016).

102. Wurtele, H. et al. Modulation of histone H3 lysine 56 acetylation as an antifungal therapeutic strategy. Nat Med 16, 774–780 (2010).

103. Rittershaus, P. C. et al. Glucosylceramide synthase is an essential regulator of pathogenicity of Cryptococcus neoformans. J Clin Invest 116, 1651–1659 (2006).

104. Fernandes, C. M., Goldman, G. H. & Del Poeta, M. Biological Roles Played by Sphingolipids in Dimorphic and Filamentous Fungi. mBio 9, e00642-18.

105. Mor, V. et al. Identification of a New Class of Antifungals Targeting the Synthesis of Fungal Sphingolipids. mBio 6, e00647-15.

106. Aeed, P. A., Young, C. L., Nagiec, M. M. & Elhammer, A. P. Inhibition of inositol phosphorylceramide synthase by the cyclic peptide aureobasidin A. Antimicrob Agents Chemother 53, 496–504 (2009).

107. Miyake, Y., Kozutsumi, Y., Nakamura, S., Fujita, T. & Kawasaki, T. Serine Palmitoyltransferase Is the Primary Target of a Sphingosine-like Immunosuppressant, ISP-1/Myriocin. Biochemical and Biophysical Research Communications 211, 396–403 (1995).

108. Delgado, A., Casas, J., Llebaria, A., Abad, J. L. & Fabrias, G. Inhibitors of sphingolipid metabolism enzymes. Biochimica et Biophysica Acta (BBA) - Biomembranes 1758, 1957–1977 (2006).

109. Rodrigues, M. L. et al. Monoclonal Antibody to Fungal Glucosylceramide Protects Mice against Lethal Cryptococcus neoformans Infection. Clin Vaccine Immunol 14, 1372–1376 (2007).

110. Rhome, R. et al. Surface Localization of Glucosylceramide during Cryptococcus neoformans Infection Allows Targeting as a Potential Antifungal. PLOS ONE 6, e15572 (2011).

111. Hogan, D. A. & Sundstrom, P. The Ras/cAMP/PKA signaling pathway and virulence in Candida albicans. Future Microbiology 4, 1263–1270 (2009).

112. Fortwendel, J. R., Panepinto, J. C., Seitz, A. E., Askew, D. S. & Rhodes, J. C. Aspergillus fumigatus rasA and rasB regulate the timing and morphology of asexual development. Fungal Genetics and Biology 41, 129–139 (2004).

113. Maurer, T. et al. Small-molecule ligands bind to a distinct pocket in Ras and inhibit SOS-mediated nucleotide exchange activity. Proc Natl Acad Sci U S A 109, 5299–5304 (2012).

114. Rubio, I. et al. Farnesylation of Ras is important for the interaction with phosphoinositide 3-kinase γ. European Journal of Biochemistry 266, 70–82 (1999).

115. Hast, M. A. et al. Structures of Cryptococcus neoformans protein farnesyltransferase reveal strategies for developing inhibitors that target fungal pathogens. J Biol Chem 286, 35149–35162 (2011).

116. Morgan, M. A., Ganser, A. & Reuter, C. W. M. Therapeutic efficacy of prenylation inhibitors in the treatment of myeloid leukemia. Leukemia 17, 1482–1498 (2003).

117. Hast, M. A. et al. Structures of Cryptococcus neoformans Protein Farnesyltransferase Reveal Strategies for Developing Inhibitors That Target Fungal Pathogens *. Journal of Biological Chemistry 286, 35149–35162 (2011).

118. Qiao, J., Gao, P., Jiang, X. & Fang, H. In vitro antifungal activity of farnesyltransferase inhibitors against clinical isolates of Aspergillus and Candida. Annals of Clinical Microbiology and Antimicrobials 12, 37 (2013).

119. Appels, N. M. G. M., Beijnen, J. H. & Schellens, J. H. M. Development of Farnesyl Transferase Inhibitors: A Review. The Oncologist 10, 565–578 (2005).

120. McGeady, P., Logan, D. A. & Wansley, D. L. A protein-farnesyl transferase inhibitor interferes with the serum-induced conversion of Candida albicans from a cellular yeast form to a filamentous form. FEMS Microbiology Letters 213, 41–44 (2002).

121. Mrak, P. et al. Discovery of the actinoplanic acid pathway in Streptomyces rapamycinicus reveals a genetically conserved synergism with rapamycin. J Biol Chem 293, 19982–19995 (2018).

122. Richard, M. et al. Complete glycosylphosphatidylinositol anchors are required in Candida albicans for full morphogenesis, virulence and resistance to macrophages. Molecular Microbiology 44, 841–853 (2002).

123. Li, H. et al. Glycosylphosphatidylinositol (GPI) anchor is required in Aspergillus fumigatus for morphogenesis and virulence. Molecular Microbiology 64, 1014–1027 (2007).

124. Shaw, K. J. et al. In Vitro and In Vivo Evaluation of APX001A/APX001 and Other Gwt1 Inhibitors against Cryptococcus. Antimicrobial Agents and Chemotherapy 62, e00523-18.

125. Yadav, U. & Khan, M. A. Targeting the GPI biosynthetic pathway. Pathog Glob Health 112, 115–122 (2018).

126. Lillie, S. H. & Pringle, J. R. Reserve carbohydrate metabolism in Saccharomyces cerevisiae: responses to nutrient limitation. Journal of Bacteriology 143, 1384–1394 (1980).

127. Perfect, J. R., Tenor, J. L., Miao, Y. & Brennan, R. G. Trehalose pathway as an antifungal target. Virulence 8, 143–149 (2017).

128. Fillinger, S. et al. Trehalose is required for the acquisition of tolerance to a variety of stresses in the filamentous fungus Aspergillus nidulans. Microbiology (Reading) 147, 1851–1862 (2001).

129. Svanström, Å., van Leeuwen, M. R., Dijksterhuis, J. & Melin, P. Trehalose synthesis in Aspergillus niger: characterization of six homologous genes, all with conserved orthologs in related species. BMC Microbiology 14, 90 (2014).

130. Al-Bader, N. et al. Role of Trehalose Biosynthesis in Aspergillus fumigatus Development, Stress Response, and Virulence. Infection and Immunity 78, 3007–3018 (2010).

131. Petzold, E. W. et al. Characterization and regulation of the trehalose synthesis pathway and its importance in the pathogenicity of Cryptococcus neoformans. Infect Immun 74, 5877–5887 (2006).

132. Ngamskulrungroj P, et al. The trehalose pathway: an integral part of virulence composite for

Cryptococcus gattii. Infect Immun. 2009; 77:4584–4596.

133. Guirao Abad, J., Sánchez-Fresneda, R., Valentin, E., Martinez-Esparza Alvargonzalez, M. & Argüelles, J.-C. Analysis of validamycin as a potential antifungal compound against Candida albicans. International Microbiology 16, 217–225 (2013).

134. Piekarska, K. et al. The activity of the glyoxylate cycle in peroxisomes of Candida albicans depends on a functional β-oxidation pathway: evidence for reduced metabolite transport across the peroxisomal membrane. Microbiology 154, 3061–3072.

135. Cheah, H.-L., Lim, V. & Sandai, D. Inhibitors of the glyoxylate cycle enzyme ICL1 in Candida albicans for potential use as antifungal agents. PLoS One 9, e95951 (2014).

136. Prado, R. S. do et al. Inhibition of Paracoccidioides lutzii Pb01 Isocitrate Lyase by the Natural Compound Argentilactone and Its Semi-Synthetic Derivatives. PLOS ONE 9, e94832 (2014).

137. Oliver, J. D. et al. F901318 represents a novel class of antifungal drug that inhibits dihydroorotate dehydrogenase. PNAS 113, 12809–12814 (2016).

138. Chatre, L. & Ricchetti, M. Are mitochondria the Achilles' heel of the Kingdom Fungi? Current Opinion in Microbiology 20, 49–54 (2014).

139. Shibata, T. et al. T-2307 Causes Collapse of Mitochondrial Membrane Potential in Yeast. Antimicrob Agents Chemother 56, 5892–5897 (2012).

140. Singh, S. B. et al. Antifungal Spectrum, In Vivo Efficacy, and Structure–Activity Relationship of Ilicicolin H. ACS Med. Chem. Lett. 3, 814–817 (2012).

141. Mitsuyama J, et al. In vitro and in vivo antifungal activities of T-2307, a novel arylamidine.

Antimicrob Agents Chemother. 2008; 52:1318–1324.

142. Silva, K. S. et al. Setting New Routes for Antifungal Drug Discovery Against Pathogenic Fungi. Current Pharmaceutical Design 26, (2020).

143. Cruz, M. C. et al. Rapamycin and Less Immunosuppressive Analogs Are Toxic to Candida albicans and Cryptococcus neoformans via FKBP12-Dependent Inhibition of TOR. Antimicrobial Agents and Chemotherapy 45, 3162–3170 (2001).

144. Hector, R. F., Zimmer, B. L. & Pappagianis, D. Evaluation of nikkomycins X and Z in murine models of coccidioidomycosis, histoplasmosis, and blastomycosis. Antimicrob Agents Chemother 34, 587–593 (1990).

145. Ganesan, L. T., Manavathu, E. K., Cutright, J. L., Alangaden, G. J. & Chandrasekar, P. H. In-vitro activity of nikkomycin Z alone and in combination with polyenes, triazoles or echinocandins against Aspergillus fumigatus. Clinical Microbiology and Infection 10, 961–966 (2004).

146. Torosantucci, A. et al. A novel glyco-conjugate vaccine against fungal pathogens. J Exp Med 202, 597–606 (2005).

147. Rachini, A. et al. An Anti-β-Glucan Monoclonal Antibody Inhibits Growth and Capsule Formation of Cryptococcus neoformans In Vitro and Exerts Therapeutic, Anticryptococcal Activity In Vivo. Infect Immun 75, 5085–5094 (2007).

148. Di Mambro, T. et al. A new humanized antibody is effective against pathogenic fungi in vitro. Sci Rep 11, 19500 (2021).

149. Krishnan, B. R. et al. CD101, a novel echinocandin with exceptional stability properties and enhanced aqueous solubility. J Antibiot 70, 130–135 (2017).

150. Walker, S. S. et al. Discovery of a novel class of orally active antifungal beta-1,3-D-glucan synthase inhibitors. Antimicrob Agents Chemother 55, 5099–5106 (2011).

151. Ribeiro, M. & Simões, M. Advances in the antimicrobial and therapeutic potential of siderophores. Environ Chem Lett 17, 1485–1494 (2019).

152. Tonziello, G., Caraffa, E., Pinchera, B., Granata, G. & Petrosillo, N. Present and future of siderophore-based therapeutic and diagnostic approaches in infectious diseases. Infectious Disease Reports 11, (2019).

153. Pfister, J. et al. Siderophore Scaffold as Carrier for Antifungal Peptides in Therapy of Aspergillus fumigatus Infections. J Fungi (Basel) 6, 367 (2020).

154. Sass, G. et al. Intermicrobial interaction: Aspergillus fumigatus siderophores protect against competition by Pseudomonas aeruginosa. PLOS ONE 14, e0216085 (2019).

155. Bastos, R. W. et al. Potential of Gallium as an Antifungal Agent. Front Cell Infect Microbiol 9, 414 (2019).

156. Nakamura, I. et al. ASP2397 Is a Novel Natural Compound That Exhibits Rapid and Potent Fungicidal Activity against Aspergillus Species through a Specific Transporter. Antimicrobial Agents and Chemotherapy 63, e02689-18.

157. Subissi, A., Monti, D., Togni, G. & Mailland, F. Ciclopirox: recent nonclinical and clinical data relevant to its use as a topical antimycotic agent. Drugs 70, 2133–2152 (2010).

158. 1.Oltu, I. et al. Current Research and New Perspectives in Antifungal Drug Development. in Advances in Microbiology, Infectious Diseases and Public Health: Volume 14 (ed. Donelli, G.) 71–83 (Springer International Publishing, 2020).

159. Grove, J. F. & Mcgowan, J. C. Identity of Griseofulvin and 'Curling-Factor'. Nature 160, 574–574 (1947).

160. Davis, S. R. An overview of the antifungal properties of allicin and its breakdown products--the possibility of a safe and effective antifungal prophylactic. Mycoses 48, 95–100 (2005).

161. Antoszczak, M. & Huczyński, A. Salinomycin and its derivatives – A new class of multiple-targeted "magic bullets". European Journal of Medicinal Chemistry 176, 208–227 (2019).

162. Koselny, K. et al. Antitumor/Antifungal Celecoxib Derivative AR-12 is a Non-Nucleoside Inhibitor of the ANL-Family Adenylating Enzyme Acetyl CoA Synthetase. ACS Infect Dis 2, 268–280 (2016).

163. Oliveira, L. V. N., Wang, R., Specht, C. A. & Levitz, S. M. Vaccines for human fungal diseases: close but still a long way to go. npj Vaccines 6, 1–8 (2021).

164. Shahi, G. et al. A detailed lipidomic study of human pathogenic fungi Candida auris. FEMS Yeast Res 20, foaa045 (2020).

165. Amarsaikhan, N. et al. Proteomic profiling of the antifungal drug response of Aspergillus fumigatus to voriconazole. Int J Med Microbiol 307, 398–408 (2017).

166. Brandt, P., Garbe, E. & Vylkova, S. Catch the wave: Metabolomic analyses in human pathogenic fungi. PLOS Pathogens 16, e1008757 (2020).

167. Kozel, T. R. & Wickes, B. Fungal Diagnostics. Cold Spring Harb Perspect Med 4, a019299 (2014).

168. Perlin, D. S., Rautemaa-Richardson, R. & Alastruey-Izquierdo, A. The global problem of antifungal resistance: prevalence, mechanisms, and management. Lancet Infect Dis 17, e383–e392 (2017).

169. Morrell, M., Fraser, V. J. & Kollef, M. H. Delaying the empiric treatment of candida bloodstream infection until positive blood culture results are obtained: a potential risk factor for hospital mortality. Antimicrob Agents Chemother 49, 3640–3645 (2005).

170. Zhang, S. X. et al. Recognition of Diagnostic Gaps for Laboratory Diagnosis of Fungal Diseases: Expert Opinion from the Fungal Diagnostics Laboratories Consortium (FDLC). Journal of Clinical Microbiology 59, e01784-20.

171. Wickes, B. L. & Wiederhold, N. P. Molecular diagnostics in medical mycology. Nat Commun 9, 5135 (2018).

172. Rodrigues, M. L. & Nosanchuk, J. D. Fungal diseases as neglected pathogens: A wake-up call to public health officials. PLoS Negl Trop Dis 14, e0007964 (2020).

173. Ostrosky-Zeichner, L. Invasive Mycoses: Diagnostic Challenges. The American Journal of Medicine 125, S14–S24 (2012).

174. Salzer, H. J. F. et al. Diagnosis and Management of Systemic Endemic Mycoses Causing Pulmonary Disease. Respiration 96, 283–301 (2018).

175. Verweij, P. E., Snelders, E., Kema, G. H. J., Mellado, E. & Melchers, W. J. G. Azole resistance in Aspergillus fumigatus: a side-effect of environmental fungicide use? Lancet Infect Dis 9, 789–795 (2009).

176. Selmecki, A., Forche, A. & Berman, J. Aneuploidy and isochromosome formation in drug-resistant Candida albicans. Science 313, 367–370 (2006).

177. Nnadi, N. E. & Carter, D. A. Climate change and the emergence of fungal pathogens. PLOS Pathogens 17, e1009503 (2021).

178. Espinel-Ingroff, A. et al. Interlaboratory Variability of Caspofungin MICs for Candida spp. Using CLSI and EUCAST Methods: Should the Clinical Laboratory Be Testing This Agent? Antimicrob Agents Chemother 57, 5836–5842 (2013).

179. Arendrup, M. C. & Patterson, T. F. Multidrug-Resistant Candida: Epidemiology, Molecular Mechanisms, and Treatment. The Journal of Infectious Diseases 216, S445–S451 (2017).

180. Mesa-Arango, A. C. et al. Cell Wall Changes in Amphotericin B-Resistant Strains from Candida tropicalis and Relationship with the Immune Responses Elicited by the Host. Antimicrob Agents Chemother 60, 2326–2335 (2016).

181. Blatzer, M. et al. Blocking Hsp70 Enhances the Efficiency of Amphotericin B Treatment against Resistant Aspergillus terreus Strains. Antimicrob Agents Chemother 59, 3778–3788 (2015).

182. Blum, G. et al. In vitro and in vivo role of heat shock protein 90 in Amphotericin B resistance of Aspergillus terreus. Clinical Microbiology and Infection 19, 50–55 (2013).

183. Linares, C. E. B. et al. Fluconazole and amphotericin-B resistance are associated with increased catalase and superoxide dismutase activity in Candida albicans and Candida dubliniensis. Rev. Soc. Bras. Med. Trop. 46, 752–758 (2013).

184. Marichal, P. et al. Contribution of mutations in the cytochrome P450 14alpha-demethylase (Erg11p, Cyp51p) to azole resistance in Candida albicans. Microbiology (Reading) 145 (Pt 10), 2701–2713 (1999).

185. Revie, N. M., Iyer, K. R., Robbins, N. & Cowen, L. E. Antifungal Drug Resistance: Evolution, Mechanisms and Impact. Curr Opin Microbiol 45, 70–76 (2018).

186. White, T. C., Marr, K. A. & Bowden, R. A. Clinical, cellular, and molecular factors that contribute to antifungal drug resistance. Clin Microbiol Rev 11, 382–402 (1998).

187. Cowen, L. E., Sanglard, D., Howard, S. J., Rogers, P. D. & Perlin, D. S. Mechanisms of Antifungal Drug Resistance. Cold Spring Harb Perspect Med 5, a019752 (2015).

188. Sanglard, D. et al. Mechanisms of resistance to azole antifungal agents in Candida albicans isolates from AIDS patients involve specific multidrug transporters. Antimicrob Agents Chemother 39, 2378–2386 (1995).

189. Sanglard, D., Ischer, F., Monod, M. & Bille, J. Cloning of Candida albicans genes conferring resistance to azole antifungal agents: characterization of CDR2, a new multidrug ABC transporter gene. Microbiology (Reading) 143 (Pt 2), 405–416 (1997).

190. Dunkel, N., Blass, J., Rogers, P. D. & Morschhäuser, J. Mutations in the multi-drug resistance regulator MRR1, followed by loss of heterozygosity, are the main cause of MDR1 overexpression in fluconazole-resistant Candida albicans strains. Mol Microbiol 69, 827–840 (2008).

191. Selmecki, A., Forche, A. & Berman, J. Genomic plasticity of the human fungal pathogen Candida albicans. Eukaryot Cell 9, 991–1008 (2010).

192. Bromley, M. et al. Mitochondrial Complex I Is a Global Regulator of Secondary Metabolism, Virulence and Azole Sensitivity in Fungi. PLOS ONE 11, e0158724 (2016).

193. Zhang, J. et al. Evolution of cross-resistance to medical triazoles in Aspergillus fumigatus through selection pressure of environmental fungicides. Proceedings of the Royal Society B: Biological Sciences 284, 20170635 (2017).

194. Chaabane, F., Graf, A., Jequier, L. & Coste, A. T. Review on Antifungal Resistance Mechanisms in the Emerging Pathogen Candida auris. Frontiers in Microbiology 10, 2788 (2019).

195. Healey, K. R. et al. Prevalent mutator genotype identified in fungal pathogen Candida glabrata promotes multi-drug resistance. Nat Commun 7, 11128 (2016).

196. Ben-Ami, R. et al. Fitness and Virulence Costs of Candida albicans FKS1 Hot Spot Mutations Associated With Echinocandin Resistance. J Infect Dis 204, 626–635 (2011).

197. Singh, S. D. et al. Hsp90 Governs Echinocandin Resistance in the Pathogenic Yeast Candida albicans via Calcineurin. PLOS Pathogens 5, e1000532 (2009).

198. Fortwendel, J. R. et al. Transcriptional Regulation of Chitin Synthases by Calcineurin Controls Paradoxical Growth of Aspergillus fumigatus in Response to Caspofungin. Antimicrob Agents Chemother 54, 1555–1563 (2010).

199. Edlind, T. D. & Katiyar, S. K. Mutational analysis of flucytosine resistance in Candida glabrata. Antimicrob Agents Chemother 54, 4733–4738 (2010).

200. Edlind, T. D. & Katiyar, S. K. Mutational Analysis of Flucytosine Resistance in Candida glabrata. Antimicrobial Agents and Chemotherapy 54, 4733–4738 (2010).

201. Gaffi - Global Action Fund for Fungal Infections. https://gaffi.org/ (2013).

202. Bongomin, F., Gago, S., Oladele, R. O. & Denning, D. W. Global and Multi-National Prevalence of Fungal Diseases—Estimate Precision. Journal of Fungi 3, 57 (2017).

203. Brown, G. D. et al. Hidden Killers: Human Fungal Infections. Science Translational Medicine 4, 165rv13-165rv13 (2012).

204. Casadevall, A. Fungal Diseases in the 21st Century: The Near and Far Horizons. Pathogens and Immunity 3, 183–196 (2018).

205. Jenks, J. D., Cornely, O. A., Chen, S. C.-A., Thompson III, G. R. & Hoenigl, M. Breakthrough invasive fungal infections: Who is at risk? Mycoses 63, 1021–1032 (2020).

206. Friedman, D. Z. P. & Schwartz, I. S. Emerging Fungal Infections: New Patients, New Patterns, and New Pathogens. J Fungi (Basel) 5, E67 (2019).

207. Lockhart, S. R. & Guarner, J. Emerging and reemerging fungal infections. Semin Diagn Pathol 36, 177–181 (2019).

208. 1.Schmiedel, Y. & Zimmerli, S. Common invasive fungal diseases: an overview of invasive candidiasis, aspergillosis, cryptococcosis, and Pneumocystis pneumonia. Swiss Medical Weekly (2016) doi:10.4414/smw.2016.14281.

209. Pal, M., Aregawi, W., N.Samajpati, & A.K.Manna. Growing role of non-Candida albicans Candida species in clinical disorders of humans and animals. Journal of Mycological Research 53, 41–48 (2015).

210. Lamoth, F., Lockhart, S. R., Berkow, E. L. & Calandra, T. Changes in the epidemiological landscape of invasive candidiasis. J Antimicrob Chemother 73, i4–i13 (2018).

211. Toda, M. Population-Based Active Surveillance for Culture-Confirmed Candidemia — Four Sites, United States, 2012–2016. MMWR Surveill Summ 68, (2019).

212. Wiederhold, N. P. Antifungal resistance: current trends and future strategies to combat. IDR 10, 249–259 (2017).

213. Satoh, K. et al. Candida auris sp. nov., a novel ascomycetous yeast isolated from the external ear canal of an inpatient in a Japanese hospital. Microbiology and Immunology 53, 41–44 (2009).

214. Tracking Candida auris | Candida auris | Fungal Diseases | CDC. https://www.cdc.gov/fungal/candida-auris/tracking-c-auris.html (2021).

215. Chow, N. A. et al. Potential Fifth Clade of Candida auris, Iran, 2018 - Volume 25, Number 9—September 2019 - Emerging Infectious Diseases journal - CDC. doi:10.3201/eid2509.190686.

216. Ahmad, S. & Alfouzan, W. Candida auris: Epidemiology, Diagnosis, Pathogenesis, Antifungal Susceptibility, and Infection Control Measures to Combat the Spread of Infections in Healthcare Facilities. Microorganisms 9, 807 (2021).

217. Forsberg, K. et al. Candida auris: The recent emergence of a multidrug-resistant fungal pathogen. Medical Mycology 57, 1–12 (2019).

218. Sathyapalan, D. T. et al. Evaluating the measures taken to contain a Candida auris outbreak in a tertiary care hospital in South India: an outbreak investigational study. BMC Infectious Diseases 21, 425 (2021).

219. Rossato, L. & Colombo, A. L. Candida auris: What Have We Learned About Its Mechanisms of Pathogenicity? Front Microbiol 9, 3081 (2018).

220. Lone, S. A. & Ahmad, A. Candida auris—the growing menace to global health. Mycoses 62, 620–637 (2019).

221. Adams, E. et al. Candida auris in Healthcare Facilities, New York, USA, 2013–2017 - Volume 24, Number 10—October 2018 - Emerging Infectious Diseases journal - CDC. doi:10.3201/eid2410.180649.

222. Bitar, D. et al. Population-Based Analysis of Invasive Fungal Infections, France, 2001–2010. Emerg Infect Dis 20, 1149–1155 (2014).

223. Alastruey-Izquierdo, A. et al. Population-based survey of filamentous fungi and antifungal resistance in Spain (FILPOP Study). Antimicrob Agents Chemother 57, 3380–3387 (2013).

224. Lionakis, M. S. et al. Increased frequency of non-fumigatus Aspergillus species in amphotericin B– or triazole–pre-exposed cancer patients with positive cultures for aspergilli. Diagnostic Microbiology and Infectious Disease 52, 15–20 (2005).

225. Baddley, J. W. et al. Aspergillosis in Intensive Care Unit (ICU) patients: epidemiology and economic outcomes. BMC Infect Dis 13, 29 (2013).

226. Crassard, N. et al. Invasive aspergillosis and allogeneic hematopoietic stem cell transplantation in children: a 15-year experience. Transpl Infect Dis 10, 177–183 (2008).

227. Enoch, D. A., Yang, H., Aliyu, S. H. & Micallef, C. The Changing Epidemiology of Invasive Fungal Infections. in Human Fungal Pathogen Identification: Methods and Protocols (ed. Lion, T.) 17–65 (Springer, 2017). doi:10.1007/978-1-4939-6515-1_2.

228. Lanjewar, D. N. The spectrum of clinical and pathological manifestations of AIDS in a consecutive series of 236 autopsied cases in mumbai, India. Patholog Res Int 2011, 547618 (2011).

229. Park, B. J. et al. Estimation of the current global burden of cryptococcal meningitis among persons living with HIV/AIDS. AIDS 23, 525–530 (2009).

230. Herkert, P. F. et al. Ecoepidemiology of Cryptococcus gattii in Developing Countries. J Fungi (Basel) 3, 62 (2017).

231. Bermas, A. & Geddes-McAlister, J. Combatting the evolution of antifungal resistance in Cryptococcus neoformans. Molecular Microbiology 114, 721–734 (2020).

232. Larsen, H. H. et al. Primary Pneumocystis Infection in Infants Hospitalized with Acute Respiratory Tract Infection. Emerg Infect Dis 13, 66–72 (2007).

233. Hubert, P. & Amigorena, S. Antibody-dependent cell cytotoxicity in monoclonal antibody-mediated tumor immunotherapy. Oncoimmunology 1, 103–105 (2012).

234. Collis, A. V. J., Brouwer, A. P. & Martin, A. C. R. Analysis of the antigen combining site: correlations between length and sequence composition of the hypervariable loops and the nature of the antigen. J Mol Biol 325, 337–354 (2003).

235. Wright, A. & Morrison, S. L. Effect of C2-associated carbohydrate structure on Ig effector function: studies with chimeric mouse-human IgG1 antibodies in glycosylation mutants of Chinese hamster ovary cells. J Immunol 160, 3393–3402 (1998).

236. Charles A Janeway, J., Travers, P., Walport, M. & Shlomchik, M. J. The distribution and functions of immunoglobulin isotypes. Immunobiology: The Immune System in Health and Disease. 5th edition (2001).

237. Vidarsson, G., Dekkers, G. & Rispens, T. IgG Subclasses and Allotypes: From Structure to Effector Functions. Front Immunol 5, 520 (2014).

238. Yusakul, G., Sakamoto, S., Pongkitwitoon, B., Tanaka, H. & Morimoto, S. Effect of linker length between variable domains of single chain variable fragment antibody against daidzin on its reactivity. Biosci Biotechnol Biochem 80, 1306–1312 (2016).

239. Whitlow, M. et al. An improved linker for single-chain Fv with reduced aggregation and enhanced proteolytic stability. Protein Eng 6, 989–995 (1993).

240. Alfaleh, M. A. et al. Phage Display Derived Monoclonal Antibodies: From Bench to Bedside. Frontiers in Immunology 11, 1986 (2020).

241. Irani, Y., Brereton, H. M., Tilton, R. G., Coster, D. J. & Williams, K. A. Production of scFv antibody fragments from a hybridoma with functional activity against human vascular endothelial growth factor. Hybridoma (Larchmt) 28, 205–209 (2009).

242. Rajput, R. et al. Diagnostic Potential of Recombinant scFv Antibodies Generated Against Hemagglutinin Protein of Influenza A Virus. Front Immunol 6, 440 (2015).

243. Hwang, W. Y. K. & Foote, J. Immunogenicity of engineered antibodies. Methods 36, 3–10 (2005).

244. Smith, K. et al. Rapid generation of fully human monoclonal antibodies specific to a vaccinating antigen. Nat Protoc 4, 372–384 (2009).

245. Clark, M. Antibody humanization: a case of the 'Emperor's new clothes'? Immunol Today 21, 397–402 (2000).

246. MAb Products: Market Trends and Projections. BioProcess International https://bioprocessintl.com/business/economics/the-market-for-therapeutic-mab-products/ (2020).

247. Torosantucci, A. et al. Protection by Anti-β-Glucan Antibodies Is Associated with Restricted β-1,3 Glucan Binding Specificity and Inhibition of Fungal Growth and Adherence. PLoS One 4, e5392 (2009).

FIGURES

Figures were built by Tania Vanzolini using images made kindly available by Servier Medical ART (https://smart.servier.com/). Servier Medical Art by Servier is licensed under a Creative Commons Attribution 3.0 Unported License (https://creativecommons.org/licenses/by/3.0/). I wish to express my sincere gratitude to Servier Medical ART.

REFERENCES FOR CHAPTER 2

1. Eggimann, P., Garbino, J. & Pittet, D. Management of Candida species infections in critically ill patients. Lancet Infect Dis 3, 772–785 (2003).Tsay, S. et al. 363. National Burden of Candidemia, United States, 2017. Open Forum Infect Dis 5, S142–S143 (2018).
2. Koehler, P. et al. Morbidity and mortality of candidaemia in Europe: an epidemiologic meta-analysis. Clinical Microbiology and Infection 25, 1200–1212 (2019).
3. Pappas, P. G., Lionakis, M. S., Arendrup, M. C., Ostrosky-Zeichner, L. & Kullberg, B. J. Invasive candidiasis. Nat Rev Dis Primers 4, 18026 (2018).
4. Kainz, K., Bauer, M. A., Madeo, F. & Carmona-Gutierrez, D. Fungal infections in humans: the silent crisis. Microbial Cell 7, 143–145 (2020).
5. Centers for Disease Control and Prevention (U.S.). Antibiotic resistance threats in the United States, 2019. https://stacks.cdc.gov/view/cdc/82532 (2019)
6. Satoh, K. et al. Candida auris sp. nov., a novel ascomycetous yeast isolated from the external ear canal of an inpatient in a Japanese hospital. Microbiology and Immunology 53, 41–44 (2009).
7. Tracking Candida auris | Candida auris | Fungal Diseases | CDC. https://www.cdc.gov/fungal/candida-auris/tracking-c-auris.html (2021).
8. de Jong, A. W. & Hagen, F. Attack, Defend and Persist: How the Fungal Pathogen Candida auris was Able to Emerge Globally in Healthcare Environments. Mycopathologia 184, 353–365 (2019).
9. Heaney, H. et al. The environmental stress sensitivities of pathogenic Candida species, including Candida auris, and implications for their spread in the hospital setting. Medical mycology 58, (2020).
10. Bravo, G. Pseudohyphal growth of the emerging pathogen Candida auris is triggered by genotoxic stress through the S phase checkpoint. 24 (2019).
11. Wang, X. et al. The first isolate of Candida auris in China: clinical and biological aspects. Emerg Microbes Infect 7, 93 (2018).
12. Garcia-Rubio, R., de Oliveira, H. C., Rivera, J. & Trevijano-Contador, N. The Fungal Cell Wall: Candida, Cryptococcus, and Aspergillus Species. Frontiers in Microbiology 10, 2993 (2020).
13. Chaffin, W. L. Candida albicans Cell Wall Proteins. Microbiology and Molecular Biology Reviews 72, 495–544 (2008).

14. Gow, N. A. R., van de Veerdonk, F. L., Brown, A. J. P. & Netea, M. G. Candida albicans morphogenesis and host defence: discriminating invasion from colonization. Nat Rev Microbiol 10, 112–122 (2011).

15. Yoshimi, A., Miyazawa, K. & Abe, K. Function and Biosynthesis of Cell Wall α-1,3-Glucan in Fungi. Journal of Fungi 3, 63 (2017).

16. Brown, G. D. Dectin-1: a signalling non-TLR pattern-recognition receptor. Nat Rev Immunol 6, 33–43 (2006).

17. Chaffin, W. L. Candida albicans cell wall proteins. Microbiol Mol Biol Rev 72, 495–544 (2008).

18. Ruiz-Herrera, J., Victoria Elorza, M., Valentín, E. & Sentandreu, R. Molecular organization of the cell wall of Candida albicans and its relation to pathogenicity. FEMS Yeast Research 6, 14–29 (2006).

19. Zamith-Miranda, D. et al. Multi-omics Signature of Candida auris, an Emerging and Multidrug-Resistant Pathogen. mSystems 4, e00257-19 (2019).

20. Navarro-Arias, M. J. et al. Differential recognition of Candida tropicalis, Candida guilliermondii, Candida krusei, and Candida auris by human innate immune cells. Infect Drug Resist 12, 783–794 (2019).

21. Di Mambro, T. et al. A new humanized antibody is effective against pathogenic fungi in vitro. Sci Rep 11, 19500 (2021).

22. Milhaud, J., Ponsinet, V., Takashi, M. & Michels, B. Interactions of the drug amphotericin B with phospholipid membranes containing or not ergosterol: new insight into the role of ergosterol. Biochimica et Biophysica Acta (BBA) - Biomembranes 1558, 95–108 (2002).

23. Gavara, N. A beginner's guide to atomic force microscopy probing for cell mechanics. Microsc Res Tech 80, 75–84 (2017).

24. Raposo, M., Ferreira, Q. & Ribeiro, P. A Guide for Atomic Force Microscopy Analysis of Soft Condensed Matter. Modern Research and Educational Topics in Microscopy 1, (2007).

25. Antonio, P. D., Lasalvia, M., Perna, G. & Capozzi, V. Scale-independent roughness value of cell membranes studied by means of AFM technique. Biochim Biophys Acta 1818, 3141–3148 (2012).

26. da Silva Junior, A. & Teschke, O. Dynamics of the Antimicrobial Peptide PGLa Action on Escherichia coli Monitored by Atomic Force Microscopy. World J Microbiol Biotechnol 21, 1103–1110 (2005).

27. Arnold, W. Force Modulation in Atomic Force Microscopy. in Encyclopedia of Nanotechnology (ed. Bhushan, B.) 1–11 (Springer Netherlands, 2014).

28. Hayashi, K. & Iwata, M. Stiffness of cancer cells measured with an AFM indentation method. Journal of the Mechanical Behavior of Biomedical Materials 49, 105–111 (2015).

29. Wheeler, R. T., Kombe, D., Agarwala, S. D. & Fink, G. R. Dynamic, Morphotype-Specific Candida albicans β-Glucan Exposure during Infection and Drug Treatment. PLoS Pathog 4, e1000227 (2008).

30. Hasim, S. et al. β-(1,3)-Glucan Unmasking in Some Candida albicans Mutants Correlates with Increases in Cell Wall Surface Roughness and Decreases in Cell Wall Elasticity. Infect Immun 85, (2017).

REFERENCES FOR CHAPTER 3

1. Perlin, D. S., Rautemaa-Richardson, R. & Alastruey-Izquierdo, A. The global problem of antifungal resistance: prevalence, mechanisms, and management. Lancet Infect Dis 17, e383–e392 (2017).

2. Colombo, A. L., Júnior, J. N. de A. & Guinea, J. Emerging multidrug-resistant Candida species. Current Opinion in Infectious Diseases 30, 528–538 (2017).

3. Forsberg, K. et al. Candida auris: The recent emergence of a multidrug-resistant fungal pathogen. Medical Mycology 57, 1–12 (2019).

4. Nnadi, N.E.; Carter, D.A. Climate Change and the Emergence of Fungal Pathogens. PLOS Pathog. 2021, 17, e1009503.

5. Ribas E Ribas, A. D. et al. Is the emergence of fungal resistance to medical triazoles related to their use in the agroecosystems? A mini review. Braz J Microbiol 47, 793–799 (2016).

6. Friedman, D. Z. P. & Schwartz, I. S. Emerging Fungal Infections: New Patients, New Patterns, and New Pathogens. J Fungi (Basel) 5, E67 (2019).

7. Seagle, E. E., Williams, S. L. & Chiller, T. M. Recent Trends in the Epidemiology of Fungal Infections. Infect Dis Clin North Am 35, 237–260 (2021).

8. Lockhart, S. R. et al. Species Identification and Antifungal Susceptibility Testing of Candida Bloodstream Isolates from Population-Based Surveillance Studies in Two U.S. Cities from 2008 to 2011. Journal of Clinical Microbiology 50, 3435–3442 (2012).

9. Mete, B. et al. Change in species distribution and antifungal susceptibility of candidemias in an intensive care unit of a university hospital (10-year experience). Eur J Clin Microbiol Infect Dis 40, 325–333 (2021).

10. Pfaller, M. A., Diekema, D. J., & International Fungal Surveillance Participant Group. Twelve years of fluconazole in clinical practice: global trends in species distribution and fluconazole susceptibility of bloodstream isolates of Candida. Clin Microbiol Infect 10 Suppl 1, 11–23 (2004).

11. Olson, J. A., Adler-Moore, J. P., Smith, P. J. & Proffitt, R. T. Treatment of Candida glabrata Infection in Immunosuppressed Mice by Using a Combination of Liposomal Amphotericin B with Caspofungin or Micafungin. Antimicrob Agents Chemother 49, 4895–4902 (2005).

12. Fidel, P. L., Vazquez, J. A. & Sobel, J. D. Candida glabrata: Review of Epidemiology, Pathogenesis, and Clinical Disease with Comparison to C. albicans. Clin Microbiol Rev 12, 80–96 (1999).

13. Choi, H. K. et al. Blood Stream Infections by Candida glabrata and Candida krusei: A Single-Center Experience. Korean J Intern Med 24, 263–269 (2009).

14. Castanheira, M. et al. Frequency of fks Mutations among Candida glabrata Isolates from a 10-Year Global Collection of Bloodstream Infection Isolates. Antimicrob Agents Chemother 58, 577–580 (2014).

15. Vandeputte, P. et al. Reduced Susceptibility to Polyenes Associated with a Missense Mutation in the ERG6 Gene in a Clinical Isolate of Candida glabrata with Pseudohyphal Growth. Antimicrob Agents Chemother 51, 982–990 (2007).

16. Tsai, H.-F. et al. Candida glabrata erg1 Mutant with Increased Sensitivity to Azoles and to Low Oxygen Tension. Antimicrob Agents Chemother 48, 2483–2489 (2004).

17. Timmermans, B., De Las Peñas, A., Castaño, I. & Van Dijck, P. Adhesins in Candida glabrata. Journal of Fungi 4, 60 (2018).

18. Rodrigues, C. F., Silva, S. & Henriques, M. Candida glabrata: a review of its features and resistance. Eur J Clin Microbiol Infect Dis 33, 673–688 (2014).

19. Silva, S., Henriques, M., Oliveira, R., Williams, D. & Azeredo, J. In Vitro Biofilm Activity of Non-Candida albicansCandida Species. Curr Microbiol 61, 534–540 (2010).

20. Di Mambro, T. et al. A new humanized antibody is effective against pathogenic fungi in vitro. Sci Rep 11, 19500 (2021).

21. da Silveira, P. V. et al. Twice-daily red and blue light treatment for Candida albicans biofilm matrix development control. Lasers Med Sci 34, 441–447 (2019).

22. Haddadin, R. n. s., Saleh, S., Al-Adham, I. s. i., Buultjens, T. e. j. & Collier, P. j. The effect of subminimal inhibitory concentrations of antibiotics on virulence factors expressed by Staphylococcus aureus biofilms. Journal of Applied Microbiology 108, 1281–1291 (2010).

23. Feoktistova, M., Geserick, P. & Leverkus, M. Crystal Violet Assay for Determining Viability of Cultured Cells. Cold Spring Harb Protoc 2016, pdb.prot087379 (2016).

24. Cleary, I. A. et al. Examination of the pathogenic potential of Candida albicans filamentous cells in an animal model of haematogenously disseminated candidiasis. FEMS Yeast Research 16, (2016).

25. Ernst, J. F. Transcription factors in Candida albicans - environmental control of morphogenesis. Microbiology (Reading) 146 (Pt 8), 1763–1774 (2000).

26. Mukaremera, L., Lee, K. K., Mora-Montes, H. M. & Gow, N. A. R. Candida albicans Yeast, Pseudohyphal, and Hyphal Morphogenesis Differentially Affects Immune Recognition. Frontiers in Immunology 8, 629 (2017).

27. Thompson, D. S., Carlisle, P. L. & Kadosh, D. Coevolution of morphology and virulence in Candida species. Eukaryot Cell 10, 1173–1182 (2011).

28. Bouklas, T. et al. Generational distribution of a Candida glabrata population: Resilient old cells prevail, while younger cells dominate in the vulnerable host. PLOS Pathogens 13, e1006355 (2017).

29. Bhattacharya, S., Bouklas, T. & Fries, B. C. Replicative Aging in Pathogenic Fungi. Journal of Fungi 7, 6 (2021).

30. Dominguez, E. et al. Conservation and Divergence in the Candida Species Biofilm Matrix Mannan-Glucan Complex Structure, Function, and Genetic Control. mBio 9, e00451-18.

31. Kumamoto, C. A. A contact-activated kinase signals Candida albicans invasive growth and biofilm development. Proc Natl Acad Sci U S A 102, 5576–5581 (2005).

32. Bor, B., Cen, L., Agnello, M., Shi, W. & He, X. Morphological and physiological changes induced by contact-dependent interaction between Candida albicans and Fusobacterium nucleatum. Sci Rep 6, 27956 (2016).

REFERENCES FOR CHAPTER 4

1. DeFrancesco, L. Drug pipeline 1Q21-the old and the new. Nat Biotechnol 39, 536–537 (2021).
2. Almeida, H., Amaral, M. H. & Lobão, P. Drugs obtained by biotechnology processing. Braz. J. Pharm. Sci. 47, 199–207 (2011).
3. Strohl, W. R. Current progress in innovative engineered antibodies. Protein Cell 9, 86–120 (2018).
4. Lu, R.-M. et al. Development of therapeutic antibodies for the treatment of diseases. Journal of Biomedical Science 27, 1 (2020).
5. Lawrence, S. The biotech drug market. Nat Biotechnol 22, 1496–1496 (2004).
6. Malik, N. N. Biotech acquisitions by big pharma: why and what is next. Drug Discovery Today 14, 818–821 (2009).
7. S, T., S, S., R, R., Semwal, B. & Yadav, P. Biotech drugs: the next boom in pharmaceutical market. Journal of pharmaceutical research and opinion 1, 76–79 (2011).
8. Emmons, C. & Hunsicker, L. G. Muromonab-CD3 (Orthoclone OKT3): the first monoclonal antibody approved for therapeutic use. Iowa Med 77, 78–82 (1987).
9. Sgro, C. Side-effects of a monoclonal antibody, muromonab CD3/orthoclone OKT3: bibliographic review. Toxicology 105, 23–29 (1995).
10. Hutchinson, M. Natalizumab: A new treatment for relapsing remitting multiple sclerosis. Ther Clin Risk Manag 3, 259–268 (2007).
11. EPIC Investigators. Use of a monoclonal antibody directed against the platelet glycoprotein IIb/IIIa receptor in high-risk coronary angioplasty. N Engl J Med 330, 956–961 (1994).
12. Nelson, A. L. Antibody fragments. MAbs 2, 77–83 (2010).
13. Torosantucci, A. et al. A novel glyco-conjugate vaccine against fungal pathogens. J Exp Med 202, 597–606 (2005).
14. Rachini, A. et al. An Anti-β-Glucan Monoclonal Antibody Inhibits Growth and Capsule Formation of Cryptococcus neoformans In Vitro and Exerts Therapeutic, Anticryptococcal Activity In Vivo. Infect Immun 75, 5085–5094 (2007).
15. Torosantucci, A. et al. Protection by Anti-β-Glucan Antibodies Is Associated with Restricted β-1,3 Glucan Binding Specificity and Inhibition of Fungal Growth and Adherence. PLoS One 4, e5392 (2009).
16. https://web.expasy.org/protparam/

17. http://www.ncbi.nlm.nih.gov/igblast/

18. Villani, M. E. et al. Humanization of a highly stable single-chain antibody by structure-based antigen-binding site grafting. Mol Immunol 45, 2474–2485 (2008).

19. Mader, A. & Kunert, R. Humanization strategies for an anti-idiotypic antibody mimicking HIV-1 gp41. Protein Eng Des Sel 23, 947–954 (2010).

20. http://www.rcsb.org/pdb/home/home.do

21. Makabe, K. et al. Thermodynamic consequences of mutations in vernier zone residues of a humanized anti-human epidermal growth factor receptor murine antibody, 528. J Biol Chem 283, 1156–1166 (2008).

22. Jordan, J. L. et al. Structural understanding of stabilization patterns in engineered bispecific Ig-like antibody molecules. Proteins 77, 832–841 (2009).

23. Teplyakov, A., Obmolova, G., Malia, T. J., Luo, J. & Gilliland, G. L. Structural evidence for a constrained conformation of short CDR-L3 in antibodies. Proteins 82, 1679–1683 (2014).

24. Scharf, L. et al. Structural basis for HIV-1 gp120 recognition by a germ-line version of a broadly neutralizing antibody. Proc Natl Acad Sci U S A 110, 6049–6054 (2013).

25. Hilden, I. et al. Hemostatic effect of a monoclonal antibody mAb 2021 blocking the interaction between FXa and TFPI in a rabbit hemophilia model. Blood 119, 5871–5878 (2012).

26. Chu, H.-M. et al. Two potential therapeutic antibodies bind to a peptide segment of membrane-bound IgE in different conformations. Nat Commun 5, 3139 (2014).

27. Fouts, A. E. et al. Mechanism for neutralizing activity by the anti-CMV gH/gL monoclonal antibody MSL-109. Proc Natl Acad Sci U S A 111, 8209–8214 (2014).

28. Foote, J. & Winter, G. Antibody framework residues affecting the conformation of the hypervariable loops. J Mol Biol 224, 487–499 (1992).

29. Tsumoto, K. et al. Effect of the order of antibody variable regions on the expression of the single-chain HyHEL10 Fv fragment in E. coli and the thermodynamic analysis of its antigen-binding properties. Biochem Biophys Res Commun 201, 546–551 (1994).

30. Anand, N. N. et al. Bacterial expression and secretion of various single-chain Fv genes encoding proteins specific for a Salmonella serotype B O-antigen. J Biol Chem 266, 21874–21879 (1991).

31. Cheng, Y. et al. A VL-linker-VH Orientation Dependent Single Chain Variable Antibody Fragment Against Rabies Virus G Protein with Enhanced Neutralizing Potency in vivo. Protein Pept Lett 23, 24–32 (2016).

32. Hamilton, S., Odili, J., Gundogdu, O., Wilson, G. D. & Kupsch, J. M. Improved production by domain inversion of single-chain Fv antibody fragment against high molecular weight proteoglycan for the radioimmunotargeting of melanoma. Hybrid Hybridomics 20, 351–360 (2001).

REFERENCES FOR CHAPTER 5

1. Tiller, K. E. & Tessier, P. M. Advances in Antibody Design. Annu Rev Biomed Eng 17, 191–216 (2015).

2. Ahmad, Z. A. et al. scFv antibody: principles and clinical application. Clin Dev Immunol 2012, 980250 (2012).

3. Nelson, A. L. Antibody fragments. MAbs 2, 77–83 (2010).

4. Chen, W., Yuan, Y. & Jiang, X. Antibody and antibody fragments for cancer immunotherapy. J Control Release 328, 395–406 (2020).

5. Fernandes, J. C. Therapeutic application of antibody fragments in autoimmune diseases: current state and prospects. Drug Discov Today 23, 1996–2002 (2018).

6. Lu, R.-M. et al. Development of therapeutic antibodies for the treatment of diseases. Journal of Biomedical Science 27, 1 (2020).

7. Xu, X., Zhang, R. & Chen, X. Application of a single-chain fragment variable (scFv) antibody for the confirmatory diagnosis of hydatid disease in non-endemic areas. Electronic Journal of Biotechnology 29, 57–62 (2017).

8. Monnier, P. P., Vigouroux, R. J. & Tassew, N. G. In Vivo Applications of Single Chain Fv (Variable Domain) (scFv) Fragments. Antibodies 2, 193–208 (2013).

9. Grilo, A. L. & Mantalaris, A. The Increasingly Human and Profitable Monoclonal Antibody Market. Trends Biotechnol 37, 9–16 (2019).

10. Kang, T. H. & Seong, B. L. Solubility, Stability, and Avidity of Recombinant Antibody Fragments Expressed in Microorganisms. Frontiers in Microbiology 11, 1927 (2020).

11. 1.Ratanji, K. D., Derrick, J. P., Dearman, R. J. & Kimber, I. Immunogenicity of therapeutic proteins: Influence of aggregation. J Immunotoxicol 11, 99–109 (2014).

12. Gourbatsi, E., Povey, J. F. & Smales, C. M. The effect of formulation variables on protein stability and integrity of a model IgG4 monoclonal antibody and translation to formulation of a model ScFv. Biotechnol Lett 40, 33–46 (2018).

13. Ebo, J. S. et al. An in vivo platform to select and evolve aggregation-resistant proteins. Nat Commun 11, 1816 (2020).

14. Martin, N. et al. Refolding of Aggregation-Prone ScFv Antibody Fragments Assisted by Hydrophobically Modified Poly(sodium acrylate) Derivatives. Macromol Biosci 17, (2017).

15. Andrade, C. et al. An Integrated Approach to Aggregate Control for Therapeutic Bispecific Antibodies Using an Improved Three Column Mab Platform-Like Purification Process. Biotechnol Prog 35, e2720 (2019).

16. Zhang, J., Liu, H. & Katta, V. Structural characterization of intact antibodies by high-resolution LTQ Orbitrap mass spectrometry. Journal of Mass Spectrometry 45, 112–120 (2010).

17. Pierleoni, R. et al. Effect of the redox state on HIV-1 tat protein multimerization and cell internalization and trafficking. Mol Cell Biochem 345, 105–118 (2010).

18. Lu, Y., Su, C., Wang, A. & Liu, H. Hyphal Development in Candida albicans Requires Two Temporally Linked Changes in Promoter Chromatin for Initiation and Maintenance. PLOS Biology 9, e1001105 (2011).

19. Chen, T. et al. Exposure of Candida albicans β (1,3)-glucan is promoted by activation of the Cek1 pathway. PLoS Genet 15, e1007892 (2019).

20. Strijbis, K. et al. Bruton's Tyrosine Kinase (BTK) and Vav1 Contribute to Dectin1-Dependent Phagocytosis of Candida albicans in Macrophages. PLoS Pathog 9, e1003446 (2013).

Additional collateral projects have led to the following outcomes:

Ghezzi, P. et al. Online Information of Vaccines: Information Quality, Not Only Privacy, Is an Ethical Responsibility of Search Engines. Frontiers in Medicine 7, 400 (2020).

Doi: https://doi.org/10.3389/fmed.2020.00400

Mehta, S., Ghezzi, D., Catalani, A., Vanzolini, T. & Ghezzi, P. Online information on face masks: analysis of websites in Italian and English returned by different search engines. BMJ Open 11, e046364 (2021).

Doi: https://doi.org/10.1101/2020.10.23.20218271

Vanzolini T., Bruschi M., Rinaldi A. C., Magnani M., Fraternale A. Multitalented synthetic antimicrobial peptides and their antibacterial, antifungal and anti-viral mechanisms – Submitted

ACKNOWLEDGEMENT

I wish to thank Marche Region for financing the Innovative Ph.D. project and the partners which collaborated with us.

Universidad Zaragoza

I personally want to express my sincere gratitude to my supervisor professor Mauro Magnani and to my co-supervisor Tomas Di Mambro for letting me have this striking experience.

I wish to thank Professor Francesco Barchiesi and his group for allowing me to work with them and learn more than I expected!

I also would like to thank all the people with whom I had the pleasure to work and discuss.

Thank you for helping, encouraging, and supporting me.

I promise that I will never lose my exuberance

and my passion and enthusiasm for research.